

**Stable isotope, major and trace element chemistry of modern
snow from Evans Piedmont Glacier, Antarctica: insights into
potential source regions and relationship of glaciochemistry
to atmospheric circulation and vigour.**

Julia Ruth Bull

A thesis submitted in partial fulfilment of the requirements for the
degree of Masters of Science in Geology, August 2009.

Victoria University of Wellington

Abstract

This thesis presents a sub-seasonally resolved, decade long record of snow pack chemistry from Evans Piedmont Glacier (EPG), southern Victoria Land coast, Antarctica. Snow chemistry measurements were made at ca. 20 analyses per year for stable isotope ratios $\delta^{18}\text{O}$ and δD , major ions Ca^+ , Cl^- , K^+ , Mg^+ , MS^- , Na^+ , NO_3^- , SO_4^{2-} by ion chromatography (IC), and major and trace element chemistry by inductively coupled plasma mass spectrometry (ICP-MS). Na, Mg, Al, Fe, Mn and Ba were measured by ICP-MS using a hydrogen flushed collision cell to reduce the formation of polyatomic ion interferences, whereas Ti, V, Cr, Ni, Cu, Zn, As, Rb, Sr, Y, Zr, Sb, Cs, Ba, La, Ce, Pb, Bi, Th and U were measured in non-collision cell mode to increase count sensitivity. ICP-MS analytical precision is typically 5 to 10 % (2 rsd) that is two orders of magnitude at minimum below natural variability (e.g. samples range between Na = 10 to 18031 ppb and Al = 5 to 3856 ppb). The presence of undigested mineral dusts in weakly acidified samples, however, complicates the measurement of elemental concentrations in snow samples by randomly entering the ICP-MS. Despite this, the range of sample concentrations (Zr = 3.0 to 5630 ppb) is still orders of magnitude higher than sample reproducibility. The dominant source regions of element chemistry transported to EPG snow are identified as marine (Na, Mg, SO_4 , Cl, K, As and Sr) and terrestrial derived aerosol (Al, Mn, Fe, Ba, Ti, V, Ni, Cr, Zn, Rb, Y, Zr, Cd, Sb, Cs, Ba, La, Ce, Pb, Th and U), with minor contributions from anthropogenic (V, Cr, Ni, Cu, Zn, As, Sb and Pb) and volcanic emissions (Bi, SO_4 and K). This is based on both elemental ratio modelling and ICP-MS time resolved analysis that identifies elements present in particulate form (mineral dusts). EPG snow chemistry is related to measured meteorological conditions at nearby Cape Ross. Winter maxima of elemental concentrations is consistent with maximum winter wind speed and low precipitation rates. Furthermore, winter snow samples that are depleted in SO_4^{2-} relative to other marine derived elements (e.g. Na), indicate the sea ice surface is an important source of marine aerosol transported to EPG in addition to an open ocean source. Annual maximum chemistry concentrations of terrestrial derived elements (e.g. Zr) are significantly correlated to maximum annual wind speed measured at Cape Ross ($r^2 = 0.68$, $p < 0.01$). Lower correlation of marine derived chemistry (e.g. Na) and maximum

wind strength reflects additional controls of source region and other meteorological parameters such as storm duration on marine derived chemistry. In contrast to elemental concentrations, elemental ratios are less sensitive to extreme wind conditions. Rather elemental ratios provide a more robust signature of changes in mean atmospheric circulation related to delivery of aerosol from different source regions and via different transport fractionation processes. Al/Na is controlled by variable delivery of terrestrial (Al) and marine (Na) aerosol to EPG, although the longer term trend is driven primarily by changes in Na. Al/Na is significantly higher between winter 2000 and summer 2006/07 with a mean value of $\text{Al/Na} = 0.15$ compared to $\text{Al/Na} = 0.02$ prior to 2000. Although sea ice extent was highly variable over this time period, there is no clear relationship between Al/Na and sea ice. Rather, Al/Na is significantly correlated to mean summer wind speed measured at Cape Ross ($r^2 = -0.51$, $p < 0.01$). This demonstrates the sensitivity of Al/Na to changes in the average transport of marine aerosol to EPG during summer, when an open ocean source is most proximal. The shift in Al/Na is also concurrent with a shift in the relationship between $\delta^{18}\text{O}$ and d excess, indicative of a changing precipitation source region to EPG. The observed changes in EPG chemistry are concurrent with shifts in mean Southern Oscillation Index (SOI), a measure of the El Niño Southern Oscillation (ENSO) strength and polarity. Al/Na is low when SOI is predominantly negative (El Niño), associated with increased summer wind strength. This is in accordance with a strong Amundsen Sea Low, positioned directly north of the Ross Sea as previously reported during El Niño years. Although the establishment of a statistically significant relationship between SOI and EPG Al/Na ratios is inhibited by the brevity of this record, this study highlights the potential for the 180 m firn core also extracted from EPG to track long-term changes in SOI. Elemental chemistry of EPG provides a high resolution tool to reconstruct atmospheric circulation changes within the southern Ross Sea region.

Table of Contents

<u>Abstract</u>	<u>2</u>
<u>Table of Contents</u>	<u>4</u>
<u>List of Figures</u>	<u>8</u>
<u>List of Tables</u>	<u>10</u>
<u>Acknowledgments</u>	<u>12</u>
<u>Chapter One: Introduction</u>	<u>14</u>
1.1.0 Prelude	14
1.2.0 Research objectives	14
1.3.0 An introduction to ice core climatology	15
1.3.1 The International Trans-Antarctic Science Expedition	16
1.3.2 NZ ITASE and coastal ice core records	17
1.4.0 Thesis outline	18
<u>Chapter Two: Antarctic climatology</u>	<u>20</u>
2.1.0 Dominant controls on Antarctic climatology	20
2.1.1 Solar radiation	20
2.1.2 Temperature	21
2.1.3 Surface inversion	22
2.1.4 Pressure systems	22
2.1.5 Antarctic surface winds	24
2.1.6 Precipitation	25
2.1.7 The El Niño Southern Oscillation	26
2.2.0 Climatology of the Victoria Land coast	27
2.2.1 Dominant drivers of Victoria Land coast climate	27
2.2.1 Temporal changes in southern Victoria Land climate	29

Chapter Three: Principles of snow and ice chemistry **31**

3.1.0 Stable isotopes	31
3.1.1 Stable isotope fractionation	31
3.1.2 Controls of stable isotopes at coastal Antarctic sites	32
3.2.0 Source regions and transport of major and trace elements in glaciochemical records	35
3.2.1 Marine aerosol	36
3.2.2 Mineral dusts	38
3.2.3 Additional sources of elemental chemistry	41
3.2.4 Trace element chemistry	41

Chapter Four: Dating of the EPG snow pit record **44**

4.1.0 Methods	44
4.2.0 Comparison of EPG accumulation with previous Victoria Land snow pit records	48

Chapter Five: Measurement and interpretation of EPG stable isotope, major and trace element chemistry **50**

Abstract	50
5.1.0 Introduction	52
5.2.0 Study site	53
5.2.1 Site location and possible aerosol source regions	53
5.2.2 Meteorology	54
5.3.0 Methods	56
5.3.1 Snow pit sampling	56
5.3.2 Stable isotopes	56
5.3.3 Ion chromatography	57
5.3.4 Inductively coupled plasma mass spectrometry (ICP-MS)	57
5.3.5 ICP-MS sample measurements	59
5.4.0 Results	60
5.4.1 Dating	60
5.4.2 Stable isotopes	60
5.4.3 Analytical accuracy and precision of ICP-MS analyses	61
5.4.4 Reproducibility of elemental chemistry measurements in EPG snow samples	63

5.4.5 Elemental concentrations of EPG snow samples	66
5.4.6 Elemental ratios of EPG snow samples	68
5.5.0 Discussion	73
5.5.1 Presence of dust particulates in EPG snow samples	73
5.5.2 Ratio source modelling	75
5.5.3 Seasonal changes in elemental chemistry in relation to local meteorology	81
5.5.4 Inter-annual changes in elemental chemistry in relation to local meteorology	83
5.6.0 Conclusions	89
 <u>Chapter Six: Synthesis and conclusions</u>	 <u>92</u>
 6.1.0 Synthesis and conclusions	 92
6.2.0 Suggestions for future work	95
 <u>References</u>	 <u>98</u>
 <u>Appendix One: Sampling and analytical techniques</u>	 <u>114</u>
 A1.1.0 Introduction	 114
A1.2.0 Snow pit sampling	114
A1.3.0 Ion chromatography analyses	115
A1.4.0 Inductively coupled plasma mass spectrometry (ICP-MS)	115
A1.4.1 Spectral interferences	115
A1.4.2 Quantification of elements	116
A1.4.3 Pulse/analogue factors	117
A1.4.4 Washout procedure	118
A1.4.5 ICP-MS analytical precision and accuracy	118
A1.5.0 References	119
 <u>Appendix Two: Whitehall Glacier study</u>	 <u>120</u>
 A2.1.0 Introduction	 120
A2.2.0 Study site	120
A2.3.0 Methodology	121
A2.4.0 Preliminary results and discussion	122
A2.4.1 Dating	122

A2.4.2 Comparison of chemistry between WHG snow profiles and Cape Hallett meteorological conditions.	124
--	-----

A2.5.0 Conclusions and future work	127
------------------------------------	-----

A2.6.0 References	127
-------------------	-----

<u>Appendix Three: Appendix Three: Stable isotope, major and trace element chemistry (ICP-MS and IC analysis), density and temperature measurements of the EPG snow profile</u>	129
---	-----

<u>Appendix Four: Stable isotope, major and trace element chemistry (ICP-OES and IC analysis), and density measurements of WHG snow profiles</u>	171
--	-----

<u>Appendix Five: Full data set of major and trace element chemistry, density and temperature measurements of EPG and WHG snow profiles</u>	CD
---	----

List of Figures

<u>Chapter One: Introduction</u>	14
1.1 Map of Antarctica showing ITASE sampling sites	16
1.2. Map of the Ross Sea region showing NZ ITASE current and future sampling sites	17
<u>Chapter Two: Antarctic climatology</u>	20
2.1 Annual average temperature across Antarctica	21
2.2 Pressure fields around Antarctica and the Antarctic Circumpolar Trough	23
2.3. Surface wind regime across Antarctica	24
2.4 Annual net accumulation across Antarctica	26
2.5 Schematic diagram of the influence of the Amundsen Sea Low on Ross Sea climatology	28
<u>Chapter Three: Principles of snow and ice chemistry</u>	31
3.1 Global meteoric water line of $\delta^{18}\text{O}$ versus δD	32
3.2 Schematic diagram of frost flower formation on the sea ice surface	37
3.3 Schematic diagram showing modes of aeolian transport of dust particles	40
<u>Chapter Four: Dating of the EPG snow pit record</u>	44
4.1 Stratigraphy, density and chemistry ($\delta^{18}\text{O}$, Na, MS, nss SO_4) of the EPG snow profile in comparison to EPG_2004 and EPG_2005 used for dating	47
<u>Chapter Five: Measurement and interpretation of EPG trace element chemistry</u>	50
5.1 Map of the Ross Sea region with the location of EPG, aerosol source regions and meteorological records. The typical wind regime measured at Cape Ross is also shown	54
5.2 Stable isotope ($\delta^{18}\text{O}$, δD , d excess) profile of the EPG snow profile	61
5.3 Microscopic images of EPG snow samples	63
5.4 Na, Mg, and Ca concentrations measured in EPG snow samples by IC versus ICP-MS	64
5.5 Collision cell vs. non-collision cell measurements of Ba in EPG snow samples	65
5.6 ICP-MS time resolved analysis of Na, Zr, Al/Na and Zr/Y for select EPG samples	66
5.7 Bivariate plots of selected major and trace elements in EPG snow samples	68

5.8 Changes of $\delta^{18}\text{O}$, Na and Al concentrations and Al/Na throughout the EPG snow pit profile	70
5.9 Changes of $\delta^{18}\text{O}$, Ti and Sr concentrations and Ti/Sr throughout the EPG snow pit profile	71
5.10 Changes of $\delta^{18}\text{O}$, Fe, Al, Zr, Y concentrations and Fe/Al and Zr/Y throughout the EPG snow pit profile	72
5.11 Modelled influence of regional geology on EPG snow chemistry	80
5.12 Comparison of maximum elemental chemistry (e.g. Zr) with maximum Cape Ross wind speed	84
5.11 Comparison of Al/Na of EPG snow with Cape Ross monthly average wind speed and wind direction	87
<u>Appendix One: Sampling and analytical techniques</u>	114
A1.1 Stratigraphy of the upper 1.7 m of the EPG snow pit profile	115
<u>Appendix Two: Whitehall Glacier study</u>	120
A2.1 Location of WHG and Cape Hallett	121
A2.2 $\delta^{18}\text{O}$, density and MS profiles of WHG_1 snow pit used for dating	123
A2.3 Comparison of EPG and WHG inferred accumulation rates with modelled precipitation rates	123
A2.4 Comparison of $\delta^{18}\text{O}$ measured in the four snow pits from WHG with Cape Hallett temperature	125
A2.5 Comparison of Na concentrations measured in the four snow pits from WHG with Cape Hallett wind speed	126
A2.6 Bivariate plots of selected major and trace element chemistry from WHG_1 in comparison to oceanic and upper continental crust ratios	126

List of Tables

<u>Chapter Three: Principles of snow and ice chemistry</u>	31
3.1 Source regions of Antarctic trace element chemistry in snow and ice core records identified by previous studies	42
<u>Chapter Four: Dating of the EPG snow pit record</u>	44
4.1 Comparison of the accumulation rates inferred from snow pit studies along the Victoria Land coast including EPG	48
<u>Chapter Five: Measurement and interpretation of EPG trace element chemistry</u>	50
5.1 Typical instrumental ICP-MS running conditions used for measurement of major and trace element chemistry in EPG snow samples	58
5.2 Analytical precision and accuracy of ICP-MS measurements and summarized EPG snow pit chemistry	62
5.3 Comparison of mean EPG snow pit chemistry with previous studies	67
5.4 Summarized source region modelling of EPG chemistry using elemental ratios	76
<u>Appendix One: Sampling and analytical techniques</u>	114
A1.1 Comparison of repeated measurements of SLRS-4 by ICP-MS with: a) hydrogen and, b) helium flushed collision cell	116
<u>Appendix Three: EPG snow chemistry, density and temperature measurements</u>	129
A3.1 Stable isotope composition of EPG snow samples ($\delta^{18}\text{O}$, δD and d excess)	130
A3.2 Major ion chemistry of EPG snow samples by IC analysis	137
A3.3 Repeated measurement of SLRS-4 by collision cell ICP-MS	144
A3.4 Standard deviations of blank measurements by collision cell ICP-MS	145
A3.5 Repeated measurement of select EPG snow samples by collision cell ICP-MS	146
A3.6 Time resolved analysis of select EPG snow samples by collision cell ICP-MS	147
A3.7 Major and trace element chemistry of EPG snow samples by collision cell ICP-MS	152

A3.8 Repeated measurement of SLRS-4 by non-collision cell ICP-MS	157
A3.9 Standard deviations of blank measurements by non-collision cell ICP-MS	158
A3.10 Time resolved analysis of select EPG snow samples by non-collision cell ICP-MS	160
A3.11 Trace element chemistry of EPG snow samples by non-collision cell ICP-MS	163
A3.12 Correlation table of EPG major and trace element chemistry measured by ICP-MS	168
A3.13 Density and temperature measurements of the EPG snow pack profile	179

Appendix Four: WHG snow profiles chemistry, density and temperature measurements

171

A4.1 Stable isotope composition of WHG_1 snow samples ($\delta^{18}\text{O}$, δD and d excess)	172
A4.2 Stable isotope composition of WHG_1b snow samples ($\delta^{18}\text{O}$, δD and d excess)	176
A4.3 Stable isotope composition of WHG_2 snow samples ($\delta^{18}\text{O}$, δD and d excess)	178
A4.4 Stable isotope composition of WHG_3 snow samples ($\delta^{18}\text{O}$, δD and d excess)	181
A4.5 Stable isotope composition of WHG_4 snow samples ($\delta^{18}\text{O}$, δD and d excess)	183
A4.6 Repeated measurement of the quality control standard (QC_2) by ICP-OES	185
A4.7 Standard deviation of blank measurements by ICP-OES	186
A4.8 Major and trace element chemistry of WHG_1 by ICP-OES	187
A4.9 Major and trace element chemistry of WHG_1b by ICP-OES	191
A4.10 Major and trace element chemistry of WHG_2 by ICP-OES	192
A4.11 Major and trace element chemistry of WHG_3 by ICP-OES	196
A4.12 Major and trace element chemistry of WHG_4 by ICP-OES	198
A4.13 Major ion chemistry of WHG_1 by IC	200
A4.14 Major ion chemistry of WHG_1b by IC	204
A4.15 WHG snow profile density measurements	206

Acknowledgments

I would like to first and foremost thank my two supervisors, Dr. Nancy Bertler and Prof. Joel Baker for their time, patience and support of this thesis. Thank you Nancy for your unwavering enthusiasm for ice core research and advice with chemistry analyses and interpretation, in addition to providing the foundations of this project. Thank you Joel for your help and in particular, patience through laboratory and analytical procedures and interpretation. Your determination to improve my writing and editing skills has been remarkable.

Rachael Rhodes deserves enumerate thanks for her support throughout this entire thesis, from field work to analytical procedures and editing. Your motivation, advice and most importantly friendship have been invaluable.

Thank you to Sharon Sneed at the University of Maine for IC analyses, and Valerie Claymore at GNS Science for stable isotope analyses and patience in teaching the complexities of the stable isotope mass spectrometer. I am also indebted to Julian Thompson at GNS Science for all his help with sampling.

I would like to thank Antarctica New Zealand for their logistical support and those who shared two field seasons in Antarctica with me shovelling snow, in particular, Shulamit Gordon, Dean Peterson, Sepp Kipfstuhl, Davie Robinson, Glen Kingan, Jodie Burton and Billy Wallace.

Thank you to New Zealand Post, Victoria University, the Transantarctic Association, and the Antarctic Research Endowed Development Fund for financial support. Data analyses for this project were jointly funded by Victoria University of Wellington and GNS Science FRST grants.

A large number of staff and students within the Victoria University Antarctic Research Centre and the School of Geography, Environment and Earth Sciences deserve an enormous amount of gratitude for their help and encouragement. In particular, thank you to Warren Dickinson for numerous discussions, MAF permitting requirements and

encouragement; Gavin Dunbar for help with dust particles and smear slide preparation; Euan Smith for statistical advice; Martin Schiller, Monica Handler and Richard Wysoczanski for help within the geochemistry laboratory; Rob McKay for help with maps; Tamsin Falconer, Michelle Dow, Alex Pyne, Mike Hannah, Tim Naish, Lionel Carter, Shona de Sain, Jill Ruthven and to anyone else who I have unconsciously left off this list. A special thank you to those I have had the privilege to spend my uni years with including Rachael C., Kim, Dan, Dave, Rory, Nettie, Julene, Martin, Evelien, Sarah, Aidan, John, Alice, Lawrence, Sam, Matt, Mark, Susanne and Heather. Thank you for your laughter on many an unproductive day, and support during the difficult ones.

In particular I would like to thank my family, Ally, Steve, Chris, George, and Jess as well Kate, Bonnie, Rosie, Jules, Kim T., Nele and Eva, who have kept in perspective what the important things in life are. Thank you to Grandpa Bull whose belief in blue sky science has been an inspiration.

Finally, to my parents.

Chapter One: Introduction

1.1.0 Prelude

Knowledge of climate system dynamics in the past is fundamental for understanding how changes in the global radiation budget may influence future climate. Continuous instrumental and observational climate records extend back at most to 1659, with more reliable data sets only available from the 1850's onwards and global scale satellite monitoring from the late 1970's (Marshall, 2007). Although critical for our understanding of present climate, instrumental records are not long enough to: a) consider 20th Century changes within the context of natural climate variability, b) compare current conditions to analogous past events and c) determine long term coupled atmospheric-oceanic controls on climate system and ice sheet dynamics. These limitations highlight the need for accurate paleoclimate proxies and archives. Ice core research has the ability to provide such records, through stable isotope and elemental analysis as well as determination of the gas chemistry trapped in the ice from past atmospheres (Alley, 2000; Augustin et al., 2004; Dansgaard et al., 1969; Jouzel, 2007; Jouzel et al., 2007; Monnin et al., 2001; Petit, 1999)

1.2.0 Research objectives

This thesis presents a chemical study of modern Antarctic snow from a 4 m snow pit, representing a seasonally resolved, 14 year record from Evans Piedmont Glacier (EPG), southern Victoria Land coast. The project is a contribution to the New Zealand International Trans-Antarctic Science Expedition (NZ ITASE) program, with the aim to develop a reliable technique for the measurement of trace elements at coastal Antarctic sites. This has been achieved using inductively coupled plasma mass spectrometry (ICP-MS) with supplementary analyses for stable water isotopes ($\delta^{18}\text{O}$ and δD) and ion chromatography (IC) for major ions. The data set provides new insights into the controls of aerosol-deposited trace element chemistry of snow and the potential to use trace element glaciochemistry for paleoclimate studies.

To achieve this, is it first important to determine the main sources of the aerosol-deposited snow chemistry. This is accomplished through comparison of chemical ratios in samples with known potential sources including regional geology, the upper ocean,

and volcanic and anthropogenic emissions. Trace element concentrations and, importantly, ratios provide a higher degree of variation in natural sources than major elements and can therefore be used to fingerprint chemical sources with a greater degree of certainty.

Secondly, temporal changes in chemistry have been evaluated. Due to the high resolution of the record, seasonal cycles have been determined which currently remain constrained by only a few studies (Hur et al., 2007; Planchon et al., 2002b). Inter-annual changes are investigated with respect to meteorological data, measured on site since 2004, and at nearby Cape Ross since 1997, which is maintained by the Italian Antarctic Research Program. At least nine-ice core records have previously been taken from the Victoria Land coast, providing the potential for important future research to extend this record back several thousand years (Bertler et al., 2004a; Bertler et al., 2004b; Bertler, 2003; Mayewski and Lyons, 1982; Mayewski et al., 1995; Patterson et al., 2005; Rhodes et al., 2009; Vimeux et al., 2002; Waddington et al., 1993; Welsh et al., 1993)

1.3.0 An introduction to ice core climatology

Ice cores provide some of the highest resolution paleoclimate records available over the last 800 kyr (EPICA community members, 2004). Dansgaard (1954) first proposed the Greenland Ice Sheet as an archive of paleo-temperatures through the measurement of the stable oxygen isotope ratio $^{18}\text{O}/^{16}\text{O}$. The earliest deep ice cores extracted from Camp Century (Greenland) and Byrd Station (Antarctica) successfully demonstrated glacial/interglacial inferred temperature changes throughout the last 100 kyr and highlighted strong similarities in climatic changes between the northern and southern hemispheres (Dansgaard et al., 1969; Epstein et al., 1970; Taylor, 2007). Ice core analyses now routinely include measurement of $\delta^{18}\text{O}$ and δD , major and trace elements, loess content and loess grain size, concentrations of gas species and their isotope ratios, organic acids, crystal structures and electric conductivity. These analyses are used as proxy indicators of temperature, windiness, circulation changes and the direct measurement of past atmospheric greenhouse gas concentrations (Augustin et al., 2004; Lambert et al., 2008; Legrand and Mayewski, 1997; Marteel et al., 2009; Mayewski et al., 1995; Monnin et al., 2001; O'Brien et al., 1995; Petit, 1999; Thompson and Mosley Thompson, 1981; Thompson et al., 1997).

Dating techniques include: a) tritium and scintillation dating which is based on identifiable spikes in the 1950s and 1960s due to atmospheric nuclear testing, b) layer counting of seasonal changes using the physical properties of snow, stable isotope ratios and elemental chemistry, c) using volcanic eruptions as time markers which are recorded in snow and ice core records by peaks in volcanic derived chemistry such as sulphate and bismuth and, less frequently, through tephra deposition, d) radiocarbon dating of carbon dioxide in gas bubbles and e) modelling approaches including Milankovitch orbital tuning and ice flow models (Alley et al., 1997; Parrenin et al., 2001; Salamin et al., 1998; Schwander et al., 2001). The spatial distribution of records has also broadened to include mid- and lower latitude records, which are important in constraining global climatology (Bradley et al., 2003; Fisher et al., 2008; Thompson et al., 1997). From ice core records, fundamental principles of paleo-climatology have been established including the relationship between temperature and atmospheric greenhouse gas concentrations over the last 800 kyr (Augustin et al., 2004; Petit, 1999). Furthermore, high resolution ice core records from Greenland have demonstrated that major readjustment of the northern hemispheric circulation systems and ocean currents, such as Dansgaard-Oeschger events, can occur in as little as 2-3 years (Alley et al., 1993; Masson-Delmotte et al., 2005; Steffensen et al., 2008).

1.3.1 The International Trans-Antarctic Science Expedition

The polar location of Antarctica makes it particularly suitable for glaciochemical studies. This is because of a) well marked seasonal chemistry cycles due to variation in temperature, atmospheric circulation, sea ice extent, photochemistry and biological activity, b) low speeds of chemical reactions due to the temperature, c) location of the oldest continuous precipitation possible and d) strong indication

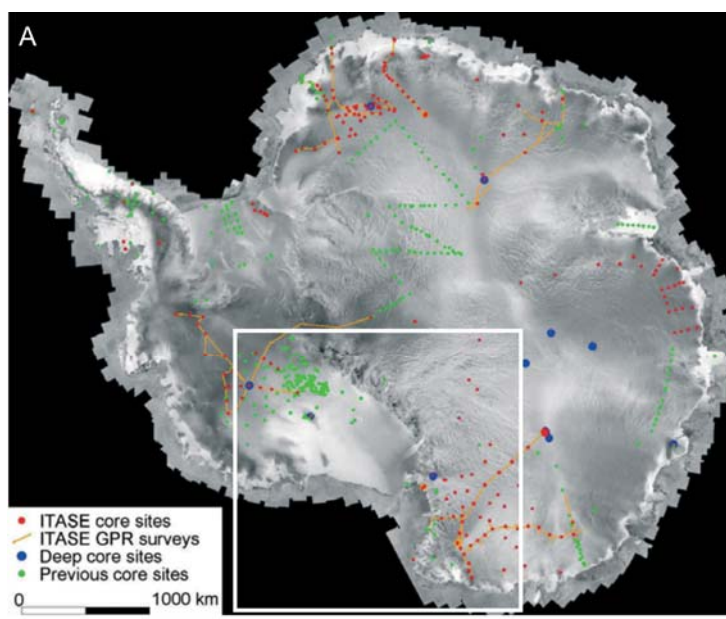


Figure 1.1 Locations of the International Trans-Antarctic Science Expedition (ITASE) ice core and snow sampling sites (Mayewski et al., 2005).

of southern ocean climate processes at coastal sites (Legrand and Mayewski, 1997). For these reasons, Antarctica is the focus of the International Trans-Antarctic Science Expedition (ITASE) with the aim to compile a comprehensive, continent wide, climatic history of Antarctica over the last 200 yr using glaciochemistry (Fig. 1.1). The time period of 200 yr was chosen to focus on natural short term climatic variability, anthropogenic induced changes since the industrial revolution (~1850 AD), and to determine how instrumental records are representative of general Antarctic climate over the last 30-40 yr (Mayewski et al., 2004).

1.3.2 NZ ITASE and coastal ice core records

The New Zealand contribution to ITASE focuses on climate reconstruction of the Victoria Land coast within the Ross Dependency (Fig. 1.2) (Mayewski and Goodwin, 1997). High accumulation rates along the coast of the Trans-Antarctic Mountains result in snow and ice core records of typically sub-seasonal resolution (Ayling and McGowan, 2006; Bertler et al., 2004a; Connolley and Cattle, 1994; Patterson et al., 2005). This is important in determining seasonal climatic variance and sub-decadal climate phenomena that may not be

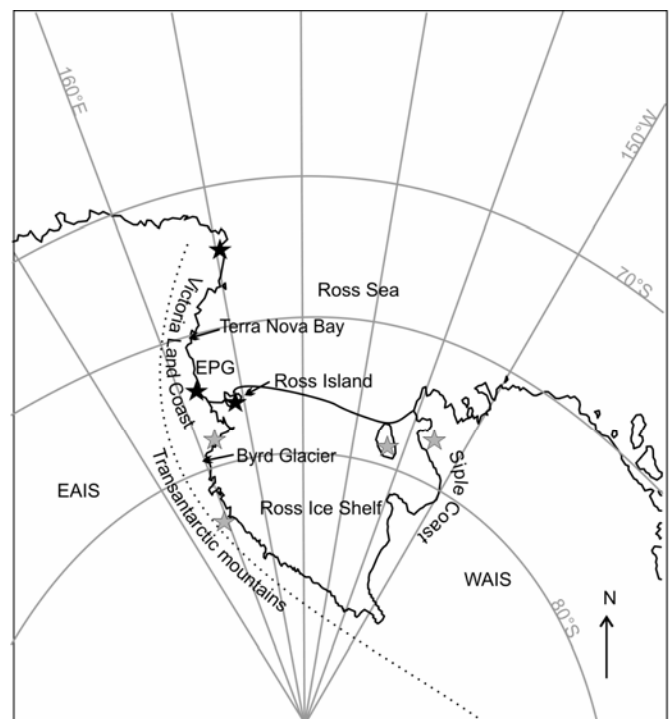


Figure 1.2 Overview of the Ross Sea region, including the focus of this study, the Evans Piedmont Glacier (EPG). The East Antarctic Ice Sheet (EAIS) and West Antarctic Ice Sheet (WAIS) are also denoted. Locations of previously drilled NZ ITASE ice core sites are shown with black stars and proposed future drilling sites with grey stars.

recorded in the Antarctic interior. Furthermore, air masses of variable origin should produce distinguishable glaciochemical signatures due to proximity of highly contrasting aerosol source regions such as the Ross Sea and local rock exposures. Long-term reconstruction of atmospheric circulation is important in establishing the influence of climate phenomena that occur within the troposphere such as the El Niño Southern Oscillation and Antarctic Oscillation on the Ross Sea climatology, the relative influence of which remain controversial due to temporal and spatial brevity of Antarctic climate

records (Turner, 2004). Furthermore, coastal glaciochemical records provide sensitive indicators of oceanic iron flux, changes in sea ice extent and associated changes in primary productivity (Atkins and Dunbar, 2009; Curran et al., 2003; Mayewski et al., 1995; Rhodes et al., 2009). Understanding the source and transport controls of glaciochemistry within this region is therefore important to utilise the potential of NZ ITASE ice core records.

1.4.0 Thesis outline

The outline of this thesis is briefly summarised below:

Chapter one: Introduction

Chapter two: Antarctic climatology

Important drivers of Antarctic climate are summarised in addition to the current understanding and complexities of decadal scale climate variability within the southern Victoria Land coast and Ross Sea region.

Chapter three: Principles of snow and ice chemistry

The principles of relating stable isotope ratios, and major and trace element chemistry in glaciochemical records to climatic conditions are reviewed.

Chapter four: Dating of the EPG snow pit record

This chapter discusses the dating method applied to the EPG snow profile and its potential uncertainty. The inferred EPG accumulation rate is compared to other snow and ice core records within southern Victoria Land for validation.

Chapter five: Measurement and interpretation of EPG stable isotope and major and trace element chemistry

This chapter is presented as a draft manuscript for submission to Earth and Planetary Science Letters under the title: “Source region and transport controls on major and trace element chemistry of snow pack from the southern Victoria Land coast, Antarctica”.

Chapter six: Synthesis and conclusions

Appendix one: Sampling and analytical techniques

Appendix two: Whitehall Glacier study

This appendix briefly outlines the aims and preliminary results of an additional glaciochemistry study conducted at Whitehall Glacier (WHG), northern Victoria Land. This study was not included in the main section of the thesis due to the brevity of the WHG snow pit records, which only represent 6 to 18 months, inhibiting meaningful correlation to the EPG record.

Appendix three: Stable isotope, major element, trace element, density and temperature measurements of the EPG snow profile

Appendix four: Stable isotope, major and trace element and density measurements of WHG snow profiles

Chapter Two: Antarctic climatology

2.1.0 Dominant controls on Antarctic climatology

Antarctic climate is controlled primarily by the polar location and high topography of the continent with an average elevation of ~2300 m compared to the next highest continent of Asia (~800 m) (King and Turner, 1997). These factors influence solar radiation, temperature, pressure, precipitation and wind fields. Understanding of present day climate and recent changes is primarily derived from instrumental records and satellite monitoring since the 1970s (Marshall, 2007). There are currently > 90 operable automatic weather stations across Antarctica (<http://amrc.ssec.wisc.edu/aws.html>), although most instrumental records are relatively brief and only 19 records extend more than 30 yr (Turner et al., 2005). Additionally, only two records greater than 30 yr in length are located at interior Antarctic sites, severely limiting spatial coverage. King and Turner (1997) provide a comprehensive review on the major aspect of Antarctic climate, which are only briefly discussed here.

2.1.1 *Solar radiation*

Solar radiation is the primary driver of temperature, atmospheric circulation, and weather systems globally and is dependent primarily on latitude and seasonality (Schwerdtfeger, 1984). Importantly, this is reduced to zero in Antarctica during winter, resulting in pronounced cooling over the entire continent and low temperature variance at interior sites (King and Turner, 1997). Atmospheric water vapour content, ozone concentration, aerosol loading, presence of clouds and elevation of the site further determine the amount of incoming solar radiation that is transmitted through the atmosphere to the surface (King and Turner, 1997). This varies inter-annually, primarily through changes in cloud coverage, which over Antarctica is primarily related to strength and position of the Antarctic Circumpolar Trough system (King and Turner, 1997). Significantly, between 75 % and 85 % of incoming solar radiation to Antarctica is reflected due to the high albedo of snow and ice surfaces (King and Turner, 1997). Seasonal changes in sea ice extent also have significant effects on the global net radiation budget by effectively doubling the area of Antarctica's high albedo surface during winter. This is particularly important during transition seasons when incoming

solar radiation is still high, concurrent with increased sea ice extent (King and Turner, 1997).

2.1.2 Temperature

Average annual temperature in Antarctica ranges between -55°C on the East Antarctic plateau to -10°C at the Antarctic Peninsula (Fig. 2.1). Although mean annual temperature is negatively correlated to elevation, slight displacement of the coldest regions over the East Antarctic ice sheet from the highest elevation, and disproportionately low temperatures of coastal ice shelves, indicates the additional influence of atmospheric circulation on site temperature (King and Turner, 1997). Seasonal temperature variation is significantly higher at interior sites, with 37°C seasonal fluctuations at Vostok station compared to 12°C at Faraday station on the Antarctic Peninsula (Comiso, 2000). Furthermore, sites within the polar circle experience a ‘coreless’ winter where temperatures are continuously low between mid-April to September with little variance, compared to more even seasonal fluctuations around the Antarctic Peninsula and coast of east Antarctica (King and Turner, 1997).

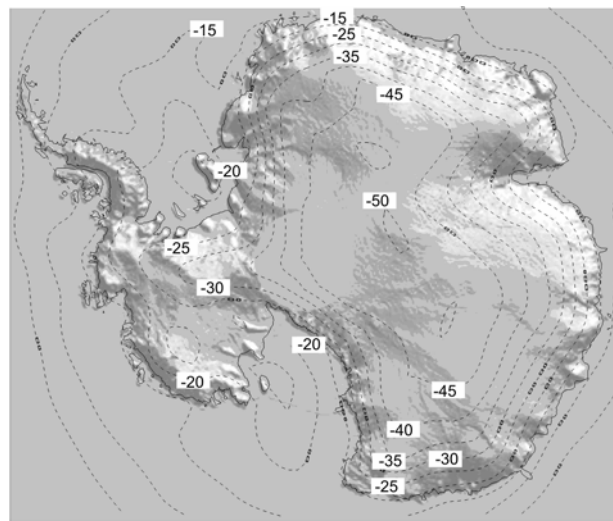


Figure 2.1 Annual average temperature ($^{\circ}\text{C}$) over Antarctica from 1950-2008 (NCEP/NCAR reanalysis data set, NOAA/ESRL Physical Sciences Division, 2009). Antarctic digital elevation model was sourced from (http://nsidc.org/data/docs/daac/nsidc0304_0305_glas_dems.gd.html)

Near surface temperature trends over the last half century show large geographic variability, although the average continent wide trend is positive (Steig et al., 2009).

While the Antarctic Peninsula is identified as one of the fastest warming regions of the world ($0.56^{\circ}\text{C decade}^{-1}$), temperature increases over the interior of West Antarctica are more subdued ($0.1^{\circ}\text{C decade}^{-1}$) and East Antarctica has arguably slightly cooled (Steig et al., 2009; Turner et al., 2005). The ability to understand East Antarctic temperature changes is limited by the scarcity of long term records. While the Vostok station temperature record shows no statistically significant change over the last 40 yr, a slight cooling over the East Antarctic plateau between 1979-1998 is reported by Comiso (2000) and a trend of $-0.17^{\circ}\text{C decade}^{-1}$ is statistically significant at the south pole Amundsen-Scott station (Turner et al., 2005). Steig et al. (2009) argued regional changes in atmospheric circulation, sea surface temperatures and sea ice extent only can explain the increased changes in West Antarctica compared to East Antarctica, rather than a simple increase of the circumpolar westerlies in response to changes in the Antarctic Oscillation as previously proposed (Turner et al., 2005).

2.1.3 Surface inversion

The surface temperature inversion is defined as the difference between surface temperature and the highest temperature within the lower troposphere. Surface inversions are typically strongest over the polar plateau during winter, up to 25°C over the interior of East Antarctica, 10°C to 15°C across western Antarctica, and 5°C at coastal sites (Connolley, 1996; Schwerdtfeger, 1984). This is an important feature of Antarctic climate which drives the development of katabatic wind flow (Connolley, 1996). The surface inversion, controlled primarily by surface temperature fluctuations with respect to relatively stable, warm air masses above, follows seasonal surface temperature trends closely, and is reduced to almost zero at coastal sites during summer.

2.1.4 Pressure systems

The pressure field of the lower troposphere over the Antarctic is dominated by two main features, the Antarctic Circumpolar Trough at a mean latitude of 66°S , and a weak surface anticyclone centred over the Antarctic continent (Fig. 2.2a) (King and Turner, 1997). The Antarctic Circumpolar Trough, is an area of intense synoptic cyclone activity (Fig. 2.2b), with cyclones typically 1000 – 6000 km across and lasting between one day to a week (King and Turner, 1997). It is located between 60° to 70°S where thermal contrast between cold Antarctic continental air meets relatively warm, moist maritime

air masses, an important control on cyclogenesis (Bromwich, 1993). Cyclonic activity varies seasonally and is strongly controlled by the position of the Antarctic Circumpolar Trough, which results in pressure maximum at coastal Antarctic sites when it is situated at its furthest position north during mid-summer and mid-winter (King and Turner, 1997). The Antarctic Circumpolar Trough, combined with the Coriolis force drives the Antarctic coastal easterlies and is also an important source of snow precipitation at coastal Antarctic sites (King and Turner, 1997; Sinclair, 2009).

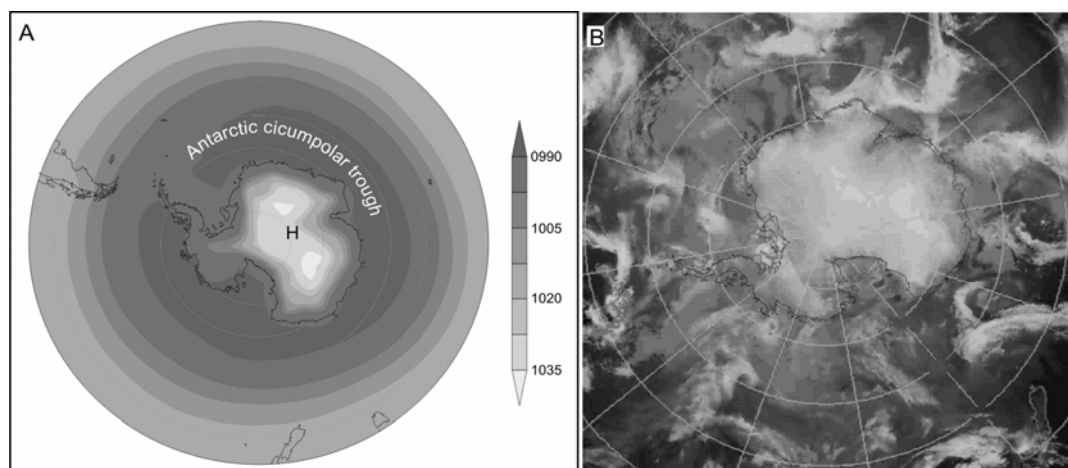


Figure 2.2 a) Annual average sea level pressure (mb) around and over Antarctica, from 1950-2008 (NCEP/NCAR reanalysis data set, NOAA/ESRL Physical Sciences Division, 2009). **b)** Satellite image of synoptic scale cyclones originating from the circumpolar trough above the Southern Ocean (University of Wisconsin).

Interannual variability of the Antarctic lower pressure field is primarily dominated by the Antarctic Oscillation (AAO), a 4 to 5 yr cycle which is dependent on changes in the strength and position of the sub-tropical jet (Fogt and Bromwich, 2006; Marshall, 2007). The AAO index is a measure of the zonal mean sea level pressure between 40°S and 65°S (Gong and Wang, 1999) and describes 30 % of natural variation of atmospheric circulation within the Southern Hemisphere (Hall and Visbeck, 2002). When AAO is positive, polar temperatures and surface pressures are anomalously low, resulting in strong circumpolar winds near 60°S (Turner, 2004), and vice versa during negative AAO. Continued positive correlation since the 1970's has been associated with an intensification of the polar vortex, and strengthening of the polar westerlies (Marshall, 2003).

The upper troposphere to stratosphere pressure field over the Antarctic is dominated by the Antarctic polar vortex, a large-scale cyclone centred over the South Pole. The polar vortex is strongest during winter when the temperature gradient between the pole and

lower latitudes is greatest and controls the strength of the high latitude westerly belt (Thompson and Wallace, 2000). Additionally, increased polar vortex strength is associated with decreased lower troposphere temperatures over the East Antarctic which will in turn influence the strength of katabatic outflow (Van den Broeke and Van Lipzig, 2002). Intensification of the polar vortex since the 1970's has been identified as a possible reason for the observed East Antarctic cooling trend over the last half century (Turner et al., 2005), although this is contentious (Steig et al., 2009).

2.1.5 Antarctic surface winds

Antarctic surface winds are predominantly controlled by katabatic flow, the drainage of cold, dense air chilled by radiation, moving gravitationally down slope from the polar plateau to the coast (Parish, 1988; Parish and Bromwich, 1987; Parish and Cassano, 2003). Flow is characteristically uni-directional, channelled by topography but also turns preferentially left under the influence of the Coriolis force (Fig. 2.3) (Parish and Bromwich, 1987). Wind speeds are strongest where the slope of terrain is high and, in particular, at outlet glaciers of the East and West Antarctic ice sheets. A stronger temperature inversion during winter results in increased strength of winter katabatic flow (King and Turner, 1997).



Figure 2.3 The pathway of dominant katabatic wind flow over Antarctica (Parish and Bromwich, 1986). In particular, surges from **a)** the Siple Coast and **b)** the Byrd Glacier region are propagated across the Ross Ice Shelf toward the Victoria Land Coast.

Synoptic and mesoscale cyclonic activity interacts with katabatic flow at the coast to produce more complex wind regimes. Synoptic scale depression systems around Antarctica enhance katabatic outflow by increasing the pressure gradient between the coast and the interior anti-cyclone (King and Turner, 1997). In turn, katabatic flow increases mesoscale cyclogenesis, in particular, within the Ross Sea region by increasing turbulence within the boundary layer (Carrasco et al., 2003). Synoptic conditions also influence flow of originally katabatic origin, propagating flow significant distances (100s of km) over ice shelves despite an effective slope gradient of zero (Schwerdtfeger, 1984).

2.1.6 Precipitation

Precipitation rates are difficult to constrain in Antarctica due to wind blown snow. Measurements include radar sensors on automatic weather stations, snow stakes, and stratigraphy and density studies of snow pack, all of which measure net accumulation rather than true precipitation (Bromwich and Parish, 1998; Cullather et al., 1996). Modelled precipitation rates are significantly lower than those in the mid-latitudes due to the typically weak nature of depression systems and significantly lower water vapour content of colder air masses (King and Turner, 1997). Furthermore, coastal sites (Fig. 2.4) receive significantly more precipitation than the Antarctic interior due to the higher influence of cyclonic activity and/or orographic lifting of marine air masses (Connolley and Cattle, 1994; Lettau, 1969; Rockey and Braaten, 1995; Schwerdtfeger, 1984). The West Antarctic Ice Sheet receives a disproportionate amount of precipitation, up to 40 % of the entire moisture flux over the Antarctic continent (Cullather et al., 1996; Lettau, 1969). Conversely, major weather systems rarely penetrate into the interior of the East Antarctic Ice Sheet due to the high elevation gradient between the coast and the East Antarctic plateau (Connolley and Cattle, 1994; King and Turner, 1997). Most interior precipitation occurs from isolated cloud (independent of weather systems) or from water vapour in clear sky air masses. Orographic lifting of air masses onto the polar plateau and irradiative cooling result in the gradual coalescence of cloud droplets which eventually fall out as ice crystals (Bromwich and Parish, 1998).

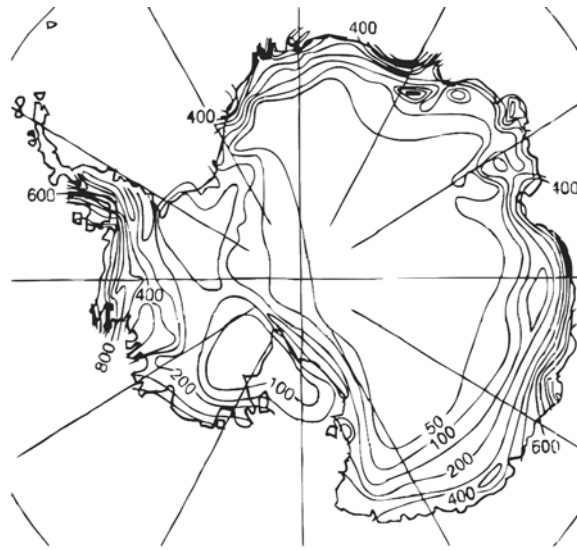


Figure 2.4 Annual net accumulation over Antarctica (mm yr⁻¹) (Connolley and Cattle, 1994 after Giovinetto and Bently, 1985).

2.1.7 The El Niño Southern Oscillation

Globally, the El Niño Southern Oscillation (ENSO) is the largest source of inter-annual climate variability (Philander, 1983) and in addition to the Antarctic Oscillation, is a major influence on Antarctic climate. The Southern Oscillation Index (SOI), defined as the normalised sea level pressure difference between Tahiti and Darwin, is a measure of ENSO strength and polarity. Links between SOI and the Antarctic climate have been found in sea ice extent, sea surface temperature, wind direction, wind speed, pressure and temperature at 500 mb and cyclonic activity with a lag of 2-4 months reported by most studies (Kwok and Comiso, 2002a; Kwok and Comiso, 2002b; Ledley and Huang, 1997; Turner, 2004; Van den Broeke and Van Lipzig, 2002; van den Broeke and van Lipzig, 2004). The most significant correlation between SOI and sea surface temperature around Antarctic occurs within the Ross Sea and Amundsen Sea, lagging tropical sea level pressure changes by three months (Fogt and Bromwich, 2006; Ledley and Huang, 1997). Positive SOI (La Niña events) are associated with low sea level pressure, cooler sea surface temperatures and warmer land conditions in the western Ross Sea and vice versa during negative SOI (El Niño) (Bertler et al., 2004a; Bertler et al., 2006a; Kwok and Comiso, 2002b).

2.2.0 Climatology of the Victoria Land coast

2.2.1 *Dominant drivers of Victoria Land coast climate*

The climate of coastal Victoria Land is driven by katabatic outflow, cyclonic activity, and on a highly localised scale, the McMurdo Dry Valley ‘monsoonal’ effect. Katabatic surges originate from both the West Antarctic Ice Sheet through the Siple coast, and the East Antarctic Ice Sheet through major outlet glaciers in the Byrd Glacier region and in the vicinity of Terra Nova Bay (Fig. 2.4) (Parish and Bromwich, 1987). Katabatic flow from Siple coast and Byrd Glacier region is propagated northward over the Ross Ice Shelf despite a reduction in slope gradient to effectively zero by synoptic scale cyclonic (Amundsen Sea Low) decay over the Marie Byrd Land coast (Bromwich, 1988). Through the influence of the Coriolis force, katabatic surges are forced eastward towards the Transantarctic Mountains, resulting in strengthened barrier winds along the Victoria Land coast (Sinclair, 1982). The position of Ross Island further increases wind strength in the McMurdo Sound by funnelling winds between the island and coast, an effect that can extend up to 100 km downstream of Ross Island (Schwerdtfeger, 1984). Local topographic features have a strong control on surface wind direction, noted in deflection of moderate strength southerlies around Minna Bluff, and Black and White Islands (Sinclair, 1982) (Fig. 5.1).

Cyclonic activity within the Ross Sea is governed primarily by the Amundsen Sea Low (L_{AS}), one of one four quasi-stationary synoptic scale low pressure centres around the Antarctic continent (Carleton and Fitch, 1993; Carrasco and Bromwich, 1994; Cullather et al., 1996; Schwerdtfeger, 1970). Dependent on its strength and position, L_{AS} forces atmospheric circulation either over the West Antarctic Ice Sheet towards the Ross Sea, increasing katabatic surges across the Ross Ice Shelf, or directly from the Ross Sea and Southern Ocean (Bertler et al., 2006a; Bromwich, 1993; Cullather et al., 1996; Kwok and Comiso, 2002b) (Fig. 2.5). Interannual variation of L_{AS} is modulated by the ENSO. Increased tropical sea surface temperatures during El Niño (negative SOI) events indirectly decrease the strength of the polar jet stream relative to sub-tropical latitudes, weakening and repositioning the L_{AS} eastward to the Marie Byrd Land coast (Bromwich et al., 1993). Conversely, during La Niña events (positive SOI), the L_{AS} is strengthened and positioned northward of the Ross Sea, increasing marine cyclonic activity (Fig 2.5)

(Bertler et al., 2004a; Bertler et al., 2006a). Modulation of L_{AS} by ENSO is also dependent on additional factors including the interaction of L_{AS} with the Antarctic Oscillation, and the eastward migration of the low-pressure system typically located over East Antarctica (Arrigo and van Dijken, 2004; Cullather et al., 1996; Fogt and Bromwich, 2006).

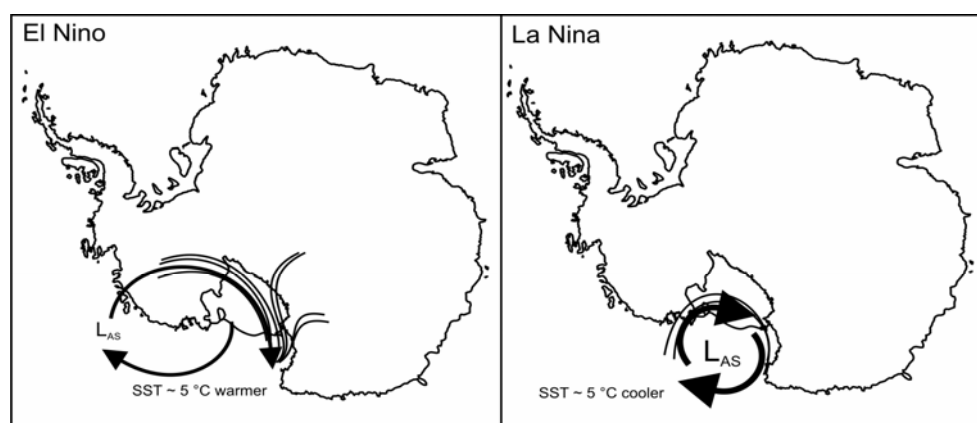


Figure 2.5 Amundsen Sea Low (L_{AS}) modulation of the Ross Sea climate in response to changes in the El Niño Southern Oscillation. Thickness of lines around the L_{AS} are used to denote strength of the low pressure cell. Adapted from Bertler et al. (2004a, after Cullather et al., 1996).

In addition to synoptic scale cyclones, mesoscale cyclonic activity is common within the Ross Sea, particularly when katabatic flow is strong and the L_{AS} is located to the north of the Ross Sea (Carrasco and Bromwich, 1994). Mesoscale cyclogenesis is focused over the western Ross Ice Shelf and 100-200 km NNE of Ross Island. This further contributes to southerly flow within the McMurdo Sound region (Carrasco and Bromwich, 1994) and is an important source of high latitude derived precipitation (Rockey and Braaten, 1995).

A unique feature of the Victoria Land coast is the McMurdo Dry Valleys, the largest ice-free area in Antarctica (Chinn, 1990). High topography of bedrock inland of the McMurdo Dry Valleys prevents ice flowing in from the East Antarctic Ice Sheet as occurs to the north and south. Additionally, the valleys are located within a precipitation shadow, whereby marine air masses deposit precipitation preferentially over Ross Island and the more coastal sites (Chinn, 1990; Fountain et al., 1998). Wind flow of the McMurdo Dry Valleys is typically bi-directional, switching between katabatic easterlies and westerly marine breezes (Doran et al., 2002). The latter develop when irradiative

warming of the exposed, low albedo surfaces during summer results in the development of a highly localised low-pressure cell, described as the McMurdo Dry Valley ‘monsoonal’ effect (Bertler et al., 2004b; Witherow, 2006). This is considered a localised effect and is unlikely to effect climatology of sites further along the Victoria Land coast.

Changes in seasonal sea ice extent are an additional control on Victoria Land coast climatology, changing moisture availability for cyclogenesis and temperature gradients between the continental and coastal air masses. Sea ice extent is at maximum during winter, forming a 20-22 km strip of fast sea ice along the western side of southern McMurdo Sound (Falconer and Pyne, 2004). Full sea ice cover is usually prevented by active polynya systems, in particular, the Ross Sea polynya which extends along the entire length of the Ross Ice Shelf, the largest to form regularly around Antarctica (Maqueda et al., 2004). The polynya is maintained predominantly by strong katabatic winds and causes relatively continuous sea ice production during winter and even when fully covered, ice thickness remains thin. Summer sea ice break out occurs between January and February following the opening of the Ross Sea, McMurdo Sound and Terra Nova polynya systems, attributed to warmer surface ocean temperatures and the influence of synoptic-scale weather systems (Bromwich and Parish, 1998; Maqueda et al., 2004).

2.2.1 Temporal changes in southern Victoria Land climate

In contrast to overall warming of the Antarctic continent since 1957 (Steig et al., 2009), the western Ross Sea sector has cooled by -0.7°C to -0.9°C decade⁻¹ since 1986 (Bertler et al., 2004a; Bertler et al., 2006a; Doran et al., 2002). This is superimposed on a longer-term warming trend of 0.29°C decade⁻¹ between 1971 to 2000 (Bertler et al., 2004a; Turner et al., 2005). The cooling of western Ross Sea is coincidental with a decrease in average wind speed measured at Lake Hoar in the McMurdo Dry Valleys of 0.23 m s^{-1} from 1986 to 1999 (Doran et al., 2002) and an insignificant decrease in average wind speeds and decrease in average pressure at Scott Base (Turner et al., 2005).

Bertler et al. (2004a; 2006a) attributed cooling of the Western Ross Sea since 1986 to strong teleconnection of the ENSO signal to the Antarctic during the 1990’s (Fogt and Bromwich, 2006) and greater dominance of the negative (El Niño) phase. El Niño

events are characterised on the Victoria Land coast by an increase in atmospheric flow from the West Antarctic Ice Sheet and a decrease in marine air masses from the Ross Sea. This is supported by high correlation of SOI and McMurdo Sound temperature anomalies inferred from glaciochemistry and instrumental records during the 1990's when the SOI and AAO are in phase but not during the 1980's (Bertler et al., 2004a; Bertler et al., 2006a).

However, Ayling and McGowan (2006) argue there has been no shift in atmospheric circulation over the last 35 yr. Assessment of tephra layers within two ice core records from the McMurdo Dry Valleys indicate there has been no significant increase in transport of material from the McMurdo Volcanic group, suggesting no change in windiness in contrast to shorter term meteorological records (Doran et al., 2002; Turner et al., 2005). This assessment is however based on 17 samples over a 35 yr period. To understand this apparently conflicting evidence, seasonally resolved records of climate are required. Elemental chemistry analysis is faster than mineralogy assessment, and therefore has the potential to provide such records.

Chapter Three: Principles of snow and ice chemistry

This chapter provides an overview of the chemistry routinely measured in snow and ice core records. Stable isotopes of oxygen and hydrogen provide estimates of temperature ($\delta^{18}\text{O}$ and δD) (Dansgaard, 1954) and precipitation source region (d excess) (Steffensen et al., 2008), while major and trace element chemistry are used to infer changes in atmospheric circulation and source region processes such as increased sea ice extent and the influence of anthropogenic pollution (Legrand and Mayewski, 1997; Petit, 1999; Planchon et al., 2002a).

3.1.0 Stable isotopes

3.1.1 Stable isotope fractionation

Fractionation of hydrogen and oxygen stable isotopes occurs during evaporation and condensation of water molecules due to the dependence of the saturation vapour pressure on isotopic mass (Jouzel, 2003). Increasing in mass, hydrogen has two stable isotopes ($^1\text{H} = 99.985\%$ atom, ^2H (D) = 0.015 % atom) and oxygen has three ($^{16}\text{O} = 99.762\%$ atom, $^{17}\text{O} = 0.038\%$ atom, $^{18}\text{O} = 0.200\%$ atom), although only ^{16}O and ^{18}O are routinely measured due to the low abundance of ^{17}O (Faure and Mensing, 2005). The δ notation, is used to express the ratio of $^2\text{H}/^1\text{H}$ (‰) or $^{18}\text{O}/^{16}\text{O}$ (‰) in the sample relative to bulk ocean seawater, the international standard VSMOW (Vienna Standard Mean Ocean Water) where

$$\delta = \left[\frac{\text{ratio in sample} - \text{ratio in VSMOW}}{\text{ratio in VSMOW}} \right] \times 1000.$$

Craig (1961) first demonstrated the strong linear correlation between $\delta^{18}\text{O}$ and δD in a study of global waters, thereby defining the Global Meteoric Water Line (GMWL) with a slope of eight (Fig. 3.1). The line is a weighted average of multiple local mean water line's (LMWL), all of which have a slope less than 8 due to seasonal variation in air mass sources. The slope approximates the ratio of H and O equilibrium factors, i.e. the fractionation of hydrogen isotopes is eight to ten times higher than that of oxygen (Jouzel, 2003).

The divergence of the GMWL from VSMOW values (e.g. when $\delta^{18}\text{O} = 0 \text{ ‰}$, $\delta\text{D} = \sim 10 \text{ ‰}$) indicates the additional non-equilibrium processes that occur during atmospheric vapour formation. The amount of kinetic fractionation is quantified by the y-axis intercept of the LMWL denoted as the *d*-excess parameter (*d*), such that $d = \delta\text{D} - 8 * \delta^{18}\text{O}$ (Dansgaard, 1954). Deuterium excess is determined primarily by kinetic effects, which are controlled by humidity at the source region during evaporation (Froehlich et al., 2002; Sharp, 2007). When humidity is low at the evaporative site, kinetic effects are proportionally more dominant compared to equilibrium evaporation effects and the *d* excess is increased. The global average of *d* excess is 10 ‰ as indicated by GMWL (Fig 3.1). Large global variation is, however, observed and *d* excess values measured in Antarctica vary between -15.4 ‰ and 28.9 ‰ (Araguas-Araguas et al., 2000; Masson-Delmotte et al., 2008; Sharp, 2007).

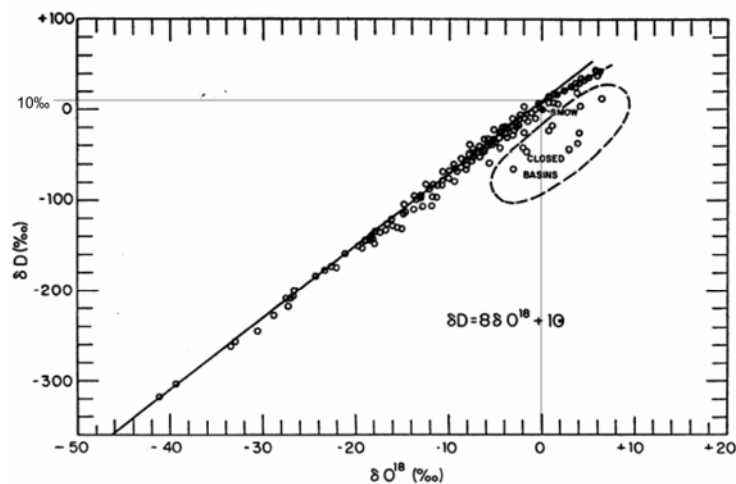


Figure 3.1 Global meteoric water line determined from $\delta^{18}\text{O}$ and δD of global waters (Craig, 1961). The global average deuterium excess (*d*) = 10 ‰.

3.1.2 Controls of stable isotopes at coastal Antarctic sites

δD and $\delta^{18}\text{O}$ are more strongly dependent on temperature with increasing latitude, altitude and distance from the coast due to greater temperature variations, and increased percentage of fractionation (Dansgaard, 1954; Sharp, 2007). Strong correlation between the spatial distribution of Antarctic mean temperature and $\delta^{18}\text{O}$ ($r^2 = -0.96$) and δD ($r^2 = -0.95$) allows reliable determination of an Antarctic ‘isotope thermometer’, in

particular, for the last 6000 to 7000 yr of constant global ice volume (Carlson et al., 2008; Masson-Delmotte et al., 2008; Masson et al., 2000).

Temporal negative correlation between δD or $\delta^{18}O$ and the d excess is expected, as low temperatures at the site of precipitation (low $\delta^{18}O$ and δD) are generally concurrent with low temperatures and hence humidity at the source region (high d) (Froehlich et al., 2002; Sharp, 2007). Negative correlation is observed at most interior Antarctic sites, with an average lag of 5 months between $\delta^{18}O$ or δD and the d excess (Aldaz and Deutsch, 1967; Ciais et al., 1995). However, coastal sites commonly show positive $\delta^{18}O$ and d excess correlation, with highest d excess values during summer at the Adélie Land coast (Ciais et al., 1995) and during early spring on Queen Maud Land coast (Schlosser, 2008). In addition to this variable phase relationship between $\delta^{18}O$, δD and d excess, a number of high resolution records indicate poor correlation of $\delta^{18}O$ and measured temperature over seasonal and inter-annual time periods (Schlosser, 2002a). These observations indicate secondary effects, which mask the primary control of temperature on stable isotope ratios $\delta^{18}O$ and δD or source humidity on d excess (Gat, 1996; Sharp, 2007). Such effects include: 1) the initial isotope composition of the moisture package, 2) the air mass trajectory pathway, 3) the seasonality of precipitation and, 4) post depositional alteration, which are briefly summarised below.

1) Warmer (cooler) sea surface temperatures at the moisture source region increases (decreases) the proportion of heavy isotopes (D and ^{18}O) evaporated and hence the initial isotope composition of a moisture package (Sharp, 2007). Additionally, increased mass of ice sheets over glacial-interglacial time scales effectively enriches the original oceanic reservoir in heavy isotopes, although this can be considered constant for the time period covered by this study.

2) The atmospheric pathway of a moisture package influences its isotope signal by changing the number of condensation and evaporation events that occur. As air masses travel further inland, the number of condensation events increases and the remaining water vapour is more depleted in $\delta^{18}O$ and δD resulting in higher d excess values (Sharp, 2007). This explains the strong negative correlation of $\delta^{18}O$ and δD , and moderate positive correlation of d excess with site temperature and distance from coast (Masson-

Delmotte et al., 2008). Additionally, air masses that reach coastal Antarctic sites from across the continent have significantly higher d excess values than air masses transported directly from their original evaporative source (Schlosser, 2004). Furthermore, precipitation that has passed over a greater distance of open water demonstrates low correlation between $\delta^{18}\text{O}$ and deposition site temperature due to re-evaporation and condensation of water vapour from variable sea surface temperatures along the air mass trajectory (Helsen et al., 2006; Schlosser, 2004).

3) Seasonality of precipitation can effect the isotopic ratio of snow by biasing the record towards the timing of precipitation, in particular, at coastal locations where precipitation occurs primarily from periodic cyclonic activity (Krinner et al., 1997; Schlosser, 2002a; Sharp, 2007). Schlosser et al. (2002a) demonstrated that interannual variability of $\delta^{18}\text{O}$ in the snow pack can be attributed to changes in the relative proportion of seasonal accumulation, with high $\delta^{18}\text{O}$ annual averages concurrent with a lower proportion of winter to early spring accumulation as measured by snow stakes. Conversely, low $\delta^{18}\text{O}$ annual averages occur when accumulation is high throughout the entire year. Accounting for seasonality of accumulation, correlations between $\delta^{18}\text{O}$ and temperature improved significantly from $r^2 = -0.13$ to $r^2 = 0.38$ (Schlosser, 2002a).

4) Finally, post depositional evaporation and recondensation of water molecules within the snow pack leads to alteration of the stable isotope ratio signal, dampening the average seasonal cycle and extreme events at sites with up to $40 \text{ g cm}^{-2} \text{ yr}^{-1}$ accumulation rates (Johnsen, 1977; Legrand and Mayewski, 1997; Schlosser, 2002b; Whillans and Grootes, 1985). At low accumulation sites ($<10 \text{ g cm}^{-2} \text{ yr}^{-1}$) the seasonal cycle is commonly lost altogether (Gat, 1996). Furthermore, high firn diffusivity and hence strong post depositional modification of δD compared to $\delta^{18}\text{O}$, results in the production of an artificial d excess signal (Johnsen et al., 2000). This commonly accounts for positive correlation between $\delta^{18}\text{O}$ and d excess signal at sites where diffusion processes are strong (Johnsen et al., 2000; Oerter, 2004). Ablation and formation of sastrugi features at the surface can further alter the integrity of the stable isotope profile with respect to temperature (Ekaykin et al., 2002).

These additional controls on $\delta^{18}\text{O}$, δD and d excess are important for interpretation of ice core stable isotope records. For example, the decreasing trend in $\delta^{18}\text{O}$ over the last century on the coast of Dronning Maud Land is attributed to a decrease in accumulation predominantly from late winter and spring, rather than a temperature change which other evidence indicates remained constant (Schlosser, 2002a). This is also observed within the EPICA Dronning Maud Land ice core record, where a downward shift in $\delta^{18}\text{O}$ and δD at 1000-1200 AD is attributed to increased accumulation as visible in annual layers (Oerter, 2004). Accumulation rate changes are also usually associated with a change in the dominant pathway of precipitation air masses. A switch from directly marine derived air masses (relatively high $\delta^{18}\text{O}$ and δD) to continentally derived air masses (low $\delta^{18}\text{O}$ and δD) will result in changes of similar or even greater magnitude than temperature driven changes (Schlosser, 2002a).

3.2.0 Source regions and transport of major and trace elements in glaciochemical records

Major and trace elemental chemistry measured in snow and ice core records is derived from atmospheric gases and aerosol sourced from the ocean, mineral dusts, volcanic emissions, biological processes, upper atmospheric processes, and anthropogenic activity (Legrand and Mayewski, 1997). Interpretation of their temporal changes with respect to climate is primarily based on knowledge of source, transport and depositional controls which are briefly reviewed here.

Aerosols are deposited to snow either with precipitation (wet) or independently of precipitation (dry). Wet deposition scavenges ionic chemistry from the atmosphere and includes snowfall, snow drifting, cloud water (fog) and clear-sky 'diamond dust' depending on the site location (Legrand and Mayewski, 1997). Dry deposition occurs through direct settling of aerosols to the surface, or filtration through the upper pack section of firn (Legrand and Mayewski, 1997). Determination of the more dominant process at a site is important as snow chemistry concentrations will overestimate the aerosol loading of the atmosphere when dry deposition is dominant (Davidson et al., 1981). To compensate for this, a chemical flux is commonly calculated where $F_{\text{ice}} = C \cdot A$ and F is the flux of elements to the snow or ice, C is the measured concentration in

snow or ice and A is the calculated accumulation rate. However use of a chemical flux will underestimate atmospheric aerosol loading when wet deposition of aerosol dominates (Kreutz and Mayewski, 1999; Legrand and Mayewski, 1997). Although Kreutz et al. (2000a) argued wet aerosol deposition is likely to be the dominant process for sites across the West Antarctic Ice Sheet, low elevation sites along the Victoria Land coast will be more sensitive to the transport of locally sourced aerosol associated with dry deposition (Ayling and McGowan, 2006; Lancaster, 2002), and therefore a chemistry flux is likely to be more appropriate for this study.

3.2.1 Marine aerosol

Marine aerosols are the most significant source of elemental chemistry in coastal Antarctic snow and ice records. Marine aerosols are typically the exclusive source of the soluble Na, Cl, SO_4 , Mg and K present in snow samples (Legrand and Mayewski, 1997). Marine aerosols are produced by two dominant mechanisms, the global phenomena of open water wave crest dispersion (sea spray) and formation of frost flowers on the surface of young sea ice at high latitudes (Fischer et al., 2007b). Relative importance of these sources is site specific and has significant implications on the interpretation of temporal changes in marine derived chemistry in snow and ice core records with respect to windiness and sea ice extent.

Traditionally, sea spray is considered the dominant mechanism of marine aerosol production. Dispersion of wave crests and bursting of air bubbles at the ocean surface produce small droplets of ocean water which are uplifted by convective cells into the boundary layer and higher atmosphere (Monahan et al., 1986). Production is most efficient during cyclonic activity due to increased turbidity of the atmospheric boundary layer, and aerosols are deposited with precipitation along the storm track (Fischer et al., 2007b). Seasonal maxima of Na during summer when sea ice extent is minimum within a number of Antarctic glaciochemical records support the open ocean as the dominant marine aerosol source (Fisher, 2004; Wagenbach, 1998). Furthermore, inter-annual variability of summer Na concentrations have been significantly correlated to summer sea ice extent and sea level pressure, an indicator of cyclonic activity (Fisher, 2004; Kreutz et al., 2000b; Wagenbach, 1998).

In addition to a sea spray source, the sea ice surface has been identified as an important region of marine aerosol production at high latitudes. During freezing of sea water, highly saline brine is ejected from the sea ice and is concentrated in elemental chemistry (Rankin and Wolff, 2002; Rankin et al., 2000; Wolff et al., 2003). Forced upwards by the large temperature gradient between the warm ocean and cold atmosphere during winter, this brine forms a slush layer on the surface of sea ice (Fig. 3.2) (Martin et al., 1996). The brine is then wicked onto frost hoar which forms at the sea ice surface due to the supersaturation of the vapour layer, resulting in the growth of highly saline crystals, hereafter denoted as frost flowers (Rankin et al., 2002).

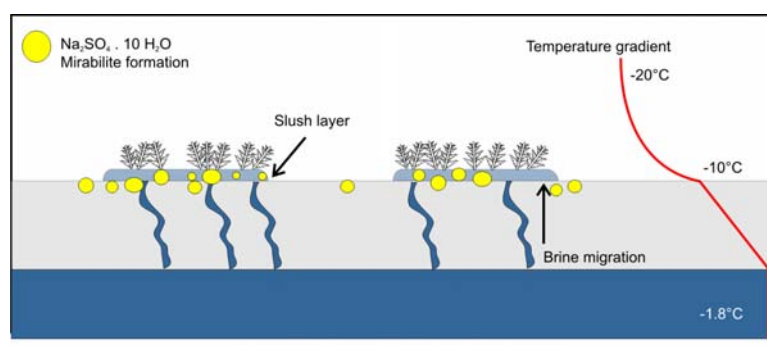


Figure 3.2 Formation of frost flowers on the sea ice surface adapted from Rankin et al. (2002).

Importantly, elemental ratios of frost flowers differ from marine values. In particular, SO_4 is depleted with respect to Na due to the precipitation of mirabilite ($\text{Na}_2\text{SO}_4 \cdot 10\text{H}_2\text{O}$) within sea ice or at the surface slush layer. The loss of sulphate and sodium into mirabilite is exponential with temperature, with half the sulphate lost at -10°C, and 90 % lost by -20°C (Rankin et al., 2002). At the normal air-ice interface temperature, almost all sulphate, and up to 13 % of sodium is lost (Rankin et al., 2002) resulting in relative depletion of sulphate, and enrichment of other trace elements with respect to Na (Rankin et al., 2002). Below -23°C other cryohydrate minerals begin precipitation, starting with halite (sodium chloride). Although this will further modify oceanic ratios, such surface temperatures are generally associated with multi-year ice where frost flower formation does not occur due to the reduced temperature gradient in thick ice (Rankin et al., 2002).

Frost flowers form abundantly around coastal Antarctica, in particular, during early winter and at sites of continual sea ice growth such as sea ice leads and polynya systems (Rankin et al., 2002). With a light, crystalline structure, frost flowers are easily transported during windy conditions and deposited independent of precipitation (dry) at coastal sites (Rankin et al., 2002). Frost flowers are identified as a significant contributor of marine derived major ions in the snow pack at a number of Antarctic sites, including Halley and Neumayer stations, Ronne Ice Shelf, South Pole and Ross Drainage region of the Siple coast. A frost flower source is associated with winter maxima of marine derived elements (Na, Cl), SO_4 depletion of snow chemistry with respect to Na and positive correlation between winter sea ice extent and Na concentrations (Kaspari et al., 2005; Minikin et al., 1998; Wagenbach et al., 1998).

Depending on the dominant source region, temporal changes of marine derived elements in snow and ice core records can indicate variable distance to open water, cyclonic activity, meridional wind strength, and sea ice extent (Fischer et al., 2004; Goodwin et al., 2004; Legrand and Mayewski, 1997; Petit et al., 1981; Petit et al., 1999; Wagenbach et al., 1998). Petit et al. (1981) attribute higher concentrations of marine derived elements during the Last Glacial Maximum to increased meridional wind strength while Fischer et al. (2007b) argue this could simply be a function of greater sea ice extent and a dominant frost flower source region of marine aerosol. Understanding of the dominant aerosol source is therefore vital. Distance to the marine aerosol source region, can be to a certain extent resolved by investigating fractionation of Cl with respect to Na. Because Cl^- bonds more easily with other ions during atmospheric transport and is therefore more rapidly precipitated out than Na^+ , Cl/Na ratio of marine aerosol decreases with distance from source region (Legrand and Mayewski, 1997).

3.2.2 Mineral dusts

Mineral dusts are the only significant source of Al, and a dominant source of Ca and a number of trace elements in Antarctic snow and ice studies (Fischer et al., 2007a; Legrand and Mayewski, 1997). Transport of mineral dusts to the snow surface is dependent on weathering of crustal sources, proximity of the source region, wind speed, wind turbulence and deposition controls. Weathering is dominated by physical processes in Antarctica due to the cold temperatures that include frost weathering,

aeolian abrasion and salt weathering (Gibson et al., 1983; Kelly and Zumberge, 1961; Pye, 1987). Chemical weathering, which occurs due to the thermodynamic instability of most minerals at surface temperatures, is relatively minimal due to the lack of water, soil and vegetation, which limits element mobility (White, 2003). However, it is noted that in the presence of melt water, which occurs at some coastal locations such as the McMurdo Dry Valleys, chemical weathering may be particularly effective due to high levels of fresh rock powder (Tranter, 2003; White, 2003). Kelly and Zumberg (1961) found chemical alteration of granodiorites at Marble Point (Victoria Land coast) is limited to Fe-oxidation only, with insignificant changes in other elements.

Entrainment of mineral dusts into the atmosphere is dependent on the size, sorting, cohesion and roughness of the source materials (Tsoar and Pye, 1987). Wind speeds required for particle entrainment range between ~ 6 to $> 16 \text{ m s}^{-1}$ for sand dunes and crustal alluvial fans respectively, with global averages for a dry, $150 \text{ }\mu\text{m}$ quartz grain ranging between 6 to 8 m s^{-1} (Clements et al., 1963). Entrainment speeds are, however, commonly lower in Antarctic due to the higher density of cold air. Ayling and McGowan (2006) report speeds of 5.5 m s^{-1} necessary for entraining and transporting dry and loose fine grained sediment in the McMurdo Dry Valleys. Depending on particle size, wind strength and wind turbulence, transport of particles occurs via sliding, rolling, bouncing (saltation) or in suspension (Fig. 3.1) (Pye, 1987). This determines how far particles are transported during sustained wind events. Mineral dust will return to the surface once the particle settling velocity exceeds the vertical component of the wind shear by either: a) reduction in wind velocity and turbulence, b) capture of particles with rough, moist or electrically charged surfaces, c) bonding of particles through chemical charge and hence settling or d) washing out of the atmosphere by precipitation (Pye, 1987).

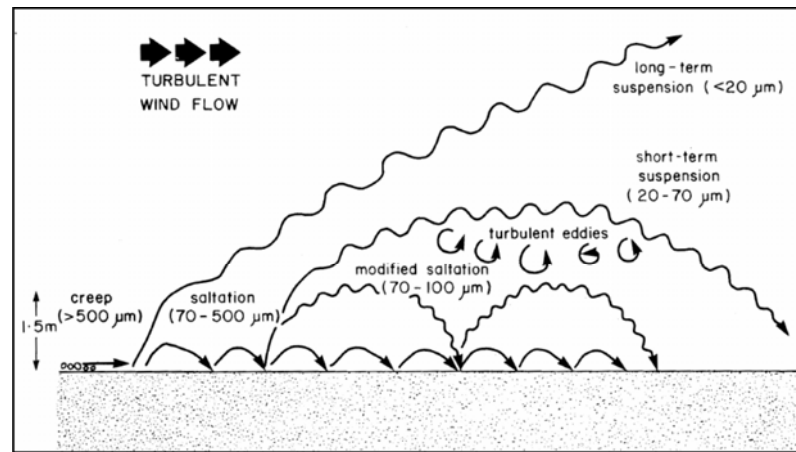


Figure 3.3 Different modes of aeolian particle transport (Pye, 1987). The size ranges transported are those for moderate wind conditions ($\sim 10 \text{ m s}^{-1}$).

While local dust sources are likely to dominate terrestrial input at coastal sites, mineral dusts transported to the interior of Antarctica are predominantly derived from global sources. Patagonia and Australia have been identified as the dominant source of dusts to the Antarctic plateau through Sr and Nd isotope analysis (Basile et al., 1997; Delmonte et al., 2004; Revel-Rolland et al., 2006; Smith et al., 2003). Global dusts can be distinguished from regional sources by the modal grain size of global dusts between 2-6 μm (Delmonte et al., 2004; Taylor and Gliozzi, 1964; Thompson and Mosley Thompson, 1981) as opposed to local dusts, which are typically $>10 \mu\text{m}$ (Atkins and Dunbar, 2009; Ayling and McGowan, 2006).

Temporal changes in mineral dust concentrations, grain size and terrestrial derived elemental chemistry have been used to infer changes in terrestrial aerosol source region aridity and atmospheric circulation. Over glacial-interglacial periods, temperature ($\delta^{18}\text{O}$ and δD) is negatively correlated to dust flux, indicating greater exposure of source regions when sea level was reduced by ca. 120 m, increased aridity and/or increased wind strength (Lambert et al., 2008; Petit et al., 1999). In particular, the correlation between global terrestrial flux to Antarctica is strong during glacial periods but decoupled during inter-glacials, and has been used to infer a greater coupling between high and low latitude climates during glacials due to a northward shift of meridional atmospheric circulation (Lambert et al., 2008).

3.2.3 Additional sources of elemental chemistry

Other sources of elemental chemistry measured in snow and ice core records involve biological, volcanic, high atmospheric and anthropogenic processes. SO_4 is predominantly derived from marine aerosol, but is also produced through atmospheric oxidation of volcanic or anthropogenic emissions of SO_2 (Kaspari et al., 2005; Legrand and Mayewski, 1997; Minikin et al., 1998). Furthermore, photo-oxidation of dimethylsulphide (DMS), a chemical produced from primary productivity at the ocean surface, produces both SO_4 and methanesulphonate (MS) (Goktas et al., 2002). Unlike SO_4 , MS has no other significant source and shows strong potential as an indicator of biological productivity and inferred sea ice extent, in particular, within ice core records from the coastal Ross Sea region (Curran et al., 2003; Goktas et al., 2002; Rhodes et al., 2009; Wolff et al., 2006).

Nitrate (NO_3) is another species commonly measured in glaciochemical records, reflective of both intrusion of stratospheric air masses and changes in soil aridity and land use (Legrand and Mayewski, 1997; Mulvaney et al., 1998; Wagenbach et al., 1998). However, understanding of its behaviour in snow and ice core records is limited. Summer annual peaks are controversial due to post depositional alteration of the signal, with up to 40 % loss of nitrate reported at sites of low accumulation (Goktas et al., 2002). Nitrate deposits are also extensive within the McMurdo Dry Valley soils, originating from stratospheric input (Michalski et al., 2005; Witherow et al., 2006) and therefore may be redistributed to glaciochemical records within the McMurdo Dry Valleys and hence primarily indicative of atmospheric circulation.

3.2.4 Trace element chemistry

Most elements present in Antarctic snow and ice core records are present in trace concentrations, in particular, elements derived from mineral dusts and anthropogenic and volcanic emissions. The first Antarctic trace element studies focussed on determining natural background levels of anthropogenic elements on the Antarctic plateau (Boutron et al., 1972; Boutron and Lorius, 1979). Further studies have documented the rise in anthropogenic Pb since 1880, and other elements including Cr, Cu, Ag, Bi and U since the early 20th Century (Vallelonga et al., 2004). All studies observed large changes in heavy metals over various temporal scales, seasonal to

centennial (Boutron and Lorius, 1979; Hur et al., 2007; Planchon et al., 2002a; Planchon et al., 2002b; Vallelonga et al., 2004).

Like major elements, the main source of trace element chemistry in snow and ice core records have been identified as marine, terrestrial, anthropogenic and volcanic aerosols. There is, however, poor agreement as to which elements are sourced from where and the main controls on transport and deposition. Possible source regions are attributed through comparison of elemental ratios in samples to oceanic and upper continental crust values and statistical techniques. However, due to the large natural variation of these sources, such calculations can only give an indication of the order of magnitude of source contributions (Barbante et al., 1997; Duce et al., 1975). Seasonality of chemistry has also been assessed which may indicate dominant source regions and transport processes, although results are variable at different sites and only a limited number of studies record sub-seasonal resolution. For example, Hur et al. (2007) sampled a 2.3 m snow pit for trace element chemistry from the Lambert Glacier in East Antarctica. Although they attribute As to a anthropogenic source and Bi to a predominantly volcanic emissions source, high correlation between the two elements is used to infer a similar atmospheric pathway. Seasonal cycles of marine derived U and V are not well defined and are attributed to the variable intrusion of marine air masses. Source regions of trace element chemistry in Antarctic snow identified by previous studies are summarized in Table 3.1.

	Planchon et al. (2002)	Vallelonga et al. (2004)	Gabrielli et al. (2005)	Hur et al. (2007)
Site	Coats Land	Law Dome	Vostok Station	Lambert Glacier
Altitude (m)	1420	1390	3488	1850
Distance from coast (~km)	200	80	1,300	160
Crustal	V, Ba, U, Cr, Mn, Co, Cu, Zn	Mn, U, V	V, Mn, Rb, Ba, U, Li, Cr, Co, Sr	V, Mn, Fe, Ba, U (20%)
Marine	minor V, Ba	Ba, Ca, Sr	Sr (40-20%)	U (40%) + minor Ba
Marine EF	V, Zn, Cd, U			V, As (13 %)
Volcanic	Bi + minor Cd, Cr	Bi, Cd + minor Co, Cu, Pb, Zn	As, Bi	V, Mn, Cd
Anthropogenic	minor Cr, Cu, Zn, Ag, Pb, Bi, U			Cu, Pb, As
Biogenic	Elements are difficult to constrain but are likely through the production of methylated metal compounds by polar marine bacteria (Heuman, 1993)			

Table 3.1 Comparison of trace element source regions identified by previous studies of Antarctic snow samples. Minor source contributions vary between 5-10%. Marine aerosol contributions are calculated both with and without the use of enrichment factors (EF) which account for elemental concentration processes at the ocean surface.

Although ion chromatography is commonly applied to measure major element chemistry (ppm to ppb concentration levels) of Antarctic snow and ice core records (Bertler et al., 2004b; Kaspari et al., 2005; Legrand and Mayewski, 1997), study of trace element concentrations (ppb to ppq) requires significantly lower detection limits and avoidance of sample contamination. ICP-MS has been chosen for this study due to its multi-element capabilities, low sample consumption and the avoidance of any pre-concentration which may introduce potential contamination (Barbante et al., 1997). The technique was first used on Antarctic and Greenland snow samples by Barbante et al. (1997) for measurements of Co, Cu, Zn, Mo, Pd, Ag, Cd, Sb, Pt, Pb, Bi, U. Detection limits were shown to be less than 1 ppt for all elements and reproducibility of Greenland snow samples of 8-25 %. Although Gabrielle et al. (Gabrielli et al., 2005) argued that inductively coupled plasma sector field mass spectrometer is required for trace element analysis of Antarctic snow and ice samples, Grotti et al. (2008) demonstrated that with a hydrogen flushed collision cell, polyatomic interferences which commonly occur during ICP-MS analysis are low enough to allow high precision trace element measurements.

Chapter Four: Dating of the EPG snow pit record

Relating glaciochemical records to climatic processes is dependent on robust dating techniques. This is particularly important when relating inter-seasonal and inter-annual variability to measured meteorological changes, a primary objective of this study. This chapter describes the basis and constraints of the EPG dating model. Accumulation rates determined by this model are compared to previous snow and ice core records along the Victoria Land coast. Full methodology, results and discussion of EPG snow pit chemistry used for dating are presented in Chapter 5 and Appendix 1.

4.1.0 Methods

The EPG snow pit profile covers the period winter 1994 to sampling in November 2007. Dating was constrained by density, stratigraphy and chemistry of the EPG snow pit profile in addition to automatic weather station measurements of EPG accumulation since 2004 (Fig. 4.1). Identified summer and winter horizons have been dated as the 1st of January and July respectively, with linear correlation between. This dating model is attributed ± 6 months error as exact timing of precipitation is unknown.

Low density and coarse grained snow layers were used to identify hoar horizons. Coupled with wind slabs of high density and fine grained crystals, changes in EPG snow stratigraphy were identified as summer/autumn (hoar) and winter (wind crust) benchmarks respectively (Alley, 1988; Alley et al., 1990; Kreutz et al., 1999). Ice layers were identified within sections of hoar, indicative of minor surface melt during summer as previously noted within nearby McMurdo Dry Valley snow records (Ayling and McGowan, 2006). Because hoar horizons may form at either the snow pack surface or up to 10 cm below the surface by sublimation during summer, slight offsets between the EPG snow stratigraphy and seasonal chemical markers are not unexpected (Alley, 1988; Kreutz et al., 1999).

EPG snow chemistry was used to confirm seasonal stratigraphy benchmarks. Chemical parameters used for dating included stable isotope ratios ($\delta^{18}\text{O}$ and the d excess) and concentrations of methanesulphonate (MS) and Na. Temperatures measured at EPG

vary on average between -7°C in summer (December to February) and -26°C in winter (June to August) as measured between 2004 and 2008. Although the dependence of $\delta^{18}\text{O}$ on temperature in Antarctic snow is well established (Dansgaard, 1954; Sharp, 2007), preservation of a seasonal signal within the snow pack may not occur due to post depositional diffusion when accumulation rates are low (Johnsen et al., 2000; Johnsen, 1977; Schlosser, 2002b). Additionally, precipitation along the Victoria Land Coast occurs episodically and primarily during summer/autumn (Carrasco and Bromwich, 1994; Carrasco et al., 2003; Monaghan et al., 2005; Mullen and Sinclair, 1990; Sinclair, 2009; Turner, 2004). This will bias stable isotope variation towards periods of precipitation. However, $\delta^{18}\text{O}$ variation of the EPG snow profile is in general agreement with snow stratigraphy changes. Although some hoar horizons are associated with subdued or absent $\delta^{18}\text{O}$ maxima (e.g. 24-35 cm depth), variation of the d excess parameter supports a seasonal change in air mass source region (Froehlich et al., 2002; Sharp, 2007).

Seasonal changes in MS and Na concentrations within the EPG snow pit profile support the dating model established by $\delta^{18}\text{O}$ and stratigraphy. The dependence of aerosol derived chemistry on seasonal changes in source region and transport efficiency is well established for dating. For example, Goktas et al. (2002) used concurrent decreases in Na peaks and increases in non-sea-salt(nss) SO_4^{2-} to indicate spring events for snow pack from coastal Dronning Maud Land. Na maxima were highest during winter due to a greater sea ice surface source region and increased wind strength. Non-sea-salt SO_4^{2-} maximum occurred during summer due to increased primary productivity within the Southern Ocean. Rhodes et al (2009) demonstrated the reliability of biologically produced MS as an indicator of summer events in snow pack from Mount Erebus, coastal Ross Sea region. Na concentrations within the EPG snow pit profile consistently occur concurrent with $\delta^{18}\text{O}$ minima indicating winter events. Summer peaks in MS are less well defined, although post depositional migration of MS towards high concentrations of other chemical species may account for this (Curran et al., 2001). Significantly, a strong MS peak is present during summer 2004 from the current dating model, but MS concentrations are subdued for the entire period winter 2000 to 2003. The period of low MS is concurrent with extensive sea ice cover within the Ross Sea, which reduced primary productivity (Rhodes et al., 2009).

Finally, annual snow accumulation measured by the EPG automatic weather station (AWS) was compared to accumulation within the EPG snow pit. AWS measurements have been made since 2004, with resetting of the accumulation sensor annually. Total accumulation measured each year was converted to water equivalent depth using the average density of the top 14cm of EPG snow pit profile. This density is considered representative of approximate compaction within a single year of accumulation. When compared to water equivalent depths of the EPG snow pit profile, the AWS time horizons are in approximate agreement with the proposed dating model. In particular, accumulation was minimal during 2007 (5 g cm^{-2}), in agreement with accumulation determined from the dated EPG snow pit profile (3 g cm^{-2}). Although snow accumulation measured by the AWS during 2006 (19 g cm^{-2}) is double that predicted by the EPG snow pit profile (10 g cm^{-2}), this is not unexpected due to natural variability of accumulation at the site such as sastrugi features observed on 10's cm scales, and error in determined compaction of the records. Importantly, both records indicate 3 years of accumulation within the top $23\text{-}30 \text{ g cm}^{-2}$ of accumulation.

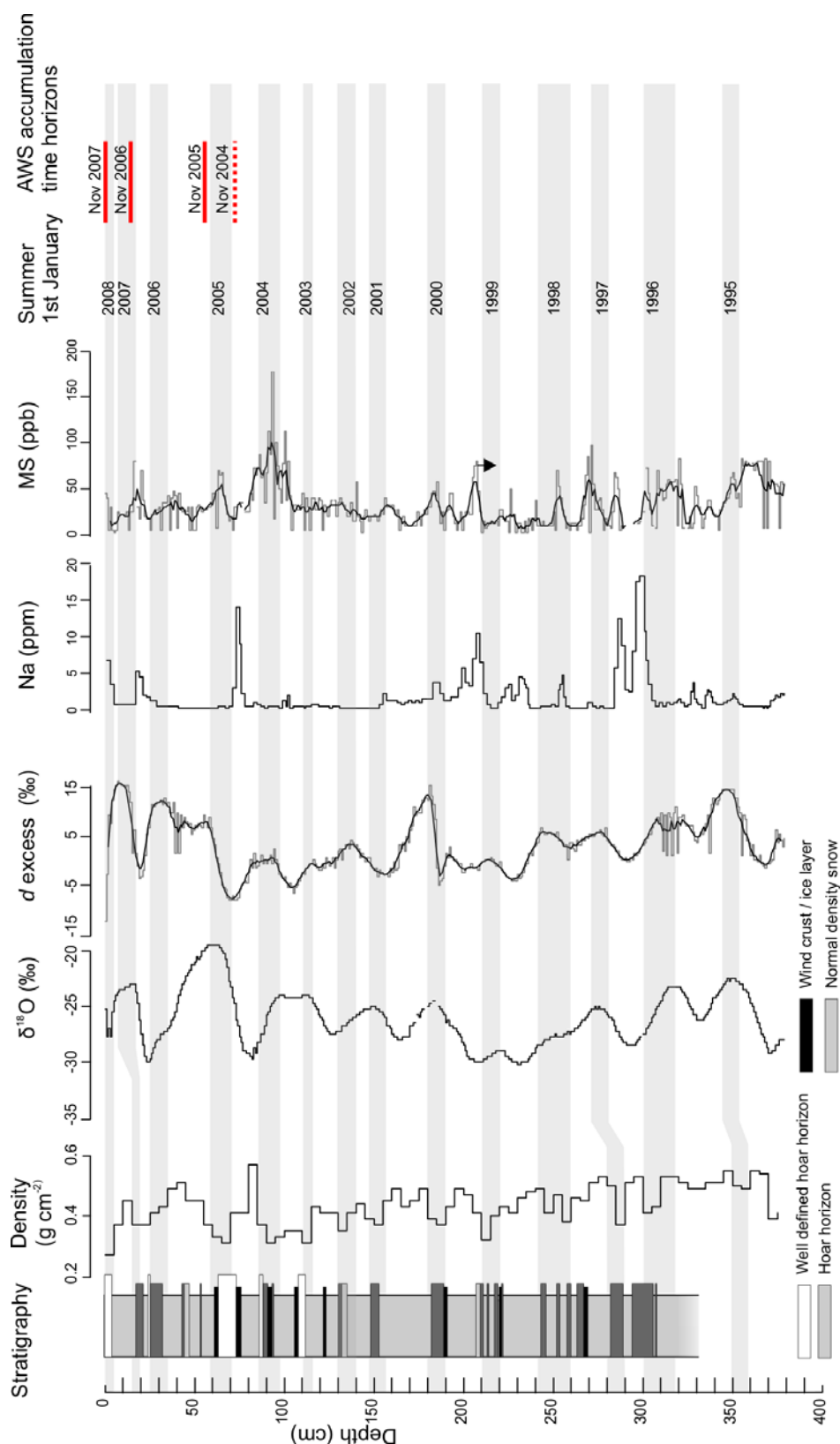


Figure 4.1 Physical and chemical properties of the EPG snow pit profile used for dating. Summer horizons (dashed lines) were identified using horizons of low density that were concurrent with stable isotope variation (typically $\delta^{18}\text{O}$ maxima) and MS maxima. Winter horizons were identified using chemistry maxima (e.g. Na shown) and stable isotope variation. Expected post-depositional migration of MS towards high chemistry concentration is shown with an arrow. Time horizons determined from AWS accumulation rates at EPG are also shown and approximate accumulation rates inferred from the dating model.

4.2.0 Comparison of EPG accumulation with previous Victoria Land snow pit records

An average accumulation rate of $12 \text{ g cm}^{-2} \text{ yr}^{-1}$ is determined from the dated EPG snow pit record. This is high in comparison to nearby McMurdo Dry Valley snow and ice core records, but is consistent with average accumulation of $11.7 \text{ cm}^{-2} \text{ yr}^{-1}$ measured by the EPG AWS between 2004 and 2008. In particular, Wilson Piedmont Glacier (WPG) is a low elevation, coastal glacier, located 50 km south of EPG but has accumulation rates that are 25 % of EPG (Table 4.1). Dating of WPG is based primarily on high frequency peaks in Na and MS which are inferred as a seasonal representation of summer open water conditions, and correlation to Victoria Lower Glacier (VLG) snow pit (Bertler, 2003). VLG dating has been independently constrained using radiogenic isotopes (β -activity age) with summer 1964/65 at 4.10 m depth (Bertler, 2003). Counting of high frequency Na and MS peaks produces a similar age ($\pm 1 \text{ yr}$) and therefore provides justification of its use at WPG (Bertler, 2003).

	Latitude (decimal)	Elevation (m)	Distance to coast (km)	Accumulation rate ($\text{g cm}^{-2} \text{ yr}^{-1}$)	Reference
Mount Erebus Saddle	-77.51	1600	10.8	11	Rhodes et al. (2009)
Victoria Lower Glacier	-77.32	624	22.5	3.3	Bertler et al. (2003)
Baldwin Valley Glacier	-77.32	1100	30	2.7	Bertler et al. (2003)
Wilson Piedmont Glacier	-77.27	50	7.5	4.5	Bertler et al. (2003)
McCarthy Ridge	-74.53	700	40	27	Piccardi et al. (1994)
Styx Glacier	-73.87	1700	50	16	Piccardi et al. (1994)
Whitehall Glacier	-72.91	500	30	71	Appendix 3
Evans Piedmont Glacier	-76.72	310	10	12	This study

Table 4.1 Comparison of accumulation rates inferred from snow pit studies along the Victoria Land coast, Antarctica. Accumulation rates measured from sites within the McMurdo Dry Valleys are italicised.

If the technique of using high frequency variation of MS or Na to represent summers instead of lower frequency, sustained MS and Na maxima is applied to EPG, it is possible to date the EPG snow profile back to 1968 with an average accumulation rate of $5 \text{ g cm}^{-2} \text{ yr}^{-1}$. Although comparable to WPG, this is not reconcilable with instrumental accumulation rates measured at EPG and chemical comparison of previous EPG snow pit records. Furthermore, EPG accumulation of $12 \text{ g cm}^{-2} \text{ yr}^{-1}$ is not anomalous in comparison to other snow pit measurements along the Victoria Land coast outside the

McMurdo Dry Valley region (Table 4.1). We therefore conclude the first dating model is more likely to capture the annual characteristics of the site, and that EPG is located just north to the boundary of the unique climate conditions which prevail over the McMurdo Dry Valleys to reduce accumulation rates and maintain an ice free zone.

Chapter Five: Measurement and interpretation of EPG stable isotope, major and trace element chemistry

This chapter is a draft manuscript for submission to Earth and Science Planetary Letters. Due to content constraints, additional description and discussion of methodology are presented in Appendix 1.

Source region and transport controls on major and trace element chemistry of snow pack from the southern Victoria Land coast, Antarctica.

Abstract

This study presents a sub-seasonally resolved, decade long, record of snow pack chemistry from Evans Piedmont Glacier, southern McMurdo Sound, Ross Sea, Antarctica. This is a region of high snow accumulation and variable aerosol sources, which are sensitive to processes in the atmospheric boundary layer, driven by interactions between the Southern Ocean and Antarctic ice sheet, that in turn are sensitive to global climate phenomena including the El Niño Southern Oscillation (ENSO). Snow chemistry measurements were made by inductively coupled plasma mass spectrometry at a resolution of ca. 20 analyses per yr. Samples were analysed for Na, Mg, Al, Fe, Mn and Ba using a hydrogen flushed collision cell to reduce interferences, and Ti, V, Cr, Ni, Cu, Zn, As, Rb, Sr, Y, Zr, Cd, Sb, Cs, Ba, La, Ce, Pb, Bi, Th and U in non-collision cell mode. Analytical precision is typically 5 to 10 % 2 rsd for all elements, which is typically two orders of magnitude less than the natural variability between samples (e.g. Na = 10 to 18031 ppb and Al = 5 to 3856 ppb). However, reproducibility of measurements made on elements largely derived from mineral dusts is affected by the presence of particulate material that is not fully dissolved during 12 hr acidification of samples. Despite this, the range of sample concentrations (e.g. Zr = 3.0 to 5630 ppb) is still orders of magnitude higher than sample reproducibility. Temporal changes in elemental chemistry are related to wind conditions measured at proximal Cape Ross (~10 km distance from EPG). Winter maxima of all elemental concentrations are consistent with increased wind strength and transport of aerosol from the south. Annual maximum chemistry concentrations of terrestrial derived elements (e.g. Zr) are significantly correlated to maximum annual wind speed measured at Cape Ross ($r^2 =$

0.68, $p < 0.01$). Lower correlation of marine derived chemistry (e.g. Na) and maximum wind strength reflects additional controls of source region and other meteorological parameters such as storm duration on marine derived chemistry. In contrast to elemental concentrations, elemental ratios are less sensitive to extreme wind conditions. Rather elemental ratios provide a more robust signature of changes in mean atmospheric circulation related to delivery of aerosol from different source regions and via different transport fractionation processes. Al/Na is controlled by variable delivery of terrestrial (Al) and marine (Na) aerosol to EPG, although the longer term trend is driven primarily by changes in Na. Al/Na is significantly higher between winter 2000 and summer 2006/07 with a mean value of $\text{Al/Na} = 0.15$ compared to $\text{Al/Na} = 0.02$ prior to 2000. Although sea ice extent was highly variable over this time period, there is no clear relationship between Al/Na and sea ice. Rather, Al/Na is significantly correlated to mean summer wind speed measured at Cape Ross ($r^2 = -0.51$, $p < 0.01$). This demonstrates the sensitivity of Al/Na to changes in the average transport of marine aerosol to EPG during summer, when an open ocean source is most proximal. The shift in Al/Na is also concurrent with a shift in the relationship between $\delta^{18}\text{O}$ and d excess, indicative of changing precipitation source region to EPG. We suggest these changes in EPG chemistry are concurrent with shifts in the mean state of the ENSO. Increased summer wind strength from, resulting in a low Al/Na ratio at EPG during negative ENSO (El Niño) period is consistent with previous models of ENSO influence on atmospheric circulation of the Ross Sea region. This study demonstrates the ability of elemental chemistry to reconstruct atmospheric circulation changes within the southern McMurdo Sound and hence the potential to extend these observations over longer time periods using ice core records.

5.1.0 Introduction

Major and trace element chemistry of snow and ice core records provide important proxy information about past environmental conditions (Curran et al., 2003; Legrand and Mayewski, 1997; Mayewski et al., 1995; Petit et al., 1999; Planchon et al., 2002a). In particular, coastal Antarctic sites from the Ross Sea region are characterised by high snow accumulation rates with records of sub-annual resolution (Connolley and Cattle, 1994). These records are sensitive to changes in tropospheric climate, and marine processes such as primary productivity (Bertler et al., 2004a; Curran et al., 2003; Patterson et al., 2005; Rhodes et al., 2009). High resolution proxy records are necessary to determine the influence of sub-decadal climate phenomena such as the El Nino Southern Oscillation (ENSO) at high latitudes where instrumental records are spatially and temporally sparse (Turner et al., 2005).

Marine derived, soluble chemistry dominates the ionic budget at coastal sites recording changes in marine source areas and transport efficiency (Legrand and Mayewski, 1997). High precision measurements of elements present in trace concentrations provide additional information about terrestrial and anthropogenic derived inputs (Hur et al., 2007; Vallelonga et al., 2004). Full utilization of major and trace element glaciochemical records still requires further understanding of source regions, transport and deposition processes. To date, the only sub-seasonally resolved Antarctic snow record with an extensive trace element profile is from the Lambert Glacier basin, East Antarctica (Hur et al., 2007). This record covers the four-year period between spring 1998 and summer 2002. Measurements of Al, V, Mn, Fe, Cu, As, Cd, Ba, Pb, Bi and U show between one and two orders of magnitude temporal variation in concentrations. Another comparable record extends back to the year 1920 from Coats Land, Weddell Sea coast, but was only sampled discretely for sub-annual resolution (Planchon et al., 2002b). Other high resolution studies have analysed for a limited number of elements and are focused typically on anthropogenic elements (Barbante et al., 1997; Wolff et al., 1999), or are too short for comprehensive assessment of seasonal changes in snow chemistry (Suttie and Wolff, 1992; Wolff and Suttie, 1994).

This study presents the first measurements of a comprehensive array of trace elements in snow pack from coastal Victoria Land (Fig. 5.1). Oxygen isotope stratigraphy and other chemical markers demonstrate the record covers the period between winter 1994 to summer 2007/08. The objective of this study is to improve our understanding of the controls on snow trace element chemistry in snow, specifically, the development of chemistry proxies for atmospheric circulation changes at coastal Antarctic sites within the Ross Sea region. This is required for the reconstruction of long term changes in sub-decadal scale climate variability. To this end, we have developed a reliable technique for rapid analysis of a wide range of major and trace elements by inductively coupled plasma mass spectrometry (ICP-MS). The specific aims of this study are to:

- 1) Model the influence of marine, terrestrial, anthropogenic and volcanic emission sources on snow chemistry, including the effects of heterogeneity within terrestrial source regions and fractionation processes during aerosol transport.
- 2) Relate seasonal and inter-annual trends in elemental chemistry concentrations and elemental ratios to atmospheric circulation changes from the on-site and regional meteorological records.

5.2.0 Study site

5.2.1 Site location and possible aerosol source regions

Evans Piedmont Glacier (76° 43.53' S, 162° 35.29 E) is a locally accumulating ice mass at 310 m elevation, selected for high annual accumulation rates ($12 \text{ g cm}^{-2} \text{ yr}^{-1}$) and strongly contrasting local aerosol source regions. Regional aerosol sources include the Ross Sea, extensive rock and soil exposures of the Transantarctic Mountains (TAM) and McMurdo Volcanic Group, emissions from the active Mt. Erebus volcano and anthropogenic activity at Ross Island, Marble Point and Terra Nova Bay (Fig. 5.1). Elemental contributions from distally derived terrestrial aerosol of Southern Hemisphere continents are considered minimal in comparison to locally sourced material (Ayling, 2001).

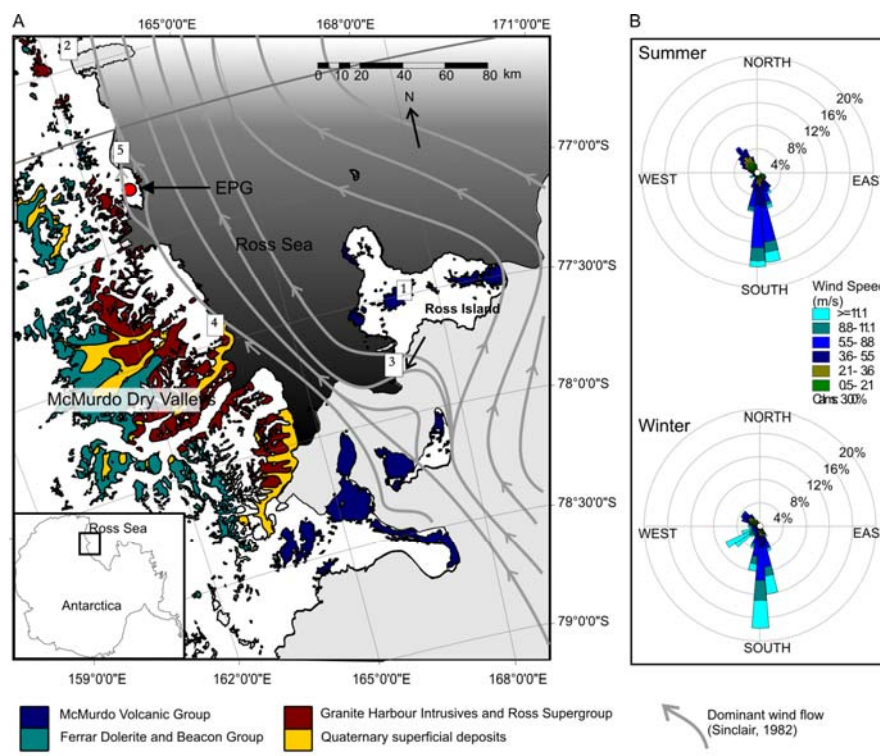


Figure 5.1 a) Location of Evans Piedmont Glacier (EPG) within the southern McMurdo Sound, Antarctica. Important aerosol sources include the Ross Sea, mineral dusts from the Transantarctic Mountains, McMurdo Dry Valleys and McMurdo Volcanic Group, volcanic emissions from Mt. Erebus (1) and Mt Melbourne (~100 km N of site 2), and anthropogenic contributions from Hut Point Peninsula (3), Marble Point (4), and Terra Nova Bay (~100 km N of site 2). Regional geology is summarised from Craddock et al. (1969) and dominant wind flow from Sinclair (1982). Automatic weather station meteorological records discussed in the text are located at Cape Ross (5), Marble Point (4) and Scott Base (3). **b)** Cape Ross AWS (Arelis 375) summer and winter wind speed and direction. Measurements are averaged over the same time period sampled by the EPG snow pit profile, 1998 to 2008. Data is accredited to <http://www.climantartide.it>

5.2.2 Meteorology

McMurdo Sound regional climate is controlled primarily by continental katabatic outflow and mesoscale ($10\,000\text{ km}^2$) cyclonic activity (Bromwich et al., 1993). Katabatic outflow originates predominantly from the Siple coast, Byrd Glacier region and Terra Nova Bay (Bromwich et al., 1993; Parish and Bromwich, 1987) and is strongest during winter due to significant cooling over the Antarctic plateau (Parish and Cassano, 2003). Interaction of katabatic winds with warmer maritime air provide conditions for mesoscale cyclogenesis when associated with a weak surface trough, which is particularly frequent within the McMurdo Sound region ($5\text{--}6$ mesoscale vortices yr^{-1}) (Carrasco et al., 2003). Katabatic and cyclonic flow is forced parallel to the Transantarctic Mountains, with the development of gale-force winds at McMurdo Station and Scott Base when

mesoscale cyclones form to the east of Ross Island (Bromwich et al., 1993; Carrasco and Bromwich, 1994; Sinclair, 1982).

We relate EPG chemistry to changes in changes in meteorological conditions measured by automatic weather stations (AWS) at EPG, Cape Ross (~10 km distance), Scott Base and Marble Point. Temperature, humidity and snow accumulation were measured at EPG between November 2004 and November 2008, excluding the period June 1st to November 1st 2005 when the AWS experienced storm damage. Hourly temperature, wind direction and speed measurements from Cape Ross AWS (Arelis 735, WMO no. 89666) are available from 1990 to the present from the Italian Antarctic Research Program (<http://www.climantartide.it>). The regional extent of wind events identified in the Cape Ross record is evaluated with respect to daily AWS data from Scott Base (station number 12740) and hourly measurements from Latitudinal Gradient Program station at Marble Point (ANT004). Data is sourced from the New Zealand national climate database (<http://www.cliflo.niwa.co.nz/>) and the Soil Climate Analysis Network (<http://www.wcc.nrcs.usda.gov>) respectively.

Wind measured at Cape Ross is dominated by flow from three directions, the SSE (160°-190°), SW (220°-250°) and NW (290-320°) (Fig. 5.1) with average frequencies over the 18 yr record of 47 %, 13 % and 15 % respectively. Strong winds ($> 10 \text{ m s}^{-1}$) occur consistently from the SW and SSE only. Winds $> 30 \text{ ms}^{-1}$ occur from the SW only. Relative humidity is highest when flow is from the S and NW (57 % and 48 % respectively) and lowest from the SW (40 %). We therefore summarise local wind directions as a) direct marine airflow from the NW, b) combined mesoscale marine cyclonic activity (high relative humidity) and katabatic outflow from the SSE and, c) extreme katabatic wind events from the either the East Antarctic or West Antarctic ice sheets (low humidity) that are strong enough to overcome the topographic barrier of EPG.

A primary research objective of the NZ ITASE program is to determine the influence of the El Niño Southern Oscillation (ENSO) on the Ross Sea climate by extending meteorological records beyond the instrumental period (~1950s) using glaciochemistry (Bertler et al., 2004a and 2006). Therefore, EPG snow pit chemistry is also related to the

southern oscillation index (SOI), a measure of ENSO strength and polarity. SOI values have been sourced from the NOAA Earth Systems Research Laboratory (<http://www.cdc.noaa.gov/data/climateindices/>).

5.3.0 Methods

5.3.1 *Snow pit sampling*

The 4 m EPG snow pit profile was sampled in November 2007 at 1 cm resolution. Sampling equipment, sample bottles and ICP-MS vials were cleaned using a method modified from Osterberg et al. (2006). Vials were triple rinsed in ultra-clean water ($>18.2\text{ M}\Omega$), soaked in 5 % analytical reagent (AR) grade HNO_3 for a minimum of two weeks, triple rinsed in ultra-clean water, soaked in ultra-clean water for two weeks, triple rinsed in ultra-clean water, shaken dry and capped immediately under class 100 HEPA conditions. IC vials were triple rinsed, soaked for two weeks and triple rinsed in ultra-clean water only, dried and capped in a class 100 HEPA clean-bench. Tyvek clean suits, face-masks and powder free polyethylene gloves were used throughout to prevent contamination.

After initial excavation, the sampling surface was cleaned back 1 m using a dedicated pre-cleaned stainless steel spade and then a further 10 cm with a ceramic knife. Samples were obtained at 1 cm resolution with an additional ceramic knife into a high-density polyethylene (HDPE) tray, directly transferred into 60 mL acid cleaned Nalgene HDPE bottles and stored frozen. Aliquots of samples were taken for ICP-MS, ion chromatography (IC) and stable isotope analyses under class 100 high efficiency particulate clean air (HEPA) conditions at GNS Science.

5.3.2 *Stable isotopes*

Oxygen ($\delta^{18}\text{O}$) and hydrogen (δD) isotope ratios were measured at the National Isotope Centre, GNS Science, by classical equilibration techniques using a GVI AquaPrep system attached to dual inlet GVI mass spectrometer. 400 μL of sample was equilibrated with 300 μL of CO_2 for 24 hr at 25.5°C. CO_2 was extracted and directly transferred for mass spectrometry analysis. Hydrogen isotope analyses (δD) were conducted by direct reduction of 100 μL of sample using a PyrOH reaction column, and measurement on

the same dual inlet mass spectrometer system. All results are reported with respect to VSMOW, normalised to internal standards INS 11, INS9 and MM1 with reported $\delta^{18}\text{O}$ values of -0.4 ‰, -17.4 ‰, -29.4 ‰, and δD values of -4.6 ‰, -131 ‰ and -241 ‰ respectively. Approximately one in every ten samples were run in duplicate with analytical precisions < 0.1 ‰ for $\delta^{18}\text{O}$ and < 1.0 ‰ for δD . The second order stable isotope parameter deuterium excess is calculated from oxygen and hydrogen isotope measurements where $d = \delta\text{D} - 8 * \delta^{18}\text{O}$ (Dansgaard, 1954). Analytical uncertainty (u) is estimated as $u(d) = \sqrt{(u\delta^2\text{H})^2 + 8 * (u\delta^{18}\text{O})^2} \approx 1.03$ ‰.

5.3.3 Ion chromatography

EPG snow samples were analysed for major ions (Ca^+ , Cl^- , K^+ , Mg^+ , Na^+ , SO_4^{2-}) by ion chromatography (IC) at the Chromatography/Glaciochemistry Laboratory, University of Maine. Un-acidified samples were measured on two Dionex ion chromatographs with chemical suppression and conductivity detectors attached to a Gilson Liquid Handler auto-sampler. This allows simultaneous anion and cation analysis. Anions were measured using an AS-18 column, 400 μL sample loop, and a Dionex Reagent Free Controller producing a KOH eluent concentration of 35 mM. Cations were measured using a CS-12A column and 500 μL loop with 25 mM methanesulphonic acid eluent. Calibration curves bracket the expected concentration range with correlation coefficients of >0.99 .

5.3.4 Inductively coupled plasma mass spectrometry (ICP-MS)

The major and trace element concentrations of EPG snow were measured using an Agilent 7500cs series ICP-MS at Victoria University of Wellington. A collision cell flushed with H_2 was used for analysis of Na, Mg, Al, Ca, Mn, Fe and Ba, reducing interferences from the formation of oxides and other polyatomic ions and, in particular, $^{40}\text{Ar}^{16}\text{O}^+$ on ^{56}Fe . Ti, V, Cr, Ni, Cu, Zn, As, Rb, Sr, Y, Zr, Sb, Cs, Ba, La, Ce, Pb, Bi, Th, U were analysed without the collision cell to obtain greater sensitivity. Oxide interferences were monitored using a 1 ppb Ce standard with the mass ratio $^{156}\text{CeO}^+ / ^{140}\text{Ce}^+$ always < 2 %. These two analytical approaches are hereafter referred to as ‘collision’ and ‘non-collision’ modes, respectively. Instrumental conditions for each are summarized in Table 5.1.

Snow samples were kept frozen until 12 hr before analysis and then acidified to 1 % HNO₃ using high purity (SeaStar) acid. Samples were transferred to the ICP-MS via a ASX-520 micro-volume autosampler and introduction kit with PFA Teflon nebuliser and quartz spray chamber maintained at 2°C to reduce the water content of aerosols entering the plasma (Hutton and Eaton, 1987). Analyte flow was maintained under self-aspiration to reduce contamination from Tygon tubing that is required for peristaltic pumping. On completion of collision cell analysis, the remaining sample was refrozen until later non-collision cell analysis. This was done to inhibit changes in sample chemistry from leaching of elements from vials and further dissolution of particulate material within the sample.

	a) Major and minor	b) Trace
Plasma conditions		
Forward power	1450 W	1500 W
RF matching	1.75 V	1.75 V
Carrier gas	0.7 L/min	1.11 L/min
Makeup gas	0.35 L/min	0 L/min
Nebulizer pump	Self aspiration	Self aspiration
Spray chamber temperature	2°C	2°C
Reaction cell	ON	OFF
H ₂ gas	3.3 mL/min	
Ion lens settings	Optimised to obtain maximal signal intensity and stability	Optimised to obtain maximal signal intensity and stability
Torch position	Optimised to obtain maximal signal intensity	Optimised to obtain maximal signal intensity
Sample		
Isotopes measured	²³ Na, ²⁴ Mg, ²⁷ Al, ⁴⁴ Ca, ⁵⁵ Mn, ⁵⁶ Fe, ¹³⁸ Ba	⁴⁷ Ti, ⁵¹ V, ⁵³ Cr, ⁶⁰ Ni, ⁶³ Cu, ⁶⁶ Zn, ⁷⁵ As, ⁸⁵ Rb, ⁸⁸ Sr, ⁸⁹ Y, ⁹⁰ Zr, ¹¹¹ Cd, ¹²¹ Sb, ¹³³ Cs, ¹³⁸ Ba, ¹³⁹ La, ¹⁴⁰ Ce, ²⁰⁸ Pb, ²⁰⁹ Bi, ²³² Th, ²³⁸ U
Uptake time	60 s	70 s
Stabilisation time	30 s	70 s
Washing time between samples	10 s H ₂ O, 60 s HNO ₃ (1), 60 s HNO ₃ (2), total 130 s	20 s H ₂ O, 180 s HNO ₃ (1), 150 s HNO ₃ (2), total 350 s
Integration time	0.15 s	0.10 s
No. of scan passes	60	30
P/A factors determined	²³ Na, ²⁷ Al, ⁴⁴ Ca, ⁵⁵ Mn, ⁵⁶ Fe	⁴⁷ Ti, ⁶³ Cu, ⁸⁸ Sr, ⁸⁹ Y, ⁹⁰ Zr, ¹³³ Cs, ¹³⁹ La, ¹⁴⁰ Ce

Table 5.1 Typical instrumental ICP-MS running conditions and measurement parameters for **a)** collision cell and **b)** non-collision cell analyses of elemental chemistry in EPG snow samples.

Initial investigation of calibration standards showed a linear relationship between elemental concentration and ICP-MS signal intensity. Therefore, a single calibration standard was analysed for each analysis mode with elemental concentrations of the standard approximating mean values expected in EPG snow samples. Dilutions of calibration standards and the external standard, the Ottawa riverine standard SLRS-4 (National Research Council Canada (CRNC)) were prepared daily. Detection limits were calculated as 3σ procedural blanks. Due to the large range of concentrations in the snow samples, pulse/analogue factors for Mg, Al, Ca, Mn and Fe during collision cell analysis and Ti, Cu, Sr, Zr, Cs, La and Ce during non-collision cell analysis were measured every four runs to calibrate the ICP-MS detector between pulse and analogue modes. Accuracy and long-term reproducibility of measurements were verified by repeated measurement of the external standard SLRS-4. This was measured approximately every 30 samples at 1:100 dilutions for collision cell mode and 1:10 dilutions for non-collision mode analyses. Analytical precision of Cr, Cu, Zn and Pb was assessed by four measurements of undiluted SLRS-4.

5.3.5 ICP-MS sample measurements

Approximately every 2nd EPG snow sample (2 cm resolution) was analysed for major and trace element concentrations by ICP-MS. Reproducibility of sample measurements across the two ICP-MS analytical modes was assessed by measurement of Ba during both collision cell and non-collision cell analysis. Furthermore, IC measurements of Na, Mg and Ca provide an independent comparison of the ICP-MS results. Reproducibility of samples within ICP-MS analytical modes was assessed by multiple (2-3) measurements of ten samples of variable concentration during a single collision cell analysis set. Additionally, select samples were measured fully by ICP-MS time resolved analysis. Time resolved analysis differs from usual spectral analysis as raw data from every scan is available rather than a single 60 and 30 scan average for collision and non-collision spectral analyses respectively.

The extent of particulate matter in EPG snow samples was also investigated by microscopic inspection of samples EPG_326, EPG _306 and EPG _172. 10 mL aliquots were centrifuged for 5 minutes at 900 rev/min to concentrate particulate

material at the bottom, from which 1 mL was transferred, evaporated and mounted on a smear slide.

5.4.0 Results

5.4.1 Dating

The EPG snow pit profile covers the period winter 1994 to sampling in November 2007. Dating was constrained using concurrent low-density hoar horizons, $\delta^{18}\text{O}$ and d excess variation (Fig. 5.2) and, methanesulphonate (MS) maxima to identify summer horizons (1st of January) (Bertler et al., 2004b; Rhodes et al., 2009). Peaks in elemental chemistry (e.g. Na and Al), concurrent with $\delta^{18}\text{O}$ minima were used to identify winter horizons (1st of July). Automatic weather station accumulation measurements acquired at EPG since 2004 confirm approximate accumulation rates inferred from the dating model. Linear extrapolation was conducted between determined seasonal horizons and our dating model is attributed ± 6 months error as exact timing of precipitation is unknown.

5.4.2 Stable isotopes

Stable isotope ratios of EPG snow samples range between $\delta^{18}\text{O} = -19.5\text{‰}$ to -30.1‰ , $\delta\text{D} = -148\text{‰}$ to -244‰ , and d excess = -12‰ to 17‰ (Fig 5.2). The mean d excess value of 3.4‰ is comparable to other coastal Antarctic snow records which range between ~ 2 and 7‰ (Ciais et al., 1995; Masson-Delmotte et al., 2008; Patterson et al., 2005). D excess positively co-varies with $\delta^{18}\text{O}$ and δD throughout the majority of the EPG snow pit profile, but lags $\delta^{18}\text{O}$ and δD by approximately 90° of the seasonal cycle between winter 2000 to summer 2004/05.

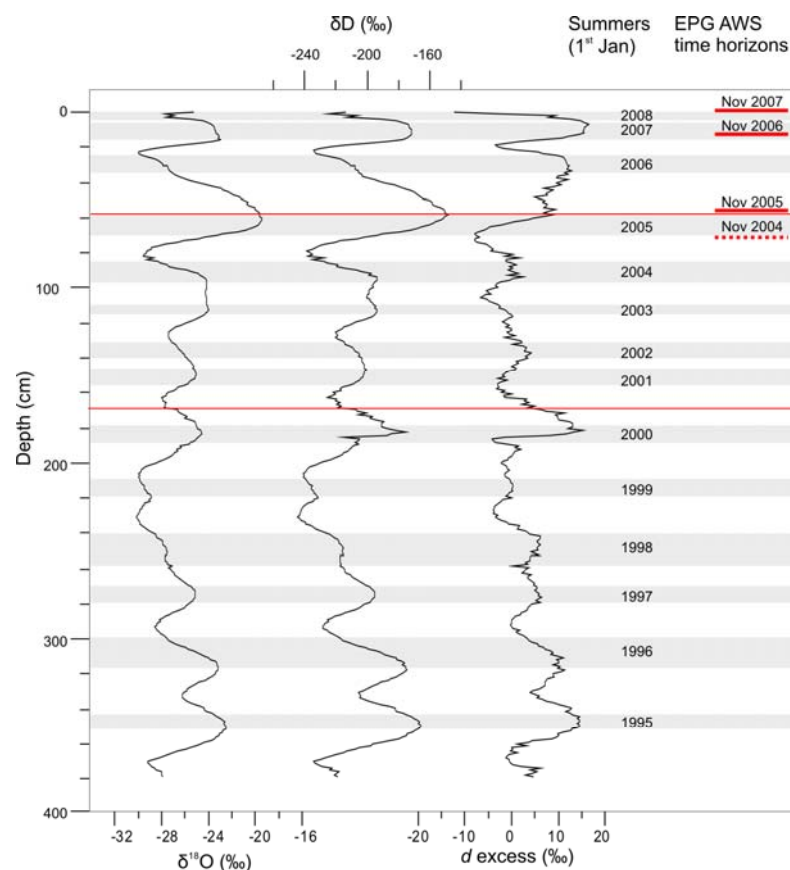


Figure 5.2 Stable isotopic ratios of the EPG snow profile. Dating is based on $\delta^{18}\text{O}$ and δD seasonal fluctuations (shown), density and elemental chemistry. Summer horizons are highlighted in grey. Measured EPG automatic weather station accumulation rates indicate the depth of November 2007 (surface), November 2006, November 2005 and minimum of November 2004 snow. Measured accumulation confirms that there is approximately 4 yr of accumulation in the top 50 cm of the snow pit profile. The second order stable isotope parameter, deuterium excess (d) is positively correlated with $\delta^{18}\text{O}$ and δD for most of the EPG snow profile, although phasing is negative between winter 2000 and summer 2004/05 (red lines).

5.4.3 Analytical accuracy and precision of ICP-MS analyses

ICP-MS analyses of SLRS-4 (Table 5.2) are within the range of certified and reported concentrations (CRNC, 1998; Osterberg et al., 2006; Rodushkin, 2003) for all elements with the exception of Ti. The determined Ti concentration is 20 % lower than Rodushkin (2003), which is currently the only other reported value. SLRS-4 analyses are highly reproducible with $< 8\%$ 2 rsd for collision cell analysis and $< 10\%$ 2 rsd for most non-collision cell analyses. Elements with precision $> 10\%$ 2 rsd (Cr, Ni, Cu, Zn, Cs, Pb and Bi) displayed low signal to background ratios when measured on the 1:10 diluted SLRS-4 solution. Precision of Ni (13 % 2 rsd) and Bi (26 % 2 rsd) are comparable to that reported by Rodushkin (2003).

Element	Applied standard concentration	SLRS certified (2 σ) and literature compilation (Environment Canada)	Osterberg et al. (2006) ($\pm 2\sigma$)	Rodushkin (2003) ($\pm 2\sigma$)	This study ($\pm 2\sigma$)	2 RSD (%)	Detection limit (3 σ blanks)	EPG samples mean	EPG samples 2 rsd (%)	EPG samples min – max	Variation of EPG samples (2 rsd) / analytical precision (2 rsd)
Major and minor elements (ppt) – collision mode											
Na	100	2400 \pm 200	-	2340 \pm 180	2120 \pm 164	8	0.21	1852	328	10 - 18031	41
Mg	10	1600 \pm 100	-	1640 \pm 40	1584 \pm 73	5	0.012	293	375	5-3856	75
Al	1	54 \pm 4	53 \pm 4	53.5 \pm 2.4	56 \pm 4	8	0.016	85	474	0.50 – 1666	59
Ca	100	6200 \pm 20	6400 \pm 400	4240 \pm 200	5731 \pm 379	7	0.10	208	355	1.5 – 2475	51
Mn	1	3.37 \pm 0.18	3.41 \pm 0.2	3.30 \pm 0.08	3.4 \pm 0.2	6	0.99	2.3	465	0.010 – 40	78
Fe	1	103 \pm 5	106 \pm 8	104 \pm 10	105 \pm 6	6	0.013	70	480	0.23 – 1358	80
Ba	1	12.2 \pm 0.6	12 \pm 1	12.7 \pm 0.4	12.5 \pm 0.7	6	0.0004	0.65	472	0.021 – 12.3	79
Al/Na					0.027 \pm 0.002	8		0.084	296	0.0009 – 0.74	37
Fe/Al					1.9 \pm 0.1	6		0.85	55	0.16 – 2.01	9
Trace elements (ppt) – non-collision mode											
Ti	1000	-	-	1250 \pm 10	1497 \pm 145	10	22	11840	330	44 – 151058	33
V	50	320 \pm 30	300 \pm 20	307 \pm 14	356 \pm 26	7	1.8	205	304	BDL – 2227	43
Cr **	50	330 \pm 20	350 \pm 20	335 \pm 8	355 \pm 45 **	13 **	27	190	275	BDL – 1735	21
Ni	50	670 *	-	709 \pm 102	825 \pm 106	13	2.8	103	317	BDL – 1246	24
Cu **	100	1810 \pm 80	1680 \pm 70	1800 \pm 280	1879 \pm 218 **	18 **	17	162	280	BDL – 1636	16
Zn **	100	930 \pm 100	-	1070 \pm 80	1359 \pm 114 **	8 **	48	288	289	BDL – 3012	36
As	40	680 \pm 60	700 \pm 40	580 \pm 80	739 \pm 47	6	6.7	220	256	BDL – 199	43
Rb	100	-	27600 \pm 1800	1440 \pm 60	1521 \pm 78	5	0.86	164	301	3.0 – 1731	60
Sr	500	26300 \pm 3200	-	27300 \pm 1000	28422 \pm 1456	5	0.62	2467	336	32 – 31450	67
Y	10	138 *	-	127 \pm 4	135 \pm 8	6	0.21	51	305	1.0 – 709	51
Zr	100	-	-	-	123 \pm 18	15	1.04	336	328	3.0 – 5630	22
Sb	10	230 \pm 40	-	253 \pm 12	257 \pm 13	5	1.2	3.0	628	BDL – 121	126
Cs	10	-	-	5.4 \pm 0.6	6.1 \pm 0.8	13	0.28	8.7	296	BDL – 95	23
Ba	100	12200 \pm 600	12000 \pm 1000	12700 \pm 400	12482 \pm 585	5	1.3	431	321	4.8 – 5841	64
La	10	320 *	-	270 \pm 16	287 \pm 15	5	0.16	105	311	1.0 – 1362	62
Ce	10	361 *	-	348 \pm 14	359 \pm 20	6	0.22	208	314	1.70 – 2665	52
Pb **	50	-	81.0 \pm 2.0	79.0 \pm 4.0	82.7 \pm 10 **	12 **	2.9	32	239	BDL – 324	20
Bi	10	-	-	1.3 \pm 0.4	2.4 \pm 0.6	26	0.41	0.39	244	BDL – 4.3	9
Th	20	-	-	17.5 \pm 1.2	201 \pm 2	10	0.29	36	643	BDL – 1339	64
U	10	50.0 \pm 3.0	50.0 \pm 8.0	47.0 \pm 2.0	49 \pm 4	9	0.30	8.9	271	BDL – 94	30
Ti/Sr				0.063 \pm 0.003	0.063 \pm 0.003	7		1.9	113	0.08 – 16	17
Zr/Y				0.91 \pm 0.10	0.91 \pm 0.10	11		6.6	77	0.22 – 17	7

Table 5.2 Analytical precision and accuracy of the ICP-MS analytical technique are determined by repeated measurement of the external riverine standard SLRS-4 in comparison to certified and previously reported values (National Research Council Canada, 1998; Rodushkin, 2003; Osterberg, 2006). Data for this study is compiled from 18 analyses of 1:100 diluted SLRS-4 for elements measured by collision cell ICP-MS and typically 30 analyses of 1:10 diluted SLRS-4 for elements measured by non-collision cell ICP-MS. Analytical precision of Cr, Cu, Zn and Pb (**) were compiled from 4 analyses of undiluted SLRS-4. Detection limits (3 σ procedural blank) and EPG snow pit chemistry are also shown.

5.4.4 Reproducibility of elemental chemistry measurements in EPG snow samples

EPG snow samples differ significantly from artificial and filtered standards due to the presence of particulate material, ranging from sub-micron to several hundred microns in size (Fig. 5.3). Although dominated by mineral grains, sample EPG_306 also contained volcanic glass (Fig. 5.3c), sponge spicules (Fig. 5.3d) and fresh water diatoms.

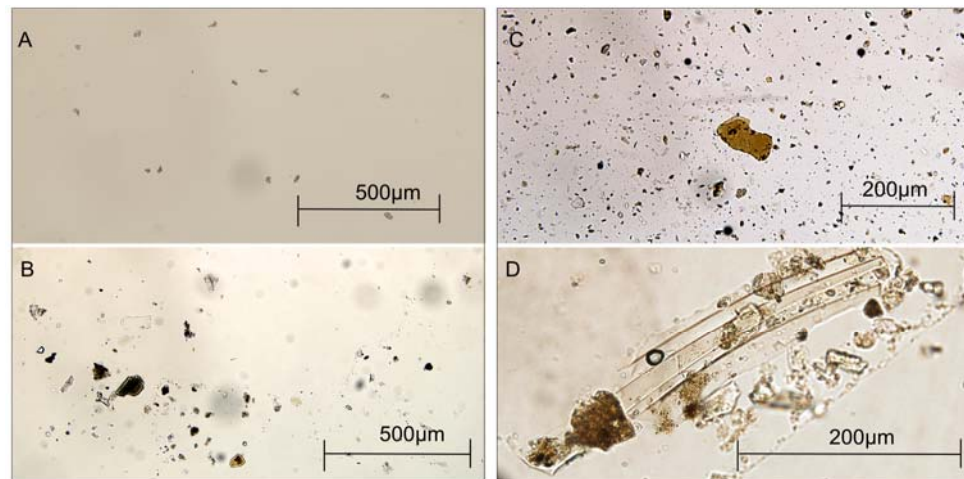


Figure 5.3 Microscope images of EPG snow samples. Samples increase progressively in expected Al concentrations as determined by ICP-MS analysis of bracketing samples. **a)** low concentration EPG_326 (Al = ~4 ppb); **b)** moderate concentration EPG_172 (Al = ~191 ppb); and **c & d)** high concentration EPG_306 (Al = ~1170 ppb). Particulate material in EPG_306 includes volcanic glass shards (**c**) and sponge spicules (**d**).

Comparison of EPG sample concentrations determined by IC and ICP-MS is $r^2 = 0.68$ for Na, $r^2 = 0.55$ for Mg and $r^2 = 0.72$ for Ca (Fig. 5.4). Although the correlation coefficient between analysis techniques is highest for Ca, this is not considered representative of measurement reproducibility due to the influence of a limited number of outliers. Rather, 70 % of sample analyses are within a 20 % envelope of either analysis for Na, within a 40 % envelope of either analysis for Mg and within a 50 % envelope of either analysis for Ca. Where significant differences are present, sample concentrations determined by ICP-MS are typically higher (e.g. 28 % of Na samples concentrations are higher when determined by ICP-MS versus 5 % of sample Na concentrations which are lower).

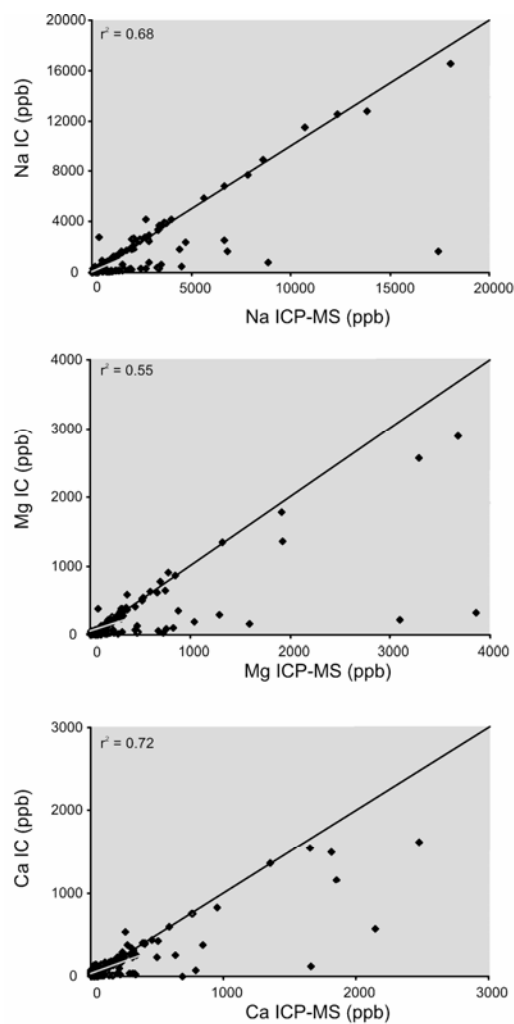


Figure 5.4 Comparison of Na, Mg and Ca concentrations measured in EPG snow samples by ICP-MS and IC. Both 1:1 (black) and linear correlation (light grey) lines are shown. Fields of grey indicate the range of 70% of all samples from 1:1 ratio, 20% for Na, 40% for Mg and 50% for Ca.

Correlation of Ba concentrations measured in EPG samples between collision cell mode ICP-MS and non-collision cell ICP-MS is $r^2 = 0.63$. Significantly, this is lower than the correlation of Ba with other elements within each analysis mode (e.g. correlation between Al and Ba, $r^2 = 0.90$ and Ti and Ba, $r^2 = 0.98$) (Fig. 5.5). There is no significant trend towards higher Ba concentrations determined by either analytical technique.

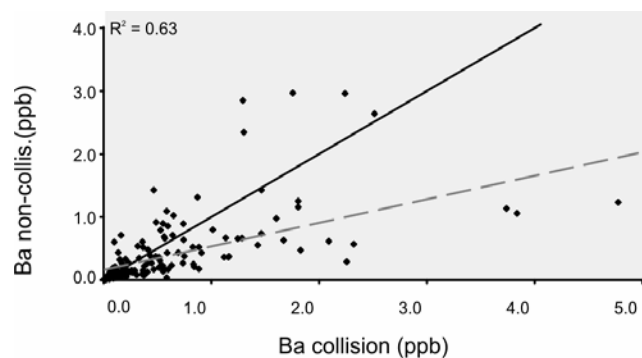


Figure 5.5 Comparison of Ba measurements between collision cell and non-collision cell ICP-MS analyses modes. The linear correlation between analyses is shown in light grey which is heavily weighted by a high concentration outlier samples. The 1:1 ratio is shown in black and considered more representative of data scatter.

Repeated measurement (2 to 3 times) of the ten samples within a single collision cell ICP-MS analysis set produces concentrations that differ from the first measurement by on average 11-12 % for Na, Mg, and Ca, 31-37 % for Al, Fe, Mn and Ba, 8 % for Al/Na and 11 % of Fe/Al. Reproducibility of sample measurements is similar to analytical precision for Na, Mg, Ca and Al/Na (analytical precision ≈ 7 % \pm 2 rsd) but worse than analytical precision for Al, Fe, Mn, Ba and Fe/Mn (analytical precision ≈ 7 % \pm 2 rsd for Al, Fe, Mn, Ba and 10 % \pm 2 rsd for Fe/Al).

ICP-MS time resolved analysis of EPG snow samples shows peaks in signal intensity extending from the modal concentration (Fig. 5.6). The magnitude and frequency of peak concentrations is both element and sample dependent, with variability of raw data highest for elements such as Al, Mn, Fe, Ti, Zr and Ba and lowest for Na, Cr, Cu and Sr. Reproducibility of 60 (collision) and 30 (non-collision) scan averages is best for Na (6 % \pm 2 rsd) and Sr (2 % \pm 2 rsd), and worst for Fe (45 % \pm 2 rsd) and Zr (90 % \pm 2 rsd) when averaged over all samples measured. This is comparable to the reproducibility of repeated sample measurements by spectral analysis, reported in the previous paragraph. Furthermore, reproducibility of scan averages for elemental ratios including Na, Sr, As and Cr (e.g. Al/Na = 24 % \pm 2 rsd) is better than ratios between elements such as Fe, Ba and Zr (e.g. Zr/Y = 86 % \pm 2 rsd) (Fig. 5.6). Variability of sample measurements is also sample dependent. The reproducibility of Zr scan averages in EPG_072 (12 % \pm 2 rsd) is an order of magnitude lower than EPG_290 (331 % \pm 2 rsd) despite comparable Zr concentrations of 97 ppt and 72 ppt respectively. The measurement of calibration

standards and the external standard SLRS-4 is highly reproducible for all elements in comparison to sample measurements.

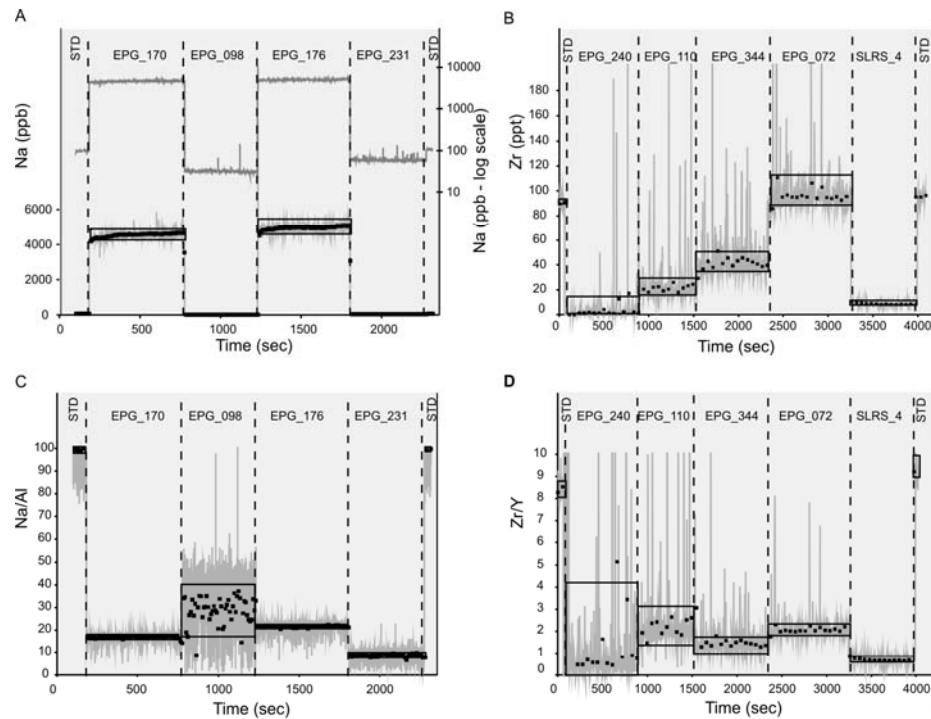


Figure 5.6 ICP-MS time resolved analysis of selected EPG snow samples for **a)** Na concentrations, **b)** Zr concentrations, **c)** Na/Al and **d)** Zr/Y. Raw scan data is shown in grey with 60 and 30 scan averages for collision cell (Na and Na/Al) and non-collision cell (Zr and Zr/Y) analyses respectively, shown as black squares. The variability of scan averages (2σ) for each sample is highlighted by black rectangles. Raw scan data of Na concentrations are also shown on a log scale (**a** - right) to observe internal variability of low concentration samples. The external standard SLRS-4 was measured for Zr concentrations and Zr/Y, and demonstrates lower internal variability than sample measurements.

5.4.5 Elemental concentrations of EPG snow samples

Elemental concentrations of EPG snow samples vary temporally by three to four orders of magnitude. Elemental variation is typically two orders of magnitude higher than ICP-MS analytical uncertainty and three times higher than natural internal sample variability for all elements (Table 5.2). Variation is highest for Th, Sb, Fe and Al and least for Pb, Cr, Bi and As. Comparably, temporal variation (ratio of maximum/minimum concentrations) is lowest for Cu and Bi, moderate for Al, high for Mn and Pb in snow samples at Lambert Glacier (Hur et al., 2007), and lowest for U, Pb, Al and Bi and highest for Fe, Mn, and V at Coats Land (Planchon et al., 2002b). Average elemental concentrations at EPG are significantly higher (up to three orders of magnitude) than average elemental concentrations at either Lambert Glacier or Coats Land (Table 5.3) (Hur et al., 2007; Planchon et al., 2002b). Pb and Bi concentrations show the lowest differences between these studies.

	Hur et al. (2007)	Planchon et al. (2002b)	This study	EPG/Lambert	EPG/Coats
Location	Lambert Glacier 70° 50'S, 77° 04'E	Coats Land 77° 34'S, 25° 22'W	Evans Piedmont Glacier 76° 43'S, 162 ° 35'E		
Time period	1998-2002	1920-1990	1997-2007		
Distance from coast (km)	160	200	10		
Altitude (m)	1850	1420	310		
Accumulation rate (g cm ⁻² y ⁻¹)	29	5.6	16		
Average elemental concentration (ppt)					
Al	165	450	85000	515	189
V	0.46	0.50	205	446	410
Cr	-	1.8	190	-	106
Mn	3.7	8.3	2300	622	277
Fe	45	-	70000	1556	-
Co	-	0.4	-	-	-
Cu	5.3	3.0	162	31	54
Zn	-	2.4	268	-	112
Ag	-	0.2	-	-	-
Ba	2.4	2.5	431	180	172
Pb	4.0	2.9	32	8	11
Bi	0.03	0.05	0.39	14	8
U	0.03	0.03	8.9	307	297

Table 5.3 Comparison of average trace element concentrations of snow samples from EPG (this study), Lambert Glacier in East Antarctica (Hur et al., 2007) and Coats Land on the Weddell Sea coast (Planchon et al., 2002b).

Na concentrations in EPG snow samples determined by ICP-MS are significantly correlated with Mg ($r^2 = 0.98$), Cr, As, and Sr ($r^2 > 0.80$) (Fig. 5.5). Samples have broadly marine ratios with slight enrichments in Mn, Cr, As and Sr towards crustal values. Al significantly correlates with Mn, Fe and Ba ($r^2 > 0.90$) and Ti co-varies with V, Ni, Rb, Y, Cs and Ba ($r^2 = 0.95$), and Cu, Zn, Zr, La, Ce, Pb, Bi, U ($r^2 > 0.84$). Relative concentrations of Al, Fe, Ti and Ba are closer to averaged regional geology whole rock ratios (Roser and Pyne, 1989) than upper continental crust (UCC) (Wedepohl, 1995).

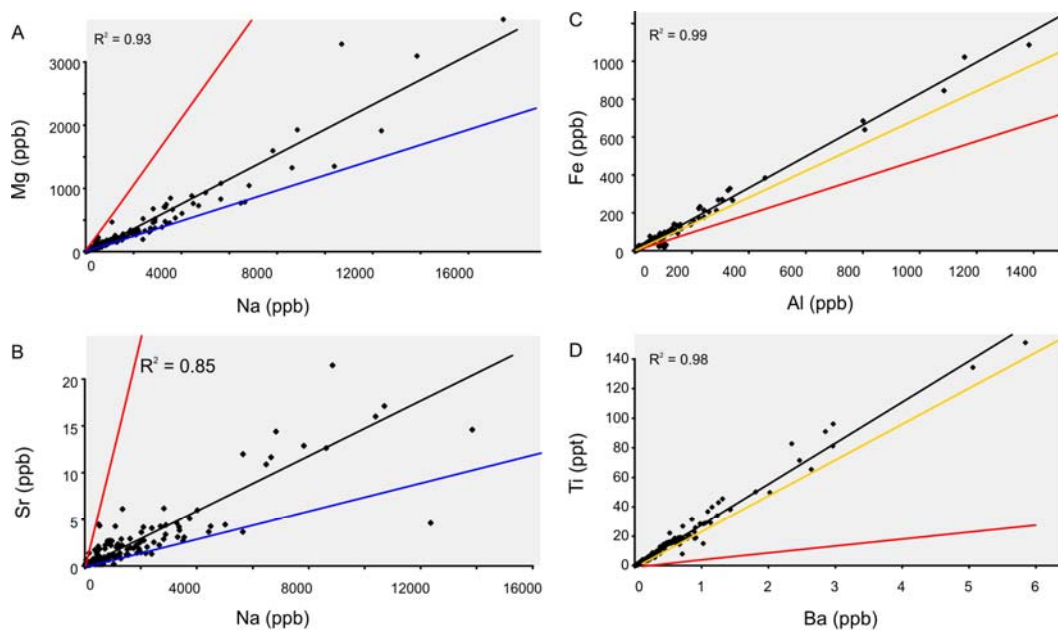


Figure 5.7 Bi-variate plots of Mg, Na, Sr, Fe, Al, Ba and Ti concentrations measured in EPG snow samples. **A,B)** Mg, Sr and Na approximate marine (blue) ratios with slight enrichment towards the average upper continental crust (red). **C,D)** Fe, Al, Ti and Ba are a closer approximation of average regional geology chemistry (orange) rather than average upper continental crust (red).

Maximum elemental concentrations typically occur during or close to winter $\delta^{18}\text{O}$ minima (Figs. 5.8 to 5.10). Concentration maxima of Na (and elements that are strongly correlated with it) occur during winters 1996, 1999 and 2004. Concentration maxima of Al, Ti (and elements correlated with them) occur during winters 1996, 2003, 2004 and 2007 (Fig. 5.8 to 5.10). Previous studies find Al, V and Cr maxima occur during late spring to summer at Coats Land (Planchon et al., 2002b), spring, summer and winter at Lambert Glacier (Hur et al., 2007) and seasonal maxima of marine derived chemical species (e.g. Na) occur both during winter (Kaspari et al., 2005; Wolff et al., 2003), and late spring/summer (Bertler et al., 2004b; Fisher et al., 2008; Wagenbach et al., 1998) depending on site location.

5.4.6 Elemental ratios of EPG snow samples

Elemental ratios are calculated between elements measured within the same ICP-MS analytical mode (collision cell or non-collision cell). Al/Na and Ti/Sr demonstrate four orders of magnitude sample-to-sample variation, an order of magnitude higher than analytical precision or intra-sample variability (Table 5.2, Fig. 5.8 and 5.9). On average, Al/Na ratio is low for the period 1997 to 2000 (Al/Na = 0.02), and high from 2001 to 2008 (Al/Na = 0.15). The Al/Na ratio changes by 156% between these time periods,

driven primarily by a reduction in average Na concentration from an average of 3101 ppb (1997 to 2000) to 1059 ppb (2001 to 2008). Ti/Sr demonstrates a similarly long-term trend to Al/Na. although the increase in Ti/Sr is more subdued, changing by 69% from an average of Ti/Sr = 3.3 (1997 to 2000) to Ti/Sr = 6.8 (2001 to 2008). Elemental ratios Fe/Al and Zr/Y vary seasonally between 1996-1998 and 2001-2008 and are consistently elevated during $\delta^{18}\text{O}$ maxima (Fig. 5.10).

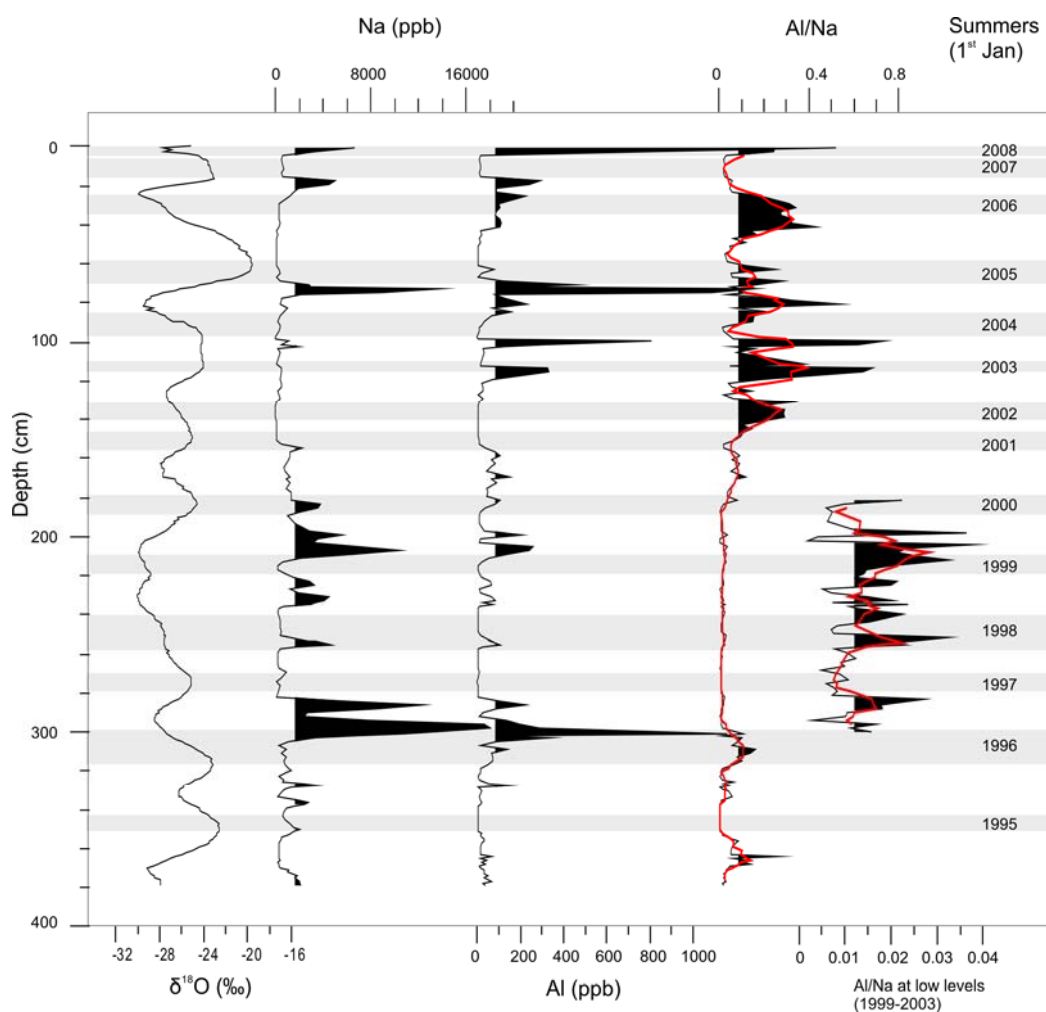


Figure 5.8 $\delta^{18}\text{O}$, Na and Al concentrations, and Al/Na ratio of the EPG snow pit profile. Winter minima in $\delta^{18}\text{O}$ are highlighted in grey shading. Samples above mean chemistry are filled in black for Na (1652 ppb) and Al (85 ppb) concentrations, and Al/Na values (0.085). A 30 point running average is shown for Al/Na ratio. Variability of Al/Na when values are extremely low (between 1996 -2000) are shown on an additional scale. Analytical error is 8 % 2 rsd for Al, Na and Al/Na.

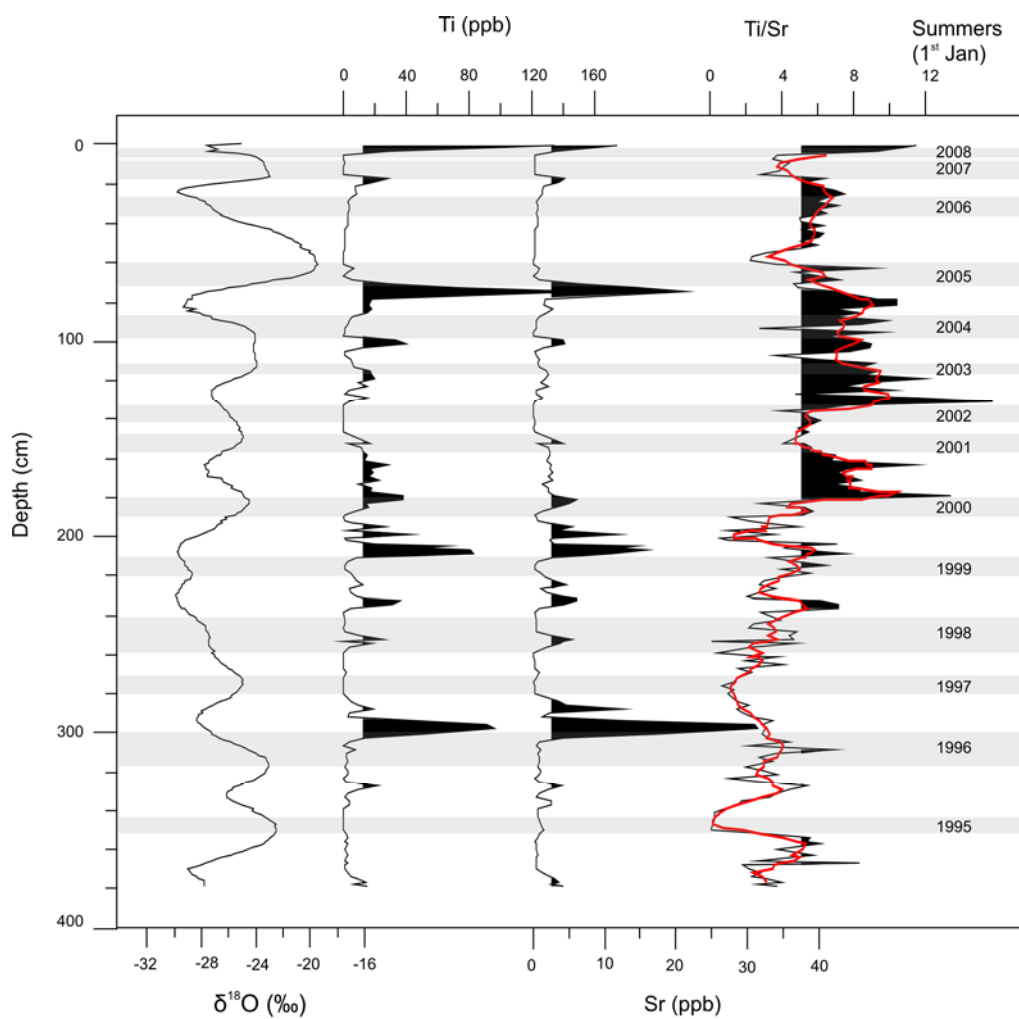


Figure 5.9 $\delta^{18}\text{O}$, Ti and Sr concentrations, and Ti/Sr of the EPG snow pit profile. Summer horizons are highlighted in grey shading. Samples above mean chemistry are filled in black for Ti (1.2 ppb) and Sr (2.5 ppb) concentrations, and Ti/Sr values (4.9). A 30 point running average is shown for Ti/Sr ratio. Analytical error is 10 %, 5 % and 7 % 2 rsd for Ti, Sr and Ti/Sr respectively.

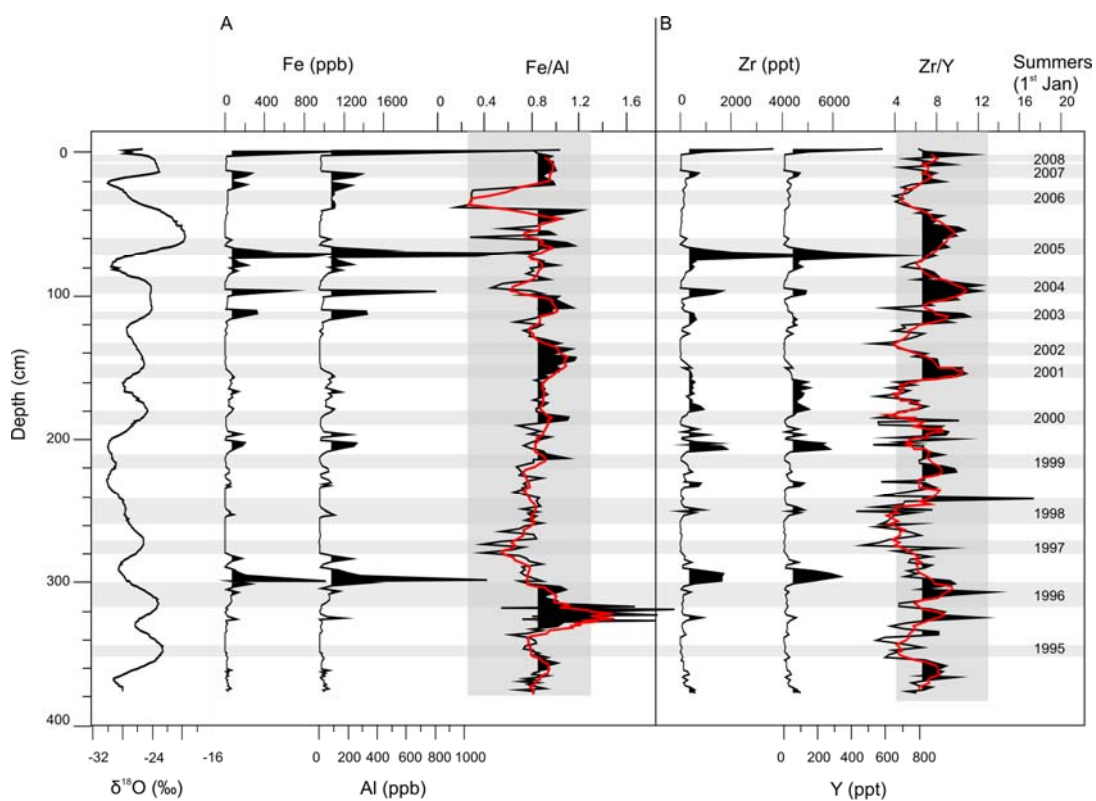


Figure 5.10 $\delta^{18}\text{O}$ of the EPG snow pit profile with summer horizons highlighted in light grey shading with respect to a) Fe and Al concentrations, and Fe/Al, and b) Zr and Y concentrations and Zr/Y. Samples above mean snow profile chemistry are filled in black for Fe (70 ppb), Al (85 ppb), Zr (336 ppt) and Y (51 ppt) concentrations and Fe/Al (0.85) Zr/Y (6.6) values. A 30 point running average is shown for Fe/Al and Zr/Y ratios. Fe/Al and Zr/Y variability displayed by regional geology whole rock chemistry is highlighted in medium grey shading (Roser and Pyne, 1989). Analytical error of EPG snow sample chemistry measurements is 6 %, 8 % and 11% 2 rsd for Al, Fe, and Al/Fe, and 14%, 6 %, 3 % 2 rsd for Zr, Y and Zr/Y

5.5.0 Discussion

5.5.1 Presence of dust particulates in EPG snow samples

Repeated measurement of the external standard SLRS-4 demonstrates ICP-MS is a reliable analytical technique for the measurement of major and trace element chemistry at concentrations similar to those present in EPG snow samples. Analytical precision is typically 5 to 10 % 2 rsd and even errors > 10 % 2 rsd are insignificant in comparison to temporal changes in elemental chemistry of snow samples. However, the reproducibility of sample measurements by ICP-MS is complicated by the presence of mineral dusts. Importantly, sample-to-sample variation is still at least three times higher than internal sample variability. The interpretation of temporal changes in elemental concentrations is therefore not affected by the reproducibility of individual sample measurements.

Mineral dusts affect sample measurements by increasing the concentration of elements in the soluble fraction when partially leached in weakly acidified ICP-MS sample aliquots. In comparison, IC aliquots are non-acidified, accounting for the systematically higher concentrations of Na, Mg and Ca determined by ICP-MS analysis when comparing the two analytical techniques. Furthermore, leaching of mineral dusts is both element and mineral specific and will alter elemental ratios present in the soluble fraction of weakly acidified samples. Easily leached elements such as Cu are relatively enriched with respect to other elements such as Al (Reimann and De Caritat, 2000; Ruth et al., 2008; Snäll and Liljefors, 2000). Because acidification was kept constant for all samples, it is unlikely this can account for observed changes in elemental ratios throughout the snow pit profile, but may be significant for elemental ratio based source modelling.

Undigested particles add additional complexity to the measurement of elemental chemistry by entering the ICP-MS and are responsible for the variability of repeated ICP-MS sample measurements. This is indicated by the poor reproducibility of Ba sample measurements between collision cell ICP-MS and non-collision cell ICP-MS (Fig. 5.5). This cannot result from variable leaching of particulate material as samples were refrozen in between analyses to inhibit chemistry changes. Additionally Ba

concentrations are not systematically higher during later non-collision cell analysis as would be expected from an increased period of acidification. Repeated measurement of samples by collision cell ICP-MS for Na, Al, Ca, Fe, Mn and Ba concentrations also show significant differences despite the completion of all analyses within an hour. This is considered too short a period of time for significant changes in chemistry after the initial 12 hr period of acidification.

Time resolved analysis most clearly demonstrates the influence of undigested particulate material on sample measurements. Strong peaks in signal intensity of terrestrial derived elements occur above the modal concentration measurement, representing the concentration of elements in particulate material and soluble chemistry respectively. Although 60 and 30 scan averages (equivalent to a single spectrum analysis for collision cell ICP-MS and non-collision cell ICP-MS respectively) are typically closer to the soluble chemistry concentration, slight differences in the number of particles analysed are responsible for the poor reproducibility of repeated sample measurements. Elemental ratios are also sensitive to the slight differences in sample analyte measured by multiple ICP-MS analysis. This is demonstrated by variation in the ratio of Ba measured by collision cell versus non-collision cell analyses between 0.15 and 15.4 rather than approximating 1 as expected. Elemental ratios are therefore calculated only between elements measured within the same analytical run.

The ICP-MS technique applied in this study measures the concentration of elements within the soluble fraction of a snow sample with variable influence of particulate material. We therefore suggest samples should be fully digested in stronger acids (HF-HNO₃) before ICP-MS analysis, adapting the procedures of Norra and Stüben (2004) or Ruth et al(2008). Contamination is however a potential problem, especially at low sample concentrations (Ruth et al., 2008). Conversely, the soluble chemistry concentration of samples could be determined from ICP-MS measurements by discounting peaks in signal intensity of the raw data and determining the modal concentration rather than an automated average. Unfortunately, this data is not available for the majority of samples measured in this study that were determined by spectral analysis.

5.5.2 Ratio source modelling

Chemical ratios are commonly used to model source regions of major and trace element chemistry in Antarctic snow and ice (Hur et al., 2007; Planchon et al., 2002b; Vallelonga et al., 2004). Modelling is based on a conservative element (C), assumed to derive from a single source such as Na from marine aerosol and Al from terrestrial dust. The contribution of each source to a sample is calculated from:

$$\text{Equation 1a: Source contribution} = \frac{C_{\text{sample concentration}}}{C_{\text{source concentration}}}$$

The percentage of an element's concentration (x) possibly derived from each source region is determined as:

Equation 1b:

$$\text{Source leverage on X (\%)} = \frac{\text{Source contribution} \times X_{\text{source concentration}}}{X_{\text{sample concentration}}} \times 100$$

Where modelled source leverage on an element (x) is > 100 %, snow chemistry is either depleted in element x or enriched in the conservative element, in comparison to source chemistry. Conversely, source leverage values < 100 % signify enrichment of element x (possibly from another source), or depletion of the conservative element relative to source ratios.

	EPG mean snow chemistry	Marine	Marine (EF)	UCC	Volcanic	Volcanic	Anthropogenic	Dominant source
Source input (%)		1,2,3	1,2,3,4,5	6	7	8,9	10,11	
References		0.015	0.015	0.0001	15% nss SO ₂	80% Bi	65% Pb	
IC	ppb	Source leverage (%)						
SO ₄	496	80			4.7			M (B + V)
nssSO ₄ ²⁻	155				15			B + V
Cl	3427	86			0.46			M
K	74	81		42	1.4	0.39		M + T
ICP-MS	ppb	Source leverage (%)						
Na	1646	100		1.7	0.48	0.02		M
Mg	292	67		5.1		0.03		M (T)
Ca	207	30		16	0.07			M + T
Al	85	0.00		100			0.09	T
Mn	2	0.00	0.02	25	1.1	0.17	0.13	T
Fe	70	0.00	0.05	48	0.50		0.16	T
Ba	1	0.43		113	0.47			T
ICP-MS	ppt	Source leverage (%)						
Ti	12618	0.00		17	0.95		0.04	T
V	217	0.14	7.1	17	1.5		2.9	T
Cr	201	0.02	0.20	12	11		1.7	T (A)
Ni	107	0.07		12	5.3		2.6	T (A)
Cu	170	0.04	7.6	5.8	38	5.3	1.6	T (M + V + A)
Zn	252	0.11	22	14	77	1.4	5.6	T (M + V + A)
As	22	1.3	265	6.1	73		5.1	M (A)
Rb	173	11		44	3.7			T (M)
Sr	2536	48		8.6				M + T
Y	54	0.00		26				T
Zr	349	0.00		47				T
Sb	2.8	1.3		7.6	34		15	T (A)
Cs	9.2	0.49		43	2.9			T
Ba	459	0.60		100				T
La	113	0.00		20	0.74			T
Ce	222	0.00		20	1.1			T
Pb	34	0.01	1.0	35		1.6	65	T + A (V)
Bi	0.40	0.79		21		80		V (T)
Th	44	0.00		16				T
U2	9.4	5.3		18				T (M)

Table 5.4 Ratio source modelling of major and trace element chemistry present in EPG snow samples. The influence (%) of each source is determined by normalising EPG elemental chemistry to concentrations of Na for marine aerosol, Al and Ba for average upper continental crust (UCC), 15% nssSO₄ and 80% Bi for volcanic emissions, and 65% Pb for anthropogenic emissions (highlighted in bold) to known source ratios. Marine source leverage is calculated both with and without the use of marine enrichment factors (EF). The dominant source region for each element is denoted as T (terrestrial), M (marine), V (volcanic), A (anthropogenic) and B (biogenic) with minor contributions shown in brackets. Source region chemistry and marine enrichment factors were derived from ¹Bruland and Lohan (2003), ²Riley and Chester (1971), ³Turekian (1968), ⁴Planchon et al. (2002b), ⁵Hur et al. (2007), ⁶Wederpohl (1995), ⁷Zreda-Gostynska and Kyle (1997), ⁸Le Cloarec and Marty (1990), ⁹Hinkley et al. (1999), ¹⁰Lantzy and McKenzie (1979) and ¹¹Pacyna (1984).

Ratio modelling provides a good first estimate of the dominant source regions of EPG major and trace element chemistry. Determined source regions are confirmed by comparison with the behaviour of elements during ICP-MS analysis, and temporal co-variance of elements. Maximum marine aerosol input was calculated using Na as a conservative element with respect to average upper ocean chemistry (Bruland and Lohan, 2003; Riley and Chester, 1971; Turekian, 1968). Although crustal material also contains significant concentrations of Na, soluble, marine derived Na is thought to

dominate at coastal Antarctic sites (Legrand and Mayewski, 1997). In addition to Na, chemistry of the average upper ocean can account for the majority of Mg, Cl, SO₄ and K present in EPG snow samples (Table 5.4). Additionally, ratio modelling indicates marine aerosols are a significant source of Sr (50 %), Ca (30 %), Rb (11 %), and U (6 %). However, previous studies have demonstrated chemical ratios of marine aerosol differ significantly from bulk upper-ocean and are frequently elevated in trace elements with respect to Na due to biological and physical processes at the ocean surface (Reimann and De Caritat, 2000). Differences are quantified using marine enrichment factors (EF), although order of magnitude differences in reported values have called their validity into question (Chester, 2000; Duce and Hoffman, 1976). Using the EF values applied by Planchon et al. (Planchon et al., 2002b) and Hur et al. (2007) marine aerosol can additionally account for all As (>100 %) and significant amounts of V, Cu and Zn (7.6 %, 8.0 % and 21 % respectively) present in EPG snow samples (Table 5.4). Strong co-variance of As with Na ($r^2 = 0.82$) and good reproducibility of As measurements during ICP-MS time resolved analysis indicates low contribution of As from particulate aerosol, suggesting As has a predominantly marine source. Similarly, strong co-variance of Cr with Na ($r^2 = 0.82$) implies marine leverage of Cr may be greater than that modelled using average upper ocean chemistry (<1 %). However, temporal co-variance may also simply suggest a similar atmospheric pathway of Cr and marine aerosol (Hur et al., 2007). These results suggest marine aerosol is an important source of Na, Cl, Mg, As, K, SO₄, Ca, Sr and to a lesser degree Rb and U present in EPG snow. These results are comparable to previous studies that determine marine aerosol as a significant source of Mg, Ca, Sr, As and Cu (Gabrielli et al., 2005; Hur et al., 2007; Planchon et al., 2002b; Vallelonga et al., 2004).

Terrestrial source contributions to EPG snow are modelled for elements measured by collision cell ICP-MS using Al with respect to average UC (Wedepohl, 1995). Despite the range in reported UCC values (Rudnick and Gao, 2003) differences are insignificant for modelling source contributions (Gabrielli et al., 2005). UCC can account for all Ba present in EPG snow but less than 50 % of Mn and Fe (Table 5.4). Using Ba as a conservative terrestrial element for trace elements measured by non-collision cell ICP-MS, UCC source leverage on all trace elements is also below 50 %.

Input of volcanic and anthropogenic emissions to Antarctic snow are difficult to constrain due to the lack of a truly conservative species and poor constraints on source ratios. Fifteen percent of non-sea-salt (nss) SO_4^{2-} in snow and ice is commonly attributed to a volcanic source (Hur et al., 2007; Planchon et al., 2002b). Average Mount Erebus gas emissions have been used to approximate volcanic source values in this study (Zreda-Gostynska and Kyle, 1997). Nss SO_4^{2-} is calculated by normalising SO_4^{2-} concentrations to Na and the upper ocean $\text{SO}_4^{2-}/\text{Na}$ ratio. In doing so, volcanic emissions are a significant source of Cr, Cu, Zn, and Sb (Table 5.4). This is considered an upper limit of volcanic contribution as biogenic activity can account for almost all nss SO_4^{2-} measured in coastal glaciochemical records (Minikin et al., 1998). Comparatively, previous studies identify volcanic emissions as the dominant source of Bi (Gabrielli et al., 2005; Hur et al., 2007). Normalising Bi present in EPG snow not attributable to UCC (80 %) to the elemental ratios of global volcanic emissions (Hinkley et al., 1999; Le Cloarec and Marty, 1990), volcanic leverage on EPG trace element chemistry is reduced by a factor of ~ 2 . In particular, estimates of volcanic Zn input are reduced by an order of magnitude, from 17 % to <1.5 %. Previous studies have found volcanic input to be only important for Bi (100 %) and V, Mn and Cd (30-40 %) (Hur et al., 2007) suggesting the latter model is more appropriate for EPG snow samples. Gabrielle et al. (2005) additionally found volcanic output is significant for As during inter-glacial periods.

Non-marine or UCC terrestrial Pb (65 %) is normalised to available global emission data (Lantzy and MacKenzie, 1979; Pacyna, 1984) to determine the leverage of anthropogenic emissions on EPG snow chemistry. In doing this, anthropogenic emissions are a potentially important source for Zn, As, V, Ni, Sb and Cr (Table 5.4), although this is only a tentative estimate, as terrestrial contribution of Pb is most probably > 35 %. Furthermore, regional anthropogenic source regions such as McMurdo Station, Scott Base, and Marble Point may emit elemental ratios which differ significantly from global estimates (Reimann and De Caritat, 2000).

A number of factors suggest terrestrial input of Mn, Fe, Ti, V, Ni, Cr, Rb, Y, Zr, Sb, Cs, La, Ce, Th, and U in EPG snow samples is significantly higher than that modelled. These include a) strong temporal correlation of elemental concentrations (e.g. Al and

Fe, $r^2 = 0.99$), b) minimal contributions from other aerosol source regions and, c) the high influence of dust particles during time resolved ICP-MS analysis. Terrestrial elemental ratios measured in snow samples are therefore either depleted in Al and Ba in comparison to UCC, or enriched in most major and trace elements. The complications when using source modelling to determine terrestrial contributions is well documented. Duce et al. (1975) and Gabrielli et al. (2005) recommended using terrestrial contribution models (fluxes or similar calculations) as an order of magnitude estimate of terrestrial contributions only. Reinmann and De Caritat (2000) have summarised the main processes responsible for poor terrestrial modelling results, which are discussed in terms of EPG snow chemistry:

(1) Differential leaching of elements from particulates alters measured elemental ratios significantly from those truly present in samples. Ruth et al. (2008) determined that 45% of Al and 30 % of Fe present in Antarctic ice samples is measured by ICP-MS analysis of samples acidified to pH 1. Assuming similar leaching rates, the influence of UCC on Fe in EPG snow samples is reduced to 32 %. However, element solubility is also dependent on mineralogy. Snäll and Liljefors (2000) measured 3.4 %, 6.2 %, 12 %, 78 % and 100 % recovery of total Al concentrations in 1 M HNO₃ solutions of powdered feldspar, muscovite, hornblende, Mg-chlorite and biotite, respectively. Furthermore, Gaspari et al. (2006) determined recovery of Fe in acidified samples (pH = 1) at Dome C is 65 % during the Last Glacial Maximum (LGM) compared to 30-40 % during the Holocene. This change has been attributed to the changing mineralogy of terrestrial aerosol transported to the Dome C, likely to be more representative of whole rock source chemistry during the LGM due to increased vigour of atmospheric circulation and greater proximity of exposed continental shelf sediments. Proximity of terrestrial source regions to EPG suggests 65 % recovery (Gaspari et al., 2006) of Fe might be more representative of element solubility in EPG samples, increasing UCC contributions to 70 %. However, further study is required to determine the elemental recovery rates for the dominant mineralogy in EPG samples.

(2) Major and trace element concentrations of crustal material vary significantly from UCC dependent on the dominant geology type of the terrestrial aerosol. Snow sample chemistry will reflect the ratios of source geology, indicated by the closer approximation

of Fe, Al, Ba and Ti in EPG snow by average McMurdo geology (Roser and Pyne, 1989) rather than UCC (Fig. 5.5) (Wedepohl, 1995). Terrestrial inputs modelled using whole rock geochemistry of McMurdo geology (Fig. 5.11) are highly variable, and when combined, have the potential to account for all elemental concentrations present within EPG snow. The McMurdo Volcanic basic group, in particular, is enriched in Fe, Ti, V, Cr, Ni and Zr with respect to Al and Ba, while Cu and V are present in high levels relative to Ba in the Ferrar Dolerite (Roser and Pyne, 1989).

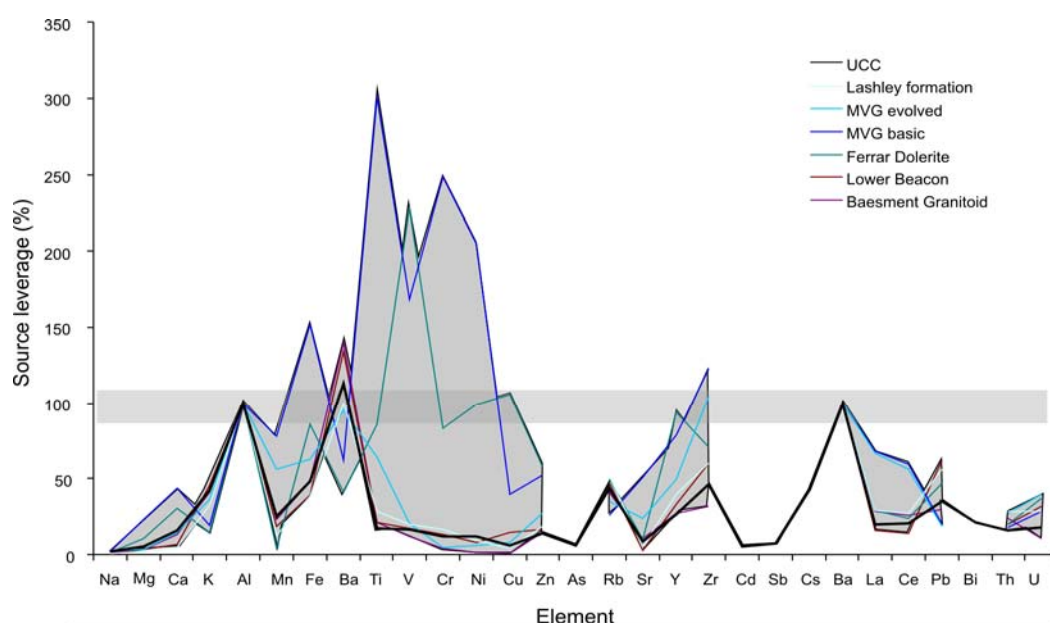


Figure 5.11 Source modelling of regional terrestrial input to EPG mean snow chemistry when normalised to regional geology (Roser and Pyne, 1989) and average upper continental crust (UCC) (Wedepohl, 1995). Large variations observed indicate the inability of UCC to reliably indicate true mineral dust input, and the potential for changing elemental ratios dependent on the source region geology.

(3) Terrestrial dust is fractionated from original source chemistry due to physical weathering and aeolian transport processes. Fine grained material preferentially transported to snow and ice core records is enriched in easily weathered, low density minerals such as quartz, feldspars, calcite, micas, chlorite, clays (Pye, 1987) and therefore associated elements such as Al, Ca, Ba, K and Na (major constituents of feldspar). Conversely, elements present in heavy minerals such as Zr (zircons), Fe and Mg (olivine) are depleted. Fractionation resulting from physical weathering is evident in the McMurdo Dry Valley soils where fine grained material < 250 µm is dominated by felsic mineralogy while coarser grains are more representative of whole rock sources (Ugolini and Jackson, 1982). Furthermore, local ice core records demonstrate felsic mineral dusts

are preferentially transported, with quartz and feldspar comprising ~ 60 to 70 % of identified grains within the Victoria Lower Glacier ice core record (Ayling and McGowan, 2006). Average EPG snow chemistry partially follows expected trends with greater depletion of Zr and Fe (UCC can account for 46 % Zr and 49 % Fe) relative to other elements such as Mn or Ti (UCC accounts for 25 % Mn and 17 % Ti). However, Fe chemistry is complex, with a number of possible sources including fine grained weathered oxides (e.g. goethite, lepidocrocite, hematite), which are abundant within the McMurdo Dry Valley soils (Bockheim, 2002; Campbell and Claridge, 1975) and local granitic surfaces (Kelly and Zumberge, 1961).

Differences between trace element concentrations measured at EPG, Lambert Glacier and Coats Land further support a predominantly terrestrial source of Al, Fe, and Ti and volcanic and anthropogenic emission sources of Pb, Bi and Cr. Average Al and Fe concentrations are the most elevated at EPG with respect to the other sites, in accordance with the proximity of terrestrial source regions at EPG. Conversely, average Pb and Bi concentrations are less than an order of magnitude higher at EPG as expected from the more regional distribution of volcanic and anthropogenic emissions. Proximity of source regions also determines the sensitivity of elemental concentrations to changes in atmospheric circulation, with highest sample-to-sample variation in terrestrial elements (Ti, Fe and Al) and the least for anthropogenic and volcanic emissions derived elements (Pb, Cr, and Bi).

5.5.3 Seasonal changes in elemental chemistry in relation to local meteorology

EPG elemental chemistry concentrations are related to meteorological conditions measured at Cape Ross. Comparison with the Scott Base and Marble Point AWS records confirms Cape Ross AWS data is representative of regional scale events. In particular, maximum wind speeds at Cape Ross are concurrent with strong winds at the other sites. Winter maxima of EPG elemental concentrations are consistent with stronger winter wind speeds. On average, winter wind speeds are $6.7 \pm 0.4 \text{ m s}^{-1}$ compared to $4.7 \pm 0.1 \text{ m s}^{-1}$ during summer. Wind strength increases from the S only (SSE and SW) indicative of stronger katabatic wind flow and mesoscale cyclonic activity (Fig. 5.1). This is supported by previous work of Ayling and McGowan (2006) who

demonstrate increased winter transport of minerals dusts in ice core records from proximal Wilson Piedmont and Victoria Lower Glaciers.

Lower rates of precipitation during winter may also partially account for high winter concentrations due to decreased dilution of dry deposited aerosol. AWS accumulation measurements at EPG demonstrate snow accumulation is dominated by episodic events rather than continuous snow precipitation. For example, 4.9 g cm^{-2} of the total 14 g cm^{-2} (35 %) accumulated during 2006 occurred over a four day interval between 24th – 27th February. Although the time period is too short to establish statistically significant seasonality, the timing of 2-3 day accumulation events greater the 2 g cm^{-2} (December 2004, January and December 2005, February, June and December 2006 and February 2007) are consistent with mid-summer to autumn precipitation maxima measured at McMurdo Station and Scott Base (Mullen and Sinclair, 1990; Rockey and Braaten, 1995). Reduced sea ice during this time period provides greater moisture for cyclonic activity over the Ross Sea, and hence increased precipitation to Victoria Land coast, especially during autumn (Carrasco and Bromwich, 1994; Carrasco et al., 2003; Monaghan et al., 2005; Mullen and Sinclair, 1990; Turner, 2004). However, low winter precipitation is not considered the dominant control on the seasonality of EPG chemistry, as chemistry peaks are not present in thin layers, rather distributed over several cm of accumulation (e.g. winter 1996 chemistry maxima over approximately 50% of the annual accumulation, 6.8 g cm^{-2} in comparison to average $12 \text{ g cm}^{-2} \text{ y}^{-1}$).

Winter maxima of marine derived chemistry (e.g. Na, Cr, As) also suggests marine aerosol are sourced from the sea ice surface, in addition to the open ocean. Transport of sea spray to EPG is unlikely to peak during winter despite increased strength of cyclonic circulation (Mullen and Sinclair, 1990) due to proximity and extent of open-ocean during summer (typically < 10 km). Additionally, mesoscale vortices that dominate McMurdo circulation are located within the region of seasonal sea ice cover and are unlikely to transport sea spray during winter (Carrasco and Bromwich, 1994). Rather, frost flowers that form on the surface of young sea ice from brine ejected during the freezing of salt water, are identified as a considerable source of marine aerosols at the polar latitudes (e.g. Thompson and Nelson, 1954; Rankin et al., 2000; Rankin et al., 2002; Wolff et al., 2003). Frost flower production is particularly efficient within the Ross

Sea due to the Ross Sea, McMurdo and Terra Nova polynya systems that force the continual growth of new sea ice (Kaspari et al., 2005; Maqueda et al., 2004; Martin et al., 2007). The contribution of frost flowers to EPG during winter is further supported by depletion of SO_4^{2-} in most winter EPG snow samples (negative nss SO_4^{2-} values calculated for 18 % of all samples). SO_4^{2-} depletion of frost flowers results from the precipitation of mirabilite ($\text{Na}_2\text{SO}_4 \cdot 10\text{H}_2\text{O}$) within sea ice (Minikin et al., 1998; Rankin et al., 2002). Kaspari et al. (2005) previously demonstrated frost flowers are an important source of marine aerosol within the coastal Ross Sea region from snow pit and ice core records from the Siple coast. These records show winter Na maxima that are associated with SO_4^{2-} depletion and are significantly correlated to sea ice extent within the Ross Sea over the last 30 yr.

Another possible source of marine chemistry is the McMurdo Dry Valleys (MDV). The MDV soils are comprised of up to 40 % (by volume) marine salts (Witherow et al., 2006). Transport of this will peak during winter due to increased katabatic wind strength. However such contributions are considered insignificant as EPG sample Na/Cl ratios (median = 0.52 ± 0.20 2σ) approximate marine values (0.55). Conversely, 90 soil samples from the MDV (Antarctic soil database) indicate strong fractionation of salts present (median = 2.8 ± 58 2σ).

5.5.4 Inter-annual changes in elemental chemistry in relation to local meteorology

Sensitivity of the EPG chemistry record to wind strength is confirmed by inter-annual changes in elemental concentrations. Calculation of an elemental flux (i.e. $F_{\text{ice}} = C_{\text{ice}} \cdot A$, where F is the flux of elements to the ice, C is the measured concentration and A the calculated accumulation rate (Legrand and Mayewski, 1997)) demonstrates the same temporal variability as chemistry concentrations. This confirms accumulation rates have remained approximately constant over the time period of interest and are not a major control on EPG chemistry concentrations. Rather, annual maximum wind speeds measured at Cape Ross is significantly ($p < 0.01$) correlated to annual maximum concentrations of Zr, Y, Ba ($r^2 > 0.65$), Ni, Cu, Mn, U ($r^2 > 0.65$), and Al, Fe, Ti, Pb, Zn, Cs, Ce, V, La and Ca ($r^2 > 0.55$) measured in EPG snow samples (Fig. 5.12). Although inter-annual peak concentrations of the remaining elements measured (e.g. Na, Mg, Sr,

Bi) also occur concurrently with maximum Cape Ross wind speeds, the correlation is less significant ($r^2 < 0.50$). This suggests additional controls on chemistry are present such as changes in source region and/or dependence on other meteorological parameters including storm duration (Dunbar et al., 2009). No significant correlations were found between EPG chemistry concentrations and annual average wind speed or wind direction. Maximum concentration of Al (and correlated elements) at EPG during winter 2004 is consistent with the highest sediment flux during the same year in a McMurdo Ice Shelf ice core for the last decade (Dunbar et al., 2009). Assuming constant precipitation rates, past changes in, in particular Y and Zr concentrations provide the most robust proxy of maximum annual wind speed at EPG.

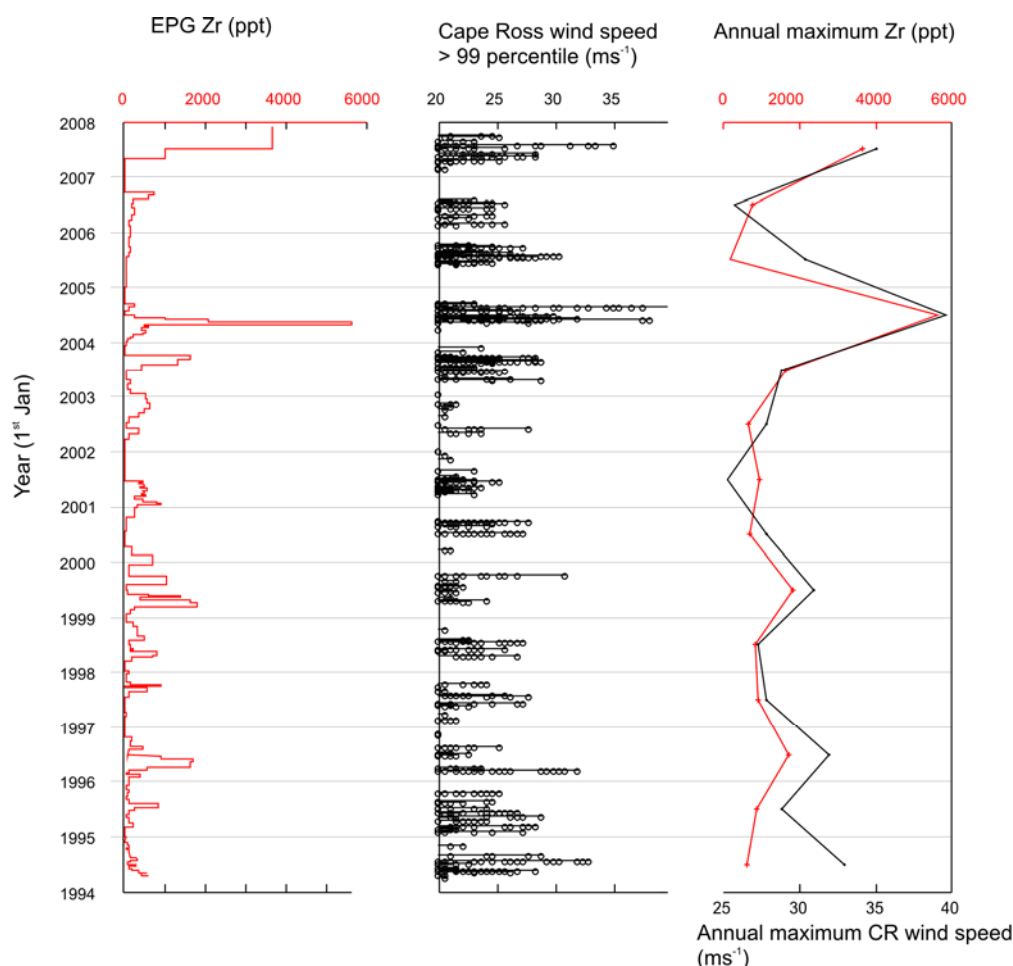


Fig. 5.12 Comparison of EPG elemental chemistry concentrations (e.g. Zr) with Cape Ross maximum wind speed. Maximum wind events are defined as > 99 percentile of all wind speed measurements.

In addition to elemental concentrations, the variation of elemental ratios of terrestrial to marine derived elements (Al/Na) is significant. Changes in Ti/Sr are slightly more subdued than Al/Na due to additional contributions of Sr from terrestrial sources in comparison to marine dominated Na. Similar changes were observed in Ca/Na ratios of non-acidified samples measured by ion chromatography taken from a snow pit sampled at EPG in November 2004 (Bertler, unpublished data). We therefore conclude observed changes in terrestrial/marine derived elemental chemistry do not simply arise from differential acidification and hence leaching of samples. Furthermore, changes in EPG terrestrial/marine elemental ratios are concurrent with changes in the phase relationship between $\delta^{18}\text{O}$ and d excess suggesting a real climate forcing of the chemistry signal.

Temporal changes in terrestrial/marine elemental ratios reflect changes in local mean wind conditions and transport of marine aerosol (Fig. 5.13). Although sea ice extent within the Ross Sea region, and hence marine aerosol source regions was highly variable during the last decade (Arrigo and Thomas, 2004; Rhodes et al., 2009), there is no apparent relationship between maximum sea ice extent and terrestrial/marine elemental ratios (Fig. 5.13). Rather, EPG annual Al/Na averages are most significantly correlated to Cape Ross summer mean wind strength. Annual mean changes in Al/Na are significantly correlated to Cape Ross mean summer wind speed ($r^2 = -0.51$, $p < 0.01$), and less significantly to summer mean wind direction ($r^2 = -0.45$, $p < 0.01$). Correlation of mean annual Ti/Sr with Cape Ross mean summer wind speed is less significant although the trend is similar ($r^2 = -0.43$, $p < 0.05$).

While extreme wind events represent maximum transport of aerosol to glacial records and hence elemental concentrations, elemental ratios reflect variation in the average background input of aerosol. Sensitivity of Al/Na changes to summer wind conditions reflects changes in the transport of Na from marine aerosol during summer when the open ocean source is most proximal. When summer wind strength is reduced, average Na input is significantly altered. Terrestrial derived elements are not as sensitive to changes in summer wind strength due to the dependence of mineral dusts of threshold wind speeds for transport. Ayling and McGowan (2006) report speeds of 5.5 m s^{-1} necessary for entraining and transporting dry and loose fine grained sediment in the McMurdo Dry Valleys. Comparatively, Cape Ross summer mean wind speeds are

consistently $< 5.5 \text{ m s}^{-1}$. Correlation of Al/Na with Cape Ross summer average wind speed is reflective of the reduction in frequency summer southerly storm events that are strong enough to travel over the topographic barrier of Evans Piedmont Glacier (i.e. SW's) (Fig. 5.1).

A change in atmospheric circulation represented by Al/Na in EPG snow is further supported by simultaneous changes in the EPG stable isotope record. $\delta^{18}\text{O}$ and d excess positively co-vary throughout the majority of the EPG snow profile, switching to negative correlation only when Al/Na are at a maximum between winter 2000 and summer 2004/05. On seasonal time scales, negative correlation between $\delta^{18}\text{O}$ and d excess is expected due to the dependence of d excess on precipitation source region humidity, which, being higher during summer results in lower d excess values (Sharp, 2007). Negative correlation of $\delta^{18}\text{O}$ and d excess in snow is demonstrated at most interior Antarctic sites (Aldaz and Deutsch, 1967; Ciais et al., 1995; Oerter, 2004) while any positive correlation is typically attributed to post depositional isotope alteration (Johnsen et al., 2000; Oerter, 2004). However, d excess is positively correlated to $\delta^{18}\text{O}$ within a snow pit profile at coastal Adélie Land where high accumulation is thought to inhibit post depositional diffusion (Ciais et al., 1995), and measurement of samples collected in real time during precipitation events at Franz Josef Glacier in New Zealand (Purdie, 2009), suggests coastal snow and ice records can demonstrate true $\delta^{18}\text{O}$, d positive correlation. Due to high accumulation rates, it is expected post deposition alteration of the EPG isotope record is minimal. Rather, we conclude positive correlation is also a true climate signal at EPG. Without isotope modelling, inferences are limited, but it is proposed that precipitation with positive correlation of $\delta^{18}\text{O}$, d excess is sourced directly from polar latitudes, where semi-arid conditions drive a greater response of d to secondary kinetic fractionation processes (Masson et al., 2000). Conversely, negative correlation suggests more distal transport of precipitation from lower latitudes, similar to that deposited at interior Antarctic sites.

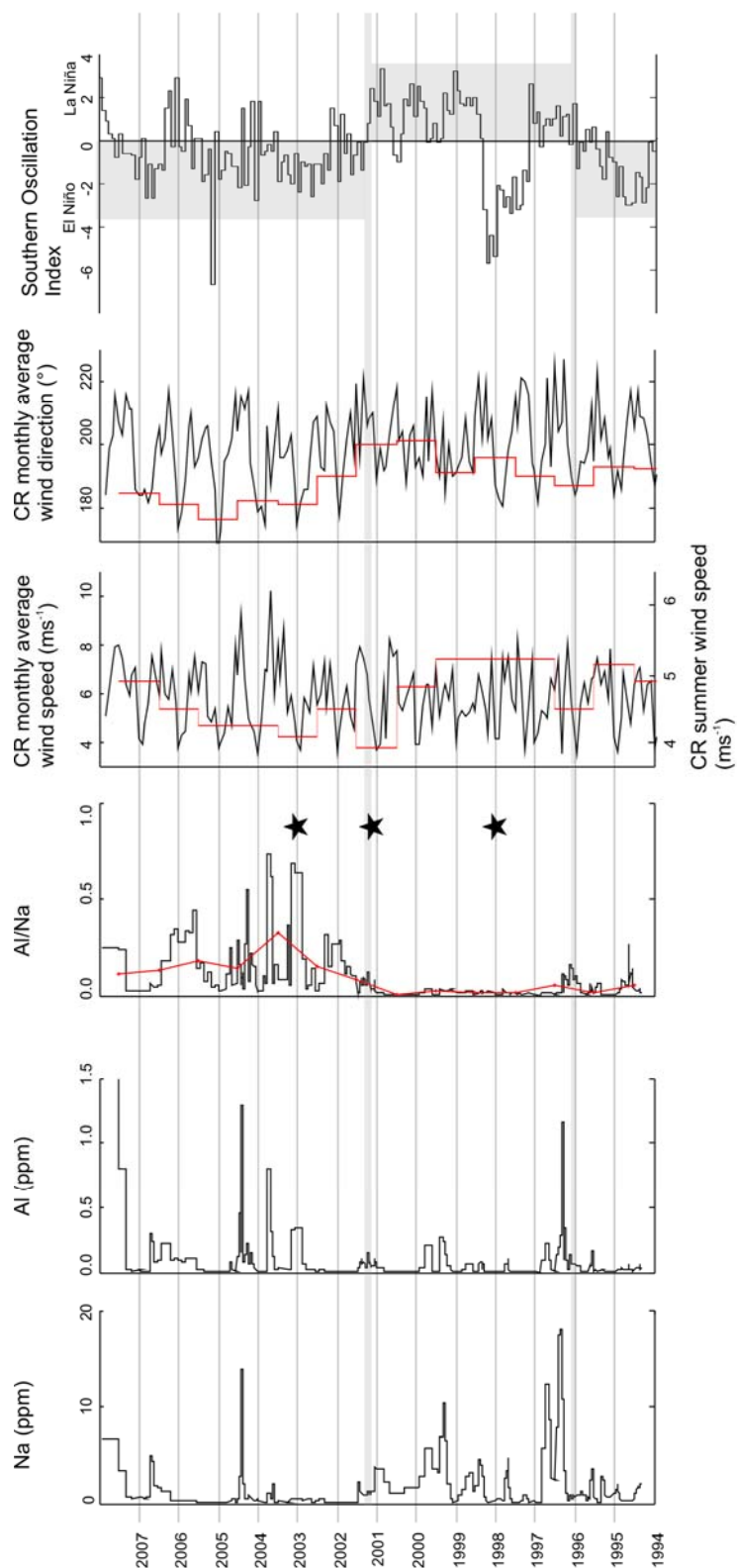


Figure 5.13 Comparison of EPG chemistry (Al, Na and Al/Na) with monthly average Cape Ross wind speed and direction (black). Average summer wind speed and wind direction are shown in red. Changes in EPG chemistry and Cape Ross wind are compared to the Southern Oscillation Index (SOI). Periods of predominantly positive and negative SOI are highlighted in grey. Years of anomalously high sea ice extent within the Ross Sea are also shown with stars (Arrigo and van Dijken, 2004; Rhodes et al., 2009).

We suggest the inter-annual variability of mean summer wind strength measured at Cape Ross, as recorded by Al/Na changes in EPG snow, is driven by mean changes in the El Niño Southern Oscillation. Over the last two decades, the Southern Oscillation Index (SOI) was in a predominantly negative (El Niño phase) between 1990 to 1996, and 2000 to 2008 (Fig. 5.13). Conversely, SOI was predominantly positive (La Niña phase) between 1996 and 2000. The changes in Cape Ross summer wind strength, and EPG Al/Na elemental ratios are consistent with the model of ENSO control on Ross Sea climate proposed by Bertler et al. (2006b). They suggest El Niño conditions are characterised by weakening and movement of the Amundsen Sea Low (L_{AS}) to the Marie Byrd Land coast. This increases the flow of air from across the West Antarctic Ice Sheet (WAIS) to the Ross Sea region, increasing the frequency of extreme katabatic wind events, but reducing the strength of marine derived cyclonic strength (mean summer wind) within the Ross Sea (high Al/Na). Conversely, La Niña conditions are characterised by a strong L_{AS} positioned directly north of the Ross Sea, associated with stronger marine cyclonic activity (mean summer wind strength) and lower katabatic wind strength during winter (low Al/Na). The strong El Niño event which developed during summer 1998/1999 is a obvious exception to this model. However, this event has been identified as unusual due to its rapid onset (McPhaden, 1999). Anomalously low maximum wind conditions prevented summer sea ice break out within the Ross Sea (Arrigo and van Dijken, 2004), suggesting the L_{AS} was not repositioned as expected. Although this EPG snow pit record is too short for significant correlation between terrestrial/marine elemental ratios with the SOI, longer ice core records may be able to confirm this relationship with measured SOI over the last half century.

Finally, ratios of elements derived from terrestrial aerosol sources vary seasonally within the EPG snow pit profile. Fe/Al and Zr/Y are highest during summer when terrestrial aerosol input relative to marine aerosol input to EPG is significant (high Al/Na values) (Fig. 5.9). As seasonal maxima of Fe/Al and Zr/Y are concurrent with element concentration minima, it is possible that ratio changes are inherited from reduced analytical precision when measurements are close to the detection limit. In particular, concentrations of Y are on average 6 times lower than Zr, and will be more sensitive to analytical precision in low concentration samples. However, no concentrations are below the measured detection limit. Rather, we propose that terrestrial/terrestrial

elemental ratios records changes in the mineralogy of terrestrial aerosol transported to EPG. This reflects changes in the dominant aerosol source geology and/or changes in the fractionation of aerosol transported to EPG. Higher Fe/Al values during summer are consistent with decreased summer wind speeds measured at Cape Ross. Lower wind speeds will relatively enrich Fe in EPG samples by preferential transport of easily transported Fe-oxide weathering products, pervasive in the McMurdo Dry Valley soils and on the surfaces of local granite (Bockheim, 2002; Campbell and Claridge, 1975; Kelly and Zumberge, 1961). Conversely, Fe/Al will be reduced during winter due to increased wind strength and a higher flux of heavy, larger dust particles with higher Al concentrations. However, if controlled by wind strength alone, Zr/Y values should also be at a maximum during winter due to the presence of Zr predominantly in high density, erosion resistant zircons that are difficult to transport during weaker summer winds (Chen et al., 2006). Summer maxima of Zr/Y may therefore represent either a change in the dominant source region sampled, or are inherited from analytical uncertainty. For example Zr/Y ratios in samples from the evolved McMurdo Volcanic Group (13.5) are ~ 3 times higher than the Ferrar Dolerite (4.9) (Roser and Pyne, 1989). Further work by micro-probe analysis on dust particles in EPG samples is required to confirm actual changes in mineralogy. However, this study illustrates the potential to relate terrestrial/terrestrial elemental ratios in snow samples to wind strength and wind direction.

5.6.0 Conclusions

ICP-MS elemental analysis of coastal Antarctic snow samples deposited from 1997 to 2008 at Evans Piedmont Glacier demonstrate:

- 1) ICP-MS provides a reliable technique for determination of a broad spectrum of major and trace elements. Detection limits are typically two orders of magnitude below the natural variability between samples.
- 2) Temporal variability of elemental concentrations between samples is at minimum three time higher than the error of repeated sample measurements. Reproducibility of sample measurements is therefore insignificant in terms of relating elemental chemistry to climatic drivers. Complexity of sample measurements arise from the presence of undigested dust particles entering the ICP-MS and is likely to be common in snow and ice core samples from Victoria

Land coastal sites. Distinction needs to be made between measurement of the purely soluble fraction of a sample and the total particulate load. It is recommended that samples are either fully digested following the procedure of Norra and Stüben (2004) or Ruth et al. (2008), or soluble concentration levels are determined from the mode of raw scan data rather than the automated average. Measurement of soluble chemistry in partially acidified samples requires consideration of differential leaching of elements and minerals.

- 3) From modelling based on elemental ratios of snow chemistry with respect to source regions, and the behaviour of elements during time resolved analysis, we conclude marine aerosols are the dominant source of Na, Mg, Cl, SO₄, Sr and As, marine and terrestrial aerosol for Ca, K, and Rb, terrestrial aerosol for Al, Mn, Fe, Ba, Ti, V, Ni, Cr, Y, Zr, Sb, Cs, La, Ce, Pb, Th and U with additional contributions from volcanic (SO₄, K, Bi, Cu, Sb) and anthropogenic (Pb, Zn and As) emissions. Inherent problems with ratio based source modelling, in particular, for particulate mineral dusts include poor constraints on source region chemistry, fractionation during aerosol formation and transport processes, and differential leaching of particulate material in snow samples which require consideration.
- 4) Concentrations of EPG elemental chemistry are a sensitive indicator of local wind strength. In particular, inter-annual variation of terrestrial derived elements are significantly correlated to maximum wind strength measured at Cape Ross (e.g. Zr, $r^2 = 0.68$, $p < 0.01$). Winter maxima of marine aerosol, that are depleted in SO₄ relative to Na, also suggests significant input of marine aerosol during winter from a sea ice surface source.
- 5) Terrestrial/marine elemental ratios provide an indication of mean summer wind conditions at EPG. Al/Na demonstrates a significant negative correlation to summer average wind speed ($r^2 = -0.51$, $p < 0.01$). This is attributed to the sensitivity of average Na concentrations to average summer wind conditions when an open ocean source is most proximal. Changes in summer average wind speed, recorded by Al/Na and concurrent with a change in the $\delta^{18}\text{O}$ and d excess relationship is related to a ENSO driven shift in atmospheric circulation. Terrestrial/ marine elemental ratios in coastal Victoria Land records therefore provide potential to track changes in ENSO back in time.

- 6) Terrestrial/terrestrial elemental ratios have the potential to provide additional proxies of atmospheric circulation, reflective of changes in specific geological source region and wind strength. Increased Fe/Al ratios during summer are concurrent with weaker summer wind flow which will transport only the finest dust particles, including low density and fine-grained secondary Fe-bearing weathering minerals.

Chapter Six: Synthesis and conclusions

6.1.0 Synthesis and conclusions

The primary aim of this work was to develop a reliable technique for trace element analysis of coastal Antarctic snow samples for future application in longer term ice core records. Trace elemental chemistry provides a complimentary data set representing changes in chemistry derived from terrestrial (e.g. Al), anthropogenic (e.g. Pb) and volcanic emission (e.g. Bi) aerosol in addition to major element chemistry which is primarily sourced from marine aerosol (e.g. Na). This has been achieved using inductively coupled plasma mass spectrometry (ICP-MS).

In addition to methodology development, two main research objectives of this work were to: a) determine the main source regions of aerosol deposited trace element chemistry at EPG, and b) to understand the dominant drivers of temporal variation in glaciochemistry with respect to measured meteorological conditions. The salient points identified within this thesis are summarised below.

1. ICP-MS provides a reliable analytical method for the measurement of trace element concentrations in coastal Antarctic snow samples. The main advantage of the ICP-MS analysis technique is its rapid and multi-element abilities coupled with low detection limits. Repeated measurement of external standard SLRS-4, demonstrated that analytical error for major and trace elements is typically below 10 % 2 rsd. In particular, the use of a hydrogen flushed collision cell enables the reliable measurement of Fe, which is an important element due to its potential effect on bio-productivity within the Ross Sea (Atkins and Dunbar, 2009; Dunbar et al., 2009). Elements with no known interferences and/or ultra trace concentrations (Ti, V, Cr, Ni, Cu, Zn, As, Rb, Sr, Y, Zr, Cd, Sb, Cs, Ba, La, Ce, Pb, Bi, Th and U) were measured without the collision cell to increase count sensitivity. Although polyatomic ion interferences may be problematic for some elements (Cr, Ni, Cu, Zn, Cs, Pb and Bi), analytical error is typically two orders of magnitude lower than sample to sample variation and therefore insignificant.

2. The minimum internal sample variability of elemental chemistry concentrations is one third of sample to sample variation and therefore inconsequential to the interpretation of temporal changes. Poor reproducibility of sample measurements is attributed to the presence of dust particles which enter into the ICP-MS. Particulate material will effect average elemental ratios through preferential leaching of some elements dependent on mineralogy and grain size, which has implications for ratio based source modelling of chemistry.

3. The behaviour of elements during ICP-MS time resolved analysis and correlation to regional source geology, allows more reliable determination of terrestrial input to EPG snow than ratio source modelling using averaged upper continental crust (UCC) ratios. Determining the terrestrial contribution of an element through comparison to a conservative element such as Al and Ba with respect to UCC is hindered by fractionation of elemental ratios both during sample acidification, and more dominantly, through natural processes such as differences in source geology and fractionation from whole rock composition during weathering and transport processes. Although all trace elements indicate < 50 % contribution from a terrestrial UCC source, we attribute mineral dusts as the dominant source of Al, Mn, Fe, Ba, Ti, V, Ni, Cr, Y, Zr, Sb, Cs, La, Ce, Pb, Th and U. This is supported by poor reproducibility of these elements when measured by time resolved analysis, due to peaks in signal intensity, resulting from high element concentrations in particulate material.

4. Concentrations of all elements, irrespective of source region, demonstrate typically winter seasonal maxima. This is attributed to the increased strength of atmospheric circulation during winter which passes over multiple aerosol source regions. Decreased winter precipitation may also effectively concentrate elemental chemistry. Winter marine aerosol is derived at least in part from the sea ice surface, in agreement with previous studies in the Ross Sea region (Kaspari et al., 2005).

5. Inter-annual variability of elemental chemistry is controlled by maximum wind speed. Concentrations of EPG elemental chemistry are a sensitive indicator of local wind strength. In particular, inter-annual variation of terrestrial derived elements are significantly correlated to maximum wind strength measured at Cape Ross (e.g. Zr, $r^2 =$

0.68, $p < 0.01$). Maximum concentration of terrestrial derived elements during winter 2004 is concurrent with the strongest wind speeds over the last decade, as observed other glacial records from the Victoria Land coastal region (Dunbar et al., 2009)

6. Elemental ratios of terrestrial/marine derived chemistry provide an indication of mean wind conditions. In particular, Al/Na demonstrates a significant negative correlation to summer average wind speed ($r^2 = -0.51$, $p < 0.01$). This is attributed to the sensitivity of average Na concentrations to average summer wind conditions when an open ocean source is most proximal.

7. Positive correlation of $\delta^{18}\text{O}$ and d excess is attributed to precipitation derived from a polar latitude source region. Previous studies attribute positive correlation of $\delta^{18}\text{O}$ and d excess to post depositional alteration of the d excess signal. This is however unlikely at EPG due to high annual accumulation rates ($12 \text{ g cm}^{-2} \text{ yr}^{-1}$). Further, changes in $\delta^{18}\text{O}$ and d excess are concurrent with high Al/Na, supporting a change in atmospheric circulation. Conversely, we interpret negative correlation, which is observed at interior Antarctic sites (Aldaz and Deutsch, 1967; Ciais et al., 1995; Oerter, 2004) as indicative of precipitation derived from a lower latitude source, transported over the Antarctic continent before arrival at EPG.

8. EPG terrestrial/marine elemental ratios and stable isotope chemistry record changes in the mean state of ENSO within the Ross Sea. Low Al/Na ratios and negative correlation of $\delta^{18}\text{O}$ and d excess in EPG snow are concurrent with a predominantly negative ENSO (El Niño). This is attributed to increased strength and position of the Amundsen Sea Low directly north of the Ross sea, increasing direct flow of marine air onto the Victoria Land coast (high summer mean wind speeds). Conversely, high Al/Na ratios and positive correlation of $\delta^{18}\text{O}$ and d excess are concurrent with positive ENSO (La Niña). This is associated with weakening and repositioning to the Amundsen Sea Low to Marie Byrd Land coast, increasing air flow across the West Antarctic Ice Sheet to the Victoria Land coast. Longer term study of this relationship is required which is currently statistically insignificant. The EPG chemistry record can be extended through analysis of the 180 m firn core drilled at EPG in summer 2004/05 (Bertler et al., 2005).

6.2.0 Suggestions for future work

This study has identified a number of complexities in trace element and stable isotope ratio chemistry of coastal Antarctic snow, which are applicable to wider ice core climatology studies. Furthermore, EPG provides a suitable site for a longer glaciochemical record. The following recommendations are therefore made to further: a) develop the methodology of trace element ICP-MS analysis further with respect to the presence of dust particulates, b) calibrate modern day glaciochemistry to climate controls and c) increase the temporal and spatial extent of coastal trace element records.

1) Trace element method development

We recommend a series of experiments to understand the effects of dust particles on snow chemistry and how elemental ratios reflect the mineralogy of terrestrial aerosols. Dust particles are likely to be present in snow and ice core records at most coastal Antarctic sites where rock outcrops are proximal. Therefore, such experiments will provide constraints for the NZ ITASE program. Furthermore, these experiments would be applicable to lower latitude ice core records, which are expected to have a high dust flux such as in the Southern Alps New Zealand (Morgenstern et al., 2006).

1. Experimental study into the leaching behaviour of trace elements when partially dissolved in 1 % HNO_3 . The effects of partial leaching of elements from dust particles are particularly important for elemental ratios used commonly in source region modelling. The study of Snäll and Liljefors (2000), who measured the leachability of K, Na, Ca, Mg, Al and Ti in acids of variable strength from different minerals and from different particle size fractions could be extended to include a wider array of trace elements which were measured in EPG snow samples. Furthermore, the leaching behaviour of the specific dusts present in EPG samples should be assessed. This could be achieved through comparison of elemental concentrations determined by ICP-MS in 1 % HNO_3 leached samples and samples fully digested using stronger acids such as HF, adapting the methodology of Ruth et al. (2008). Duration of acidification with respect to leaching of elements from the sample tubes, how the size fraction of particulate material effects the time required for sample digestion, and the scavenging of some elements by other compounds should also be addressed through laboratory control experiments.

2. *Study into the viability of centrifuging samples to analyse soluble snow chemistry.* An alternative approach to the presence of particulate material in samples would be to extract particulate material and analyse soluble chemistry only. The soluble fraction of terrestrial derived elements may be more indicative of wider regional source processes, with finer, more soluble material transported greater distances. Soluble chemistry could potentially be measured by centrifuging samples and analysing the upper portion of analyte only. Preliminary work is required to understand what fractionation of particulate material is then analysed, potential contamination errors and viability of this on a large number of samples which need to be analysed for ice core records. An alternative method utilises acid washed syringe filter systems, which allows contamination free removal of particulates. Such an approach would also permit a quantitative study of particulate concentration in each sample and would provide material for geochemical and petrographic analyses.

3. *Microprobe study of the temporal changes in mineralogy of dust particles in snow samples with respect to elemental ratio changes.* EPG snow pit chemistry demonstrated temporal fluctuations in elemental ratios between terrestrial elements such as Fe/Al or Zr/Y. It is hypothesised these ratios reflect changes in the dominant mineralogy of terrestrial aerosol transported to EPG and are therefore indicative of wind strength and/or direction. However, all maxima are concurrent with low elemental concentrations and it is also possible ratio changes are inherited from reduced analytical precision close to the detection limit. To determine the potential of terrestrial/terrestrial elemental ratios to reflect climatic driven changes in terrestrial aerosol mineralogy, the composition of dust needs to be assessed through microprobe analysis. Furthermore, grain size measurements using a coulter-counter system (e.g. Petit et al., 1999) would confirm increases in windiness, reflected through larger grain sizes and transport of heavier minerals (e.g. zircon). If fully understood, terrestrial/terrestrial elemental ratios have the potential to indicate wind speed and wind direction rather than time consuming mineralogy studies and grain size analysis.

2) Understanding meteorological controls on trace element chemistry

The simultaneous controls of aerosol source region, atmospheric transport and post-depositional alteration of snow pack chemistry, in addition to seasonal dating resolution,

complicate the correlation of glaciochemistry to atmospheric circulation at sub-seasonal resolution. Rather, daily collection of fresh snow samples over an extended time period (weeks to months) would allow more robust comparison and hence greater understanding of chemistry source regions and climatic controls. In particular, the true nature of the $\delta^{18}\text{O}$, d excess relationship at coastal Antarctic sites should be established without the potential error of post depositional diffusion. Back trajectory models such as TRAJKS (Stohl, 2001) and HYSPLIT (Air Resource Laboratory) can determine the pathway of an air mass over days prior to arriving at a specified location. This is useful for identification of precipitation source regions and potential controls on the isotope ratio signature of precipitation (Schlosser, 2004). Furthermore, Global Circulation Modelling of precipitation packages sourced from high latitude oceans may increase insight into how a positive $\delta^{18}\text{O}$, d excess signal is produced (Jouzel et al., 2007).

3) Temporal and spatial extension of coastal glaciochemistry

We have demonstrated that EPG provides a site of high snow accumulation and hence high resolution of sub-seasonal changes in glaciochemistry that are sensitive to changes in local wind strength and direction. The EPG firn core record has the potential to demonstrate annual changes in regional climate, and should be extended for major and trace element chemistry in addition to stable isotope ratios. Relation of this record to the long term Scott Base meteorological record which extends back to 1957 will allow more robust correlation between climatic controls and glaciochemistry. Furthermore, increased spatial distribution of trace element chemistry studies will increase our understanding of present day controls, in a similar manner that major element chemistry has been related to elevation, distance inland and proximity to source region (Bertler et al., 2005).

References

- Aldaz, L., and Deutsch, S. (1967). On a relationship between air temperature and oxygen isotope ratio of snow and firn in south pole region *Earth and Planetary Science Letters* **3**, 267-274.
- Alley, R., Meese, D., Shuman, A., Gow, A., Taylor, K., Grootes, P., White, J., Ram, M., Waddington, E., Mayewski, P., and Zielinski, G. (1993). Abrupt increase in Greenland snow accumulation at the end of the Younger Dryas event. *Nature* **362**, 527-529.
- Alley, R. B. (1988). Concerning the deposition and diagenesis of strata in polar firn. *Journal of Glaciology* **34**, 283-290.
- Alley, R. B. (2000). The Younger Dryas cold interval as viewed from central Greenland. *Quaternary Science Reviews* **19**, 213-226.
- Alley, R. B., Saltzman, E. S., Cuffey, K. M., and Fitzpatrick, J. J. (1990). Summertime formation of depth hoar in central Greenland. *Geophysical Research Letters* **17**, 2393-2396.
- Alley, R. B., Shuman, C. A., Meese, D. A., Gow, A. J., Taylor, K. C., Cuffey, K. M., Fitzpatrick, J. J., Grootes, P. M., Zielinski, G. A., Ram, M., Spinelli, G., and Elder, B. (1997). Visual-stratigraphic dating of the GISP2 ice core: Basis, reproducibility, and application. *Journal of Geophysical Research-Oceans* **102**, 26367-26381.
- Araguas-Araguas, L., Froehlich, K., and Rozanski, K. (2000). Deuterium and oxygen-18 isotope composition of precipitation and atmospheric moisture. *Hydrological Processes* **14**, 1341-1355.
- Arrigo, K. R., and Thomas, D. N. (2004). Large scale importance of sea ice biology in the Southern Ocean. *Antarctic Science* **16**, 471-486.
- Arrigo, K. R., and van Dijken, G. L. (2004). Annual changes in sea-ice, chlorophyll a, and primary production in the Ross Sea, Antarctica. *Deep-Sea Research Part II-Topical Studies in Oceanography* **51**, 117-138.
- Atkins, C. B., and Dunbar, G. B. (2009). Aeolian sediment flux from sea ice into Southern McMurdo Sound, Antarctica. *Global and Planetary Change* **69**, 133-141.
- Augustin, L., Barbante, C., Barnes, P. R. F., Barnola, J. M., Bigler, M., Castellano, E., Cattani, O., Chappellaz, J., Dahljensen, D., Delmonte, B., Dreyfus, G., Durand, G., Falourd, S., Fischer, H., Fluckiger, J., Hansson, M. E., Huybrechts, P., Jugie, R., Johnsen, S. J., Jouzel, J., Kaufmann, P., Kipfstuhl, J., Lambert, F., Lipenkov, V. Y., Littot, G. V. C., Longinelli, A., Lorrain, R., Maggi, V., Masson-Delmotte, V., Miller, H., Mulvaney, R., Oerlemans, J., Oerter, H., Orombelli, G., Parrenin, F., Peel, D. A., Petit, J. R., Raynaud, D., Ritz, C., Ruth, U., Schwander, J., Siegenthaler, U., Souchez, R., Stauffer, B., Steffensen, J. P., Stenni, B., Stocker, T. F., Tabacco, I. E., Udisti, R., van de Wal, R. S. W., van den Broeke, M.,

- Weiss, J., Wilhelms, F., Winther, J. G., Wolff, E. W., Zucchelli, M., and Members, E. C. (2004). Eight glacial cycles from an Antarctic ice core. *Nature* **429**, 623-628.
- Ayling, B. (2001). "Dust accumulation on the Victoria Lower Glacier and Wilson Piedmont, coastal south Victoria Land, Antarctica, and its potential as a paleowind indicator." Victoria University of Wellington.
- Ayling, B. F., and McGowan, H. A. (2006). Niveo-eolian sediment deposits in coastal South Victoria Land, Antarctica: Indicators of regional variability in weather and climate. *Arctic Antarctic and Alpine Research* **38**, 313-324.
- Barbante, C., Bellomi, T., Mezzadri, G., Cescon, P., Scarpon, G., Morel, C., Jay, S., Van de Velde, K., Ferrari, C., and Bouton, C. (1997). Direct determination of heavy metals at picogram per gram levels in Greenland and Antarctic snow by double focused inductively coupled plasma mass spectrometry. *Journal of analytical atomic spectrometry* **12**, 925-931.
- Basile, I., Grousset, F., Revel, M., Petit, J., Biscaye, P., and Barkov, N. (1997). Patagonian origin of glacial dust deposited in East Antarctica (Vostok and Dome C) during glacial stages 2,4 and 6. *Earth and Planetary Science Letters* **146**, 573-589.
- Bertler, N., Barrett, P., Mayewski, P., Fogt, R., Kreutz, K., and Shulmeister, J. (2004a). El Nino suppresses Antarctic warming. *Geophysical Research Letters* **31**, L15207.
- Bertler, N., Mayewski, P., Barrett, P., Sneed, S., Handley, M., and Kreutz, K. (2004b). Monsoonal circulation of the McMurdo Dry Valleys, Ross Sea region, Antarctica: signal from the snow chemistry. *Annals of Glaciology* **39**, 139-145.
- Bertler, N., Mayewski, P., Sneed, S., Naish, T., Morgenstern, U., and Barrett, P. (2005). Solar forcing recorded by aerosol concentrations in coastal Antarctic glacier ice, McMurdo Dry Valleys. *Annals of Glaciology* **41**, 52-56.
- Bertler, N., Naish, T., Oerter, H., Kipfstuhl, S., Barrett, P., Mayewski, P., and Kreutz, K. (2006a). The effect of joint ENSO-Antarctic Oscillation forcing on the McMurdo Dry Valleys, Antarctica. *Antarctic Science* **18**, 507-514.
- Bertler, N. A. N. (2003). "Understanding the Climate Behaviour of the McMurdo Dry Valleys, Antarctica, from Coastal Ice Cores: A Thesis Submitted to the Victoria University of Wellington in Fulfilment of the Requirements for the Degree of Doctor of Philosophy in Geology." Victoria University of Wellington.
- Bertler, N. A. N. (unpublished data). EPG snow pit record from 2004.
- Bertler, N. A. N., Naish, T.R., Mayewski, P.A., Barrett, R.J. (2006b). Opposing oceanic and atmospheric ENSO influences on the Ross Sea region, Antarctica. *Advances in Geosciences* **6**, 83-86.
- Bockheim, J. G. (2002). Landform and soil development in the McMurdo Dry Valleys, Antarctica: a regional synthesis. *Arctic Antarctic and Alpine Research* **34**, 308-317.

- Boutron, C., Echevin, M., and Lorius, C. (1972). Chemistry of polar snows. Estimation of rates of deposition in Antarctica. *Geochimica Et Cosmochimica Acta* **36**, 1029-1041.
- Boutron, C., and Lorius, C. (1979). Trace metals in Antarctic snow since 1914. *Nature* **277**, 551-554.
- Bradley, R. S., Vuille, M., Hardy, D., and Thompson, L. G. (2003). Low latitude ice cores record Pacific sea surface temperatures. *Geophysical Research Letters* **30**.
- Bromwich, D., Carrasco, J., Liu, Z., Tzeng, R.Y. (1993). Hemispheric atmospheric variations and oceanographic impacts associated with katabatic surges across the Ross Ice Shelf, Antarctica. *Journal of Geophysical Research* **98**, 13045-13062.
- Bromwich, D. H. (1988). Snowfall in high southern latitudes. *Reviews of Geophysics* **26**, 149-168.
- Bromwich, D. H., Carrasco, J. F., Liu, Z., and Tzeng, R. Y. (1993). Hemispheric atmospheric variations and oceanographic impacts associated with katabatic surges across the Ross Ice Shelf, Antarctica. *Journal of Geophysical Research-Atmospheres* **98**, 13045-13062.
- Bromwich, D. H., and Parish, T. R. (1998). Meteorology of the Antarctic. *Meteorological Monographs* **49**, 175-200.
- Bruland, K. W., and Lohan, M. C. (2003). Controls of Trace Metals in Seawater. In "Treatise on Geochemistry." (K. K. Turekian, and H. D. Holland, Eds.).
- Campbell, I. B., and Claridge, G. G. C. (1975). Morphology and age relationships of Antarctic soil. In "Quaternary Studies: Selected Papers from IX INQUA Congress." pp. 87. Royal Society of New Zealand, Christchurch, New Zealand.
- Carleton, A. M., and Fitch, M. (1993). Synoptic aspects of Antarctic mesocyclones *Journal of Geophysical Research-Atmospheres* **98**, 12997-13018.
- Carlson, A. E., Legrande, A. N., Oppo, D. W., Came, R. E., Schmidt, G. A., Anslow, F. S., Licciardi, J. M., and Obbink, E. A. (2008). Rapid early Holocene deglaciation of the Laurentide ice sheet. *Nature Geoscience* **1**, 620-624.
- Carrasco, J. F., and Bromwich, D. H. (1994). Climatological aspects of mesoscale cyclogenesis over the Ross Sea and Ross Ice Shelf regions of Antarctica. *Monthly Weather Review* **122**, 2405-2425.
- Carrasco, J. F., Bromwich, D. H., and Monaghan, A. J. (2003). Distribution and characteristics of mesoscale cyclones in the Antarctic: Ross Sea eastward to the Weddell Sea. *Monthly Weather Review* **131**, 289-301.
- Chen, J., Chen, Y., Liu, L. W., Ji, J. F., Balsam, W., Sun, Y. B., and Lu, H. Y. (2006). Zr/Rb ratio in the Chinese loess sequences and its implication for changes in the East Asian winter monsoon strength. *Geochimica Et Cosmochimica Acta* **70**, 1471-1482.

- Chester, R. (2000). "Marine Geochemistry." Blackwell Science Ltd, Oxford UK.
- Chinn, T. (1990). "The Dry Valleys." DSIR Publishing, Wellington.
- Ciais, P., White, J. W. C., Jouzel, J., and Petit, J. R. (1995). The origin of present-day Antarctic precipitation from surface snow deuterium excess data. *Journal of Geophysical Research-Atmospheres* **100**, 18917-18927.
- Clements, T., Stone, R. O., Mann, J. F., and Eymann, J. L. (1963). A study of windborne sand and dust in desert areas. In "Technical Report." Army Natick Labs, Ma, Earth Science Lab.
- Comiso, J. C. (2000). Variability and trends in Antarctic surface temperatures from in situ and satellite infrared measurements. *Journal of Climate* **13**, 1674-1696.
- Connolley, W. M. (1996). The Antarctic temperature inversion. *International Journal of Climatology* **16**, 1333-1342.
- Connolley, W. M., and Cattle, H. (1994). The Antarctic Climate of the UKMO Unified Model. *Antarctic Science* **6**, 115-122.
- Craig, H. (1961). Isotopic variations in meteoric waters. *Science* **133**, 1702-1703.
- CRNC, N. R. C. C. (1998). SLRS-4 River water reference material for trace metals.
- Cullather, R. I., Bromwich, D. H., and Van Woert, M. L. (1996). Interannual variations in Antarctic precipitation related to El Nino southern oscillation. *Journal of Geophysical Research-Atmospheres* **101**, 19109-19118.
- Curran, M., Ommen, T., Morgan, V., Phillips, K., and Palmers, A. (2003). Ice core evidence for Antarctic sea ice decline since the 1950s. *Science* **302**, 1203-1206.
- Curran, M. A. J., Palmer, A. S., Van Ommen, T. D., Morgan, V. I., Phillips, K., McMorrow, A. J., and Mayewski, P. A. (2001). Post-depositional movement of methanesulphonic acid at Law Dome, Antarctica, and the influence of accumulation rate. In "International Symposium on Ice Cores and Climate." (E. W. Wolff, Ed.), pp. 333-339, Kangerlussuaq, Greenland.
- Dansgaard, W. (1954). The O¹⁸- abundance in fresh water. *Geochimica et Cosmochimica Acta* **6**, 241-260.
- Dansgaard, W., Johnsen, S., Moller, J., and Langway, C. (1969). One thousand centuries of climatic record from Camp Century on the Greenland ice. *Science* **166**, 377-380.
- Davidson, C. I., Chu, L., Grimm, T. C., Nasta, M. A., and Qamoos, M. P. (1981). Wet and dry deposition of trace-elements onto the Greenland Ice-Sheet. *Atmospheric Environment* **15**, 1429-1437.
- Delmonte, B., Petit, J. R., Andersen, K. K., Basile-Doelseh, I., Maggi, V., and Lipenkov, V. Y. (2004). Dust size evidence for opposite regional atmospheric circulation

changes over east Antarctica during the last climatic transition. *Climate Dynamics* **23**, 427-438.

Doran, P. T., Priscu, J. C., Lyons, W. B., Walsh, J. E., Fountain, A. G., McKnight, D. M., Moorhead, D. L., Virginia, R. A., Wall, D. H., Clow, G. D., Fritsen, C. H., McKay, C. P., and Parsons, A. N. (2002). Antarctic climate cooling and terrestrial ecosystem response. *Nature* **415**, 517-520.

Duce, R., Hoffman, G., and Zoller, W. (1975). Atmospheric trace metals at remote Northern and Southern Hemisphere sites: pollution or natural? *Science* **187**, 59-61.

Duce, R. A., and Hoffman, E. J. (1976). Chemical fractionation at the air/sea interface. *Annual review of earth and planetary sciences* **4**, 187-228.

Dunbar, G. B., Bertler, N. A. N., and McKay, R. M. (2009). Sediment flux through the McMurdo Ice Shelf in Windless Bight, Antarctica. *Global and Planetary Change* **69**, 87-93.

Ekaykin, A., Lipenkov, V., Barkov, N., Petit, J., and Masson-Delmotte, V. (2002). Spatial and temporal variability in isotopic composition of recent snow in the vicinity of Vostok station, Antarctica: implications for ice-core record interpretation. *Annals of Glaciology* **35**, 181-186.

Epstein, S., Sharp, R. P., and Gow, A. J. (1970). Antarctic Ice Sheet - Stable isotope analysis of Byrd Station cores and inter-hemispheric climate implications. *Science* **168**, 1570-1572.

Falconer, T. R., and Pyne, A. R. (2004). Ice breakout history in southern McMurdo Sound, Antarctica (1988-2002). In "Antarctic Data Series."

Faure, G., and Mensing, T. M. (2005). "Isotopes: principles and applications." John Wiley and Sons Inc. .

Fischer, H., Fundel, F., Ruth, U., Twarloh, B., Wegner, A., Udisti, R., Becagli, S., Castellano, E., Morganti, A., Severi, M., Wolff, E., Littot, G., Rothlisberger, R., Mulvaney, R., Hutterli, M. A., Kaufmann, P., Federer, U., Lambert, F., Bigler, M., Hansson, M., Jonsell, U., de Angelis, M., Boutron, C., Siggaard-Andersen, M. L., Steffensen, J. P., Barbante, C., Gaspari, V., Gabrielli, P., and Wagenbach, D. (2007a). Reconstruction of millennial changes in dust emission, transport and regional sea ice coverage using the deep EPICA ice cores from the Atlantic and Indian Ocean sector of Antarctica. *Earth and Planetary Science Letters* **260**, 340-354.

Fischer, H., Siggaard-Andersen, M. L., Ruth, U., Rothlisberger, R., and Wolff, E. (2007b). Glacial/interglacial changes in mineral dust and sea-salt records in polar ice cores: Sources, transport, and deposition. *Reviews of Geophysics* **45**.

Fischer, H., Traufetter, F., Oerter, H., Weller, R., and Miller, H. (2004). Prevalence of the Antarctic Circumpolar Wave over the last two millenia recorded in Dronning Maud Land ice. *Geophysical Research Letters* **31**.

- Fisher, D., Osterberg, E., Dyke, A., Dahl-Jensen, D., Demuth, M., Zdanowicz, C., Bourgeois, J., Koerner, R. M., Mayewski, P., Wake, C., Kreutz, K., Steig, E., Zheng, J., Yalcin, K., Goto-Azuma, K., Luckman, B., and Rupper, S. (2008). The Mt Logan Holocene-late Wisconsinan isotope record: Tropical Pacific-Yukon connections. *Holocene* **18**, 667-677.
- Fisher, H., Traufetter, F., Oerter, H., Weller, R., Miller, H. (2004). Prevalence of the Antarctic Circumpolar Wave over the last two millenia recorded in Dronning Maud Land ice. *Geophysical research letters* **31**.
- Fogt, R., and Bromwich, D. (2006). Decadal variability of the ENSO teleconnection to the high-latitude South Pacific governed by coupling with the Southern Annular Mode. *Journal of climate* **19**, 979-997.
- Fountain, A. G., Dana, G. L., Lewis, K. J., Vaughn, D., McKnight, D., and Priscu, J. C. (1998). "Glaciers of the McMurdo Dry Valleys, southern Victoria Land, Antarctica." American Geophysical Union, Washington, DC.
- Froehlich, K., Gibson, J. J., and Aggarwal, P. (2002). Deuterium excess in precipitation and its climatological significance. *Isotope Techniques. C & S Papers Series* **13**, 54-66.
- Gabrielli, P., Planchon, F., Hong, S., Hyun Lee, K., Hur, S., Barbante, C., Ferrari, C., Petit, J., Lipenkov, V., Cascon, P., and Bouton, C. (2005). Trace elements in Vostok Antarctic ice during the last four climate cycles. *Earth and Planetary Science Letters* **234**, 249-259.
- Gaspari, V., Barbante, C., Cozzi, G., Cescon, P., Boutron, C. F., Gabrielli, P., Capodaglio, G., Ferrari, C., Petit, J. R., and Delmonte, B. (2006). Atmospheric iron fluxes over the last deglaciation: Climatic implications. *Geophysical Research Letters* **33**.
- Gat, J. R. (1996). Oxygen and hydrogen isotopes in the hydrologic cycle. *Annual Review of Earth and Planetary Sciences* **24**, 225-262.
- Gibson, E. K., Wentworth, S. J., and McKay, D. S. (1983). Chemical Weathering and Diagenesis of a Cold Desert Soil from Wright Valley, Antarctica: An Analogue of Martian Weathering Processes. *Journal of Geophysical Research* **88(Supplement)** A912-A928.
- Goktas, F., Fischer, H., Oerter, H., Weller, R., Sommer, S., and Miller, H. (2002). A glacio-chemical characterization of the new EPICA deep-drilling site on Amundsenisen, Dronning Maude Land, Antarctica. *Annals of Glaciology* **35**, 347-354.
- Gong, D. Y., and Wang, S. W. (1999). Definition of Antarctic Oscillation Index. *Geophysical Research Letters* **26**, 459-462.
- Goodwin, I. D., van Ommen, T. D., Curran, M. A. J., and Mayewski, P. A. (2004). Mid latitude winter climate variability in the South Indian and southwest Pacific regions since 1300 AD. *Climate Dynamics* **22**, 783-794.

- Grotti, M., Soggia, F., and Todoli, J. (2008). Ultra-trace analysis of Antarctic snow samples by reaction cell inductively coupled plasma mass spectrometry using a total-consumption micro-sample-introduction system. *Analyst* **133**, 1388-1394.
- Hall, A., and Visbeck, M. (2002). Synchronous variability in the southern hemisphere atmosphere, sea ice, and ocean resulting from the annular mode. *Journal of Climate* **15**, 3043-3057.
- Helsen, M. M., van de Wal, R. S. W., van den Broeke, M. R., Masson-Delmotte, V., Meijer, H. A. J., Scheele, M. P., and Werner, M. (2006). Modelling the isotopic composition of Antarctic snow using backward trajectories: Simulation of snow pit records. *Journal of Geophysical Research-Atmospheres* **111**.
- Hinkley, T. K., Lamothe, P. J., Wilson, S. A., Finnegan, D. L., and Gerlach, T. M. (1999). Metal emissions from Kilauea, and a suggested revision of the estimated worldwide metal output by quiescent degassing of volcanoes. *Earth and Planetary Science Letters* **170**, 315-325.
- Hur, S., Cunde, X., Hong, S., Barbante, C., Gabrielli, P., Lee, K., Bouton, C., and Ming, Y. (2007). Seasonal patterns of heavy metal deposition to the snow on Lambert Glacier basin, East Antarctica. *Atmospheric Environment* **41**, 8567-8578.
- Hutton, R. C., and Eaton, A. N. (1987). Role of aerosol water vapour loading in inductively coupled plasma mass spectrometry. *Journal of Analytical Spectrometry* **2**, 595-598.
- Johnsen, S., Clausen, J., Henrick, B., Cuffey, K., Hoffmann, G., Schwander, J., and Creyts, T. (2000). Diffusion of stable isotopes in polar firn and ice: the isotope effect in firn diffusion. *Physics of Ice Core Records*, 121-140.
- Johnsen, S. J. (1977). Stable isotope homogenization of polar firn and ice. *International Association of Hydrological Sciences Publication*, **118**, 210-219.
- Jouzel, J. (2003). Water stable isotopes: Atmospheric composition and applications in polar ice core studies. In "Treatise on Geochemistry." (H. D. Holland, and K. K. Turekian, Eds.), pp. 213-239. The Atmosphere. Elsevier.
- Jouzel, J. (2007). Water Stable Isotopes: Atmospheric Composition and Applications in Polar Ice Core Studies. *Treatise of Geochemistry* **4.08**, 213-243.
- Jouzel, J., Stievenard, M., Johnsen, S. J., Landais, A., Masson-Delmotte, V., Sveinbjornsdottir, A., Vimeux, F., von Grafenstein, U., and White, J. W. C. (2007). The GRIP deuterium-excess record. *Quaternary Science Reviews* **26**, 1-17.
- Kaspari, S., Sixon, D. A., Sneed, S. B., and Handley, M. J. (2005). Sources and transport pathways of marine aerosol species into West Antarctica. *Annals of Glaciology* **41**, 1-9.
- Kelly, W. C., and Zumberge, J. H. (1961). Weathering of a quartz diorite at Marble Point, McMurdo Sound, Antarctica. *Journal of Geology* **69**, 433-446.

- King, J. C., and Turner, J. (1997). "Antarctic meteorology and climatology." Cambridge University Press.
- Kreutz, K., and Mayewski, P. (1999). Spatial variability of Antarctic surface snow glaciochemistry: implications for paleo-atmospheric circulation reconstructions. *Antarctic Science* **11**, 105-118.
- Kreutz, K. J., Mayewski, P. A., Meeker, L. D., Twickler, M. S., and Whitlow, S. I. (2000a). The effect of spatial and temporal accumulation rate variability in West Antarctica on soluble ion deposition. *Geophysical Research Letters* **27**, 2517-2520.
- Kreutz, K. J., Mayewski, P. A., Pittalwala, II, Meeker, L. D., Twickler, M. S., and Whitlow, S. I. (2000b). Sea level pressure variability in the Amundsen Sea region inferred from a West Antarctic glaciochemical record. *Journal of Geophysical Research-Atmospheres* **105**, 4047-4059.
- Kreutz, K. J., Mayewski, P. A., Twickler, M. S., Whitlow, S. I., White, J. W. C., Shuman, C. A., Raymond, C. F., Conway, H., and McConnell, J. R. (1999). Seasonal variations of glaciochemical, isotopic and stratigraphic properties in Siple Dome (Antarctica) surface snow. *Annals of Glaciology* **29**, 38-44.
- Krinner, R., Jouzel, J., Suozzo, R., Russel, G., Broecker, W., Rind, D., and Eagleson, P. (1997). Global sources of local precipitations as determined by the NASA/GISS GCM. *Geophysical research letters* **43**, 121-124.
- Kwok, R., and Comiso, J. (2002a). Spatial patterns of variability in Antarctica surface temperature: connections to the Southern Hemisphere Annular Mode and the Southern Oscillation. *Geophysical research letters* **29**, 1705.
- Kwok, R., and Comiso, J. C. (2002b). Southern Ocean climate and sea ice anomalies associated with the Southern Oscillation. *Journal of Climate* **15**, 487-501.
- Lambert, S., Delmonte, B., Petit, J., Bigler, M., Kaufmann, P., Hutterli, M., Stocker, T., Ruth, U., Steffensen, J., and Maggi, V. (2008). Dust - climate couplings over the past 800,000 years from the EPICA Dome C ice core. *Nature* **452**, 616-618.
- Lancaster, N. (2002). Flux of eolian sediment in the McMurdo Dry Valleys, Antarctica: a preliminary assessment. *Arctic Antarctic and Alpine Research* **34**, 318-323.
- Lantzy, R., and MacKenzie, F. T. (1979). Atmospheric trace metals: global cycles and assessment of man's impact. *Geochimica et Cosmochimica Acta* **43**, 511-525.
- Le Cloarec, M. F., and Marty, B. (1990). Volatile fluxes from Volcanoes. *Terra Review* **3**, 17-27.
- Ledley, T., and Huang, Z. (1997). A possible ENSO signal in the Ross Sea. *Geophysical research letters* **24**, 3253-3256.
- Legrand, M., and Mayewski, P. (1997). Glaciochemistry of polar ice core: a review. *Reviews of Geophysics* **35**, 219-243.

- Lettau, B. (1969). Transport of moisture into Antarctic interior. *Tellus* **21**, 331-340.
- Maqueda, M. A. M., Willmott, A. J., and Biggs, N. R. T. (2004). Polynya dynamics: A review of observations and modelling. *Reviews of Geophysics* **42**.
- Marshall, G. (2003). Trends in the Southern Annular Mode from Observations and Reanalysis. *Journal of climate* **16**, 4134-4143.
- Marshall, G. (2007). Half-century seasonal relationships between the Southern Annular Mode and Antarctic temperatures. *International Journal of Climatology* **27**, 373-383.
- Marteel, A., Gaspari, V., Boutron, C. F., Barbante, C., Gabrielli, P., Cescon, P., Cozzi, G., Ferrari, C. P., Dommergue, A., Rosman, K., Hong, S. M., and Hur, S. D. (2009). Climate-related variations in crustal trace elements in Dome C (East Antarctica) ice during the past 672 kyr. *Climatic Change* **92**, 191-211.
- Martin, S., Drucker, R. S., and Kwok, R. (2007). The areas and ice production of the western and central Ross Sea polynyas, 1992-2002, and their relation to the B-15 and C-19 iceberg events of 2000 and 2002. *Journal of Marine Systems* **68**, 201-214.
- Martin, S., Yu, Y. L., and Drucker, R. (1996). The temperature dependence of frost flower growth on laboratory sea ice and the effect of the flowers on infrared observations of the surface. *Journal of Geophysical Research-Oceans* **101**, 12111-12125.
- Masson-Delmotte, V., Hou, S., Ekaykin, A., Jouzel, J., Aristarain, A., Bernardo, R. T., Bromwich, D., Cattani, O., Delmotte, M., Falourd, S., Frezzotti, M., Gallee, H., Genoni, L., Isaksson, E., Landais, A., Helsen, M. M., Hoffmann, G., Lopez, J., Morgan, V., Motoyama, H., Noone, D., Oerter, H., Petit, J. R., Royer, A., Uemura, R., Schmidt, G. A., Schlosser, E., Simoes, J. C., Steig, E. J., Stenni, B., Stievenard, M., van den Broeke, M. R., de Wal, R., de Berg, W. J. V., Vimeux, F., and White, J. W. C. (2008). A review of Antarctic surface snow isotopic composition: Observations, atmospheric circulation, and isotopic modeling. *Journal of Climate* **21**, 3359-3387.
- Masson-Delmotte, V., Jouzel, J., Landais, A., Stievenard, M., Johnsen, S. J., White, J. W. C., Werner, M., Sveinbjornsdottir, A., and Fuhrer, K. (2005). GRIP deuterium excess reveals rapid and orbital-scale changes in Greenland moisture origin. *Science* **309**, 118-121.
- Masson, V., Vimeux, F., Jouzel, J., Morgan, V., Delmotte, M., Ciais, P., Hammer, C., Johnsen, S., Lipenkov, V. Y., Mosley-Thompson, E., Petit, J. R., Steig, E. J., Stievenard, M., and Vaikmae, R. (2000). Holocene climate variability in Antarctica based on 11 ice-core isotopic records. *Quaternary Research* **54**, 348-358.
- Mayewski, P., and Goodwin, I. (1997). ITASE Science and Implementation Plan. In "Join PAGES/GLOCANT Report."

- Mayewski, P., and Lyons, W. (1982). Source and climate implications of reactive iron and reactive silicate concentrations found in an ice core from Meserve Glacier, Antarctica. *Geophysical Research Letters* **9**, 190-192.
- Mayewski, P., Lyons, W. B., Zielinski, G., Twickler, M., Whitlow, S., Dibb, J., Grootes, P., Taylor, K., Whung, P. Y., and Fosberry, L. (1995). An ice core based late Holocene history for the Transantarctic Mountains, Antarctica. *Antarctic Research Series* **67**, 33-45.
- Mayewski, P. A., Frezzotti, M., Bertler, N., Van Ommen, T., Hamilton, G., Jacka, T. H., Welch, B., Frey, M., Qin, D., Ren, J. W., Simoes, J., Fily, M., Oerter, H., Nishio, F., Isaksson, E., Mulvaney, R., Holmund, P., Lipenkov, V., and Goodwin, I. (2004). The International Trans-Antarctic Scientific Expedition (ITASE): an overview. In "28th Symposium of the Scientific-Committee on Antarctic Research." (G. Hamilton, Ed.), pp. 180-185, Bremen, Germany.
- McPhaden, M. J. (1999). Genesis and evolution of the 1997-98 El Nino. *Science* **283**, 950-954.
- Michalski, G., Bockheim, J. G., Kendall, C., and Thiemens, M. (2005). Isotopic composition of Antarctic Dry Valley nitrate: Implications for NO_y sources and cycling in Antarctica. *Geophysical Research Letters* **32**.
- Minikin, A., Legrand, M., Hall, J., Wagenbach, D., Kleefeld, C., Wolff, E., Pasteur, E. C., and Ducroz, F. (1998). Sulfur-containing species (sulfate and methanesulfonate) in coastal Antarctic aerosol and precipitation. *Journal of Geophysical Research-Atmospheres* **103**, 10975-10990.
- Monaghan, A. J., Bromwich, D. H., Powers, J. G., and Manning, K. W. (2005). The climate of the McMurdo, Antarctica, region as represented by one year of forecasts from the Antarctic Mesoscale Prediction System. *Journal of Climate* **18**, 1174-1189.
- Monahan, E., Spiel, D., and Davidson, K. (1986). "A model of marine aerosol generation via whitecaps and wave disruption." Norwell Mass.
- Monnin, E., Indermuhle, A., Dallenbach, A., Fluckiger, J., Stauffer, B., Stocker, T. F., Raynaud, D., and Barnola, J. M. (2001). Atmospheric CO₂ concentrations over the last glacial termination. *Science* **291**, 112-114.
- Morgenstern, U., Mayewski, P. A., Bertler, N., and Ditchburn, R. G. (2006). Ice core research in the New Zealand Southern Alps. *Geochimica Et Cosmochimica Acta* **70**, A430-A430.
- Mullen, A., and Sinclair, M. (1990). Climate and weather. In "Antarctica, the Ross Sea region." pp. 98-117. DSIR publishing, Wellington, New Zealand.
- Mulvaney, R., Wagenbach, D., and Wolff, E. W. (1998). Post-depositional change in snow-pack nitrate from observation of year-round near-surface snow in coastal Antarctica. *Journal of Geophysical Research-Atmospheres* **103**, 11021-11031.

- Norra, S., and Stuben, D. (2004). Trace element patterns and seasonal variability of dust precipitation in a low polluted city - The example of Karlsruhe/Germany. *Environmental Monitoring and Assessment* **93**, 203-228.
- O'Brien, S. R., Mayewski, P. A., Meeker, L. D., Meese, D. A., Twickler, M. S., and Whitlow, S. I. (1995). Complexity of Holocene climate as reconstructed from a Greenland ice core *Science* **270**, 1962-1964.
- Oerter, H., Graf, W., Meyer H., Wilhelms, F. (2004). The EPICA ice core from Dronning Maud Land: first results from stable-isotope measurements. *Annals of Glaciology* **39**, 307-312.
- Osterberg, E., Handley, M., Sneed, S., Mayewski, P., and Kreutz, K. (2006). Continuous ice core melter system with discrete sampling for major ion, trace element, and stable isotope analysis. *Environmental Science Technology* **40**, 3355-3361.
- Pacyna, J. (1984). Estimations of the atmospheric emissions of trace elements from anthropogenic sources in Europe. *Atmospheric Environment* **18**, 41-50.
- Parish, T. (1988). Surface winds over the Antarctic continent: A review. *Reviews of Geophysics* **26**, 169-180.
- Parish, T. R., and Bromwich, D. H. (1987). The surface windfield over the Antarctic ice sheets. *Nature* **328**, 51-54.
- Parish, T. R., and Cassano, J. J. (2003). The role of katabatic winds on the Antarctic surface wind regime. *Monthly Weather Review* **131**, 317-333.
- Parrenin, F., Jouzel, J., Waelbroeck, C., Ritz, C., and Barnola, J. M. (2001). Dating the Vostok ice core by an inverse method. *Journal of Geophysical Research-Atmospheres* **106**, 31837-31851.
- Patterson, N., Bertler, N., Naish, T., and Morgenstern, U. (2005). ENSO variability in the deuterium-excess record of a coastal Antarctic ice core from McMurdo Dry Valleys, Victoria Land. *Annals of Glaciology* **41**, 140-146.
- Petit, J., et al. (1999). Climate and atmospheric history of the past 420,000 years from the Vostok ice core, Antarctica. *Nature* **399**, 429-436.
- Petit, J. R., Briat, M., and Royer, A. (1981). Ice-age aerosol content from East Antarctic ice core samples and past wind strength *Nature* **293**, 391-394.
- Petit, J. R., Jouzel, J., Raynaud, D., Barkov, N. I., Barnola, J. M., Basile, I., Bender, M., Chappellaz, J., Davis, M., Delaygue, G., Delmotte, M., Kotlyakov, V. M., Legrand, M., Lipenkov, V. Y., Lorius, C., Pepin, L., Ritz, C., Saltzman, E., and Stievenard, M. (1999). Climate and atmospheric history of the past 420,000 years from the Vostok ice core, Antarctica. *Nature* **399**, 429-436.
- Philander, S. G. H. (1983). El-Nino Southern Oscillation phenomena. *Nature* **302**, 295-301.

- Planchon, F. A. M., Boutron, C. F., Barbante, C., Cozzi, G., Gaspari, V., Wolff, E. W., Ferrari, C. P., and Cescon, P. (2002a). Changes in heavy metals in Antarctic snow from Coats Land since the mid-19th to the late-20th century. *Earth and Planetary Science Letters* **200**, 207-222.
- Planchon, F. A. M., Boutron, C. F., Barbante, C., Cozzi, G., Gaspari, V., Wolff, E. W., Ferrari, C. P., and Cescon, P. (2002b). Short-term variations in the occurrence of heavy metals in Antarctic snow from Coats Land since the 1920s. *Science of the Total Environment* **300**, 129-142.
- Purdie, H. (2009). PhD Candidate (V. U. o. W. Antarctic Research Centre, Ed.), Wellington.
- Pye, K. (1987). Aeolian dust and dust deposits. Academic Press, London.
- Rankin, A. M., and Wolff, E. W. (2002). Frost flowers: Implications for tropospheric chemistry and ice core interpretation. *Journal of Geophysical Research* **107**.
- Rankin, A. M., Wolff, E. W., and Auld, V. (2000). Frost Flowers as a source of fractionated sea salt aerosol in the polar regions. *Geophysical Research Letters* **27**, 3469-3472.
- Rankin, A. M., Wolff, E. W., and Martin, S. (2002). Frost flowers: Implications for tropospheric chemistry and ice core interpretation. *Journal of Geophysical Research-Atmospheres* **107**.
- Reimann, C., and De Caritat, P. (2000). Intrinsic flaws of element enrichment factors (EFs) in environmental geochemistry. *Environmental Science & Technology* **34**, 5084-5091.
- Revel-Rolland, M., De Deckker, P., Delmonte, B., Hesse, P. P., Magee, J. W., Basile-Doelsch, I., Grousset, F., and Bosch, D. (2006). Eastern Australia: A possible source of dust in East Antarctica interglacial ice. *Earth and Planetary Science Letters* **249**, 1-13.
- Rhodes, R. H., Bertler, N. A. N., Baker, J. A., Sneed, S. B., Oerter, H., and Arrigo, K. R. (2009). Sea ice variability and primary productivity in the Ross Sea, Antarctica, from methylsulphonate snow record. *Geophysical Research Letters* **36**.
- Riley, J. P., and Chester, R. (1971). Introduction to marine chemistry. Academic Press, London and New York.
- Rockey, C. C., and Braaten, D. A. (1995). Characterization of polar cyclonic activity and relationship to observed snowfall events at McMurdo Station, Antarctica. *Fourth Conference on Polar Meteorology and Oceanography*, 244-245.
- Roduskin, I. (2003). Use of semi-quantitative calibration mode for rapid sample screening. In "Analytica AB, Application note: AN30005_E." Thermo Electro Corporation.

- Roser, B. P., and Pyne, A. R. (1989). Wholerock geochemistry. In "Antarctic Cenozoic history from the CIROS-1 drillhole, McMurdo Sound." (P. J. Barrett, Ed.), pp. 175-184. DSIR, Wellington, New Zealand.
- Rudnick, R. L., and Gao, S. (2003). Composition of the Continental Crust. In "Treatise on Geochemistry." (H. D. Holland, and K. K. Turekian, Eds.), pp. 1-64. Elsevier.
- Ruth, U., Barbante, C., Bigler, M., Delmonte, B., Fischer, H., Gabrielli, P., Gaspari, V., Kaufmann, P., Lambert, F., Maggi, V., Marino, F., Petit, J. R., Udisti, R., Wagenbach, D., Wegner, A., and Wolff, E. W. (2008). Proxies and measurement techniques for mineral dust in antarctic ice cores. *Environmental Science & Technology* **42**, 5675-5681.
- Salamatin, A. N., Lipenkov, V. Y., Barkov, N. I., Jouzel, J., Petit, J. R., and Raynaud, D. (1998). Ice core age dating and paleo-thermometer calibration based on isotope and temperature profiles from deep boreholes at Vostok Station (East Antarctica). *Journal of Geophysical Research-Atmospheres* **103**, 8963-8977.
- Schlosser, E., Oerter, H., (2002a). Seasonal variations of accumulation and the isotope record in ice cores: a study with surface snow samples and firn cores from Neumayer station, Antarctica. *Annals of Glaciology* **35**, 97-101.
- Schlosser, E., Oerter, H., (2002b). Shallow firn cores from Neumayer, Ekstromisen, Antarctica: a comparison of accumulation rates and stable-isotope rates. *Annals of Glaciology* **35**.
- Schlosser, E., Oerter, H., Masson-Delmotte, V., Reigmer, C., . (2008). Atmospheric influence on the deuterium excess signal in polar firn - implications for ice core interpretation. *Journal of glaciology* **54**, 117-124
- Schlosser, E., Reijmer, C., Oerter, H., Graf, W., (2004). The influence of precipitation origin on the d18O-T relationship at Neumayer station, Ekstromisen, Antarctica. *Annals of Glaciology* **39**.
- Schwander, J., Jouzel, J., Hammer, C. U., Petit, J. R., Udisti, R., and Wolff, E. (2001). A tentative chronology for the EPICA Dome Concordia ice core. *Geophysical Research Letters* **28**, 4243-4246.
- Schwerdtfeger, W. (1970). The climate of the Antarctic. Climates of the Polar Regions. In "World Survey of Climatology." (H. E. Landsberg, Ed.), pp. 253-355. Elsevier.
- Schwerdtfeger, W. (1984). "Weather and climate of the Antarctic." Elsevier, Amsterdam.
- Sharp, Z. (2007). Principles of Stable Isotope Geochemistry. *Perason Prentice Hall Publishers, USA*.
- Sinclair, K. (2009). Post Doctoral Fellow in Ice Core Research (G. Science, Ed.), Wellington.

- Sinclair, M. R. (1982). Weather observations in the Ross Island Area, Antarctica. New Zealand Meteorological Service, Wellington.
- Smith, J., Vance, D., Kemp, R., Archer, C., Toms, P., King, M., and Zarate, M. (2003). Isotopic constraints on the source of Argentinian loess - with implications for atmospheric circulation and the provenance of Antarctic dust during recent glacial maxima. *Earth and Planetary Science Letters* **212**, 181-196.
- Snäll, S., and Liljefors, T. (2000). Leachability of major elements from minerals in strong acids. *Journal of Geochemical Exploration* **71**, 1-12.
- Steffensen, J. P., Andersen, K. K., Bigler, M., Clausen, H. B., Dahl-Jensen, D., Fischer, H., Goto-Azuma, K., Hansson, M., Johnsen, S. J., Jouzel, J., Masson-Delmotte, V., Popp, T., Rasmussen, S. O., Rothlisberger, R., Ruth, U., Stauffer, B., Siggaard-Andersen, M. L., Sveinbjornsdottir, A. E., Svensson, A., and White, J. W. C. (2008). High-resolution Greenland Ice Core data show abrupt climate change happens in few years. *Science* **321**, 680-684.
- Steig, E. J., Schneider, D. P., Rutherford, S. D., Mann, M. E., Comiso, J. C., and Shindell, D. T. (2009). Warming of the Antarctic ice-sheet surface since the 1957 International Geophysical Year. *Nature* **457**, 459-U4.
- Stohl, A., Heimberger, M., Scheele, M., Wernli, H. (2001). An intercomparison of results from three trajectory models. *Meteorology applications* **8**.
- Suttie, E. D., and Wolff, E. W. (1992). Seasonal input of heavy metals to Antarctic snow. *Tellus* **44B**, 351-357.
- Taylor, K. (2007). Ice Cores: History of Research, Greenland and Antarctica. In "Encyclopedia of Quaternary Science." (S. Elias, Ed.). Elsevier.
- Taylor, L., and Gligozi, J. (1964). "Distribution of particulate matter in a firn core from Eights Station, Antarctica." American Geophysical Union, Washington DC.
- Thompson, D. W. J., and Wallace, J. M. (2000). Annular modes in the extra-tropical circulation. Part I: Month-to-month variability. *Journal of Climate* **13**, 1000-1016.
- Thompson, L. G., and Mosley Thompson, E. (1981). Micro-particle concentration variations linked with climatic change - evidence from polar ice cores *Science* **212**, 812-815.
- Thompson, L. G., Yao, T., Davis, M. E., Henderson, K. A., MosleyThompson, E., Lin, P. N., Beer, J., Synal, H. A., ColeDai, J., and Bolzan, J. F. (1997). Tropical climate instability: The last glacial cycle from a Qinghai-Tibetan ice core. *Science* **276**, 1821-1825.
- Tranter, M. (2003). Geochemical weathering in glacial and pro-glacial environments. In "Treatise on geochemistry" (H. D. Holland, and K. K. Turekian, Eds.), pp. 190-203. Elsevier.

- Tsoar, H., and Pye, K. (1987). Dust transport and the question of loess formation. *Sedimentology* **34**, 139-153.
- Turekian, K. K. (1968). Oceans. Prentice-Hall, Englewood, Cliffs.
- Turner, J. (2004). Review: The El Nino-Southern Oscillation and Antarctica. *International Journal of Climatology* **24**.
- Turner, J., Colwell, S., Marshall, G., Lachlan-Cope, T., Carleton, A., Jones, P., Lagun, V., Reid, P., and Iagovinka, S. (2005). Antarctic climate change during the last 50 years. *International Journal of Climatology* **25**, 279-294.
- Ugolini, F. C., and Jackson, M. L. (1982). Weathering and mineral synthesis in Antarctic soil. In "Antarctic Geoscience." pp. 1101-1108. University of Madison, Wisconsin.
- Vallelonga, P., Barbante, C., Cozzi, G., Gaspari, V., Candelone, J., Van de Velde, K., Morgan, V., Rosman, K., Bouton, C., and Cescon, P. (2004). Elemental indicators of natural and anthropogenic aerosol inputs to Law Dome, Antarctica. *Annals of Glaciology* **39**.
- Van den Broeke, M. R., and Van Lipzig, N. P. M. (2002). Impact of polar vortex variability on the wintertime low-level climate of East Antarctica: results of a regional climate model. *Tellus Series a-Dynamic Meteorology and Oceanography* **54**, 485-496.
- van den Broeke, M. R., and van Lipzig, N. P. M. (2004). Changes in Antarctic temperature, wind and precipitation in response to the Antarctic Oscillation. *Annals of Glaciology, Vol 39, 2005* **39**, 119-126.
- Vimeux, F., Cuffey, K. M., and Jouzel, J. (2002). New insights into Southern Hemisphere temperature changes from Vostok ice cores using deuterium excess correction. *Earth and Planetary Science Letters* **203**, 829-843.
- Waddington, E., Morse, D., Grootes, P., and Steig, E. (1993). The connection between ice dynamics and paleoclimate from ice cores: a study of Taylor Dome, Antarctica. In "Ice in the Climate System." (W. Peltier, Ed.), pp. 499-518. Springer Verlag, Berlin.
- Wagenbach, D., Ducroz, F., Mulvaney, R., Keck, L., Minikin, A., Legrand, M., Hall, J. S., and Wolff, E. W. (1998). Sea-salt aerosol in coastal Antarctic regions. *Journal of Geophysical Research-Atmospheres* **103**, 10961-10974.
- Wagenbach, D., Ducroz, F., Mulvaney, R., Keck, L., Minikin, A., Legrand, M., Hall, J. S., Wolff, E. W., (1998). Sea-salt aerosol in coastal Antarctic regions. *Journal of Geophysical Research* **103**, 10961-10974.
- Wedepohl, K. H. (1995). The composition of the continental crust. *Geochimica et Cosmochimica Acta* **59**, 1217-1232.

- Welsh, K., Mayewski, P., and Whitlow, S. (1993). Methanesulfonic acid in coastal Antarctic snow related to sea ice extent. *Geophysical Research Letters* **20**, 443-446.
- Whillans, I., and Grootes, P. (1985). Isotope diffusion in cold snow and firn. *Journal of Geophysical Research-Atmospheres* **90**, 3910-3918.
- White, A. F. (2003). Natural weathering rates of silicate minerals. In "Treatise on Geochemistry." (H. D. Holland, and K. K. Turekian, Eds.), pp. 134-164. Elsevier.
- Witherow, R., Lyons, B., Bertler, N., and 6 others. (2006). The aeolian flux of calcium, chloride, and nitrate to the McMurdo Dry Valleys landscape: evidence from snow pit analysis. *Antarctic Science* **18**, 497-505.
- Witherow, R. A., Lyons, W. B., Bertler, N. A. N., Welch, K. A., Mayewski, P. A., Sneed, S. B., Nylen, T., Handley, M. J., and Fountain, A. (2006). The aeolian flux of calcium, chloride and nitrate to the McMurdo Dry Valleys landscape: evidence from snow pit analysis. *Antarctic Science* **18**, 497-505.
- Wolff, E., Rankin, A., and Rothlisberger, R. (2003). An ice core indicator of Antarctic sea ice production. *Geophysical research letters* **30**, 2158.
- Wolff, E. W., Fischer, H., Fundel, F., Ruth, U., Twarloh, B., Littot, G. C., Mulvaney, R., Rothlisberger, R., de Angelis, M., Boutron, C. F., Hansson, M., Jonsell, U., Hutterli, M. A., Lambert, F., Kaufmann, P., Stauffer, B., Stocker, T. F., Steffensen, J. P., Bigler, M., Siggaard-Andersen, M. L., Udisti, R., Becagli, S., Castellano, E., Severi, M., Wagenbach, D., Barbante, C., Gabrielli, P., and Gaspari, V. (2006). Southern Ocean sea-ice extent, productivity and iron flux over the past eight glacial cycles. *Nature* **440**, 491-496.
- Wolff, E. W., and Suttie, E. D. (1994). Antarctic snow record of Southern Hemisphere lead pollution. *Geophysical Research Letters* **21**, 781-784.
- Wolff, E. W., Suttie, E. D., and Peel, D. A. (1999). Antarctic snow record of cadmium, copper, and zinc content during the twentieth century. *Atmospheric Environment* **33**, 1535-1541.
- Zreda-Gostynska, G., and Kyle, P. R. (1997). Volcanic gas emissions from Mount Erebus and their impact on the Antarctic environment. *Journal of Geophysical Research* **102**, 15039-15055.

Appendix One: Sampling and analytical techniques

A1.1.0 Introduction

This appendix provides additional description of the Evans Piedmont Glacier (EPG) snow profile sampling and analytical techniques described in Chapter 5.3.

A1.2.0 Snow pit sampling

A 4 m deep snow profile was sampled at EPG from two separate ~2 m accessible sections. A well developed hoar horizon at 190 cm depth and 3 cm of overlapping samples were used to correlate between the two sections. Stable isotope ratios of equivalent samples demonstrate comparable values with $\delta^{18}\text{O} = -26.7\text{‰}$, -26.3‰ and -26.4‰ at 188 cm, 189 cm and 190 cm depths, respectively, from the lower section and $\delta^{18}\text{O} = -27.1\text{‰}$, -26.3‰ and -25.4‰ at 188 cm, 189 cm and 190 cm depths, respectively, from the upper section compared to an average seasonal variation of $\delta^{18}\text{O} = 7\text{‰}$. Elemental chemistry of samples from the lower section increase up to a peak (Na = 2846 ppb at 190 cm depth, Na = 2625 ppb at 189 cm depth and Na 3252 ppb at 188 cm depth) which is not sampled by the upper section (Na = 520 ppb at 190 cm depth, Na = 647 ppb at 189 cm depth and Na = 710 ppb at 188 cm depth). This is attributed to differential deposition of aerosol at the site.

Physical description of crystal structure and approximate crystal size were noted during and after sampling. The upper 1.5 m section of the sampling wall was constructed into a thin (1-3 cm) translucent section to determine stratigraphy more clearly (Fig A1.1). Snow density measurements were made on a freshly cut surface of the snow pit profile after chemistry sampling was completed. Cylinders that were 5 cm in diameter were inserted horizontally at 2.5 cm overlapping intervals, filled with care to avoid compaction, and weighed. Density and physical description are used together to determine the location and width of hoar horizons and snow and ice layers used for dating (Fig. 4.1).

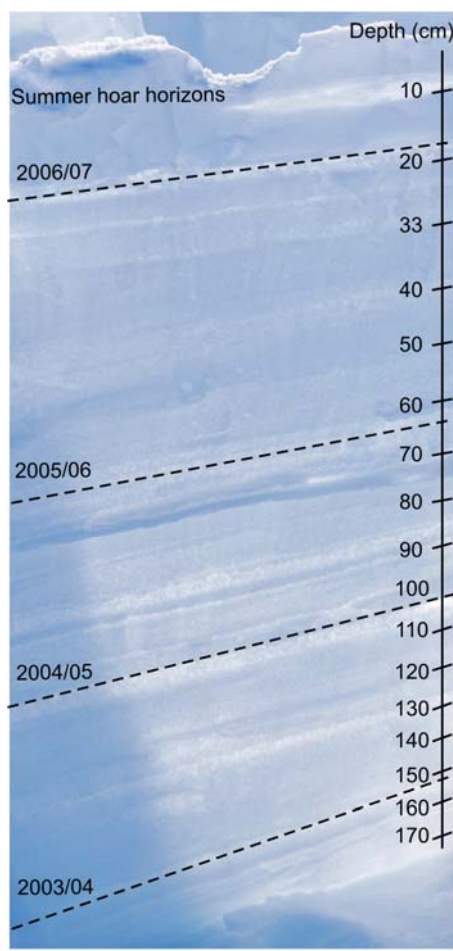


Figure A1.1 Snow stratigraphy of the upper 1.7 m of the EPG snow pit profile. Summer hoar horizons are shown with dashed lines.

A1.3.0 Ion chromatography analyses

In addition to Ca^+ , Cl^- , K^+ , Mg^+ , Na^+ , SO_4^{2-} described in Chapter 5, ionic species methylsulphonate (MS^-) and nitrate (NO_3^-) (Table A2.2) were also measured by ion chromatography using the same anion methodology. MS is particularly useful for dating of EPG_2004 and EPG_2005 snow pit profiles (Fig. 4.1).

A1.4.0 Inductively coupled plasma mass spectrometry (ICP-MS)

A1.4.1 Spectral interferences

A hydrogen flushed collision cell was used during ICP-MS analysis of Na, Mg, Ca, Fe, Mn and Ba to reduce polyatomic ion interferences from oxidation of the argon carrier gas, in particular, $^{40}\text{Ar}^{16}\text{O}$ on ^{56}Fe . Initial tests demonstrated that flushing the collision

cell with hydrogen rather than helium was more effective in removing polyatomic species and does not effect the reproducibility of other elements (Table A1.1). This is supported by the previous study of Iglesias et al. (2002).

	Na (ppb)	Mg (ppb)	Ca (ppb)	Mn (ppb)	Fe (ppb)	Sr (ppb)	Ba (ppb)
Certified SLRS-4 values	2400	1600	6200	3.4	103	26	12.2
a) He flushed collision cell							
SLRS-4 1	2236	1605	596	3.6	86	29	12.5
SLRS-4 2	2274	1592	612	3.5	69	29	12.8
SLRS-4 3	2429	1592	647	3.6	82	29	12.7
SLRS-4 4	2047	1622	644	3.5	119	29	11.9
Average	2247	1603	625	3.5	89	29	12.5
2 σ	314	29	49	0.05	42	0.4	0.78
2 rsd (%)	14	2	8	1	48	2	6
Difference from certified value (%)	-6	0	-90	5	-14	10	2
b) H flushed collision cell							
SLRS-4 1	2454	1625	2692	3.4	107	29	11.5
SLRS-4 2	2549	1654	2692	3.5	110	29	12.6
SLRS-4 3	2796	1677	2721	3.5	111	30	12.8
SLRS-4 4	2697	1654	2779	3.5	108	29	12.3
SLRS-4 5	2688	1684	2965	3.4	109	29	12.3
Average	2637	1659	2770	3.5	109	29	12.3
2 σ	270	46	229	0.09	3.0	0.60	0.96
2 rsd (%)	10	3	8	3	3	2	8
Difference from certified value (%)	10	4	-55	3	6	11	1

Table A1.1 Comparison of repeated measurement of the external standard SLRS-4 (Environment Canada, 1998) by ICP-MS with **a)** He flushed collision cell and **b)** H flushed collision cell. Analytical precision of Ca was greatly improved for sample measurements since these initial tests.

Spectral interferences were kept minimal for all analyses by optimising plasma conditions. The highest effective temperature within the plasma was achieved by adjusting the carrier gas flow rate. Additionally, the sample introduction spray chamber was maintained at a constant 2°C to reduce the water loading of the plasma (Hutton and Eaton, 1987) and nitric acid was chosen as the preferred analytical matrix as it does not increase polyatomic interferences (Tan and Horlick, 1986).

A1.4.2 Quantification of elements

Elemental concentrations were determined from ICP-MS count data using bracketing analyses of in-house calibration standards. These were measured after every ~5 samples to monitor temporal drift in instrument sensitivity which is affected by external factors

including ambient room temperature and sample uptake rate. Standards were acidified to 1 % HNO₃ and prepared daily from 5 % HNO₃ acidified stock solution to avoid precipitation of elements over the extended analysis period. Elemental concentrations in the calibration standards were made to approximate average sample concentrations. This was determined as necessary by initial ICP-MS collision cell analysis of EPG snow samples and external standard SLRS-4, using a 1 ppb element standard. The signal intensity of the blank corrected, 1 ppb calibration standard decreased considerably for Na, Ca and Mg during analysis due to increasing background levels from residue of high sample concentrations (e.g. mean EPG Na concentration of 1652 ppb). Blank measurements increased from close to detection limit to ~1-2 ppb Na over the analytical period of 15 samples. Although in comparison to sample concentration, such background levels are insignificant, errors introduced on the calibration standard significantly altered the determined concentration, resulting in up to 100 % error on SLRS-4 analyses of Na. When calibrated to the 10 ppb standard measured at the beginning of the analysis, SLRS-4 errors were reduced to 15 %. Therefore standards for both collision cell and non-collision cell ICP-MS analyses were prepared with concentrations approximating sample concentrations (Table 5.2). Further, samples with concentrations >900 ppb Mg measured within collision cell ICP-MS analysis were run separately for trace element analysis during non-collision cell ICP-MS analysis to reduce increasing background levels. This also allowed the use of a more suitable calibration standard, which was ten times in higher concentration than that used for the bulk of non-collision cell ICP-MS analyses.

A1.4.3 Pulse/analogue factors

The two to three order of magnitude variability between sample concentrations required the calibration of pulse/analog (P/A) factors for ²³Na, ²⁴Mg, ²⁷Al, ⁴⁴Ca, ⁵⁶Fe, ⁴⁷Ti, ⁶³Cu, ⁸⁸Sr, ⁹⁰Zr, ¹³³Cs, ¹³⁹La and ¹⁴⁰Ce. This is the calibration between changing pulse (high counts) and analogue (low counts) counting modes of the ICP-MS detector system. P/A factors were measured every three days using a separate standard with approximately one million counts of each element with concentrations dependent on daily sensitivity. The bulk standard was not used to avoid the introduction of high background levels into the ICP-MS, for example, of the high Na and Ca concentrations required to gain enough counts of Fe and Al during major element analyses.

A1.4.4 Washout procedure

Background levels between samples were kept at a minimum by washout of ICP-MS system by progressively aspirating ultra-clean water ($>18.2\text{ M}\Omega$), sub-boiled 5 % HNO_3 , and SeaStar grade 1 % HNO_3 (Table 5.1). Additionally, the ICP-MS system was cleaned with HNO_3 for 20 min between each analysis set of ~ 30 samples. When this was considered insufficient (as determined by blank measurements), the spray chamber was soaked in 5 % HNO_3 for ~ 12 hr.

A1.4.5 ICP-MS analytical precision and accuracy

Measured Na and Ca concentrations of SLRS-4 are systemically lower than Environment Canada certified values, but within the range reported in the literature (Rodushkin et al., 2003; Osterberg et al., 2006). Differences are therefore attributed to real variability in SLRS-4 aliquots. Although determination of low concentrations could also arise from contamination of the calibration standard, this was extensively tested, including preparation of a new bulk calibration solution after initial analysis, after which the Na and Ca deficit remained.

However, Na is easily contaminated during vial cleaning, snow sampling and standard preparation. Although all steps were taken to prevent this, high Na concentrations were still measured in occasional blanks. Therefore all sections of the EPG record with high Na concentrations have been measured at single sample resolution (1 cm) to demonstrate well sloped changes up to a maximum rather than an individual erratic peak suggestive of contamination during sample preparation.

Analytical precision on trace element analyses are typically between 5-10 % and again much lower than the variability observed between samples (Table 5.2). Notable exceptions with high 2σ errors are Cr, Cu, Zn, and Bi. High analytical errors are attributed to molecular interferences such as $^{37}\text{Cl}^{16}\text{O}$ on ^{53}Cr , and $^{47}\text{Ti}^{16}\text{O}$ or $^{36}\text{Ar}^{27}\text{Al}$ on ^{63}Cu resulting in relatively large background levels relative to the count rate on calibration standards. Additionally, Ti, V, Ni, Zn, As, Cs, Pb and Th are all $\sim 15\%$ higher than the average values reported by of Environment Canada (certified values), Osterberg et al. (2006) and Rodushkin et al.(2003). With the exception of V and Ni, all

measurements are however within the 2σ range of the variation between different published data, or have only been published by Rodushkin et al. (2003). Further, measurement of Ni ($780 \text{ ppt} \pm 70$) and Pb ($82 \text{ ppt} \pm 10$) are closer to certified values (670 ± 80 and 86 ± 7 2σ of Ni and Pb respectively) when measured on undiluted SLRS-4. Notably Bi is 140 % higher than the value found by Rodushkin et al. (2003) at $2.6 \pm 0.6 \text{ ppt}$ compared to 1.3 ± 0.4 . All other elements are within error of certified values.

A1.5.0 References

- Hutton, R. C. & A. N. Eaton. 1987. Role of aerosol water vapour loading in inductively coupled plasma mass spectrometry. *Journal of Analytical Atomic Spectrometry* 2(6), 595-598.
- Iglesias, M., N. Gilon, E. Poussel & J. M. Mermet. 2002. Evaluation of an ICP-collision/reaction cell-MS system for the sensitive determination of spectrally interfered and non-interfered elements using the same gas conditions. *Journal of Analytical Atomic Spectrometry* 17(10), 1240-1247.
- Osterberg, E. C., M. J. Handley, S. B. Sneed, P. A. Mayewski & K. J. Kreutz. 2006. Continuous ice core melter system with discrete sampling for major ion, trace element and stable isotope analyses. *Environmental Science Technology* 40, 3355-3361.
- Rodushkin, I. 2003. Use of the semi-quantitative calibration mode for rapid sample screening. *Thermo Electron Corporation*.
http://www.thermo.com/cThermo/CMA/PDFs/Various/File_24914.pdf.
- Tan, S. H. and G. Horlick. 1986. Background spectral features in inductively coupled plasma mass spectrometry. *Applied Spectroscopy* 40(4), 445-460.

Appendix Two: Whitehall Glacier study

A2.1.0 Introduction

In addition to the Evans Piedmont Glacier (EPG) snow profile study, glaciochemistry of Whitehall Glacier (WHG), northern Victoria Land coast was investigated from four different snow profiles. Sampling was completed in November 2006 in conjunction with the retrieval of a 105 m firn core. The specific aims of this study were to:

- 1) Determine how representative a single glaciochemical record such as a firn core is of temporal chemistry changes at WHG.
- 2) Establish the site specific controls on stable isotope ratios and major element chemistry with respect to measured meteorology at nearby Cape Hallett.
- 3) Compare the controls on glaciochemistry between northern and southern Victoria Land coastal sites.

However, unexpectedly high accumulation rates ($71 \text{ g cm}^{-2} \text{ y}^{-1}$) restricted the length of the four $\sim 1\text{-}3$ m snow pit profiles to between 6 to 18 months. Although this indicates excellent temporal resolution for the WHG firn core record, the obtained snow profiles are too short for robust seasonality assessment of elemental chemistry and comparison with the decade long EPG record. Therefore, only a brief outline of the research, methods and discussion of preliminary results are presented here which may be useful for future research in combination with the firn core, but is outside the scope of this study.

A2.2.0 Study site

The Whitehall Glacier ice divide ($72^{\circ} 54' \text{ S}$, $169^{\circ} 5' \text{ E}$, 500 m a.s.l.) is located in northern Victoria Land and is 12 km from the open ocean (Fig. A2.1). The proximal location of WHG to the Antarctic Circumpolar Trough results in frequent and intense cyclonic activity. Interannual climatic variability is therefore primarily controlled by the Antarctic Oscillation (Turner, 2004). Katabatic outflow from the East Antarctic Ice Sheet is

expected from the SSW, due to local topography. Meteorological conditions have been measured at Cape Hallett, located 71 km NNE of WHG intermittently since 1957. Wind speed, wind direction and air temperature are available from the Long Term Ecological Network between December 2003 to December 2007 (data attributed to Lyons, 2009, <http://bprc.osu.edu/capehallett/chaws.html>).

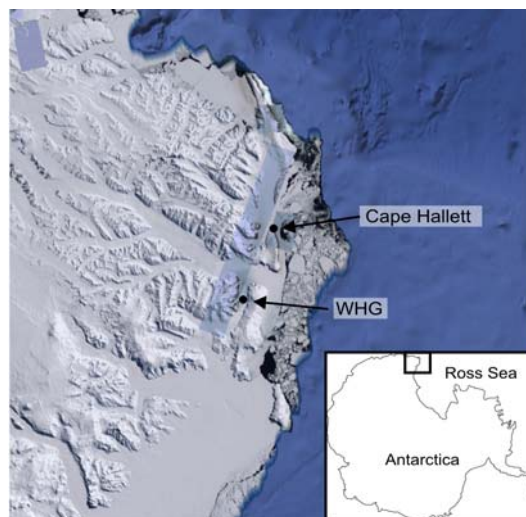


Figure A2.1 Location of Whitehall Glacier (WHG) on the northern Victoria Land coast, Antarctica. Location of Cape Hallett is also shown. Image is sourced from Google Earth, 2007 (Europa Technologies)

A2.3.0 Methodology

Four snow pits were sampled at Whitehall Glacier (WHG) in November 2006, to depths of 288 cm (WHG_1), 170 cm (WHG_2), 112 cm (WHG_3) and 102 cm (WHG_4). WHG_1 was sampled from two sections, WHG_1 from 9cm to 222 cm depth and WHG_1b from 188 cm to 288 cm depth. A dominant hoar horizon at 180 cm depth was used to correlate between the two sections, which demonstrate good overlap of density and Na chemistry concentrations (Fig. A2.2, A2.5). Samples were taken at 1cm resolution using the same methodology applied at EPG (Chapter 5.3). However, pre-cleaned HDPE vials were not used, and samples were collected into NASCO whirl-pack bags. Although this is insignificant for major element chemistry, it is possible samples are contaminated for trace elements. Furthermore, WHG_1 was sampled from a fresh surface of the 3 m pit used for ice core drilling, an additional source of potential trace element contamination. Snow density and temperature measurements were made at 5 cm resolution after chemistry sampling was completed.

Samples from each WHG snow profile were analysed for $\delta^{18}\text{O}$ and δD at the GNS National Isotope Centre and Al, Ca, K, Mg, Na, S, Si and Sr by inductively coupled plasma optical emission spectrometry (ICP-OES) at the Chromatography/Glaciochemistry Laboratory, University of Maine. ICP-OES detection limits are determined as the 3σ error of 10 blank measurements (Table A4.7). Analytical error was assessed through 53 measurements of an internal quality control standard which was

measured in addition to calibration standards (Table A4.6). Errors are typically between 10 – 30 % 2 rsd, which is an order of magnitude below temporal variation between samples. Both calibration and quality control standards were made to approximate mean snow sample concentrations. Ca^+ , Cl^- , K^+ , Mg^+ , MS^- , Na^+ , NO_3^- , SO_4^{2-} were also measured in WHG_1 samples by ion chromatography (IC) at the Chromatography/Glaciochemistry Laboratory, University of Maine. Methodology of stable isotope and IC measurements are described fully in Chapter 5.3.

A2.4.0 Preliminary results and discussion

A2.4.1 Dating

The stable isotope profile of WHG_1 demonstrates two frequencies of $\delta^{18}\text{O}$ variation. Fluctuations between 10-50 cm occur on top of a lower frequency signal which is maximum between 150–110 cm depth (Fig. A2.2). The lower frequency signal is considered indicative of seasonal temperature changes due to a concurrent increase in MS. MS maxima represents increased biological activity within the Ross Sea and Southern Ocean during summer when sea ice extent is at a minimum (e.g. Wolff et al., 2003, Rhodes et al. 2009). Additionally, density measurements display the same low frequency fluctuation. An age model for WHG_1 is therefore established between winter (July) 2005 to sampling in November 2006.

An accumulation rate of $71 \text{ g cm}^{-2} \text{ y}^{-1}$ is determined between July 2005 and July 2006. This complies with the general Victoria Land coast trend of increasing precipitation with decreasing latitude (A2.3) ($r^2 = 0.89$, $n = 30$). $71 \text{ g cm}^{-2} \text{ y}^{-1}$ is however double the snow precipitation rate predicted by Giovinetto and Bentley (1985) (Fig. A2.3) and a single year is considered too short to robustly characterize snow accumulation at WHG.

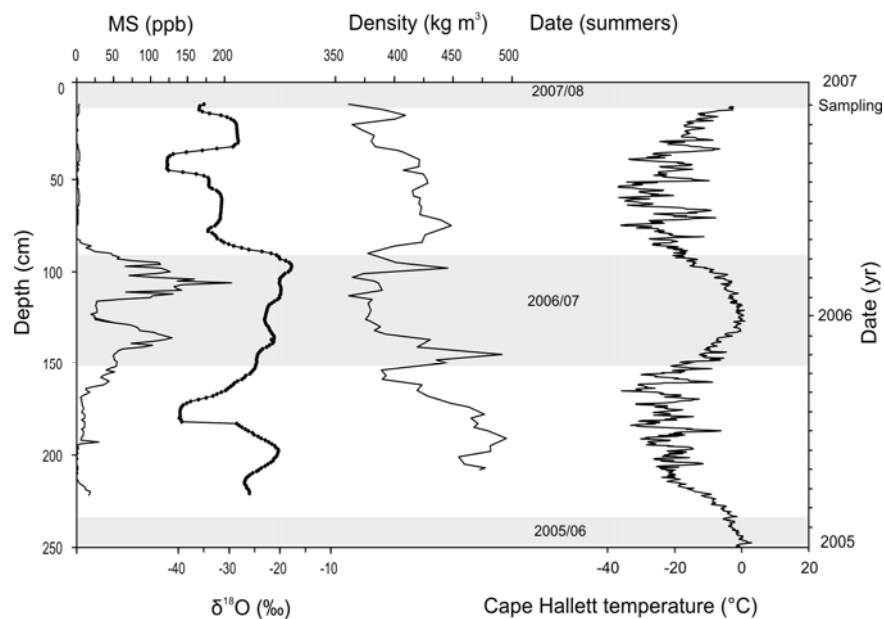


Figure A2-2. Dating of WHG_1 snow pit profile. The 2005/06 summer is determined by concurrent MS maxima, $\delta^{18}\text{O}$ maxima and density minima. Sampling in November 2006 provides a maximum age constraint.

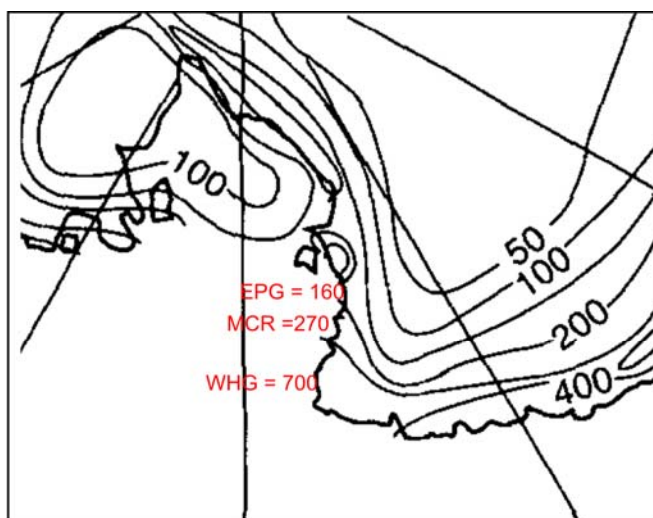


Figure A2.3 Comparison of accumulation rates ($\text{g mm}^{-2} \text{yr}^{-1}$) inferred from snow pit studies at WHG, McCarthy Ridge (Piccardi et al., 1994) and EPG, with modelled accumulation contours (from Connolley and Cattle (1994, adapted from Giovinetto and Bentley, 1985).

A2.4.2 Comparison of chemistry between WHG snow profiles and Cape Hallett meteorological conditions.

The four WHG snow profiles demonstrate similar sub-seasonal variation of $\delta^{18}\text{O}$ and elemental chemistry (Figs. A2.4, A2.5). WHG_4 alone displays relative homogeneity of $\delta^{18}\text{O}$ within the upper 60 cm of snow pack, attributed to extremely localised post depositional mixing of snow through wind drift. Assuming high frequency $\delta^{18}\text{O}$ fluctuations are representative of sub-seasonal temperature changes, WHG snow pit records are dated at sub-seasonal resolution through comparison with the Cape Hallett temperature record (Fig. A2.4). WHG_1, WHG_2 and WHG_3 demonstrate strong correlation with Cape Hallett temperature of $r^2 = 0.72$, $r^2 = 0.81$ and $r^2 = 0.52$ respectively.

Four maxima of elemental concentrations are identified in the WHG snow profiles (e.g. Na concentrations in Fig. A2.5). Slight differences between the records is reflective of heterogeneous deposition of aerosol to the snow surface, dependent on surface roughness and sastrugi features. For example, the highest maxima of Na concentrations in WHG_1 (peak 2) is present at slightly lower concentrations in WHG_2 and WHG_4, but absent from the WHG_3 record. Similarly, peak 1 is observed in WHG_2 and WHG_3 but is absent from WHG_4. Despite these slight differences, the dominant control on WHG elemental chemistry is still atmospheric circulation, evident through the simple relationship of WHG chemistry to wind strength measured at Cape Hallett. Chemistry peaks 1,2 and 4 are all approximately concurrent (within uncertainty of snow pit dating), with daily averaged, maximum wind speed measurements $> 10 \text{ m s}^{-1}$. Peak 3, which was sampled in WHG_1, occurs when there are no available wind measurements at Cape Hallett. However the most probable cause of automatic weather station damage is storm events, and hence increased wind strength.

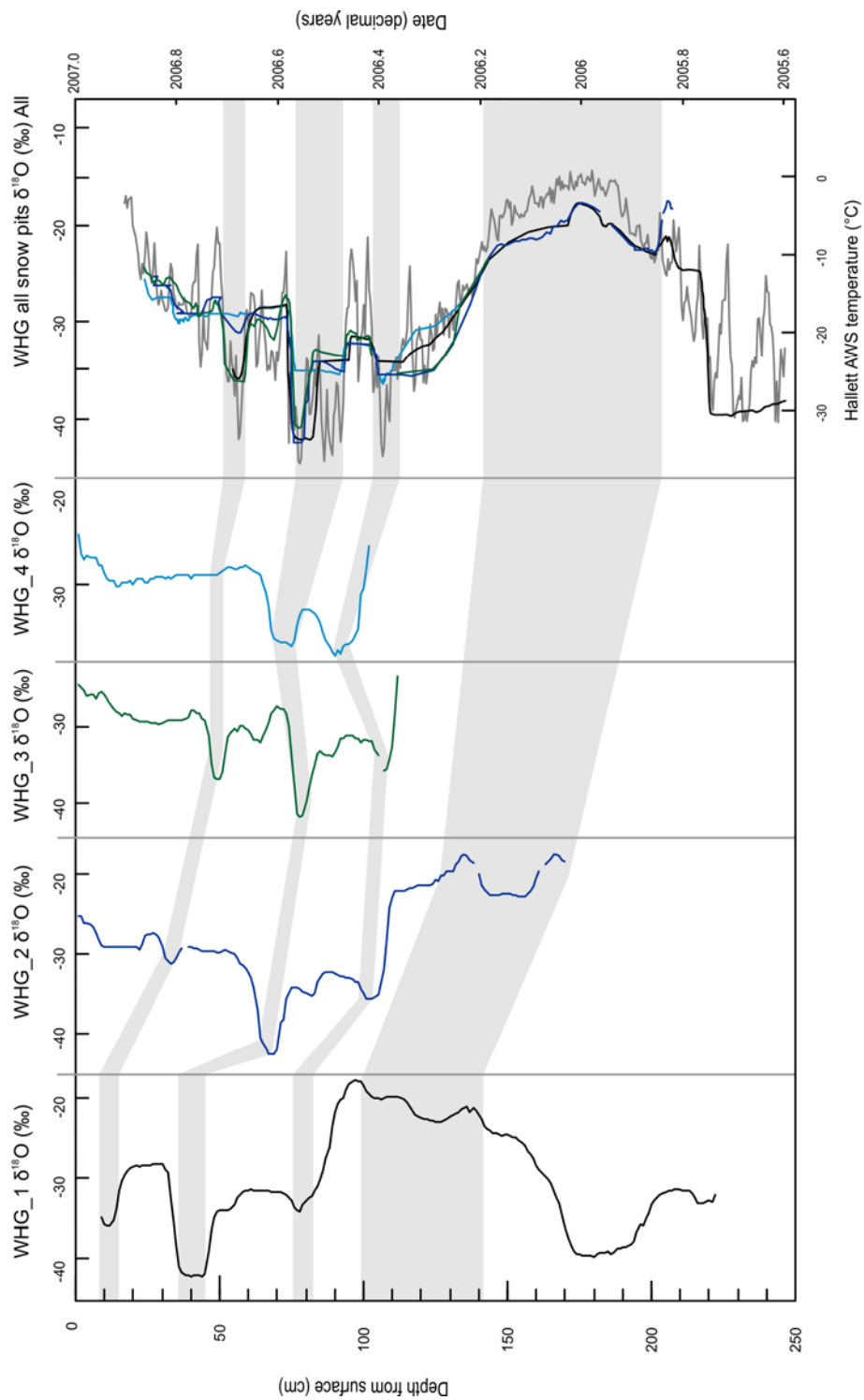


Fig A2.4 Comparison of $\delta^{18}\text{O}$ in WHG_1, WHG_2, WHG_3 and WHG_4 snow profiles and sub-seasonal temperature variation measured at Cape Hallett (Lyons, 2009). $\delta^{18}\text{O}$ analytical error is typically $< 0.1\text{‰}$.

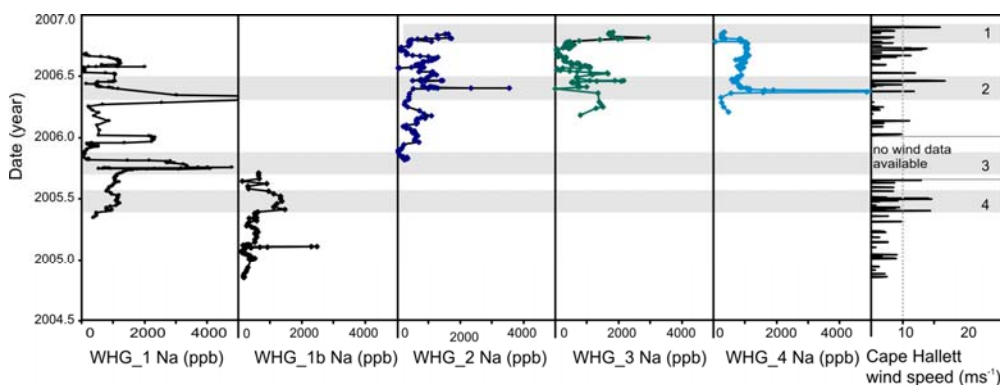


Fig A2.5 Comparison of Na concentrations measured by ICP-OES in WHG_1, WHG_2, WHG_3 and WHG_4 snow profiles with daily averaged wind speeds measured at Cape Hallett. Analytical error of Na measurements is typically 30 % (2 rsd). Na concentration maxima are labelled 1-4 as discussed in the text. Dating of the WHG snow profiles is based on comparison of sub-seasonal $\delta^{18}\text{O}$ fluctuations with Cape Hallett temperature.

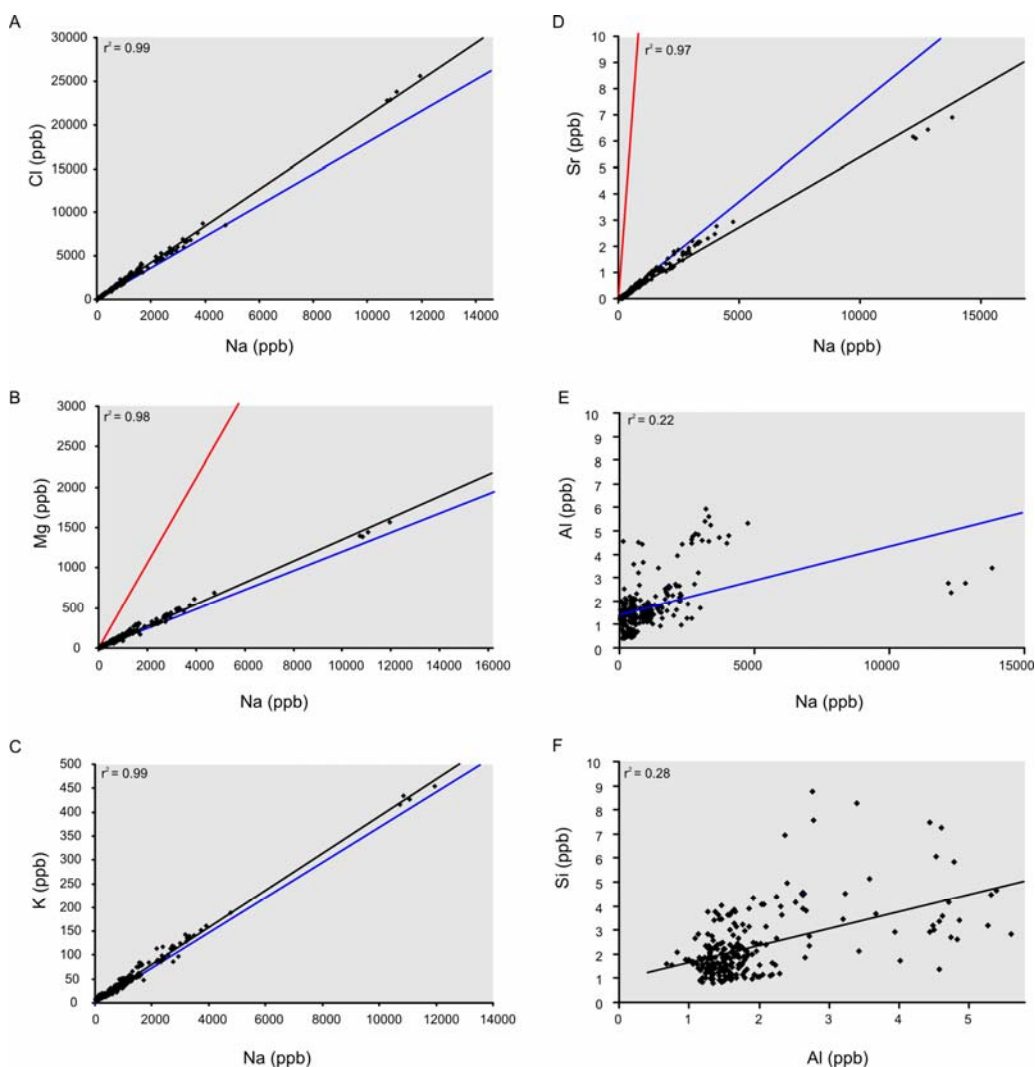


Fig A2.6 Correlation of elemental concentrations measured in the WHG_1 snow profile. Analytical errors for ICP-OES analysis are presented in Table A4.5 and are typically 10-30 %. Linear correlation between elements is shown in black. Where appropriate, marine ratios (blue) and upper continental crust (red) values are shown for comparison. **a-c)** IC measurements of Cl, Mg and K versus Na. **d-f)** ICP-OES measurements of Sr and Al versus Na.

Elemental ratios of WHG snow samples are similar to upper ocean values indicating a dominant marine source of Cl, Mg, K (Turekian, 1968; Riley and Chester, 1971; Bruland and Lohan, 2003) (Fig. A2.6). Conversely, elements derived from mineral dust such as Al and Si are poorly correlated, considered reflective of the detection limits of ICP-OES analysis.

A2.5.0 Conclusions and future work

Preliminary results indicate that the WHG firn core has the potential to track sub-seasonal resolution changes in temperature ($\delta^{18}\text{O}$) and increased wind strength (elemental chemistry concentrations) at WHG. This is supported by correlation of WHG glaciochemistry to the Cape Hallett meteorological record and similarity of chemistry trends in the four snow pit records. Slight, sub-seasonal differences that are observed between the WHG snow profiles, which are dependent on the exact sampling location, will be inconsequential in interpretation of a compacted firn core record. Although IC and ICP-OES allow robust determination of marine derived, major element chemistry (Na, Mg, K, Cl), further analysis using ICP-MS is recommended to determine the variation of predominantly terrestrial derived, trace element chemistry (e.g. Al and Ti) which is present at concentrations close or below ICP-OES detection limits. As at EPG, terrestrial derived chemistry might provide constraints on the direction of atmospheric circulation in addition to simple wind strength.

A2.6.0 References

- Bruland, K. W. & M. C. Lohan. 2003. Controls of trace metals in seawater. *Treatise on Geochemistry* 6, 23–49.
- Connolley, W.M. & H. Cattle. 1994. The Antarctic Climate of the UKMO Unified Model. *Antarctic Science*, 6(01), 115-122.
- Giovinetto, M. B. & C. R. Bentley. 1985. Surface balance in ice drainage systems of Antarctica. *Antarctic Journal of the USA*, 20(4) 6-13.
- Piccardi, G., R. Udisti & F. Casella. 1994. Seasonal Trends and Chemical Composition of Snow at Terra Nova Bay (Antarctica). *International Journal of Environmental Analytical Chemistry*, 55(1), 219.

- Rhodes, R. H., N.A. Bertler, J. A. Baker, S. B. Sneed, H. Oerter & K. R. Arrigo. 2009. Sea ice variability and primary productivity in the Ross Sea, Antarctica, from methylsulphonate snow record. *Geophysical Research Letters*, 36. doi:10.1029/2009GL037311
- Riley, J. P. & R. Chester. 1971. *Introduction to marine chemistry*. London and New York: Academic Press.
- Turekian, K.K. 1968. *Oceans*. Englewoods, Cliffs: Prentice Hall.
- Turner, J. 2004. The El Nino–southern oscillation and Antarctica. *International Journal of Climatology* 24(1), 1-31.
- Wolff, E. W., A. M. Rankin & R. Rothlisberger. 2003. An ice core indicator of Antarctic sea ice production. *Geophysical Research Letters*, 30(22), 2158.

**Appendix Three: Appendix Three: Stable isotope, major and trace
element chemistry (ICP-MS and IC analysis), density and
temperature measurements of the EPG snow profile**

Table A3.1 Oxygen ($\delta^{18}\text{O}$) and hydrogen (δD) isotopic ratios of EPG snow samples. Deuterium excess (d) is calculated as $d = \delta\text{D} - 8 \cdot \delta^{18}\text{O}$. Analytical precision is typically $< 0.1\text{‰}$ for $\delta^{18}\text{O}$, $< 1.0\text{‰}$ δD , and $< 1\text{‰}$ for d excess. Dating is based on seasonal maxima of $\delta^{18}\text{O}$ and δD (bold) with linear extrapolation in between. Accumulation rates have been inferred from this dating.

Sample	Date (decimal yr)	Depth (cm)	Accumulation (cm yr ⁻¹)	$\delta^{18}\text{O}$ (‰)	2 σ	DH (‰)	2 σ	d excess (‰)	2 σ
Average			34	-26.0	0.02	-205	0.7	3	0.7
2 σ			29	4.9		44		11	
2 rsd (%)			84	19.0		22		336	
Min		0	7	-30.1	0.00	-244	0.0	-12	0.0
Max		379	66	-19.5	0.10	-148	3.7	16	2.7
EGP_07_380	2007.92	0	7	-25.2		-214	0.1	-12	
EGP_07_379	2007.78	1	7	-27.7		-225	0.0	-3	
EGP_07_378	2007.64	2	7	-26.9		-206	0.0	9	
EGP_07_377	2007.50	3	12	-27.6		-213	0.3	8	
EGP_07_376	2007.42	4	12	-25.5		-191	0.0	13	
EGP_07_375	2007.33	5	12	-24.5		-181	0.4	15	
EGP_07_374	2007.25	6	12	-24.1		-177	0.1	15	
EGP_07_373	2007.17	7	12	-23.8		-174	0.2	16	
EGP_07_372	2007.08	8	12	-23.6	0.00	-173	0.1	16	0.1
EGP_07_371	2007.00	9	30	-23.5	0.02	-173	0.1	15	0.1
EGP_07_370	2006.97	10	30	-23.4		-172	0.3	16	
EGP_07_369	2006.93	11	30	-23.4		-172	0.1	15	
EGP_07_368	2006.90	12	30	-23.3		-171	0.3	15	
EGP_07_367	2006.87	13	30	-23.2		-172	0.2	14	
EGP_07_366	2006.83	14	30	-23.1		-173	0.2	12	
EGP_07_365	2006.80	15	30	-23.1		-174	0.2	11	
EGP_07_364	2006.77	16	30	-23.0		-178	0.0	6	
EGP_07_363	2006.73	17	30	-23.6		-187	0.1	2	
EGP_07_362	2006.70	18	30	-24.8		-200	0.1	-1	
EGP_07_361	2006.67	19	30	-26.2		-213	0.1	-3	
EGP_07_360	2006.63	20	30	-27.6		-224	0.1	-3	
EGP_07_359	2006.60	21	30	-28.6		-230	0.1	-2	
EGP_07_358	2006.57	22	30	-29.4		-234	0.5	1	
EGP_07_357	2006.53	23	30	-29.9		-234	0.6	6	
EGP_07_356	2006.50	24	18	-30.0		-233	0.4	7	
EGP_07_355	2006.44	25	18	-29.6		-228	0.1	9	
EGP_07_354	2006.39	26	18	-29.2		-223	0.1	11	
EGP_07_353	2006.33	27	18	-28.6		-218	0.1	11	
EGP_07_352	2006.28	28	18	-28.3	0.10	-215	0.1	12	0.1
EGP_07_351	2006.22	29	18	-27.9	0.01	-211	0.2	12	0.2
EGP_07_350	2006.17	30	18	-27.9		-211	0.4	12	
EGP_07_349	2006.11	31	18	-27.6		-208	0.6	12	
EGP_07_348	2006.06	32	18	-27.4		-207	0.6	12	
EGP_07_347	2006.00	33	22	-27.3		-205	0.0	13	
EGP_07_346	2005.95	34	22	-27.1		-205	1.9	11	
EGP_07_345	2005.91	35	22	-26.9		-203	1.4	12	
EGP_07_344	2005.86	36	22	-26.7		-203	0.8	10	
EGP_07_343	2005.82	37	22	-26.2		-200	0.3	10	
EGP_07_342	2005.77	38	22	-25.9		-195	0.6	12	
EGP_07_341	2005.73	39	22	-25.4		-193	0.8	11	
EGP_07_340	2005.68	40	22	-24.8		-189	1.2	10	
EGP_07_339	2005.64	41	22	-24.1		-183	0.7	11	
EGP_07_338	2005.59	42	22	-23.6		-180	0.7	9	
EGP_07_337	2005.55	43	22	-22.9		-176	0.8	7	
EGP_07_336	2005.50	44	22	-22.8		-173	3.1	9	
EGP_07_335	2005.45	45	22	-22.3		-170	1.3	8	
EGP_07_334	2005.41	46	22	-22.1		-169	1.6	7	
EGP_07_333	2005.36	47	22	-21.8		-167	1.0	8	
EGP_07_332	2005.32	48	22	-21.4	0.00	-166	0.1	5	0.1

Table A3.1 continued

Sample	Date (decimal yr)	Depth (cm)	Accumulation (cm yr ⁻¹)	$\delta^{18}\text{O}$ (‰)	2 σ	DH (‰)	2 σ	dexcess (‰)	2 σ
EGP_07_331	2005.27	49	22	-21.2	0.01	-164	1.0	6	1.0
EGP_07_330	2005.23	50	22	-20.9		-160	0.6	7	
EGP_07_329	2005.18	51	22	-20.6		-158	1.4	7	
EGP_07_328	2005.14	52	22	-20.7		-158	0.9	8	
EGP_07_327	2005.09	53	22	-20.6		-157	0.8	7	
EGP_07_326	2005.05	54	22	-20.0		-153	1.8	7	
EGP_07_325	2005.00	55	28	-20.1		-151	0.5	9	
EGP_07_324	2004.96	56	28	-19.8		-151	0.4	8	
EGP_07_323	2004.93	57	28	-19.7		-150	1.1	7	
EGP_07_322	2004.89	58	28	-19.6		-148	0.7	9	
EGP_07_321	2004.86	59	28	-19.6		-150	1.9	7	
EGP_07_320	2004.82	60	28	-19.5		-151	0.7	5	
EGP_07_319	2004.79	61	28	-19.5		-153	0.2	3	
EGP_07_318	2004.75	62	28	-19.6		-156	1.5	1	
EGP_07_317	2004.71	63	28	-19.7		-158	1.6	-1	
EGP_07_316	2004.68	64	28	-19.8		-160	0.2	-2	
EGP_07_315	2004.64	65	28	-20.0		-165	0.2	-5	
EGP_07_314	2004.61	66	28	-20.4		-168	1.4	-5	
EGP_07_313	2004.57	67	28	-20.8		-172	1.1	-6	
EGP_07_312	2004.54	68	28	-21.5	0.01	-179	0.6	-7	0.6
EGP_07_311	2004.50	69	50	-22.8	0.01	-190	0.8	-8	0.8
EGP_07_310	2004.48	70	50	-23.2		-194	1.0	-8	
EGP_07_309	2004.46	71	50	-24.4		-202	0.1	-7	
EGP_07_308	2004.44	72	50	-24.8		-207	0.1	-8	
EGP_07_307	2004.42	73	50	-26.2		-217	0.7	-8	
EGP_07_306	2004.40	74	50	-26.6		-220	0.4	-7	
EGP_07_305	2004.38	75	50	-27.7		-227	0.5	-5	
EGP_07_304	2004.36	76	50	-28.2		-231	0.2	-5	
EGP_07_303	2004.34	77	50	-28.9					
EGP_07_302	2004.32	78	50	-28.9		-235	0.4	-4	
EGP_07_301	2004.30	79	50	-29.3		-239	0.9	-4	
EGP_07_300	2004.28	80	50	-29.3		-237	0.5	-2	
EGP_07_299	2004.26	81	50	-29.5		-235	1.7	0	
EGP_07_298	2004.24	82	50	-29.6		-238	1.1	-1	
EGP_07_297	2004.22	83	50	-28.7		-228	2.3	2	
EGP_07_296	2004.20	84	50	-29.3		-235	0.3	-1	
EGP_07_295	2004.18	85	50	-28.3		-228	0.0	-1	
EGP_07_294	2004.16	86	50	-28.1		-225	0.1	0	
EGP_07_293	2004.14	87	50	-27.5		-219	0.3	1	
EGP_07_292	2004.12	88	50	-27.4		-220	0.5	0	
EGP_07_291	2004.10	89	50	-26.8	0.02	-214	1.6	0	1.6
EGP_07_290	2004.08	90	50	-25.8	0.01	-207	0.1	-1	0.1
EGP_07_289	2004.06	91	50	-25.4		-203	1.0	0	
EGP_07_288	2004.04	92	50	-24.9		-198	1.7	1	
EGP_07_287	2004.02	93	50	-24.7		-199	0.6	-1	
EGP_07_286	2004.00	94	22	-24.5		-193	2.4	2	
EGP_07_285	2003.95	95	22	-24.2		-194	2.2	0	
EGP_07_284	2003.91	96	22	-24.1		-194	0.2	-1	
EGP_07_283	2003.86	97	22	-24.1	0.01	-195	0.4	-2	0.4
EGP_07_282	2003.82	98	22	-24.1		-196	0.3	-3	
EGP_07_281	2003.77	99	22	-24.1		-197	1.2	-3	
EGP_07_280	2003.73	100	22	-24.1		-196	0.8	-3	
EGP_07_279	2003.68	101	22	-24.2		-198	1.3	-5	
EGP_07_278	2003.64	102	22	-24.2		-199	0.2	-5	
EGP_07_277	2003.59	103	22	-24.3		-199	0.6	-4	
EGP_07_276	2003.55	104	22	-24.3		-200	1.0	-5	
EGP_07_275	2003.50	105	22	-24.2		-200	2.0	-7	
EGP_07_274	2003.45	106	22	-24.2		-199	1.0	-5	
EGP_07_273	2003.41	107	22	-24.2		-198	0.9	-5	

Table A3.1 continued

Sample	Date (decimal yr)	Depth (cm)	Accumulation (cm yr ⁻¹)	$\delta^{18}\text{O}$ (‰)	2 σ	DH (‰)	2 σ	dexcess (‰)	2 σ
EGP_07_272	2003.36	108	22	-24.1		-197	0.9	-4	
EGP_07_271	2003.32	109	22	-24.1		-196	2.4	-3	
EGP_07_270	2003.27	110	22	-24.0		-195	1.0	-2	
EGP_07_269	2003.23	111	22	-24.0		-195	0.6	-3	
EGP_07_268	2003.18	112	22	-24.0		-194	1.2	-2	
EGP_07_267	2003.14	113	22	-24.1		-194	0.4	-1	
EGP_07_266	2003.09	114	22	-24.2		-195	0.8	-1	
EGP_07_265	2003.05	115	22	-24.4		-195	0.9	0	
EGP_07_264	2003.00	116	24	-24.7	0.00	-197	0.9	0	0.9
EGP_07_263	2002.96	117	24	-24.9	0.01	-200	1.3	-1	1.3
EGP_07_262	2002.92	118	24	-25.2		-203	0.8	-1	
EGP_07_261	2002.88	119	24	-25.7		-207	0.2	-2	
EGP_07_260	2002.83	120	24	-26.0		-209	0.2	-1	
EGP_07_259	2002.79	121	24	-26.4		-211	0.9	0	
EGP_07_258	2002.75	122	24	-26.8		-215	1.0	-1	
EGP_07_257	2002.71	123	24	-27.0		-216	2.2	0	
EGP_07_256	2002.67	124	24	-27.2		-218	0.1	0	
EGP_07_255	2002.63	125	24	-27.4		-220	0.7	-1	
EGP_07_254	2002.58	126	24	-27.4		-220	2.3	0	
EGP_07_253	2002.54	127	24	-27.4		-219	2.6	1	
EGP_07_252	2002.50	128	18	-27.4		-221	0.3	-1	
EGP_07_251	2002.44	129	18	-27.3		-219	0.6	0	
EGP_07_250	2002.39	130	18	-27.3		-216	0.1	2	
EGP_07_249	2002.33	131	18	-27.1		-215	0.3	2	
EGP_07_248	2002.28	132	18	-26.8		-215	0.2	0	
EGP_07_247	2002.22	133	18	-26.7		-211	0.0	3	
EGP_07_246	2002.17	134	18	-26.6		-210	1.2	3	
EGP_07_245	2002.11	135	18	-26.5		-209	1.2	3	
EGP_07_244	2002.06	136	18	-26.3	0.00	-208	1.2	3	1.2
EGP_07_243	2002.00	137	30	-26.2	0.00	-205	0.8	4	0.8
EGP_07_242	2001.97	138	30	-26.1		-205	1.7	4	
EGP_07_241	2001.93	139	30	-26.0		-205	1.4	3	
EGP_07_240	2001.90	140	30	-25.8		-203	2.7	4	
EGP_07_239	2001.87	141	30	-25.7		-203	0.4	2	
EGP_07_238	2001.83	142	30	-25.5		-203	0.4	1	
EGP_07_237	2001.80	143	30	-25.5		-202	0.0	1	
EGP_07_236	2001.77	144	30	-25.3		-202	1.1	1	
EGP_07_235	2001.73	145	30	-25.2		-202	0.3	0	
EGP_07_234	2001.70	146	30	-25.3		-202	0.1	1	
EGP_07_233	2001.67	147	30	-25.2		-200	0.5	1	
EGP_07_232	2001.63	148	30	-25.1		-202	0.5	-1	
EGP_07_231	2001.60	149	30	-25.0		-202	0.3	-1	
EGP_07_230	2001.57	150	30	-25.1		-203	0.9	-2	
EGP_07_229	2001.53	151	30	-25.2		-203	0.0	-2	
EGP_07_228	2001.50	152	66	-25.1		-204	0.2	-3	
EGP_07_227	2001.48	153	66	-25.4		-205	0.3	-1	
EGP_07_226	2001.47	154	66	-25.6		-207	1.1	-2	
EGP_07_225	2001.45	155	66	-25.7		-209	0.7	-3	
EGP_07_224	2001.44	156	66	-26.0	0.00	-211	0.2	-3	0.2
EGP_07_223	2001.42	157	66	-26.6	0.02	-216	1.2	-3	1.2
EGP_07_222	2001.41	158	66	-26.7		-217	1.1	-3	
EGP_07_221	2001.39	159	66	-26.9		-217	0.4	-1	
EGP_07_220	2001.38	160	66	-27.4		-222	1.8	-2	
EGP_07_219	2001.36	161	66	-27.6		-221	1.5	0	
EGP_07_218	2001.35	162	66	-27.6		-223	0.8	-2	
EGP_07_217	2001.33	163	66	-28.0		-225	0.5	-1	
EGP_07_216	2001.32	164	66	-27.9		-220	0.5	3	
EGP_07_215	2001.30	165	66	-27.9		-220	0.7	3	
EGP_07_214	2001.29	166	66	-27.6		-217	0.6	4	

Table A3.1 continued

Sample	Date (decimal yr)	Depth (cm)	Accumulation $\delta^{18}\text{O}$ (cm yr ⁻¹) (‰)	2 σ	DH (‰)	2 σ	dexcess (‰)	2 σ
EGP_07_213	2001.27	167	66	-27.7	-219	0.2	2	
EGP_07_212	2001.26	168	66	-27.7	-217	0.6	5	
EGP_07_211	2001.24	169	66	-27.8	-219	0.9	4	
EGP_07_210	2001.23	170	66	-26.6	-207	0.1	6	
EGP_07_209	2001.21	171	66	-26.7	-206	0.3	7	
EGP_07_208	2001.20	172	66	-26.5	-200	0.2	11	
EGP_07_207	2001.18	173	66		-205	0.4		
EGP_07_206	2001.17	174	66	-25.8	-197	0.7	10	
EGP_07_205	2001.15	175	66	-26.0	-198	0.3	10	
EGP_07_204	2001.14	176	66	-25.6	-195	0.6	10	0.6
EGP_07_203	2001.12	177	66	-25.2	-189	2.0	12	2.0
EGP_07_202	2001.11	178	66		-191	1.3		
EGP_07_201	2001.09	179	66		-191	0.2		
EGP_07_200	2001.08	180	66	-24.9	-187	0.3	12	
EGP_07_199	2001.06	181	66	-24.6	-182	3.7	15	
EGP_07_198	2001.05	182	66		-175	0.8		
EGP_07_197	2001.03	183	66	-24.6	-185	3.7	12	
EGP_07_196	2001.02	184	66		-187	0.3		
EGP_07_195	2001.00	185	11		-215	1.0		
EGP_07_194	2000.91	186	11	-25.1	-205	0.4	-4	
EGP_07_193	2000.82	187	11	-25.2	-206	0.7	-4	
EGP_07_192	2000.74	188	11	-25.5	-208	0.1	-3	
EGP_07_191	2000.65	189	11	-25.6	-206	0.3	-1	
EGP_07_190	2000.56	190	11	-26.4	-209	0.0	2	
EGP_07_189	2000.47	191	11	-26.3	-210	0.3	1	
EGP_07_188	2000.38	192	11	-26.7	-212	0.5	2	
EGP_07_187	2000.29	193	11	-26.6	-212	0.8	1	
EGP_07_186	2000.21	194	11	-26.9	-215	0.5	0	
EGP_07_185	2000.12	195	11	-27.0	-216	0.3	0	
EGP_07_184	2000.03	196	11	-27.3	-218	0.1	0	
EGP_07_183	1999.94	197	11	-27.6	-221	0.1	-1	0.1
EGP_07_182	1999.85	198	11	-27.8	-223	0.8	-1	0.8
EGP_07_181	1999.76	199	11	-28.2	-227	0.2	-2	
EGP_07_180	1999.68	200	11	-28.5	-230	0.0	-2	
EGP_07_179	1999.59	201	11	-29.0	-233	0.2	-1	
EGP_07_178	1999.50	202	30	-29.4	-236	0.1	-1	
EGP_07_177	1999.47	203	30	-29.6	-238	0.1	-1	
EGP_07_176	1999.43	204	30	-29.8	-239	0.5	-1	
EGP_07_175	1999.40	205	30	-29.8	-239	0.4	-1	
EGP_07_174	1999.37	206	30	-29.9	-241	0.2	-1	
EGP_07_173	1999.33	207	30	-29.9	-240	0.3	-1	
EGP_07_172	1999.30	208	30	-30.0	-241	0.2	-1	
EGP_07_171	1999.27	209	30	-29.9	-240	0.4	0	
EGP_07_170	1999.23	210	30	-29.8	-239	0.6	0	
EGP_07_169	1999.20	211	30	-29.8	-238	0.0	0	
EGP_07_168	1999.17	212	30	-29.7	-237	0.0	0	
EGP_07_167	1999.13	213	30	-29.4	-235	0.4	0	
EGP_07_166	1999.10	214	30	-29.5	-236	0.3	0	
EGP_07_165	1999.07	215	30	-29.4	-235	0.5	0	
EGP_07_164	1999.03	216	30	-29.3	-234	0.7	0	
EGP_07_163	1999.00	217	24	-29.3	-235	0.3	0	0.3
EGP_07_162	1998.96	218	24	-29.0	-233	0.1	-1	0.1
EGP_07_161	1998.92	219	24	-28.9	-232	0.1	-1	
EGP_07_160	1998.88	220	24	-28.9	-231	0.5	0	
EGP_07_159	1998.83	221	24	-29.0	-234	0.3	-2	
EGP_07_158	1998.79	222	24	-29.0	-234	0.3	-2	
EGP_07_157	1998.75	223	24	-29.4	-238	0.2	-3	
EGP_07_156	1998.71	224	24	-29.5	-239	0.7	-3	
EGP_07_155	1998.67	225	24	-29.7	-241	0.6	-4	

Table A3.1 continued

Sample	Date (decimal yr)	Depth (cm)	Accumulation (cm yr ⁻¹)	$\delta^{18}\text{O}$ (‰)	2 σ	DH (‰)	2 σ	dexcess (‰)	2 σ
EGP_07_154	1998.63	226	24	-29.7		-241	0.0	-4	
EGP_07_153	1998.58	227	24	-29.8		-242	0.7	-4	
EGP_07_152	1998.54	228	24	-29.9		-243	0.7	-4	
EGP_07_151	1998.50	229	32	-29.9		-243	0.7	-4	
EGP_07_150	1998.47	230	32	-30.1		-244	0.3	-3	
EGP_07_149	1998.44	231	32	-30.1		-244	0.1	-4	
EGP_07_148	1998.41	232	32	-30.0		-243	0.3	-3	
EGP_07_147	1998.38	233	32	-30.0		-242	0.2	-2	
EGP_07_146	1998.34	234	32	-29.8		-240	0.1	-1	
EGP_07_145	1998.31	235	32	-29.9		-240	0.2	-1	
EGP_07_144	1998.28	236	32	-29.7		-236	0.2	2	
EGP_07_143	1998.25	237	32	-29.5	0.04	-234	0.8	1	0.8
EGP_07_142	1998.22	238	32	-29.3	0.00	-233	0.0	1	0.0
EGP_07_141	1998.19	239	32	-29.1		-230	0.3	3	
EGP_07_140	1998.16	240	32	-28.8		-227	0.6	3	
EGP_07_139	1998.13	241	32	-28.5		-224	0.4	4	
EGP_07_138	1998.09	242	32	-28.5		-222	0.6	6	
EGP_07_137	1998.06	243	32	-28.4		-221	0.0	6	
EGP_07_136	1998.03	244	32	-28.1		-219	0.0	6	
EGP_07_135	1998.00	245	32	-27.9		-218	0.0	5	
EGP_07_134	1997.97	246	32	-27.9		-218	0.5	6	
EGP_07_133	1997.94	247	32	-27.9		-217	0.2	6	
EGP_07_132	1997.91	248	32	-27.7		-216	0.5	6	
EGP_07_131	1997.88	249	32	-27.6		-215	0.2	6	
EGP_07_130	1997.84	250	32	-27.6		-216	0.4	6	
EGP_07_129	1997.81	251	32	-27.5		-216	1.0	4	
EGP_07_128	1997.78	252	32	-27.6		-215	0.2	6	
EGP_07_127	1997.75	253	32	-27.7		-217	0.4	4	
EGP_07_126	1997.72	254	32	-27.7		-217	0.1	4	
EGP_07_125	1997.69	255	32	-27.7		-218	0.7	4	
EGP_07_124	1997.66	256	32	-27.5		-217	0.5	3	
EGP_07_123	1997.63	257	32	-27.5	0.03	-216	0.0	3	0.0
EGP_07_122	1997.59	258	32	-27.2	0.10	-217	0.7	0	0.7
EGP_07_121	1997.56	259	32	-27.4	0.03	-215	0.8	4	0.8
EGP_07_120	1997.53	260	32	-27.2		-215	0.9	3	
EGP_07_119	1997.50	261	36	-27.1		-215	0.1	3	
EGP_07_118	1997.47	262	36	-27.0		-213	0.3	2	
EGP_07_117	1997.44	263	36	-26.9		-211	0.2	4	
EGP_07_116	1997.42	264	36	-26.7		-210	0.3	3	
EGP_07_115	1997.39	265	36	-26.5		-208	0.2	3	
EGP_07_114	1997.36	266	36	-26.3		-207	0.0	4	
EGP_07_113	1997.33	267	36	-26.1		-205	0.4	4	
EGP_07_112	1997.31	268	36	-25.9		-202	0.3	5	
EGP_07_111	1997.28	269	36	-25.7		-201	0.1	5	
EGP_07_110	1997.25	270	36	-25.5		-198	0.5	6	
EGP_07_109	1997.22	271	36	-25.3		-197	0.1	5	
EGP_07_108	1997.19	272	36	-25.1		-196	0.1	5	
EGP_07_107	1997.17	273	36	-25.1		-196	0.2	5	
EGP_07_106	1997.14	274	36	-25.1		-195	0.3	6	
EGP_07_105	1997.11	275	36	-25.1		-195	0.2	6	
EGP_07_104	1997.08	276	36	-25.2		-195	0.6	6	
EGP_07_103	1997.06	277	36	-25.3		-196	0.6	6	
EGP_07_102	1997.03	278	36	-25.4	0.01	-198	0.1	5	0.1
EGP_07_101	1997.00	279	26	-25.5	0.02	-198	0.7	6	0.7
EGP_07_100	1996.96	280	26	-25.7		-202	0.4	4	
EGP_07_099	1996.92	281	26	-25.9		-203	0.7	4	
EGP_07_098	1996.88	282	26	-26.0		-205	1.0	3	
EGP_07_097	1996.85	283	26	-26.3		-207	0.3	3	
EGP_07_096	1996.81	284	26	-26.8		-211	0.3	3	

Table A3.1 continued

Sample	Date (decimal yr)	Depth (cm)	Accumulation $\delta^{18}\text{O}$ (cm yr ⁻¹) (‰)	2 σ	DH (‰)	2 σ	dexcess (‰)	2 σ
EGP_07_095	1996.77	285	26	-27.1	-215	0.6	2	
EGP_07_094	1996.73	286	26	-27.3	-216	0.2	2	
EGP_07_093	1996.69	287	26	-27.7	-221	0.4	1	
EGP_07_092	1996.65	288	26	-27.9	-223	0.2	1	
EGP_07_091	1996.62	289	26	-28.2	-226	0.3	0	0.3
EGP_07_090	1996.58	290	26	-28.1	-225	0.0	0	
EGP_07_089	1996.54	291	26	-28.4	-227	0.2	0	
EGP_07_088	1996.50	292	46	-28.4	-228	0.1	0	
EGP_07_087	1996.48	293	46	-28.6	-228	0.7	0	
EGP_07_086	1996.46	294	46	-28.5	-228	0.0	0	
EGP_07_085	1996.43	295	46	-28.4	-225	0.0	2	
EGP_07_084	1996.41	296	46	-28.2	-225	0.4	1	
EGP_07_083	1996.39	297	46	-28.1	-223	0.0	2	
EGP_07_082	1996.37	298	46	-27.8	-220	0.4	2	
EGP_07_080	1996.35	299	46	-27.5	-216	0.4	3	
EGP_07_079	1996.33	300	46	-27.4	-216	0.5	4	
EGP_07_078	1996.30	301	46	-27.1	-212	1.0	5	
EGP_07_077	1996.28	302	46	-26.8	-209	0.0	6	
EGP_07_076	1996.26	303	46	-26.5	-206	0.9	6	
EGP_07_075	1996.24	304	46	-26.0	-201	0.9	7	
EGP_07_074	1996.22	305	46	-25.7	-199	0.5	7	
EGP_07_073	1996.20	306	46	-25.2	-193	1.5	8	
EGP_07_072	1996.17	307	46	-24.9	-191	0.5	9	
EGP_07_071	1996.15	308	46	-24.7	-189	0.2	8	0.2
EGP_07_070	1996.13	309	46	-24.4	-185	0.9	10	0.9
EGP_07_069	1996.11	310	46	-24.0	-181	0.7	11	
EGP_07_068	1996.09	311	46	-23.9	-181	0.6	10	
EGP_07_067	1996.07	312	46	-23.4	-177	0.7	10	
EGP_07_066	1996.04	313	46	-23.3	-176	1.1	10	
EGP_07_065	1996.02	314	46	-23.3	-178	1.1	9	
EGP_07_064	1996.00	315	30	-23.2	-175	2.3	10	
EGP_07_063	1995.97	316	30	-23.2	-176	0.7	10	
EGP_07_062	1995.93	317	30	-23.2	-174	1.0	11	
EGP_07_061	1995.90	318	30	-23.4	-176	2.1	11	
EGP_07_060	1995.87	319	30	-23.4	-178	0.8	9	
EGP_07_059	1995.83	320	30	-23.5	-179	0.9	9	
EGP_07_058	1995.80	321	30	-23.8	-181	0.1	9	
EGP_07_057	1995.77	322	30	-24.1	-185	0.0	8	
EGP_07_056	1995.73	323	30	-24.3	-187	0.9	7	
EGP_07_055	1995.70	324	30	-24.8	-191	0.6	7	
EGP_07_054	1995.67	325	30	-25.1	-193	1.4	7	
EGP_07_053	1995.63	326	30	-25.4	-196	0.5	7	
EGP_07_052	1995.60	327	30	-25.8	-201	0.4	6	
EGP_07_051	1995.57	328	30	-25.8	-202	2.1	4	2.1
EGP_07_050	1995.53	329	30	-26.1	-205	0.1	4	
EGP_07_049	1995.50	330	34	-26.2	-205	0.2	5	
EGP_07_048	1995.47	331	34	-26.3	-204	0.5	6	
EGP_07_047	1995.44	332	34	-26.3	-205	1.3	6	
EGP_07_046	1995.41	333	34	-26.1	-202	0.2	7	
EGP_07_045	1995.38	334	34	-25.8	-199	1.1	7	
EGP_07_044	1995.35	335	34	-25.5	-195	1.2	9	
EGP_07_043	1995.32	336	34	-25.2	-191	0.2	10	
EGP_07_042	1995.29	337	34	-24.7	-186	0.6	12	
EGP_07_041	1995.26	338	34	-24.3	-182	0.4	13	
EGP_07_040	1995.24	339	34	-24.4	-182	0.3	13	
EGP_07_039	1995.21	340	34	-24.1	-181	0.2	12	
EGP_07_038	1995.18	341	34	-23.7	-177	0.0	13	
EGP_07_037	1995.15	342	34	-23.4	-174	0.7	13	
EGP_07_036	1995.12	343	34	-23.3	-172	0.8	15	

Table A3.1 continued

Sample	Date (decimal yr)	Depth (cm)	Accumulation (cm yr ⁻¹)	$\delta^{18}\text{O}$ (‰)	2 σ	DH (‰)	2 σ	dexcess (‰)	2 σ
EGP_07_035	1995.06	345	34	-23.0		-170	1.1	14	
EGP_07_034	1995.03	346	34	-22.8		-168	0.2	15	
EGP_07_033	1995.00	347	46	-22.6		-166	0.1	14	
EGP_07_032	1994.98	348	46	-22.7		-167	0.6	14	
EGP_07_031	1994.96	349	46	-22.6	0.01	-166	1.1	14	1.1
EGP_07_030	1994.93	350	46	-22.5	0.01	-166	1.4	14	1.4
EGP_07_029	1994.91	351	46	-22.5		-168	0.1	13	
EGP_07_028	1994.89	352	46	-22.7		-169	0.8	13	
EGP_07_027	1994.87	353	46	-22.8		-171	1.6	11	
EGP_07_026	1994.85	354	46	-23.1		-175	1.1	10	
EGP_07_025	1994.83	355	46	-23.1		-175	0.6	10	
EGP_07_024	1994.80	356	46	-23.4		-178	0.0	10	
EGP_07_023	1994.78	357	46	-23.5		-179	1.2	9	
EGP_07_022	1994.76	358	46	-23.8		-186	1.9	4	
EGP_07_021	1994.74	359	46	-24.3		-191	2.0	4	
EGP_07_020	1994.72	360	46	-24.7		-196	0.4	1	
EGP_07_019	1994.70	361	46	-25.1		-197	1.0	3	
EGP_07_018	1994.67	362	46	-25.6		-204	0.1	0	
EGP_07_017	1994.65	363	46	-26.0		-208	0.5	0	
EGP_07_016	1994.63	364	46	-26.6		-213	0.5	0	
EGP_07_015	1994.61	365	46	-27.0		-215	2.1	1	
EGP_07_014	1994.59	366	46	-27.4		-220	0.5	0	
EGP_07_013	1994.57	367	46	-27.8		-223	0.4	-1	
EGP_07_012	1994.54	368	46	-28.2		-227	0.2	-1	
EGP_07_011	1994.52	369	46	-28.7	0.01	-230	1.8	-1	1.8
EGP_07_010	1994.50	370	46	-29.2		-234	1.9	0	
EGP_07_009	1994.48	371	46	-29.2		-233	1.5	0	
EGP_07_008	1994.46	372	46	-29.0		-232	0.3	0	
EGP_07_007	1994.43	373	46	-28.9		-229	0.0	2	
EGP_07_006	1994.41	374	46	-28.6					
EGP_07_005	1994.39	375	46	-28.5		-224	2.3	4	
EGP_07_004	1994.37	376	46	-28.0		-218	2.0	5	
EGP_07_003	1994.35	377	46	-28.0		-220	0.1	4	
EGP_07_002	1994.33	378	46	-28.0		-221	2.2	3	
EGP_07_001	1994.30	379		-27.9	0.00	-219	2.7	5	2.7
Section overlap									
EGP_07_188B				-27.1		-217	0.3	0	
EGP_07_189B				-26.3		-211		0	
EGP_07_190B				-25.8		-207		-1	
Fresh snow samples									
EPG_07_FS_001				-27.2		-208	0.1	10	
EPG_07_FS_002				-27.2		-209	0.2	8	

Table A3.2 Major ionic chemistry of EPG snow samples by ion chromatography analysis.

Sample	Depth (cm)	Na ⁺ (ppb)	K ⁺ (ppb)	Mg ⁺ (ppb)	Ca ⁺ (ppb)	MS ⁻ (ppb)	Cl ⁻ (ppb)	SO ₄ ²⁻ (ppb)	NO ₃ ⁻ (ppb)
Average		1374	73	222	161	38	3466	451	118
2σ		5060	333	877	509	77	13178	991	196
2 rsd (%)		368	456	395	316	199	380	220	166
Min		12	1	2	2	2	69	41	15
Max		17017	1251	3027	1633	368	40666	3691	726
EGP_07_380	0	1979	101	303	277	44	3995	538	279
EGP_07_379	1	2584	138	296	567	39	4759	1047	96
EGP_07_378	2	1298	67	168	292	21	2404	534	55
EGP_07_377	3	1151	58	146	200	28	2121	419	66
EGP_07_376	4	313	10	41	27	21	574	113	38
EGP_07_375	5	269	9	38	30	20	501	94	35
EGP_07_374	6	260	9	38	22	21	478	89	31
EGP_07_373	7	244	5	35	20	22	448	86	32
EGP_07_372	8	237	8	39	22	22	449	91	32
EGP_07_371	9	255	8	41	36	22	486	93	37
EGP_07_370	10	284	10	40	25	21	528	100	34
EGP_07_369	11	283	10	39	23	20	525	99	29
EGP_07_368	12	273	10	43	25	24	520	100	40
EGP_07_367	13	276	10	43	26	21	528	95	39
EGP_07_366	14	283	10	47	28	23	550	101	43
EGP_07_365	15	277	11	53	37	25	575	112	45
EGP_07_364	16	817	33	129	93	79	1567	369	92
EGP_07_363	17	2064	106	369	258	225	3785	1413	224
EGP_07_362	18	2224	124	421	284	209	4258	1107	191
EGP_07_361	19	1820	98	345	256	151	3589	809	148
EGP_07_360	20	962	53	175	115	68	1983	200	74
EGP_07_359	21	1004	58	188	136	37	2113	180	77
EGP_07_358	22	1863	89	284	325	19	3753	432	120
EGP_07_357	23	622	32	109	95	17	1289	88	42
EGP_07_356	24	585	26	97	104	16	1187	94	50
EGP_07_355	25	505	22	79	145	21	987	211	61
EGP_07_354	26	359	13	66	157	22	655	367	61
EGP_07_353	27	306	10	53	134	22	542	307	79
EGP_07_352	28	314	10	54	137	27	521	355	93
EGP_07_351	29	303	10	50	126	27	510	312	132
EGP_07_350	30	300	10	47	120	28	507	298	92
EGP_07_349	31	298	10	52	130	30	505	315	101
EGP_07_348	32	295	10	53	138	33	502	354	120
EGP_07_347	33	312	10	52	134	32	507	336	112
EGP_07_346	34	298	10	51	127	33	507	301	111
EGP_07_345	35	296	10	52	126	41	509	304	113
EGP_07_344	36	307	11	52	122	40	501	309	115
EGP_07_343	37	305	10	52	142	39	511	317	126
EGP_07_342	38	311	11	52	120	45	514	306	112
EGP_07_341	39	299	10	51	126	41	506	297	162
EGP_07_340	40	324	12	49	135	50	527	338	106
EGP_07_339	41	261	8	41	140	45	411	393	87
EGP_07_338	42	124	4	26	44	27	223	133	54
EGP_07_337	43	117	4	23	35	23	209	109	39
EGP_07_336	44	122	4	23	31	26	211	113	36
EGP_07_335	45	116	4	22	31	24	209	104	34
EGP_07_334	46	114	4	21	39	28	204	110	28
EGP_07_333	47	114	4	21	48	30	208	108	30
EGP_07_332	48	116	4	20	32	29	210	105	26
EGP_07_331	49	114	4	21	40	31	209	101	28
EGP_07_330	50	115	4	21	24	30	211	99	28
EGP_07_329	51	118	4	20	22	30	214	99	21

Table A3.2 continued.

Sample	Depth (cm)	Na ⁺ (ppb)	K ⁺ (ppb)	Mg ⁺ (ppb)	Ca ⁺ (ppb)	MS ⁻ (ppb)	Cl ⁻ (ppb)	SO ₄ ²⁻ (ppb)	NO ₃ ⁻ (ppb)
EGP_07_328	52	117	4	21	22	31	211	98	27
EGP_07_327	53	123	4	23	22	29	220	99	32
EGP_07_326	54	126	4	21	20	25	231	81	22
EGP_07_325	55	121	4	21	16	27	224	74	26
EGP_07_324	56	118	4	19	26	27	220	69	25
EGP_07_323	57	114	4	18	13	28	211	68	15
EGP_07_322	58	93	3	17	16	28	178	59	25
EGP_07_321	59	81	3	14	26	32	159	62	26
EGP_07_320	60	80	3	16	51	43	156	80	54
EGP_07_319	61	50	3	15	23	43	112	58	65
EGP_07_318	62	200	9	35	84	61	374	271	201
EGP_07_317	63	286	12	44	94	70	486	396	250
EGP_07_316	64	309	13	49	87	63	528	413	272
EGP_07_315	65	439	17	64	64	66	724	527	340
EGP_07_314	66	163	7	34	47	41	371	342	266
EGP_07_313	67	31	4	24	44	32	199	173	217
EGP_07_312	68	32	4	34	53	22	153	135	200
EGP_07_311	69	369	24	102	133	14	809	196	157
EGP_07_310	70	953	58	213	253	20	2085	381	260
EGP_07_309	71	2664	157	520	501	30	5775	766	392
EGP_07_308	72	2465	154	499	434	28	5484	594	369
EGP_07_307	73	12782	716	2141	1612	250	29075	2198	634
EGP_07_306	74	12810	689	2065	1633	368	27554	2416	618
EGP_07_305	75	8304	459	1359	1154	222	17404	1645	443
EGP_07_304	76	1832	100	276	398	35	3644	504	145
EGP_07_303	77	1157	65	168	314	29	2254	395	109
EGP_07_302	78	481	29	60	230	23	863	286	74
EGP_07_301	79	466	26	56	171	24	861	250	74
EGP_07_300	80	407	22	45	127	23	755	187	69
EGP_07_299	81	444	35	77	264	45	827	265	148
EGP_07_298	82	327	21	69	263	37	655	209	81
EGP_07_297	83	1060	48	155	334	72	1949	465	133
EGP_07_296	84	881	38	133	230	64	1603	351	165
EGP_07_295	85	768	34	111	196	72	1377	357	105
EGP_07_294	86	820	38	118	224	87	1497	404	138
EGP_07_293	87	457	23	76	101	62	855	172	146
EGP_07_292	88	549	26	87	142	70	1013	223	188
EGP_07_291	89	233	15	63	126	35	509	217	165
EGP_07_290	90	454	30	96	226	66	849	515	147
EGP_07_287	93	453	17	66	67	177	796	672	103
EGP_07_286	94	334	11	45	75	151	574	577	105
EGP_07_285	95	64	5	21	88	100	177	221	129
EGP_07_283	97	12	3	21	39	48	89	120	82
EGP_07_282	98	20	5	40	69	34	158	124	78
EGP_07_281	99	1128	83	221	380	76	2161	683	295
EGP_07_280	100	2104	135	336	594	111	3887	1175	485
EGP_07_279	101	928	83	175	533	36	1807	745	262
EGP_07_278	102	1966	197	328	1363	78	3649	2075	726
EGP_07_277	103	455	27	65	138	41	876	292	187
EGP_07_276	104	159	5	33	71	31	515	158	149
EGP_07_275	105	149	5	29	24	32	525	150	156
EGP_07_274	106	199	7	34	28	31	627	179	185
EGP_07_273	107	380	13	54	45	26	855	339	254
EGP_07_272	108	516	18	79	66	27	964	628	258
EGP_07_271	109	486	17	73	80	31	932	552	264
EGP_07_270	110	296	11	56	72	44	605	330	192
EGP_07_269	111	315	13	58	91	30	584	297	133
EGP_07_268	112	329	12	61	98	39	598	307	129

Table A3.2 continued.

Sample	Depth (cm)	Na ⁺ (ppb)	K ⁺ (ppb)	Mg ⁺ (ppb)	Ca ⁺ (ppb)	MS ⁻ (ppb)	Cl ⁻ (ppb)	SO ₄ ²⁻ (ppb)	NO ₃ ⁻ (ppb)
EGP_07_267	113	302	13	59	123	28	586	269	107
EGP_07_266	114	373	19	63	170	30	715	291	128
EGP_07_265	115	458	33	66	202	39	874	319	141
EGP_07_264	116	517	26	75	229	38	988	358	153
EGP_07_263	117	490	27	77	223	27	957	347	157
EGP_07_262	118	439	24	76	207	26	879	329	137
EGP_07_261	119	436	23	92	124	38	819	358	100
EGP_07_260	120	422	21	100	85	35	868	259	67
EGP_07_259	121	558	27	105	100	40	1103	261	84
EGP_07_258	122	762	35	92	203	32	1429	364	145
EGP_07_257	123	538	22	65	214	28	1081	375	153
EGP_07_256	124	302	15	62	159	19	669	196	94
EGP_07_255	125	183	8	54	120	31	462	99	59
EGP_07_252	128	686	24	72	87	36	1163	249	130
EGP_07_251	129	480	19	73	108	18	834	448	121
EGP_07_250	130	136	6	35	62	33	318	360	75
EGP_07_249	131	26	2	12	26	40	170	202	135
EGP_07_248	132	13	1	7	18	34	154	122	64
EGP_07_247	133	13	2	8	15	31	124	123	70
EGP_07_246	134	14	1	10	17	27	113	116	81
EGP_07_245	135	15	2	10	19	19	94	123	78
EGP_07_244	136	17	2	11	22	19	80	127	82
EGP_07_243	137	16	3	14	25	35	72	125	101
EGP_07_242	138	16	4	15	28	15	69	122	84
EGP_07_241	139	20	4	25	40	13	76	164	92
EGP_07_239	141	24	2	9	17	18	97	138	80
EGP_07_238	142	33	2	12	17	15	127	151	77
EGP_07_237	143	40	2	11	22	20	152	166	61
EGP_07_236	144	44	3	13	32	20	167	172	63
EGP_07_235	145	45	3	12	22	26	168	175	66
EGP_07_234	146	47	4	15	21	19	171	179	63
EGP_07_233	147	52	3	16	24	15	176	185	67
EGP_07_232	148	58	3	17	28	18	181	185	84
EGP_07_231	149	59	6	20	24	20	188	168	111
EGP_07_230	150	122	7	33	31	21	291	170	143
EGP_07_229	151	123	7	37	32	19	287	167	152
EGP_07_228	152	397	17	73	59	13	688	412	128
EGP_07_227	153	574	25	107	60	18	945	516	85
EGP_07_226	154	1026	43	175	111	26	1679	798	91
EGP_07_225	155	2448	100	370	226	22	3926	1675	150
EGP_07_224	156	5443	192	760	461	38	8495	3691	289
EGP_07_223	157	1249	63	199	130	30	2247	527	73
EGP_07_222	158	865	44	171	108	32	1781	163	77
EGP_07_221	159	1253	61	217	147	30	2519	191	112
EGP_07_220	160	1240	62	212	141	32	2483	183	129
EGP_07_219	161	1173	56	203	174	27	2368	183	107
EGP_07_218	162	920	44	172	122	22	1905	154	94
EGP_07_217	163	927	45	168	121	27	1927	152	97
EGP_07_216	164	842	42	141	151	31	1732	249	93
EGP_07_215	165	704	38	136	180	16	1460	226	67
EGP_07_214	166	502	23	98	114	17	1028	155	54
EGP_07_213	167	809	34	135	174	10	1607	229	62
EGP_07_212	168	934	45	154	197	9	1864	248	69
EGP_07_211	169	1210	55	177	226	9	2334	308	76
EGP_07_210	170	828	36	140	175	10	1636	222	66
EGP_07_209	171	891	45	136	176	9	1708	264	49
EGP_07_208	172	941	37	143	187	10	1771	289	60
EGP_07_207	173	1210	46	186	249	9	2265	362	73

Table A3.2 continued.

Sample	Depth (cm)	Na ⁺ (ppb)	K ⁺ (ppb)	Mg ⁺ (ppb)	Ca ⁺ (ppb)	MS ⁻ (ppb)	Cl ⁻ (ppb)	SO ₄ ²⁻ (ppb)	NO ₃ ⁻ (ppb)
EGP_07_206	174	2021	121	251	661	24	1780	1925	105
EGP_07_205	175	929	37	128	113	16	1685	259	48
EGP_07_204	176	1417	56	169	162	10	2595	388	58
EGP_07_203	177	1250	49	148	156	22	2250	368	61
EGP_07_202	178	1186	50	139	149	25	2126	342	63
EGP_07_201	179	1263	47	143	167	22	2245	362	67
EGP_07_200	180	1532	64	183	214	28	2769	459	82
EGP_07_199	181	1377	62	161	217	29	2488	434	72
EGP_07_198	182	2141	96	273	336	44	3992	649	110
EGP_07_197	183	3863	173	542	387	47	7341	1000	136
EGP_07_196	184	2993	140	451	288	42	5838	705	110
EGP_07_195	185	3673	220	865	268	56	7936	851	221
EGP_07_194	186	2147	104	369	199	30	4121	738	114
EGP_07_193	187	2267	102	389	196	12	4393	802	135
EGP_07_192	188	2439	110	423	200	24	4800	879	130
EGP_07_191	189	1061	49	194	87	31	2044	494	68
EGP_07_190	190	521	22	100	45	23	917	371	76
EGP_07_189	191	648	28	119	65	26	1121	409	80
EGP_07_188	192	710	39	126	72	43	1232	360	139
EGP_07_187	193	80	6	21	5	43	4576	1069	325
EGP_07_186	194	181	9	35	11	19	4672	721	293
EGP_07_185	195	498	24	83	28	12	1024	99	74
EGP_07_184	196	538	22	93	26	20	1681	167	63
EGP_07_183	197	776	34	135	40	15	8691	1140	167
EGP_07_182	198	721	29	104	26	23	12571	1613	243
EGP_07_181	199	701	27	91	26	21	18342	1887	351
EGP_07_180	200	547	23	70	22	19	14681	780	223
EGP_07_179	201	621	25	68	23	25	11254	247	90
EGP_07_178	202	611	26	61	26	23	10104	189	89
EGP_07_177	203	1025	44	132	75	22	9851	189	76
EGP_07_176	204	1814	80	222	100	22	11399	561	70
EGP_07_175	205	1653	66	189	75	61	20460	1809	253
EGP_07_174	206	1403	52	163	65	73	29705	2586	449
EGP_07_173	207	1098	41	115	55	80	31081	2726	444
EGP_07_172	208	712	23	61	32	46	31981	2980	515
EGP_07_171	209	456	13	37	16	25	18854	1925	322
EGP_07_170	210	164	4	16	3	20	9522	793	102
EGP_07_169	211	23	1	2	BDL	14	5518	596	81
EGP_07_168	212	53	1	6	BDL	5	1881	219	45
EGP_07_167	213	75	1	10	2	8	1245	153	53
EGP_07_166	214	97	2	15	5	12	612	105	40
EGP_07_165	215	214	10	47	24	13	502	74	35
EGP_07_164	216	191	10	50	28	12	477	67	37
EGP_07_163	217	244	15	64	34	12	582	90	38
EGP_07_162	218	515	26	93	53	15	1018	191	61
EGP_07_161	219	905	43	115	87	8	1617	344	139
EGP_07_160	220	302	20	54	29	25	2367	641	123
EGP_07_159	221	1650	67	212	123	27	2678	870	123
EGP_07_158	222	1917	109	385	159	15	3849	699	104
EGP_07_157	223	3004	158	499	196	13	6217	339	73
EGP_07_156	224	3065	159	521	198	14	6403	249	75
EGP_07_155	225	3750	195	766	287	20	7838	703	141
EGP_07_154	226	2580	158	461	160	50	5448	192	55
EGP_07_153	227	1360	194	259	87	18	2938	88	70
EGP_07_152	228	1193	195	261	84	21	2709	89	56
EGP_07_151	229	2088	164	342	167	20	4342	247	46
EGP_07_150	230	3821	157	623	287	12	7867	419	64
EGP_07_149	231	4721	195	809	340	12	10083	490	114

Table A3.2 continued.

Sample	Depth (cm)	Na ⁺ (ppb)	K ⁺ (ppb)	Mg ⁺ (ppb)	Ca ⁺ (ppb)	MS ⁻ (ppb)	Cl ⁻ (ppb)	SO ₄ ²⁻ (ppb)	NO ₃ ⁻ (ppb)
EGP_07_148	232	5023	216	866	363	10	10676	530	99
EGP_07_147	233	4155	186	622	313	11	8529	516	93
EGP_07_146	234	3411	169	491	267	13	6870	453	72
EGP_07_145	235	2990	156	366	227	11	5731	459	61
EGP_07_144	236	756	47	108	50	15	1518	100	31
EGP_07_143	237	262	16	61	29	13	615	47	27
EGP_07_142	238	127	5	45	24	4	368	41	32
EGP_07_141	239	180	7	32	30	15	376	67	46
EGP_07_140	240	278	18	42	44	37	509	130	83
EGP_07_139	241	360	12	54	35	9	638	162	54
EGP_07_138	242	368	17	55	33	8	665	160	53
EGP_07_137	243	417	17	62	31	10	740	173	60
EGP_07_136	244	428	16	64	34	13	760	180	106
EGP_07_135	245	456	17	65	34	8	799	184	55
EGP_07_134	246	448	15	66	35	9	803	185	57
EGP_07_133	247	577	19	72	42	10	982	213	65
EGP_07_132	248	333	13	75	50	8	690	187	48
EGP_07_131	249	398	25	104	62	8	912	184	54
EGP_07_130	250	2130	107	302	212	23	4020	573	192
EGP_07_129	251	2779	126	382	280	30	5313	714	243
EGP_07_128	252	4771	250	726	492	68	9385	1086	527
EGP_07_127	253	4179	216	580	382	52	8132	768	403
EGP_07_126	254	3206	141	412	303	40	6360	498	293
EGP_07_125	255	2442	96	301	227	26	4731	336	214
EGP_07_124	256	1749	80	223	161	20	3421	263	159
EGP_07_123	257	470	30	93	55	7	1066	137	51
EGP_07_122	258	187	7	61	27	12	520	117	45
EGP_07_121	259	172	4	36	44	4	394	114	51
EGP_07_120	260	178	5	32	18	12	386	118	83
EGP_07_119	261	185	4	30	22	11	385	126	86
EGP_07_118	262	182	5	28	22	12	380	121	93
EGP_07_117	263	168	5	26	24	2	364	118	119
EGP_07_116	264	171	4	28	20	10	373	120	120
EGP_07_115	265	179	4	34	17	10	396	129	107
EGP_07_114	266	160	5	37	20	17	430	119	98
EGP_07_113	267	243	8	52	25	32	600	136	82
EGP_07_112	268	653	21	88	46	63	1147	289	95
EGP_07_111	269	906	28	112	59	84	1528	372	106
EGP_07_110	270	959	33	120	61	101	1602	397	107
EGP_07_109	271	1007	32	104	61	96	1670	371	107
EGP_07_108	272	466	13	63	32	54	860	353	68
EGP_07_107	273	162	4	33	12	27	369	323	67
EGP_07_106	274	81	3	18	15	26	178	245	122
EGP_07_105	275	99	6	22	13	35	200	189	114
EGP_07_104	276	369	10	50	20	38	557	327	96
EGP_07_103	277	361	9	55	23	25	552	491	61
EGP_07_102	278	210	5	40	17	21	399	318	58
EGP_07_101	279	138	5	36	18	16	282	210	70
EGP_07_100	280	130	5	48	23	12	286	196	80
EGP_07_099	281	73	7	34	21	9	187	144	87
EGP_07_098	282	40	8	41	19	7	164	96	92
EGP_07_097	283	156	18	76	40	24	534	97	70
EGP_07_096	284	5839	325	906	396	65	12383	997	148
EGP_07_095	285	8393	443	1288	572	62	18081	1217	163
EGP_07_094	286	12500	663	1776	827	49	26856	1772	202
EGP_07_093	287	9108	461	1412	618	30	19742	1329	142
EGP_07_092	288	8943	449	1344	596	8	19124	1219	117
EGP_07_091	289	7356	364	1066	469	BDL	15331	1014	87

Table A3.2 continued.

Sample	Depth (cm)	Na ⁺ (ppb)	K ⁺ (ppb)	Mg ⁺ (ppb)	Ca ⁺ (ppb)	MS ⁻ (ppb)	Cl ⁻ (ppb)	SO ₄ ²⁻ (ppb)	NO ₃ ⁻ (ppb)
EGP_07_090	290	2839	173	372	166	BDL	5693	277	54
EGP_07_089	291	2181	161	264	124	BDL	4387	176	23
EGP_07_088	292	2489	161	260	135	BDL	4913	169	55
EGP_07_087	293	3613	223	514	260	BDL	7688	310	50
EGP_07_086	294	7713	473	1509	758	BDL	18833	900	139
EGP_07_085	295	16175	1211	2908	1571	BDL	40383	1903	262
EGP_07_084	296	17017	1251	2896	1545	BDL	40666	1873	120
EGP_07_083	297	16939	1231	2946	1447	12	40559	1905	106
EGP_07_082	298	16553	1220	3027	1497	105	39728	1858	174
EGP_07_080	300	15045	1098	3000	1600	240	36215	1840	452
EGP_07_079	301	11523	830	2562	1107	192	27566	1650	386
EGP_07_078	302	6834	332	900	748	72	13149	2170	169
EGP_07_077	303	3693	236	644	258	43	7484	978	81
EGP_07_076	304	2135	120	266	135	26	3933	727	60
EGP_07_075	305	1168	60	132	66	8	2001	512	39
EGP_07_074	306	488	18	89	45	BDL	846	458	44
EGP_07_073	307	310	14	76	45	7	647	432	43
EGP_07_072	308	1553	57	185	138	68	2594	874	242
EGP_07_071	309	909	42	122	80	49	1632	457	154
EGP_07_070	310	813	32	114	72	49	1477	428	132
EGP_07_069	311	515	22	89	49	37	1057	275	107
EGP_07_068	312	470	21	87	49	39	1016	226	76
EGP_07_067	313	932	33	126	81	53	1686	386	109
EGP_07_066	314	960	38	146	84	58	1713	458	111
EGP_07_065	315	765	31	144	86	54	1413	478	95
EGP_07_064	316	886	35	142	82	56	1625	483	97
EGP_07_063	317	846	32	142	75	56	1541	480	93
EGP_07_062	318	888	35	144	82	59	1616	492	99
EGP_07_061	319	1213	44	158	98	71	2105	590	141
EGP_07_060	320	1354	48	159	107	82	2278	667	149
EGP_07_059	321	991	34	109	76	55	1651	563	130
EGP_07_058	322	236	9	45	35	7	503	375	51
EGP_07_057	323	320	12	54	29	BDL	585	427	60
EGP_07_056	324	442	17	73	36	BDL	742	508	45
EGP_07_055	325	714	22	119	69	6	1190	587	48
EGP_07_054	326	599	24	134	88	18	1202	481	58
EGP_07_053	327	2657	141	521	306	61	5674	807	194
EGP_07_052	328	3919	195	613	428	101	7875	991	249
EGP_07_051	329	1506	66	191	171	51	2831	372	119
EGP_07_050	330	803	41	129	59	41	1602	101	70
EGP_07_049	331	639	27	108	75	29	1321	148	60
EGP_07_048	332	341	18	98	68	22	863	114	60
EGP_07_047	333	207	12	91	48	7	653	97	31
EGP_07_046	334	1193	47	180	98	17	2281	384	62
EGP_07_045	335	2205	77	274	141	26	4018	651	54
EGP_07_044	336	2890	89	357	153	37	5259	810	63
EGP_07_043	337	2807	86	338	138	37	5090	778	64
EGP_07_042	338	1618	62	205	75	25	2927	479	43
EGP_07_041	339	949	40	133	44	22	1728	293	40
EGP_07_040	340	1037	41	135	51	22	1866	307	30
EGP_07_039	341	786	30	107	42	19	1426	241	30
EGP_07_038	342	607	17	95	36	21	1147	204	53
EGP_07_037	343	682	20	103	33	26	1275	233	31
EGP_07_036	344	789	22	113	42	29	1432	258	40
EGP_07_035	345	915	27	127	43	33	1658	286	48
EGP_07_034	346	1071	34	142	51	36	1899	321	65
EGP_07_033	347	1306	41	173	59	40	2314	397	104
EGP_07_032	348	1306	42	174	61	43	2328	393	74

Table A3.2 continued.

Sample	Depth (cm)	Na ⁺ (ppb)	K ⁺ (ppb)	Mg ⁺ (ppb)	Ca ⁺ (ppb)	MS ⁻ (ppb)	Cl ⁻ (ppb)	SO ₄ ²⁻ (ppb)	NO ₃ ⁻ (ppb)
EGP_07_031	349	1714	53	221	81	61	3037	519	103
EGP_07_030	350	1857	57	235	100	66	3259	569	136
EGP_07_029	351	1725	55	207	142	58	2973	538	148
EGP_07_028	352	1346	57	192	540	39	2131	521	166
EGP_07_027	353	1138	35	139	80	43	1996	489	125
EGP_07_026	354	602	21	85	66	29	1094	404	106
EGP_07_025	355	589	22	96	67	81	1061	413	110
EGP_07_024	356	363	13	73	50	74	681	369	113
EGP_07_023	357	356	13	73	49	78	673	375	122
EGP_07_022	358	336	11	60	40	73	611	353	120
EGP_07_021	359	343	11	55	36	BDL	635	349	128
EGP_07_020	360	364	12	57	41	BDL	660	351	136
EGP_07_019	361	370	12	60	39	76	672	357	148
EGP_07_018	362	369	11	62	45	69	677	347	131
EGP_07_017	363	374	11	64	47	73	678	356	133
EGP_07_016	364	330	10	61	35	78	642	266	122
EGP_07_015	365	293	12	53	37	79	601	198	119
EGP_07_014	366	285	9	55	48	78	595	153	112
EGP_07_013	367	238	9	52	56	6	528	107	111
EGP_07_012	368	359	20	62	143	82	704	82	112
EGP_07_011	369	286	10	63	38	5	642	59	90
EGP_07_010	370	476	22	131	56	78	1171	66	58
EGP_07_009	371	1298	67	218	112	56	2681	185	77
EGP_07_008	372	1141	55	195	101	55	2385	186	61
EGP_07_007	373	1707	76	259	143	53	3437	291	95
EGP_07_006	374	2078	91	299	183	54	4096	393	95
EGP_07_005	375	2106	93	304	177	52	4129	390	88
EGP_07_004	376	2359	92	337	191	51	4607	504	83
EGP_07_003	377	2678	94	381	220	56	5199	600	98
EGP_07_002	378	2074	86	294	167	53	4027	427	82
EGP_07_001	379	2727	92	367	220	54	5206	599	98

Table A3.3 Repeated measurement of the external standard SLRS-4 (National Research Council, Canada) at 1:100 dilution by collision cell ICP-MS to determine analytical precision and accuracy.

Standard	Na (ppb)	Mg (ppb)	Al (ppb)	Ca (ppb)	Mn (ppb)	Fe (ppb)	Ba (ppb)	Al/Na	Fe/Al
Average	2120	1584	56	5731	3.4	105	12.5	0.027	1.9
2 σ	164	73	4	379	0.2	6	0.71	0.002	0.1
2 rsd (%)	8	5	8	7	6	6	6	8	6
1:100 dilution of SLRS-4 measured									
Average	21	15.8	0.56	57	0.034	1.05	0.125	0.027	1.86
2 σ	2	0.7	0.04	4	0.002	0.06	0.007	0.002	0.10
SLRS-4_1	2086	1557	56	5717	3.3	104	12.1	0.027	1.9
SLRS-4_2	2075	1559	62	5848	3.3	105	12.5	0.030	1.7
SLRS-4_3	2031	1533	54	5663	3.2	101	12.3	0.027	1.9
SLRS-4_4	2092	1583	56	5450	3.4	105	12.8	0.027	1.9
SLRS-4_5	2142	1627	56	5546	3.4	106	12.6	0.026	1.9
SLRS-4_6	2129	1605	57	5906	3.4	108	12.7	0.027	1.9
SLRS-4_7	2112	1598	57	5819	3.4	107	12.7	0.027	1.9
SLRS-4_8	2088	1551	54	5479	3.2	99	11.7	0.026	1.8
SLRS-4_9	2090	1565	55	5498	3.2	100	11.9	0.026	1.8
SLRS-4_10	2090	1565	55	5498	3.2	100	11.9	0.026	1.8
SLRS-4_11	2207	1627	58	5979	3.5	107	12.7	0.026	1.9
SLRS-4_12	2175	1615	57	5909	3.4	108	12.7	0.026	1.9
SLRS-4_13	2282	1650	58	6028	3.5	109	12.9	0.025	1.9
SLRS-4_14	2251	1638	59	5990	3.5	108	12.8	0.026	1.8
SLRS-4_15	1956	1528	53	5619	3.3	103	12.5	0.027	1.9
SLRS-4_16	2009	1567	55	5793	3.4	105	12.7	0.027	1.9
SLRS-4_17	2183	1574	55	5726	3.3	104	12.4	0.025	1.9
SLRS-4_18	2163	1561	55	5680	3.3	103	12.3	0.025	1.9

Table A3.4 Standard deviations of blank measurements used to determine the detection limits of elements measured by collision cell ICP-MS.

Blank σ	Na (ppb)	Mg (ppb)	Al (ppb)	Ca (ppb)	Mn (ppb)	Fe (ppb)	Ba (ppt)
Average 3 σ	0.21	0.012	0.016	0.10	0.99	0.013	0.0039
Blank_1	0.02	0.003	0.003	0.03	0.27	0.002	0.0007
Blank_2	0.02	0.003	0.003	0.03	0.22	0.001	0.0003
Blank_3	0.02	0.003	0.002	0.04	0.27	0.001	0.0004
Blank_4	0.02	0.004	0.002	0.03	0.18	0.009	0.0003
Blank_5	0.02	0.006	0.002	0.03	0.23	0.001	0.0014
Blank_6	0.03	0.005	0.003	0.03	0.28	0.002	0.0009
Blank_7	0.02	0.004	0.006	0.02	0.21	0.002	0.0017
Blank_8	0.02	0.005	0.008	0.04	0.26	0.002	0.0018
Blank_9	0.04	0.008	0.013	0.09	0.29	0.007	0.0019
Blank_10	0.02	0.008	0.017	0.04	0.35	0.003	0.0017
Blank_11	0.03	0.005	0.018	0.03	0.31	0.002	0.0015
Blank_12	0.02	0.007	0.009	0.04	0.25	0.053	0.0013
Blank_13	0.02	0.005	0.009	0.02	0.25	0.003	0.0017
Blank_14	0.02	0.006	0.006	0.02	0.28	0.003	0.0016
Blank_15	0.02	0.005	0.007	0.02	0.34	0.003	0.0018
Blank_16	0.02	0.005	0.006	0.02	0.26	0.002	0.0015
Blank_17	0.45	0.005	0.011	0.04	0.43	0.015	0.0015
Blank_18	0.09	0.004	0.004	0.02	0.35	0.001	0.0009
Blank_19	0.16	0.003	0.005	0.02	0.40	0.006	0.0015
Blank_20	0.08	0.003	0.005	0.01	0.37	0.001	0.0006
Blank_21	0.11	0.010	0.008	0.09	0.81	0.044	0.0051
Blank_22	0.08	0.003	0.006	0.03	0.47	0.005	0.0019
Blank_23	0.07	0.004	0.007	0.04	0.53	0.006	0.0019
Blank_24	0.09	0.002	0.004	0.04	0.41	0.001	0.0013
Blank_25	0.08	0.002	0.003	0.16	0.31	0.001	0.0015
Blank_26	0.08	0.002	0.004	0.05	0.38	0.004	0.0016
Blank_27	0.09	0.001	0.003	0.03	0.33	0.001	0.0006
Blank_28	0.07	0.002	0.003	0.02	0.31	0.004	0.0012
Blank_29	0.07	0.002	0.003	0.02	0.27	0.001	0.0004
Blank_30	0.06	0.006	0.003	0.03	0.45	0.001	0.0007
Blank_31	0.06	0.001	0.003	0.01	0.34	0.001	0.0004
Blank_32	0.06	0.003	0.004	0.04	0.36	0.001	0.0024
Blank_33	0.10	0.004	0.007	0.03	0.32	0.001	0.0009
Blank_34	0.06	0.003	0.003	0.01	0.32	0.001	0.0006
Blank_35	0.06	0.002	0.003	0.01	0.29	0.001	0.0006
Blank_36	0.06	0.002	0.003	0.02	0.27	0.001	0.0018
Blank_37	0.07	0.005	0.003	0.02	0.30	0.001	0.0011
Blank_38	0.05	0.004	0.003	0.02	0.29	0.001	0.0012
Blank_39	0.09	0.002	0.006	0.01	0.26	0.001	0.0020
Blank_40	0.07	0.002	0.007	0.01	0.31	0.001	0.0023
Blank_41	0.07	0.003	0.005	0.02	0.43	0.002	0.0017
Blank_42	0.08	0.006	0.005	0.08	0.32	0.002	0.0017
Blank_43	0.13	0.011	0.004	0.02	0.30	0.001	0.0005
Blank_44	0.09	0.004	0.006	0.04	0.38	0.001	0.0025
Blank_45	0.07	0.007	0.008	0.03	0.40	0.001	0.0007
Blank_46	0.07	0.003	0.003	0.02	0.31	0.001	0.0007
Blank_47	0.06	0.002	0.004	0.03	0.31	0.001	0.0010
Blank_48	0.07	0.003	0.004	0.05	0.33	0.001	0.0008
Blank_49	0.10	0.003	0.004	0.04	0.33	0.001	0.0006

Table A3.5 Repeated measurement of select EPG snow samples by collision cell ICP-MS.

Sample	Measurement	Na (ppb)	Mg (ppb)	Al (ppb)	Ca (ppb)	Mn (ppb)	Fe (ppb)	Ba (ppb)	Al/Na	Fe/Al
EPG_231	1	43	11	5.0	11	0.13	6.0	0.031	0.84	1.2
EPG_231	2	43	10	4.0	11	0.11	3.8	0.024	1.1	0.95
EPG_098	1	60	21	1.2	7.5	0.034	0.77	0.009	1.6	0.64
EPG_098	2	44	15	0.83	5.8	0.024	0.51	0.006	1.6	0.61
EPG_229	1	136	24	6.3	18	0.22	5.1	0.034	1.2	0.81
EPG_229	2	131	23	6.2	17	0.20	5.4	0.032	1.1	0.88
EPG_027	1	1500	214	60	128	1.1	65	0.29	0.93	1.1
EPG_027	2	1248	171	36	100	0.75	39	0.18	0.94	1.1
EPG_178	1	3126	432	4.7	110	0.13	2.9	0.035	1.6	0.62
EPG_178	2	3074	423	4.2	109	0.14	3.0	0.039	1.4	0.72
EPG_170	1	3601	325	39	308	1.5	32	0.38	1.2	0.83
EPG_170	2	3725	336	42	325	1.8	40	0.52	1.0	0.96
EPG_170	3	3798	339	37	327	1.7	35	0.41	1.1	0.94
EPG_176	1	4006	385	20	223	0.94	17	0.23	1.2	0.85
EPG_176	2	3992	384	25	232	1.1	21	0.31	1.2	0.85
EPG_176	3	3978	382	24	230	1.1	21	0.26	1.2	0.86
EPG_180	1	4743	745	23	287	0.78	18	0.19	1.3	0.78
EPG_180	2	4728	743	27	291	1.0	24	0.26	1.1	0.90
EPG_180	3	4456	704	41	283	1.1	36	0.32	1.1	0.88
EPG_096	1	12498	2172	245	925	4.5	210	1.1	1.2	0.86
EPG_096	2	9506	1623	108	639	2.5	92	0.54	1.2	0.85
EPG_94	1	28042	5133	441	2060	10	401	2.3	1.1	0.91
EPG_94	2	22069	3957	230	1600	5.5	204	1.2	1.1	0.89
EPG_94	3	17113	3034	131	1238	3.3	109	0.75	1.2	0.84
Difference from the first measurement of each sample (%)										
EPG_231	2	0	5	21	0	12	37	21	26	21
EPG_098	2	27	28	31	23	29	34	33	4	4
EPG_229	2	4	5	2	4	5	5	6	7	8
EPG_027	2	17	20	40	22	35	40	38	1	1
EPG_178	2	2	2	10	1	4	4	11	14	16
EPG_170	2	3	3	8	5	24	26	38	14	16
EPG_170	3	5	5	4	6	19	10	10	12	14
EPG_176	2	0	0	23	4	17	22	35	1	1
EPG_176	3	1	1	22	3	16	23	14	1	1
EPG_180	2	0	0	18	1	33	36	39	13	15
EPG_180	3	6	5	78	1	44	102	75	12	13
EPG_096	2	24	25	56	31	45	56	50	1	1
EPG_94	2	21	23	48	22	45	49	46	3	2
EPG_94	3	39	41	70	40	67	73	68	9	8
Average difference (%)		11	12	31	12	28	37	35	8	9
Max difference (%)		39	41	78	40	67	102	75	26	21
Min difference (%)		0	0	2	0	4	4	6	1	1

Table A3.6 60 scan averages of time resolved, collision cell ICP-MS analysis of select EPG snow samples.

Sample	Time (sec)	Na (ppb)	Mg (ppb)	Al (ppb)	Ca (ppb)	Mn (ppb)	Fe (ppb)	Ba (ppb)	Al/Na	Fe/Al
Average 2 rsd of samples		6	6	26	6	20	45	27	24	46
Average 2 rsd of 1ppb std.		3	4	5	6	3	4	4	3	2
1ppb_std	102	99	9.9	0.99	69	0.97	0.95	0.97	0.010	0.97
1ppb_std	111	99	9.7	0.99	69	0.97	0.96	0.97	0.010	0.97
1ppb_std	120	99	9.9	1.00	68	0.96	0.96	0.97	0.010	0.96
1ppb_std	130	99	9.9	0.99	69	0.97	0.95	0.96	0.010	0.96
1ppb_std	139	99	9.9	1.01	69	0.97	0.96	0.97	0.010	0.95
1ppb_std	148	100	10.0	1.00	69	0.98	0.97	0.97	0.010	0.96
1ppb_std	158	99	9.9	0.96	68	0.97	0.95	0.95	0.010	1.00
1ppb_std	167	99	9.8	0.99	69	0.97	0.96	0.97	0.010	0.97
1ppb_std	176	99	9.9	0.98	69	0.98	0.96	0.96	0.010	0.98
1ppb_std	185	91	9.1	0.89	63	0.89	0.88	0.88	0.010	0.98
EPG 170	250	4205	461	246	296	5.3	255	1.2	0.058	1.04
EPG 170	260	4282	463	255	301	5.2	289	1.3	0.060	1.13
EPG 170	269	4337	481	257	305	5.4	253	1.3	0.059	0.99
EPG 170	278	4373	476	267	307	5.3	261	1.3	0.061	0.98
EPG 170	287	4407	491	255	310	5.3	260	1.3	0.058	1.02
EPG 170	297	4355	476	268	307	5.3	257	1.2	0.062	0.96
EPG 170	306	4355	474	266	310	5.3	259	1.2	0.061	0.97
EPG 170	315	4400	482	260	311	5.4	260	1.3	0.059	1.00
EPG 170	324	4416	478	261	310	5.6	263	1.3	0.059	1.01
EPG 170	334	4396	481	258	311	5.4	254	1.3	0.059	0.99
EPG 170	343	4403	481	267	311	5.4	262	1.3	0.061	0.98
EPG 170	352	4447	489	267	314	5.5	335	1.3	0.060	1.26
EPG 170	362	4487	488	262	317	5.5	260	1.3	0.058	0.99
EPG 170	371	4466	486	269	318	5.5	292	1.3	0.060	1.08
EPG 170	380	4483	486	260	315	5.5	263	1.3	0.058	1.01
EPG 170	389	4505	486	270	319	5.5	264	1.3	0.060	0.98
EPG 170	399	4528	490	266	320	5.8	269	1.3	0.059	1.01
EPG 170	408	4549	496	267	325	5.5	269	1.3	0.059	1.01
EPG 170	417	4531	492	268	325	5.6	270	1.3	0.059	1.01
EPG 170	426	4550	495	269	322	6.4	272	1.3	0.059	1.01
EPG 170	436	4587	497	265	323	5.6	275	1.3	0.058	1.04
EPG 170	445	4586	502	269	324	5.6	280	1.3	0.059	1.04
EPG 170	454	4566	500	270	323	5.7	271	1.3	0.059	1.00
EPG 170	464	4592	499	270	323	5.8	275	1.3	0.059	1.02
EPG 170	473	4595	498	288	325	5.6	273	1.3	0.063	0.95
EPG 170	482	4568	499	270	323	5.6	267	1.3	0.059	0.99
EPG 170	491	4602	500	268	325	5.7	271	1.3	0.058	1.01
EPG 170	501	4622	505	273	325	5.8	270	1.3	0.059	0.99
EPG 170	510	4589	496	271	323	5.7	270	1.3	0.059	0.99
EPG 170	519	4573	497	268	322	5.7	274	1.3	0.059	1.02
EPG 170	528	4595	501	265	326	5.6	277	1.3	0.058	1.05
EPG 170	538	4587	498	266	323	5.7	274	1.3	0.058	1.03
EPG 170	547	4586	500	264	326	5.7	274	1.3	0.058	1.04
EPG 170	556	4596	500	268	326	5.6	286	1.3	0.058	1.07
EPG 170	566	4588	497	265	326	5.6	275	1.4	0.058	1.03
EPG 170	575	4598	504	269	324	5.6	274	1.3	0.058	1.02
EPG 170	584	4617	501	276	326	5.7	270	1.4	0.060	0.98
EPG 170	593	4624	507	270	327	5.8	271	1.3	0.058	1.00
EPG 170	603	4613	501	265	324	5.9	273	1.3	0.057	1.03
EPG 170	612	4619	502	269	328	5.7	271	1.3	0.058	1.01
EPG 170	621	4607	502	268	325	5.7	273	1.3	0.058	1.02

Table A3.6 continued.

Sample	Time (sec)	Na (ppb)	Mg (ppb)	Al (ppb)	Ca (ppb)	Mn (ppb)	Fe (ppb)	Ba (ppb)	Al/Na	Fe/Al
EPG 170	630	4636	506	270	327	5.6	276	1.4	0.058	1.02
EPG 170	640	4636	505	269	326	5.7	280	1.4	0.058	1.04
EPG 170	649	4608	505	266	326	5.7	276	1.3	0.058	1.03
EPG 170	658	4588	499	265	324	5.7	270	1.4	0.058	1.02
EPG 170	668	4656	500	271	326	5.7	280	1.4	0.058	1.03
EPG 170	677	4616	504	272	324	5.7	279	1.3	0.059	1.03
EPG 170	686	4612	510	267	324	5.8	279	1.3	0.058	1.05
EPG 170	695	4608	503	267	326	6.0	269	1.3	0.058	1.01
EPG 170	705	4600	503	269	325	5.7	275	1.3	0.058	1.02
EPG 170	714	4629	504	266	326	5.6	270	1.3	0.058	1.01
EPG 170	723	4644	505	266	327	5.8	277	1.4	0.057	1.04
EPG 170	732	4641	507	269	329	5.7	274	1.3	0.058	1.02
EPG 170	742	4647	506	274	331	5.7	281	1.3	0.059	1.03
EPG 170	751	4642	504	268	329	5.7	286	1.4	0.058	1.07
EPG 170	760	4603	500	265	326	6.0	282	1.3	0.058	1.06
EPG 170	770	4685	505	271	336	5.8	288	1.3	0.058	1.06
EPG 170	779	4674	507	271	330	5.8	284	1.4	0.058	1.05
EPG 170	788	4674	507	269	333	5.7	275	1.3	0.057	1.02
EPG 170	797	4654	504	270	329	5.7	287	1.3	0.058	1.06
EPG 170	807	4689	511	274	332	5.9	285	1.3	0.058	1.04
EPG 170	816	4692	509	276	332	5.9	289	1.3	0.059	1.05
EPG 170	825	4685	515	283	333	5.7	282	1.3	0.060	1.00
EPG 170	834	4702	511	287	339	5.9	290	1.4	0.061	1.01
EPG 170	844	4662	537	312	339	6.2	410	2.1	0.067	1.31
EPG 170	853	3574	411	250	262	5.1	290	1.3	0.070	1.16
EPG_098	1085	32	11.4	0.94	16	0.025	0.75	0.005	0.029	0.80
EPG_098	1094	32	11.4	0.92	17	0.027	0.83	0.005	0.029	0.90
EPG_098	1103	32	11.3	1.69	16	0.029	0.72	0.006	0.053	0.43
EPG_098	1113	32	11.4	1.85	16	0.026	0.81	0.005	0.058	0.44
EPG_098	1122	31	11.2	1.18	16	0.030	0.76	0.005	0.038	0.64
EPG_098	1131	32	11.2	1.13	16	0.028	4.12	0.008	0.036	3.64
EPG_098	1140	32	11.3	0.94	16	0.026	0.82	0.005	0.030	0.87
EPG_098	1150	32	11.2	1.19	16	0.029	0.96	0.006	0.038	0.80
EPG_098	1159	32	11.3	0.99	16	0.025	0.74	0.005	0.031	0.74
EPG_098	1168	31	11.3	3.56	16	0.025	0.78	0.006	0.113	0.22
EPG_098	1178	32	11.3	1.06	17	0.027	2.15	0.005	0.033	2.03
EPG_098	1187	32	11.2	0.90	16	0.027	0.80	0.007	0.028	0.90
EPG_098	1196	32	11.3	0.90	16	0.027	0.86	0.009	0.029	0.95
EPG_098	1205	32	11.3	1.23	17	0.025	1.34	0.006	0.039	1.09
EPG_098	1215	32	11.3	1.06	16	0.026	0.74	0.006	0.033	0.69
EPG_098	1224	32	11.3	1.05	17	0.026	1.29	0.005	0.033	1.23
EPG_098	1233	32	11.3	0.90	16	0.031	1.45	0.007	0.028	1.60
EPG_098	1242	32	11.3	1.05	16	0.073	0.91	0.007	0.033	0.87
EPG_098	1252	31	11.3	1.26	16	0.027	2.15	0.009	0.040	1.70
EPG_098	1261	32	11.4	1.18	16	0.026	0.83	0.006	0.037	0.71
EPG_098	1270	32	11.3	1.11	16	0.026	0.75	0.005	0.035	0.68
EPG_098	1280	32	11.3	1.03	16	0.030	0.74	0.006	0.033	0.72
EPG_098	1289	32	11.4	1.12	16	0.026	0.93	0.005	0.035	0.83
EPG_098	1298	32	11.6	1.14	16	0.025	0.98	0.005	0.036	0.86
EPG_098	1307	31	11.0	1.50	16	0.035	1.17	0.007	0.048	0.78
EPG_098	1317	32	11.2	0.94	16	0.025	0.75	0.008	0.030	0.81
EPG_098	1326	32	11.4	1.05	17	0.033	0.75	0.005	0.033	0.72
EPG_098	1335	32	11.3	1.54	16	0.032	0.74	0.005	0.049	0.48
EPG_098	1344	32	11.1	1.46	16	0.028	0.76	0.005	0.046	0.52
EPG_098	1354	31	11.2	1.06	16	0.027	1.47	0.004	0.034	1.38

Table A3.6 continued.

Sample	Time (sec)	Na (ppb)	Mg (ppb)	Al (ppb)	Ca (ppb)	Mn (ppb)	Fe (ppb)	Ba (ppb)	Al/Na	Fe/Al
EPG_098	1363	32	11.3	1.01	16	0.027	0.85	0.007	0.032	0.84
EPG_098	1372	31	11.0	0.94	16	0.027	0.76	0.006	0.030	0.81
EPG_098	1382	31	11.0	1.11	16	0.026	0.74	0.011	0.035	0.67
EPG_098	1391	31	11.1	1.26	16	0.027	0.73	0.011	0.040	0.58
EPG_098	1400	31	11.2	1.01	16	0.025	1.53	0.006	0.033	1.52
EPG_098	1409	31	11.1	0.86	16	0.031	0.71	0.006	0.028	0.83
EPG_098	1419	31	11.0	1.10	16	0.025	0.90	0.006	0.036	0.82
EPG_098	1428	31	11.0	0.88	16	0.026	2.45	0.011	0.029	2.78
EPG_098	1437	32	10.9	0.87	16	0.036	0.79	0.006	0.027	0.91
EPG_098	1446	30	10.9	0.89	16	0.026	0.81	0.007	0.029	0.91
EPG_098	1456	30	10.9	2.10	16	0.025	1.23	0.007	0.069	0.58
EPG_098	1465	30	10.8	1.10	16	0.030	1.45	0.006	0.036	1.32
EPG_098	1474	30	11.3	0.93	16	0.025	0.75	0.013	0.030	0.81
EPG_098	1484	31	10.8	0.94	16	0.025	0.78	0.006	0.031	0.83
EPG_098	1493	30	10.7	1.13	16	0.026	0.85	0.006	0.038	0.76
EPG_098	1502	30	10.8	1.23	16	0.026	0.82	0.007	0.041	0.67
EPG_098	1511	30	11.0	1.27	16	0.055	2.20	0.007	0.042	1.74
EPG_098	1521	30	10.9	1.23	16	0.024	0.71	0.005	0.041	0.57
EPG_098	1530	31	11.2	0.91	16	0.026	0.82	0.005	0.030	0.91
EPG_098	1539	30	10.8	1.05	16	0.026	0.71	0.005	0.035	0.67
EPG_098	1548	31	10.8	0.93	16	0.025	0.73	0.009	0.030	0.79
EPG_176	1688	4588	495	210	235	3.9	330	1.1	0.046	1.57
EPG_176	1697	4756	523	220	246	4.0	218	1.0	0.046	0.99
EPG_176	1706	4832	529	221	247	4.1	238	1.0	0.046	1.08
EPG_176	1715	4842	533	227	247	4.0	221	1.1	0.047	0.97
EPG_176	1725	4835	532	224	249	4.0	235	1.0	0.046	1.05
EPG_176	1734	4858	537	229	249	4.0	219	1.0	0.047	0.96
EPG_176	1743	4918	543	227	253	4.0	225	1.0	0.046	0.99
EPG_176	1752	4858	537	221	249	4.0	218	1.0	0.045	0.99
EPG_176	1762	4883	538	227	250	4.0	226	1.0	0.047	1.00
EPG_176	1771	4872	540	226	252	4.0	226	1.0	0.046	1.00
EPG_176	1780	4925	543	227	251	4.8	242	1.0	0.046	1.06
EPG_176	1790	4916	542	232	254	4.0	217	1.0	0.047	0.94
EPG_176	1799	4936	543	230	251	4.0	229	1.0	0.047	0.99
EPG_176	1808	4957	546	227	254	4.2	222	1.0	0.046	0.98
EPG_176	1817	4967	545	228	254	4.0	221	1.0	0.046	0.97
EPG_176	1827	4956	546	229	254	4.2	221	1.0	0.046	0.96
EPG_176	1836	4968	546	242	254	4.0	229	1.0	0.049	0.95
EPG_176	1845	4942	547	227	253	4.1	224	1.0	0.046	0.99
EPG_176	1854	5020	550	232	256	4.0	226	1.0	0.046	0.98
EPG_176	1864	5009	550	232	254	4.1	224	1.0	0.046	0.97
EPG_176	1873	4968	547	231	254	4.0	221	1.1	0.046	0.96
EPG_176	1882	4959	546	232	256	4.1	225	1.0	0.047	0.97
EPG_176	1892	4999	552	231	255	4.0	222	1.2	0.046	0.96
EPG_176	1901	4993	548	233	255	4.1	227	1.0	0.047	0.97
EPG_176	1910	4969	547	234	254	4.1	239	1.0	0.047	1.02
EPG_176	1919	4982	547	237	255	4.0	224	1.0	0.048	0.94
EPG_176	1929	5010	550	230	256	4.1	219	1.0	0.046	0.95
EPG_176	1938	4995	549	238	254	4.1	226	1.0	0.048	0.95
EPG_176	1947	4991	550	236	254	4.4	222	1.0	0.047	0.94
EPG_176	1957	4971	549	230	255	4.0	234	1.0	0.046	1.02
EPG_176	1966	4971	549	233	254	4.0	226	1.0	0.047	0.97
EPG_176	1975	4952	545	232	252	4.0	222	1.0	0.047	0.96
EPG_176	1984	4982	547	227	254	4.0	221	1.1	0.046	0.97
EPG_176	1994	5017	553	235	256	4.0	229	1.0	0.047	0.97

Table A3.6 continued.

Sample	Time (sec)	Na (ppb)	Mg (ppb)	Al (ppb)	Ca (ppb)	Mn (ppb)	Fe (ppb)	Ba (ppb)	Al/Na	Fe/Al
EPG_176	2003	5020	553	232	254	4.0	227	1.0	0.046	0.98
EPG_176	2012	4971	546	240	252	4.0	228	1.0	0.048	0.95
EPG_176	2021	4939	542	228	252	4.0	220	1.0	0.046	0.97
EPG_176	2031	4995	550	231	254	4.0	222	1.0	0.046	0.96
EPG_176	2040	4975	547	232	254	4.1	235	1.0	0.047	1.01
EPG_176	2049	4948	544	232	252	4.0	220	1.0	0.047	0.95
EPG_176	2059	4962	549	227	252	4.1	235	1.0	0.046	1.03
EPG_176	2068	4982	544	228	253	4.0	221	1.0	0.046	0.97
EPG_176	2077	4988	550	228	252	4.0	225	1.0	0.046	0.98
EPG_176	2086	4940	546	227	251	4.0	220	1.0	0.046	0.97
EPG_176	2096	4979	547	230	255	4.0	225	1.0	0.046	0.98
EPG_176	2105	4943	545	229	252	4.0	218	1.0	0.046	0.95
EPG_176	2114	5006	553	228	255	4.0	248	1.0	0.046	1.09
EPG_176	2123	5000	550	228	255	4.1	222	1.0	0.046	0.97
EPG_176	2133	5007	546	230	254	4.0	229	1.0	0.046	1.00
EPG_176	2142	5003	552	224	251	4.0	219	1.0	0.045	0.98
EPG_176	2151	5018	551	230	255	4.0	221	1.0	0.046	0.96
EPG_176	2161	5015	553	233	257	4.1	236	1.0	0.047	1.01
EPG_176	2170	5004	553	231	256	4.1	218	1.0	0.046	0.95
EPG_176	2179	5031	549	230	254	4.0	228	1.0	0.046	0.99
EPG_176	2188	5078	558	228	259	4.1	239	1.0	0.045	1.05
EPG_176	2198	5075	555	230	257	4.0	223	1.0	0.045	0.97
EPG_176	2207	5053	557	228	257	4.1	230	1.0	0.045	1.01
EPG_176	2216	5072	558	232	256	4.1	225	1.0	0.046	0.97
EPG_176	2225	5127	561	239	262	4.1	228	1.1	0.047	0.95
EPG_176	2235	5074	560	235	256	4.1	228	1.0	0.046	0.97
EPG_176	2244	5113	562	242	259	4.1	228	1.1	0.047	0.94
EPG_176	2253	5059	558	238	256	4.1	231	1.0	0.047	0.97
EPG_176	2263	5126	567	237	264	4.1	232	1.1	0.046	0.98
EPG_176	2272	3087	344	145	158	2.5	139	0.6	0.047	0.96
EPG_231	2392	61	13.2	6.7	15	0.18	6.8	0.044	0.11	1.01
EPG_231	2402	60	12.9	7.6	15	0.20	8.9	0.046	0.13	1.18
EPG_231	2411	60	12.9	6.6	14	0.18	6.4	0.043	0.11	0.96
EPG_231	2420	60	12.7	7.3	15	0.18	6.6	0.044	0.12	0.90
EPG_231	2429	60	12.9	6.8	15	0.17	6.9	0.040	0.11	1.00
EPG_231	2439	59	13.0	7.3	15	0.18	6.0	0.047	0.12	0.83
EPG_231	2448	59	12.7	6.6	15	0.18	6.3	0.039	0.11	0.96
EPG_231	2457	59	12.7	6.9	15	0.18	7.5	0.043	0.12	1.08
EPG_231	2467	59	12.7	6.6	15	0.18	8.2	0.040	0.11	1.24
EPG_231	2476	60	12.9	6.5	15	0.17	6.3	0.048	0.11	0.97
EPG_231	2485	60	12.6	6.7	14	0.17	12.3	0.044	0.11	1.84
EPG_231	2494	59	12.6	6.5	15	0.18	6.3	0.054	0.11	0.97
EPG_231	2504	59	12.8	7.0	15	0.18	6.6	0.043	0.12	0.94
EPG_231	2513	59	12.8	7.0	15	0.19	6.6	0.052	0.12	0.95
EPG_231	2522	59	12.7	7.5	14	0.18	7.9	0.041	0.13	1.05
EPG_231	2531	59	12.7	6.9	15	0.17	6.9	0.042	0.12	1.01
EPG_231	2541	59	12.7	6.6	14	0.18	6.6	0.043	0.11	1.00
EPG_231	2550	59	12.8	7.2	14	0.19	11.0	0.050	0.12	1.52
EPG_231	2559	59	13.4	6.4	15	0.18	8.9	0.048	0.11	1.39
EPG_231	2569	59	12.7	7.3	15	0.18	6.3	0.042	0.12	0.87
EPG_231	2578	59	12.6	6.6	15	0.18	8.0	0.041	0.11	1.21
EPG_231	2587	58	12.5	6.4	14	0.17	7.3	0.041	0.11	1.14
EPG_231	2596	59	12.5	6.4	14	0.18	6.2	0.042	0.11	0.98
EPG_231	2606	58	12.6	6.1	14	0.20	6.6	0.041	0.11	1.08
EPG_231	2615	58	12.9	6.2	14	0.19	6.8	0.045	0.11	1.09

Table A3.6 continued.

Sample	Time (sec)	Na (ppb)	Mg (ppb)	Al (ppb)	Ca (ppb)	Mn (ppb)	Fe (ppb)	Ba (ppb)	Al/Na	Fe/Al
EPG_231	2624	58	12.5	6.4	15	0.19	7.7	0.041	0.11	1.20
EPG_231	2633	58	12.6	6.7	14	0.17	8.1	0.041	0.12	1.20
EPG_231	2643	58	12.6	6.1	14	0.18	6.6	0.046	0.11	1.07
EPG_231	2652	58	12.4	6.4	14	0.17	7.3	0.041	0.11	1.15
EPG_231	2661	57	12.3	6.8	14	0.18	6.2	0.041	0.12	0.91
EPG_231	2671	58	12.4	6.0	14	0.17	6.8	0.044	0.10	1.13
EPG_231	2680	57	12.5	6.6	14	0.18	6.0	0.041	0.12	0.91
EPG_231	2689	59	12.6	6.7	14	0.18	7.0	0.055	0.11	1.05
EPG_231	2698	57	12.2	6.3	14	0.17	6.2	0.069	0.11	0.98
EPG_231	2708	57	12.6	6.4	14	0.18	6.9	0.043	0.11	1.09
EPG_231	2717	58	12.4	6.4	15	0.17	7.7	0.045	0.11	1.21
EPG_231	2726	59	12.6	6.8	15	0.18	7.2	0.041	0.12	1.07
EPG_231	2735	58	12.8	6.1	14	0.17	6.0	0.046	0.11	0.98
EPG_231	2745	57	12.4	7.4	15	0.18	7.0	0.046	0.13	0.94
EPG_231	2754	58	12.4	8.7	14	0.18	5.9	0.044	0.15	0.68
EPG_231	2763	57	12.7	6.8	14	0.17	6.1	0.047	0.12	0.90
EPG_231	2773	57	12.3	6.1	15	0.17	5.8	0.046	0.11	0.95
EPG_231	2782	57	12.4	7.0	14	0.18	6.1	0.058	0.12	0.86
EPG_231	2791	58	12.3	6.0	14	0.17	6.6	0.041	0.10	1.09
EPG_231	2800	58	12.7	6.5	14	0.17	7.7	0.044	0.11	1.19
EPG_231	2810	57	12.7	6.4	14	0.17	6.6	0.041	0.11	1.03
EPG_231	2819	58	12.3	5.9	14	0.18	6.2	0.043	0.10	1.04
EPG_231	2828	58	12.7	7.0	14	0.18	6.6	0.042	0.12	0.95
EPG_231	2837	57	12.7	6.6	14	0.18	7.2	0.044	0.12	1.08
EPG_231	2847	58	12.4	6.2	14	0.17	6.9	0.040	0.11	1.12
EPG_231	2856	57	12.3	6.8	15	0.17	6.1	0.040	0.12	0.90
EPG_231	2865	57	12.1	7.4	14	0.17	6.1	0.039	0.13	0.83
EPG_231	2875	56	12.2	7.1	14	0.18	6.0	0.046	0.13	0.84
1ppb_std	2958	105	10.6	1.07	135	1.07	1.08	1.1	0.010	1.01
1ppb_std	2967	105	10.5	1.06	131	1.07	1.09	1.1	0.010	1.03
1ppb_std	2977	106	10.7	1.06	135	1.08	1.09	1.1	0.010	1.03
1ppb_std	2986	106	10.6	1.05	142	1.08	1.09	1.1	0.010	1.04
1ppb_std	2995	104	10.4	1.04	133	1.06	1.06	1.1	0.010	1.02
Average concentration										
1ppb_std		98	9.8	0.98	68	0.96	0.95	0.958	0.010	0.97
EPG_170		4546	496	268	322	5.6	276	1.331	0.059	1.03
EPG_098		31	11.2	1.17	16	0.029	1.06	0.007	0.037	0.97
EPG_176		4940	544	229	252	4.03	226	1.024	0.046	0.99
EPG_231		58	12.6	6.7	14	0.18	7.0	0.045	0.115	1.05
1ppb_std		105	10.6	1.05	135	1.07	1.08	1.076	0.010	1.03
2σ										
1ppb_std		5	0.5	0.07	4	0.050	0.05	0.05	0.0003	0.03
EPG_170		325	32.6	17.4	23	0.431	41	0.21	0.004	0.11
EPG_098		1	0.4	0.85	1	0.016	1.2	0.004	0.027	1.2
EPG_176		501	54.6	23.8	25	0.456	37	0.12	0.001	0.16
EPG_231		2	0.5	1.00	1	0.013	2.4	0.01	0.017	0.36
1ppb_std		2	0.2	0.02	8	0.018	0.03	0.02	0.0002	0.02
2 rsd (%)										
1ppb_std		5	5	7	6	5	6	6	3	3
EPG_170		7	7	6	7	8	15	16	7	11
EPG_098		4	4	73	4	55	115	58	73	120
EPG_176		10	10	10	10	11	16	11	3	16
EPG_231		4	4	15	4	7	34	23	15	35
1ppb_std		2	2	2	6	2	3	2	2	2

Table A3.7 Major and trace element chemistry of EPG snow samples measured by collision cell ICP-MS. Values below the detection limit are shown in grey.

Sample	Depth (cm)	Na (ppb)	Mg (ppb)	Al (ppb)	Ca (ppb)	Mn (ppb)	Fe (ppb)	Ba (ppb)	Al/Na	Fe/Al
Average		1652	293	85	208	2.3	70	0.65	0.084	0.85
2 σ		5411	1101	405	737	11	337	3.1	0.25	0.47
2 rsd (%)		328	375	474	355	465	480	472	296	55
Min		10	4.8	0.50	1.5	0.010	0.23	0.0021	0.0009	0.16
Max		18031	3856	1666	2475	40.25	1358	12	0.74	2.0
EGP_379	1	6656	1296	1666	2143	37.1	1358	9.5	0.25	0.82
EPG_377	3	3319	704	801	872	20.0	685	3.8	0.24	0.86
EPG_375	5	594	69	17	34	0.37	17	0.12	0.029	0.97
EPG_373	7	517	63	11	30	0.20	9.7	0.045	0.021	0.92
EPG_371	9	602	81	16	42	0.35	15	0.086	0.026	0.98
EPG_369	11	661	72	13	36	0.28	13	0.084	0.020	0.98
EPG_367	13	507	62	10	34	0.25	10	0.14	0.020	0.99
EPG_365	15	599	72	14	37	0.32	14	0.090	0.024	1.0
EPG_363	17	5012	934	293	636	7.7	268	1.6	0.059	0.92
EPG_361	19	4431	885	242	637	7.1	214	1.2	0.055	0.88
EPG_359	21	1874	343	86	214	2.2	80	0.52	0.046	0.93
EPG_357	23	1558	282	88	217	2.1	86	0.75	0.056	0.98
EPG_355	25	1232	257	224	371	4.8	224	1.1	0.18	1.0
EPG_351	29	317	82	100	138	2.1	30	0.60	0.31	0.30
EPG_349	31	303	81	103	133	2.2	30	0.63	0.34	0.29
EPG_347	33	316	75	88	140	1.9	25	0.55	0.28	0.28
EPG_345	35	306	75	84	141	1.7	24	0.47	0.27	0.28
EPG_343	37	320	78	106	174	2.0	30	0.56	0.33	0.28
EPG_341	39	340	84	109	139	1.9	31	0.51	0.32	0.28
EPG_339	41	238	68	104	167	2.4	16	0.88	0.44	0.16
EPG_337	43	120	24	17	26	0.45	21	0.13	0.14	1.2
EPG_335	45	127	27	21	27	0.40	24	0.11	0.17	1.1
EPG_333	47	117	19	7.6	23	0.21	7.0	0.043	0.065	0.92
EPG_331	49	110	19	13	19	0.26	13	0.12	0.12	1.0
EPG_329	51	108	15	5.3	17	0.17	4.6	0.031	0.049	0.87
EPG_327	53	113	19	5.8	17	0.16	5.0	0.038	0.051	0.86
EPG_325	55	109	16	2.7	7.6	0.057	1.5	0.011	0.025	0.56
EPG_323	57	112	15	3.4	7.1	0.071	3.2	0.026	0.030	0.95
EPG_321	59	78	11	2.9	5.4	0.064	2.9	0.021	0.037	0.99
EPG_319	61	46	10	5.4	13	0.047	1.5	0.019	0.12	0.28
EPG_317	63	298	61	75	95	1.7	68	0.74	0.25	0.90
EPG_315	65	404	58	21	47	0.54	23	0.17	0.052	1.1
EPG_313	67	30	5.0	1.7	3.6	0.043	1.9	0.014	0.056	1.2
EPG_311	69	414	119	117	142	2.5	102	0.84	0.28	0.87
EPG_309	71	2824	678	457	695	16.5	384	3.7	0.16	0.84
EPG_308	72	2895	520	150	458	4.7	93	1.1	0.052	0.62
EPG_307	73	13847	3098	1286	2475	40.2	1087	12.3	0.093	0.85
EPG_305	75	8847	1927	1085	1855	35.7	845	12.0	0.12	0.78
EPG_304	76	2127	332	81	391	4.1	65	0.65	0.038	0.81
EPG_302	78	491	105	130	220	3.7	117	1.3	0.27	0.90
EPG_301	79	490	118	160	230	4.3	139	1.5	0.33	0.87
EPG_299	81	419	151	228	300	6.7	233	2.1	0.54	1.0

Table A3.7 continued.

Sample	Depth (cm)	Na (ppb)	Mg (ppb)	Al (ppb)	Ca (ppb)	Mn (ppb)	Fe (ppb)	Ba (ppb)	Al/Na	Fe/Al
EPG_297	83	963	153	71	306	3.2	56	0.55	0.074	0.79
EPG_295	85	714	149	157	213	4.5	127	1.4	0.22	0.81
EPG_291	89	210	46	31	37	0.82	27	0.26	0.15	0.85
EPG_289	91	370	51	18	36	0.45	17	0.11	0.048	0.94
EPG_287	93	420	55	6.4	27	0.18	4.1	0.032	0.015	0.64
EPG_286	94	303	33	6.4	25	0.19	3.5	0.036	0.021	0.55
EPG_283	97	10	5.1	0.50	1.5	0.029	0.23	0.0021	0.051	0.45
EPG_282	98	15	13	0.91	3.6	0.11	0.55	0.0039	0.063	0.60
EPG_281	99	1094	471	807	848	18.6	639	4.8	0.74	0.79
EPG_279	101	497	188	306	261	7.6	270	1.8	0.62	0.88
EPG_278	102	1962	317	125	1354	5.8	92	0.98	0.064	0.74
EPG_277	103	155	32	25	20	0.57	26	0.14	0.16	1.0
EPG_275	105	379	54	30	33	0.55	29	0.14	0.078	1.0
EPG_269	111	41	12	15	22	0.46	18	0.17	0.38	1.1
EPG_268	112	294	49	15	47	0.44	13	0.10	0.049	0.90
EPG_267	113	477	200	327	299	7.0	318	2.3	0.69	0.97
EPG_265	115	520	226	333	339	9.1	328	2.3	0.64	0.99
EPG_261	119	362	94	69	131	2.0	54	1.0	0.19	0.79
EPG_259	121	492	93	19	62	1.2	13	0.20	0.039	0.66
EPG_257	123	482	69	27	206	1.6	24	0.36	0.056	0.89
EPG_255	125	175	42	25	48	0.62	21	0.24	0.14	0.84
EPG_253	127	299	45	5.5	30	0.39	4.0	0.043	0.018	0.73
EPG_251	129	428	67	27	99	1.2	21	0.32	0.062	0.79
EPG_249	131	25	11	8.2	15	0.20	6.4	0.070	0.32	0.78
EPG_247	133	13	4.8	2.3	7.0	0.057	2.0	0.013	0.18	0.90
EPG_245	135	15	6.1	4.3	12	0.069	4.5	0.026	0.29	1.0
EPG_243	137	15	7.8	4.4	8.2	0.073	4.1	0.021	0.28	0.93
EPG_241	139	14	6.9	4.2	7.6	0.079	4.8	0.024	0.29	1.1
EPG_239	141	22	6.7	4.2	7.9	0.081	4.4	0.025	0.19	1.1
EPG_237	143	35	8.2	3.5	8.3	0.11	3.3	0.024	0.099	0.93
EPG_235	145	41	9.5	5.8	9.0	0.16	6.9	0.056	0.14	1.2
EPG_233	147	45	11	4.8	9.5	0.12	5.5	0.033	0.11	1.2
EPG_231	149	50	11	4.7	10	0.15	4.9	0.039	0.094	1.1
EPG_229	151	114	21	7.7	14	0.21	7.6	0.050	0.068	0.99
EPG_227	153	529	75	11	36	0.33	11	0.099	0.021	1.0
EPG_225	155	2226	319	40	200	1.5	41	0.48	0.018	1.0
EPG_223	157	1189	199	84	141	2.8	74	0.91	0.071	0.88
EPG_221	159	1162	221	104	146	2.7	98	0.83	0.089	0.94
EPG_219	161	1127	202	64	138	2.0	53	0.69	0.057	0.83
EPG_217	163	878	183	81	160	2.2	72	0.65	0.092	0.89
EPG_215	165	728	152	60	204	2.2	52	0.74	0.082	0.86
EPG_213	167	812	141	42	169	1.7	38	0.49	0.051	0.91
EPG_211	169	1235	225	148	313	3.8	134	1.7	0.12	0.90
EPG_209	171	902	154	68	191	2.2	63	0.74	0.075	0.94
EPG_207	173	1250	208	87	224	2.7	77	1.2	0.070	0.88
EPG_205	175	929	136	43	141	1.0	35	0.53	0.047	0.81
EPG_203	177	1304	161	49	163	1.6	45	0.64	0.038	0.93
EPG_201	179	1306	151	44	159	1.5	40	0.47	0.034	0.90
EPG_199	181	1344	171	106	221	2.9	88	1.5	0.079	0.84
EPG_197	183	3746	533	84	407	2.7	70	1.1	0.022	0.84
EPG_195	185	3549	847	35	241	1.4	32	0.37	0.010	0.92

Table A3.7continued.

Sample	Depth (cm)	Na (ppb)	Mg (ppb)	Al (ppb)	Ca (ppb)	Mn (ppb)	Fe (ppb)	Ba (ppb)	Al/Na	Fe/Al
EPG_193	187	2171	360	13	173	1.1	14	0.16	0.0060	1.1
EPG_191	189	1032	188	7.4	75	0.49	8.2	0.10	0.0072	1.1
EPG_187	193	1628	229	10	117	0.64	7.0	0.084	0.0063	0.68
EPG_183	197	2886	475	34	292	1.4	29	0.26	0.012	0.87
EPG_181	199	5652	1080	206	614	6.4	160	1.8	0.036	0.78
EPG_179	201	3509	454	14	135	0.44	14	0.15	0.0041	0.96
EPG_177	203	3184	388	6.3	107	0.18	5.4	0.056	0.0020	0.86
EPG_175	205	6830	1045	260	791	6.5	206	2.5	0.038	0.79
EPG_173	207	10391	1351	243	1036	6.6	177	2.2	0.023	0.73
EPG_171	209	6480	769	139	785	4.7	109	1.3	0.021	0.79
EPG_169	211	2108	268	55	174	1.2	49	0.51	0.026	0.90
EPG_167	213	563	75	18	43	0.52	17	0.19	0.033	0.92
EPG_165	215	191	36	3.8	17	0.15	4.1	0.037	0.020	1.1
EPG_163	217	214	45	3.1	18	0.12	2.5	0.024	0.015	0.81
EPG_161	219	825	101	12	61	0.47	9.5	0.11	0.014	0.82
EPG_159	221	1517	181	19	109	0.76	13	0.15	0.012	0.67
EPG_157	223	2817	460	60	186	1.5	41	0.41	0.021	0.69
EPG_155	225	3276	706	65	240	1.8	47	0.44	0.020	0.72
EPG_153	227	1225	224	6.3	61	0.31	4.4	0.059	0.0052	0.69
EPG_151	229	1931	304	13	144	0.60	12	0.11	0.0070	0.88
EPG_149	231	4493	763	68	330	1.6	52	0.45	0.015	0.76
EPG_147	233	4022	605	83	325	2.0	61	0.59	0.021	0.73
EPG_146	234	3317	479	24	253	1.2	18	0.26	0.0072	0.75
EPG_145	235	2897	374	69	255	2.1	52	0.60	0.024	0.76
EPG_144	236	729	104	8.1	49	0.39	5.8	0.097	0.011	0.72
EPG_143	237	233	50	3.0	17	0.14	2.2	0.026	0.013	0.73
EPG_141	239	173	23	3.9	16	0.17	2.5	0.020	0.023	0.65
EPG_137	243	340	45	5.3	25	0.20	4.6	0.056	0.016	0.86
EPG_135	245	385	50	3.2	21	0.095	2.7	0.031	0.0083	0.84
EPG_133	247	420	54	2.9	22	0.10	2.5	0.025	0.0070	0.85
EPG_131	249	532	59	4.0	28	0.16	3.5	0.033	0.0076	0.88
EPG_129	251	372	78	12	35	0.29	8.7	0.11	0.033	0.71
EPG_127	253	2699	370	67	276	2.5	56	0.58	0.025	0.85
EPG_126	254	3380	447	61	318	2.8	47	0.57	0.018	0.77
EPG_125	255	4719	727	107	500	4.3	83	0.88	0.023	0.78
EPG_124	256	1734	238	23	168	0.85	19	0.20	0.014	0.83
EPG_123	257	429	84	3.3	45	0.13	2.7	0.061	0.0078	0.82
EPG_121	259	163	26	1.7	11	0.051	1.2	0.0095	0.010	0.74
EPG_119	261	170	25	2.1	13	0.064	1.9	0.012	0.012	0.89
EPG_117	263	156	20	1.4	11	0.054	1.1	0.011	0.0092	0.74
EPG_115	265	169	27	1.7	12	0.057	1.2	0.0093	0.010	0.69
EPG_113	267	230	37	1.1	11	0.042	0.61	0.0076	0.0049	0.54
EPG_111	269	848	104	7.5	48	0.22	6.1	0.053	0.0088	0.82
EPG_108	272	474	76	5.1	26	0.10	4.2	0.038	0.011	0.83
EPG_106	274	90	14	0.55	4.3	0.010	0.29	0.0036	0.0061	0.53
EPG_104	276	388	56	3.0	8.6	0.084	1.1	0.0083	0.0076	0.39
EPG_102	278	232	37	1.9	13	0.048	1.4	0.016	0.0084	0.73
EPG_100	280	144	21	1.0	6.2	0.018	0.65	0.0044	0.0072	0.63
EPG_098	282	36	15	1.0	3.2	0.019	0.38	0.0035	0.027	0.38
EPG_096	284	5643	832	100	410	1.8	70	0.55	0.018	0.70
EPG_094	286	12361	1913	226	952	4.1	170	1.2	0.018	0.75

Table A3.7 continued.

Sample	Depth (cm)	Na (ppb)	Mg (ppb)	Al (ppb)	Ca (ppb)	Mn (ppb)	Fe (ppb)	Ba (ppb)	Al/Na	Fe/Al
EPG_092	288	8621	1327	91	596	1.8	70	0.56	0.011	0.78
EPG_090	290	2654	309	27	142	0.66	24	0.17	0.010	0.89
EPG_088	292	2386	195	7.3	94	0.37	5.2	0.054	0.0031	0.72
EPG_086	294	7826	1597	132	770	3.2	97	0.87	0.017	0.74
EPG_084	296	17458	3676	196	1651	4.9	138	1.3	0.011	0.71
EPG_082	298	18031	3856	286	1819	6.4	212	1.8	0.016	0.74
EPG_079	301	10700	3286	1157	1663	27.4	1022	7.1	0.11	0.88
EPG_078	302	6650	786	90	760	2.4	63	0.74	0.014	0.69
EPG_077	303	3369	749	343	350	8.4	266	1.8	0.10	0.78
EPG_075	305	1065	158	88	94	1.7	92	0.55	0.083	1.0
EPG_073	307	277	66	16	21	0.27	17	0.11	0.058	1.1
EPG_071	309	847	166	138	111	3.0	140	0.83	0.16	1.0
EPG_069	311	460	100	64	54	1.2	59	0.37	0.14	0.92
EPG_067	313	847	135	69	88	1.4	62	0.36	0.081	0.91
EPG_065	315	689	153	70	85	1.4	71	0.41	0.10	1.0
EPG_063	317	788	147	48	75	0.93	49	0.31	0.061	1.0
EPG_061	319	1100	153	16	64	0.61	27	0.29	0.014	1.7
EPG_060	320	1272	156	13	96	0.41	6.7	0.079	0.010	0.54
EPG_059	321	889	114	13	47	0.46	27	0.37	0.015	2.0
EPG_057	323	281	42	1.1	10	0.038	1.3	0.036	0.0038	1.3
EPG_055	325	641	105	9.2	33	0.30	17	0.16	0.014	1.9
EPG_054	326	546	116	34	69	0.83	28	0.28	0.063	0.80
EPG_053	327	2394	523	53	202	2.2	76	0.88	0.022	1.4
EPG_052	328	3629	667	163	506	5.7	117	1.3	0.045	0.72
EPG_051	329	1331	177	5.4	106	0.63	10	0.15	0.0041	1.9
EPG_050	330	758	128	13	48	0.39	12	0.097	0.017	0.94
EPG_049	331	571	108	23	78	0.77	24	0.24	0.040	1.1
EPG_047	333	185	79	11	40	0.48	11	0.090	0.060	1.0
EPG_045	335	1986	267	17	141	0.60	14	0.18	0.0085	0.81
EPG_044	336	2739	340	20	148	0.54	18	0.13	0.0074	0.88
EPG_043	337	2469	331	15	141	0.53	12	0.14	0.0060	0.81
EPG_042	338	1517	194	5.0	68	0.21	3.8	0.041	0.0033	0.76
EPG_041	339	856	125	3.1	37	0.061	2.0	0.021	0.0037	0.62
EPG_039	341	726	103	1.3	32	0.035	0.98	0.0089	0.0017	0.78
EPG_037	343	614	95	1.2	27	0.032	1.0	0.011	0.0020	0.82
EPG_035	345	833	118	1.7	38	0.046	1.4	0.014	0.0020	0.84
EPG_033	347	1158	159	1.5	53	0.043	1.1	0.012	0.0013	0.74
EPG_031	349	1488	203	1.3	70	0.045	0.94	0.011	0.0009	0.73
EPG_030	350	2009	306	2.2	76	0.044	1.8	0.013	0.0011	0.81
EPG_029	351	1505	195	4.1	73	0.12	3.3	0.028	0.0027	0.81
EPG_028	352	1286	201	19	74	0.42	17	0.15	0.015	0.86
EPG_027	353	994	138	14	82	0.44	12	0.13	0.014	0.83
EPG_026	354	515	89	20	60	0.54	18	0.13	0.039	0.89
EPG_025	355	524	94	30	65	0.81	28	0.28	0.058	0.94
EPG_024	356	368	90	31	54	0.61	27	0.17	0.085	0.87
EPG_023	357	315	71	23	45	0.54	21	0.18	0.073	0.92
EPG_021	359	305	52	17	35	0.40	17	0.11	0.056	1.0
EPG_019	361	323	55	17	39	0.43	16	0.12	0.053	0.93
EPG_017	363	326	60	17	39	0.42	16	0.11	0.053	0.94
EPG_016	364	256	68	68	53	1.3	60	0.37	0.27	0.88
EPG_015	365	253	48	16	32	0.36	14	0.13	0.062	0.87

Table A3.7 continued.

Sample	Depth (cm)	Na (ppb)	Mg (ppb)	Al (ppb)	Ca (ppb)	Mn (ppb)	Fe (ppb)	Ba (ppb)	Al/Na	Fe/Al
EPG_014	366	333	60	42	39	0.69	34	0.21	0.13	0.82
EPG_013	367	210	43	23	33	0.47	18	0.17	0.11	0.80
EPG_012	368	294	67	40	39	0.69	38	0.21	0.14	0.93
EPG_011	369	242	46	11	22	0.24	9.3	0.067	0.044	0.86
EPG_010	370	414	114	17	38	0.43	13	0.13	0.042	0.75
EPG_009	371	1087	192	34	100	0.99	28	0.27	0.031	0.83
EPG_008	372	1023	188	32	99	0.83	22	0.23	0.031	0.70
EPG_007	373	1369	217	30	125	1.0	25	0.22	0.022	0.85
EPG_006	374	1836	295	47	188	1.3	36	0.38	0.026	0.77
EPG_005	375	1620	245	34	152	1.1	28	0.33	0.021	0.80
EPG_003	377	2018	316	66	213	1.8	60	0.59	0.033	0.91
EPG_002	378	1968	286	28	146	0.90	20	0.23	0.014	0.70
EPG_001	379	2091	323	40	206	1.4	33	0.41	0.019	0.83

Table A3.8 Repeated measurement of the external standard SLRS-4 (National Research Council, Canada) by non-collision cell ICP-MS to determine analytical precision and accuracy. Measurements were made at 1:10 dilution. Analyses which are not considered reliable are shown in grey.

SLRS-4 1:10 dilution	Ti	V	Cr	Ni	Cu	Zn	As	Rb	Sr	Y	Zr	Sb	Cs	Ba	La	Ce	Pb	Bi	Th	U	Ti/Sr	Zr/Y
Average	1497	356	1217	825	1742	1158	739	1521	28422	135	123	257	6.1	12482	287	359	93	2.4	20.9	49	0.053	0.91
2 σ	145	26	2958	106	563	1705	47	78	1456	8	18	13	0.8	565	15	20	144	0.6	2.1	4	0.003	0.10
2 rsd	10	7	243	13	32	147	6	5	5	6	15	5	13	5	5	6	154	26	10	9	7	11
Average of select SLRS-4	-	-	315	-	1857	1000	-	-	-	-	-	-	-	-	-	-	79	-	-	-	-	-
2 σ	95	339	295	30	18	30											7					
2 rsd	30	30	30														9					
SLRS-4_1	1419	338	261	779	1645	1236	714	1499	28160	132	113	257	6.1	12523	287	360	101	2.5	21	51	0.050	0.86
SLRS-4_2	1380	328	278	748	1577	1046	709	1465	27544	130	111	252	6.6	12297	282	355	80	2.1	21	50	0.050	0.86
SLRS-4_3	1472	344	285	795	1905	1110	736	1510	28345	133	112	258	6.0	12479	288	358	76	2.2	21	49	0.052	0.84
SLRS-4_4	1431	338	280	780	1674	1069	729	1501	28161	133	111	259	6.4	12444	285	357	76	2.2	20	49	0.051	0.84
SLRS-4_5	1452	339	294	768	1636	772	713	1467	28392	130	111	255	6.0	12292	283	351	77	2.2	20	50	0.051	0.86
SLRS-4_6	1515	346	420	776	1584	807	730	1500	28757	133	113	262	6.7	12408	286	356	78	2.2	21	48	0.053	0.85
SLRS-4_7	1499	347	332	811	1976	2014	725	1484	28669	129	122	250	6.3	12108	276	344	370	3.3	20	46	0.052	0.95
SLRS-4_8	1529	346	358	807	2011	1810	739	1481	28546	130	122	251	6.3	12056	276	344	330	3.3	20	46	0.054	0.94
SLRS-4_9	1507	352	315	802	1689	789	738	1498	28829	131	125	251	5.8	12252	277	347	77	2.5	20	48	0.052	0.95
SLRS-4_10	1498	352	332	789	1664	797	731	1503	28877	133	119	250	5.8	12354	278	347	78	2.2	19	48	0.052	0.89
SLRS-4_11	1503	343	497	786	1942	1161	742	1469	27644	132	111	256	6.0	12152	279	350	77	2.0	20	45	0.054	0.84
SLRS-4_12	1579	350	649	790	1718	1037	758	1488	27963	133	110	255	6.3	12190	279	352	74	2.2	20	46	0.056	0.82
SLRS-4_13	1672	375	489	802	1284	486	751	1612	30329	142	140	261	5.7	12924	306	382	85	2.5	24	55	0.055	0.99
SLRS-4_14	1645	370	425	791	1261	459	738	1593	29892	142	135	265	5.7	12812	303	382	77	2.6	23	54	0.055	0.95
SLRS-4_15	1556	367	352	843	2069	454	760	1583	29562	140	120	263	6.1	12986	296	371	21	1.9	22	52	0.053	0.86
SLRS-4_16	1589	373	361	841	2108	1177	747	1561	29280	140	129	254	7.0	12804	294	368	97	2.5	22	50	0.054	0.92
SLRS-4_17	1561	369	1039	868	1973	1416	731	1545	28466	138	130	262	6.3	12673	289	363	80	2.2	21	49	0.055	0.94
SLRS-4_18	1585	364	1522	928	2161	1659	748	1548	28770	139	133	260	5.9	12777	294	367	95	2.4	20	51	0.055	0.96
SLRS-4_19	1545	365	740	847	1887	898	714	1537	28226	137	125	255	6.2	12622	291	364	85	2.3	20	50	0.055	0.91
SLRS-4_20	1423	359	3229	920	1945	995	718	1527	28157	136	127	255	6.0	12562	290	364	95	2.5	19	49	0.051	0.93
SLRS-4_21	1478	375	6701	910	1994	3827	737	1546	28179	137	136	260	6.1	12840	289	364	48	2.4	22	50	0.052	1.00
SLRS-4_22	1513	369	4049	925	1923	4026	746	1544	28085	136	133	259	6.7	12798	289	363	34	2.5	22	50	0.054	0.98
SLRS-4_23	1425	362	1878	836	1866	1016	741	1510	27739	137	128	256	5.6	12336	285	355	79	2.4	20	47	0.051	0.94
SLRS-4_24	1465	362	3250	882	1898	999	739	1515	28062	136	130	254	6.2	12525	288	361	82	2.6	21	49	0.052	0.96
SLRS-4_25	1491	353	642	772	1176	394	719	1520	28102	136	128	250	6.5	12246	289	361	59	2.4	21	50	0.053	0.94
SLRS-4_26	1495	354	525	782	1173	396	728	1529	28356	137	128	249	6.3	12312	289	361	60	2.6	21	50	0.053	0.94
SLRS-4_27	1407	356	767	809	1394	600	748	1502	27378	135	125	248	5.5	12052	281	348	71	1.9	20	48	0.051	0.93
SLRS-4_28	1438	348	1085	798	1409	613	743	1534	28038	137	127	252	5.3	12344	287	359	71	2.3	22	49	0.051	0.93
SLRS-4_29	1383	344	2464	842	1837	1084	758	1480	26924	132	109	264	6.5	12303	284	354	86	2.5	21	48	0.051	0.88
SLRS-4_30	1451	379	2684	917	1887	592	838	1590	29237	143	125	280	6.4	13000	301	375	81	2.6	22	49	0.050	0.88
SLRS-4 conc_1	1550	378	380	820	2005	1425	942	1681	29629	150	113	312	7.5	13772	324	404	89	2.7	23	55	0.052	0.76
SLRS-4 conc_2	1394	344	345	764	1820	1331	877	1497	26536	134	104	281	6.5	12187	288	360	80	2.5	21	49	0.053	0.77
SLRS-4 conc_3	1403	341	339	757	1812	1322	875	1500	26467	133	104	282	6.5	12254	288	360	80	2.5	21	49	0.053	0.78

Table A3.9 Standard deviations of blank measurements by non-collision cell ICP-MS used to determine detection limits.

Blank	Ti ppt	V ppt	Cr ppt	Ni ppt	Cu ppt	Zn ppt	As ppt	Rb ppt	Sr ppt	Y ppt	Zr ppt	Sb ppt	Cs ppt	Ba ppt	La ppt	Ce ppt	Pb ppt	Bi ppt	Th ppt	U ppt
Average 3σ	22	1.8	27	2.8	17	48	6.7	0.86	0.62	0.21	1.04	1.2	0.28	1.3	0.16	0.22	2.9	0.41	0.29	0.30
Blank_1	12	0.6	6.3	0.9	1.1	1.8	1.4	0.25	0.26	0.07	2.8	0.4	0.12	0.5	0.10	0.13	0.5	0.46	0.20	0.16
Blank_2	13	0.7	6.5	1.0	1.4	4.7	1.1	0.27	0.28	0.06	1.2	0.4	0.10	0.3	0.08	0.12	0.7	0.47	0.19	0.23
Blank_3	15	0.7	6.3	1.1	1.0	2.5	1.2	0.21	0.14	0.07	0.5	0.5	0.10	0.3	0.11	0.11	0.4	0.24	0.19	0.16
Blank_4	12	0.7	7.7	0.8	1.0	2.7	1.4	0.22	0.73	0.07	0.6	0.5	0.10	0.5	0.08	0.17	0.3	0.33	0.20	0.15
Blank_5	12	0.6	7.0	1.0	1.0	9.3	1.6	0.21	0.45	0.07	0.2	0.4	0.08	0.3	0.11	0.11	0.4	0.37	0.18	0.18
Blank_6	26	0.8	6.8	1.0	2.5	10	1.4	0.18	0.28	0.07	1.0	0.4	0.11	0.6	0.08	0.22	1.2	0.36	0.27	0.23
Blank_7	13	0.5	6.9	0.9	0.9	2.7	1.3	0.20	0.48	0.06	0.3	0.4	0.10	0.4	0.09	0.55	0.4	0.36	0.17	0.20
Blank_8	15	0.7	6.2	0.9	1.1	3.7	1.7	0.26	0.21	0.07	0.2	0.4	0.10	0.2	0.09	0.12	0.5	0.36	0.24	0.13
Blank_9	14	0.7	8.2	1.2	1.0	1.8	1.6	0.16	0.23	0.06	0.6	0.5	0.09	0.2	0.08	0.13	0.3	0.31	0.16	0.16
Blank_10	13	0.7	7.8	1.0	1.2	2.3	1.3	0.18	0.18	0.06	0.7	0.4	0.10	0.3	0.09	0.15	0.5	0.39	0.23	0.25
Blank_11	9.0	0.7	6.2	1.0	1.0	15	1.8	0.22	1.09	0.06	0.2	0.5	0.11	2.1	0.09	0.13	1.0	0.33	0.17	0.19
Blank_12	10	0.5	4.6	0.9	1.3	2.2	1.2	0.19	0.18	0.05	0.6	0.4	0.11	0.3	0.07	0.11	0.5	0.35	0.23	0.21
Blank_13	11	0.6	7.3	0.8	0.9	1.3	1.3	0.19	0.12	0.08	0.3	0.4	0.10	0.2	0.09	0.11	0.4	0.42	0.23	0.20
Blank_14	8.4	0.8	6.6	0.8	0.9	1.3	1.5	0.21	0.16	0.07	0.7	0.5	0.10	0.2	0.08	0.10	0.3	0.40	0.23	0.16
Blank_15	7.6	0.6	6.1	0.8	1.0	1.6	1.3	0.22	0.11	0.06	0.2	0.5	0.10	0.2	0.06	0.14	0.3	0.32	0.20	0.21
Blank_16	19	0.6	7.5	1.1	2.6	22	1.2	0.25	0.57	0.07	1.3	0.6	0.09	0.6	0.09	0.20	0.5	0.34	0.21	0.24
Blank_17	5.7	0.4	4.1	0.7	0.6	1.5	1.8	0.19	0.06	0.06	0.2	0.4	0.09	0.1	0.04	0.05	0.1	0.09	0.06	0.10
Blank_18	5.4	0.4	5.6	0.7	67	2.5	1.7	0.20	0.12	0.06	0.1	0.3	0.08	0.2	0.04	0.04	0.1	0.07	0.07	0.07
Blank_19	4.6	0.4	4.8	0.7	2.7	2.5	1.4	0.19	0.07	0.05	2.2	0.4	0.07	0.1	0.03	0.04	0.2	0.08	0.07	0.07
Blank_20	5.9	0.4	5.5	0.6	4.7	2.0	1.6	0.19	0.07	0.06	0.2	0.3	0.08	0.1	0.04	0.05	0.2	0.09	0.07	0.07
Blank_21	5.1	0.4	6.2	0.8	1.3	2.1	1.4	0.26	0.07	0.06	0.2	0.3	0.09	0.1	0.03	0.04	0.2	0.08	0.07	0.07
Blank_22	5.8	0.4	6.6	0.7	1.3	2.0	1.7	0.27	0.07	0.07	0.2	0.3	0.08	0.1	0.03	0.04	0.2	0.07	0.06	0.06
Blank_23	4.3	0.5	5.3	0.5	2.4	2.4	1.5	0.27	0.07	0.06	0.2	0.4	0.08	0.1	0.04	0.05	0.2	0.08	0.07	0.08
Blank_24	4.9	0.4	6.9	0.7	0.5	2.5	1.4	0.29	0.08	0.06	0.2	0.3	0.08	0.1	0.03	0.03	0.1	0.08	0.06	0.07
Blank_25	4.8	0.4	5.7	0.9	7.7	19	1.7	0.22	0.19	0.07	0.2	0.3	0.10	0.8	0.04	0.05	1.7	0.07	0.06	0.08
Blank_26	8.1	0.4	5.4	0.8	1.9	1.9	1.8	0.27	0.07	0.09	0.2	0.4	0.10	0.1	0.04	0.04	0.1	0.08	0.06	0.09
Blank_27	7.0	0.5	8.8	0.8	12	2.3	1.7	0.24	0.07	0.05	0.7	0.4	0.10	0.1	0.04	0.05	0.1	0.08	0.07	0.06
Blank_28	6.1	0.6	6.8	0.8	3.6	2.1	2.3	0.22	0.06	0.06	0.2	0.4	0.07	0.1	0.04	0.04	0.1	0.08	0.08	0.08
Blank_29	4.8	0.5	5.5	0.7	0.9	2.0	1.4	0.28	0.06	0.06	0.3	0.4	0.08	0.1	0.04	0.04	0.1	0.07	0.05	0.07
Blank_30	5.0	0.4	5.7	0.7	0.8	1.9	1.3	0.30	0.07	0.06	0.2	0.3	0.09	0.1	0.03	0.04	0.1	0.07	0.06	0.05
Blank_31	6.2	0.5	6.2	0.7	1.1	2.4	1.5	0.21	0.08	0.08	0.2	0.3	0.08	0.1	0.03	0.04	0.1	0.08	0.06	0.07
Blank_32	8.1	0.6	6.2	0.6	19	2.6	1.7	0.26	0.09	0.06	0.2	0.3	0.07	0.1	0.04	0.04	0.1	0.06	0.05	0.06
Blank_33	5.8	0.6	6.0	0.6	1.8	1.6	1.3	0.29	0.05	0.05	0.2	0.3	0.08	0.1	0.03	0.04	0.1	0.07	0.06	0.06
Blank_34	4.7	0.5	6.6	0.8	1.4	6.3	1.4	0.24	0.08	0.06	0.2	0.3	0.09	0.1	0.04	0.04	0.1	0.07	0.06	0.05
Blank_35	4.2	0.5	5.4	0.9	1.0	1.6	1.6	0.21	0.05	0.06	0.1	0.3	0.09	0.1	0.04	0.04	0.1	0.09	0.07	0.07
Blank_36	5.3	0.5	6.1	0.8	2.3	1.7	1.5	0.25	0.05	0.07	0.2	0.3	0.06	0.1	0.04	0.05	0.1	0.07	0.06	0.05
Blank_37	4.6	0.4	26	0.7	1.5	4.2	1.8	0.18	0.06	0.04	0.1	0.4	0.07	0.1	0.04	0.04	0.1	0.09	0.09	0.06
Blank_38	4.1	0.5	25	0.7	0.6	3.9	1.6	0.22	0.09	0.07	0.3	0.3	0.07	5.0	0.03	0.05	0.1	0.06	0.08	0.07
Blank_39	6.1	0.5	24	1.1	1.2	5.0	3.1	0.23	0.05	0.07	0.2	0.6	0.09	0.1	0.03	0.04	0.1	0.06	0.07	0.09

Table A3.9 continued.

Blank	Ti	V	Cr	Ni	Cu	Zn	As	Rb	Sr	Y	Zr	Sb	Cs	Ba	La	Ce	Pb	Bi	Th	U
Blank_40	7.7	0.8	24	1.8	29	216	2.4	0.32	0.72	0.08	0.6	1.4	0.10	1.8	0.09	0.06	7.9	0.09	0.07	0.11
Blank_41	6.8	0.8	30	2.0	13	17	2.5	0.41	0.13	0.08	0.2	0.7	0.13	0.2	0.07	0.07	0.5	0.08	0.08	0.10
Blank_42	5.9	0.6	29	1.2	30	14	3.0	0.43	0.13	0.10	0.2	0.8	0.09	0.3	0.08	0.06	0.4	0.08	0.07	0.09
Blank_43	7.8	0.9	21	1.3	46	63	2.6	0.34	0.23	0.09	0.2	0.6	0.13	0.7	0.09	0.08	2.2	0.08	0.07	0.14
Blank_44	6.6	0.6	7.1	2.5	34	82	1.8	0.31	0.85	0.08	0.5	0.3	0.10	2.6	0.06	0.11	11.4	0.13	0.09	0.12
Blank_45	7.8	0.8	6.9	1.1	1.7	4.3	1.9	0.29	0.33	0.11	0.1	0.4	0.07	0.4	0.03	0.05	0.7	0.09	0.08	0.11
Blank_46	4.5	0.7	6.2	0.9	1.7	5.0	2.2	0.33	0.53	0.11	0.2	0.4	0.14	0.2	0.06	0.05	0.5	0.12	0.08	0.11
Blank_47	6.7	0.7	7.7	1.1	1.5	3.3	2.5	0.42	0.13	0.05	0.2	0.5	0.08	0.2	0.05	0.06	0.5	0.11	0.09	0.11
Blank_48	5.1	0.6	7.6	1.3	15	35	2.6	0.43	0.37	0.08	0.3	0.4	0.17	1.1	0.07	0.07	4.6	0.13	0.09	0.12
Blank_49	6.4	0.7	7.9	1.1	2.5	5.3	2.6	0.35	0.10	0.11	0.3	0.5	0.15	0.3	0.05	0.05	0.8	0.09	0.09	0.10
Blank_50	7.2	0.6	8.3	1.1	2.9	5.4	2.2	0.49	0.14	0.09	0.2	0.5	0.15	0.4	0.04	0.05	0.8	0.10	0.09	0.12
Blank_51	5.9	0.6	8.0	1.6	2.6	3.8	2.8	0.46	0.10	0.11	0.3	0.4	0.10	0.2	0.05	0.06	0.3	0.13	0.09	0.12
Blank_52	5.7	0.9	7.7	1.4	1.7	2.8	2.5	0.43	0.11	0.11	0.2	0.4	0.14	0.2	0.06	0.05	0.3	0.14	0.10	0.13
Blank_53	7.8	0.7	11	0.9	3.5	2.5	2.4	0.33	0.06	0.09	0.2	0.4	0.10	0.2	0.04	0.05	0.1	0.07	0.06	0.05
Blank_54	6.9	0.7	11	1.3	4.3	391	2.0	1.18	0.68	0.07	0.2	0.3	0.11	1.1	0.05	0.06	8.1	0.06	0.04	0.06
Blank_55	8.8	0.7	12	1.4	6.1	9.3	2.9	0.34	0.13	0.09	0.3	0.3	0.13	0.6	0.05	0.05	1.0	0.06	0.05	0.06
Blank_56	8.0	0.9	14	0.9	4.5	5.1	1.8	0.44	0.09	0.09	0.3	0.3	0.10	0.3	0.04	0.08	0.4	0.07	0.07	0.06
Blank_57	8.6	0.9	15	1.0	8.7	3.2	3.0	0.35	0.10	0.08	0.3	0.4	0.12	0.2	0.05	0.06	0.1	0.09	0.06	0.07
Blank_58	7.7	0.8	11	1.3	2.1	3.0	2.9	0.37	0.08	0.09	0.3	0.4	0.11	0.2	0.05	0.06	0.2	0.08	0.05	0.04
Blank_59	7.8	0.8	15	1.1	0.7	3.3	2.9	0.41	0.07	0.10	0.2	0.4	0.12	0.1	0.05	0.06	0.2	0.06	0.05	0.06
Blank_60	8.8	0.7	14	0.9	0.8	2.6	2.4	0.49	0.07	0.08	0.3	0.4	0.12	0.1	0.05	0.06	0.1	0.07	0.06	0.07
Blank_61	8.4	0.9	12	1.2	0.7	3.0	2.3	0.47	0.08	0.09	0.3	0.4	0.13	0.1	0.05	0.05	0.1	0.08	0.06	0.06
Blank_62	7.4	0.7	12	1.2	0.8	2.6	2.5	0.45	0.06	0.08	0.2	0.3	0.12	0.1	0.05	0.05	0.2	0.10	0.04	0.06
Blank_63	6.3	0.8	12	1.2	0.9	2.9	3.0	0.36	0.17	0.09	0.2	0.4	0.11	0.2	0.05	0.05	0.2	0.07	0.05	0.05
Blank_64	8.1	0.9	14	1.2	0.9	3.4	2.9	0.36	0.08	0.09	0.2	0.5	0.10	0.1	0.04	0.07	0.3	0.07	0.06	0.06
Blank_65	7.2	0.8	13	2.1	29	93	2.8	0.48	0.73	0.10	0.4	0.5	0.13	2.8	0.05	0.13	9.8	0.09	0.05	0.07
Blank_66	7.5	0.9	13	0.9	3.6	11	2.0	0.46	0.13	0.10	0.3	0.4	0.11	0.4	0.05	0.06	1.1	0.08	0.04	0.07
Blank_67	6.7	0.8	11	1.0	1.1	28	2.7	0.39	0.26	0.09	0.2	0.3	0.12	0.9	0.06	0.07	3.1	0.07	0.05	0.05
Blank_68	7.9	0.8	10	1.0	0.7	3.2	2.5	0.29	0.05	0.09	0.2	0.5	0.10	0.1	0.05	0.06	0.2	0.08	0.05	0.06
Blank_69	7.9	0.8	11	1.2	0.7	2.8	2.4	0.37	0.08	0.13	0.3	0.3	0.13	0.1	0.06	0.05	0.1	0.06	0.07	0.05
Blank_70	7.9	0.9	12	0.9	0.8	3.0	2.5	0.39	0.07	0.10	0.2	0.4	0.12	0.1	0.04	0.05	0.2	0.08	0.04	0.06
Blank_71	8.2	0.7	12	0.9	0.7	2.4	3.0	0.38	0.08	0.09	0.2	0.4	0.11	0.1	0.04	0.05	0.1	0.07	0.06	0.06
Blank_72	3.3	0.2	2.6	0.4	0.9	2.5	3.9	0.08	0.22	0.03	0.2	0.2	0.04	0.1	0.04	0.05	0.2	0.08	0.08	0.08
Blank_73	3.3	0.3	2.5	0.3	0.6	1.7	4.9	0.08	0.26	0.03	0.2	0.2	0.04	0.1	0.03	0.05	0.2	0.08	0.10	0.07
Blank_74	3.3	0.7	3.6	0.3	2.5	5.8	0.7	0.08	0.32	0.02	0.2	0.3	0.04	0.2	0.04	0.04	0.5	0.09	0.07	0.09
Blank_75	2.6	0.3	2.4	0.4	0.4	1.1	6.2	0.06	0.53	0.02	0.1	0.2	0.03	0.1	0.02	0.04	0.1	0.07	0.07	0.06
Blank_76	3.0	0.6	2.8	0.2	0.9	2.2	6.6	0.08	0.06	0.02	0.1	0.2	0.03	0.2	0.03	0.04	0.2	0.07	0.07	0.08
Blank_77	3.2	0.4	2.6	1.4	20	57	3.0	0.08	0.32	0.02	0.4	0.3	0.04	1.6	0.04	0.08	6.0	0.08	0.07	0.07
Blank_78	4.3	0.4	2.3	0.3	2.8	6.4	6.4	0.07	0.16	0.03	0.2	0.3	0.04	0.2	0.03	0.04	0.8	0.07	0.07	0.07
Blank_79	3.8	0.3	2.5	0.3	4.3	3.3	3.0	0.06	0.55	0.02	0.1	0.2	0.05	0.3	0.03	0.04	0.1	0.06	0.09	0.06
Blank_80	3.5	0.2	1.9	0.3	0.7	1.6	4.3	0.07	0.08	0.02	0.2	0.2	0.03	0.1	0.03	0.03	0.2	0.05	0.07	0.08

Table A3.10 30 scan averages of time resolved, non-collision cell ICP-MS analysis of select EPG snow samples and SLRS-4.

	Time sec	Ti ppt	V ppt	As ppt	Rb ppt	Sr ppt	Y ppt	Zr ppt	Cs ppt	Ba ppt	La ppt	Ce ppt	Bi ppt	Th ppt	U ppt	Ti/Sr	Zr/Y
Average 2 rsd of samples		10	7	12	7	3	16	110	12	9	3	5	99	10	9	9	106
Average 2 rsd of stds.		6	4	3	3	3	4	9	7	3	4	3	14	7	3	4	8
10 ppb Mg_std	88	1292	124	217	221	1076	10.9	90	10.3	62	9.9	9.7	9.2	10.0	9.6	1.20	8.3
10 ppb Mg_std	147	1277	124	222	219	1063	10.7	91	10.1	63	10.1	9.9	9.5	9.9	9.7	1.20	8.5
EPG_240	561	296	7.7	3.8	7.0	74	2.5	1.2	0.31	1.2	3.5	7.1	0.04	0.92	0.88	4.03	0.48
EPG_240	620	273	8.1	3.6	6.8	74	2.5	1.2	0.34	1.1	3.6	7.7	0.03	0.84	0.71	3.71	0.47
EPG_240	679	269	7.7	4.1	7.1	72	2.4	1.7	0.36	1.2	3.5	7.2	0.06	0.92	0.75	3.74	0.71
EPG_240	738	273	7.8	3.7	6.5	73	2.6	1.5	0.38	1.2	3.6	7.1	0.04	0.91	0.89	3.74	0.57
EPG_240	797	294	7.9	3.4	6.7	71	2.5	1.4	0.36	1.1	3.8	7.3	0.04	0.89	0.70	4.12	0.58
EPG_240	856	277	7.9	3.6	6.5	74	2.5	4.2	0.32	1.1	3.5	7.3	0.03	0.92	0.73	3.76	1.64
EPG_240	916	273	7.2	3.2	6.2	74	2.5	1.3	0.37	1.4	3.6	7.2	0.04	0.86	0.85	3.70	0.53
EPG_240	975	291	7.3	3.0	6.8	74	2.5	1.1	0.31	1.1	3.5	7.3	0.05	0.81	0.68	3.96	0.46
EPG_240	1034	285	8.9	3.5	6.9	72	2.5	1.3	0.39	1.1	3.6	7.2	0.05	1.05	0.87	3.94	5.2
EPG_240	1093	267	7.2	3.9	6.7	72	2.4	2.0	0.38	1.1	3.6	7.3	0.07	1.01	0.74	3.72	0.83
EPG_240	1152	291	6.9	3.4	6.6	74	5.0	17	0.31	1.3	3.6	7.5	0.05	0.92	0.75	3.92	3.4
EPG_240	1211	241	7.1	3.7	6.6	72	2.5	2.2	0.31	1.1	3.6	7.1	0.07	0.96	0.66	3.34	0.89
EPG_240	1270	254	7.4	3.8	6.7	71	2.4	1.8	0.35	1.1	3.5	7.3	0.07	0.91	0.67	3.60	0.76
EPG_110	1743	1703	40	6.9	26	835	11	21	0.79	3.9	14	29	-	2.7	1.8	2.0	1.9
EPG_110	1802	1733	38	7.4	26	844	12	18	0.77	4.4	14	29	-	2.6	1.9	2.1	1.5
EPG_110	1862	1706	38	7.8	27	853	9.4	22	0.72	4.3	15	30	-	2.8	1.9	2.0	2.4
EPG_110	1921	1668	38	7.4	26	844	9.3	23	0.82	4.4	15	30	0.04	2.7	1.9	2.0	2.4
EPG_110	1980	1690	39	7.8	27	845	10	19	0.79	4.1	15	29	0.00	2.7	1.8	2.0	1.9
EPG_110	2039	1718	39	7.5	27	852	9.3	21	0.82	4.2	15	30	-	3.6	1.8	2.0	2.2
EPG_110	2098	1725	38	7.7	27	847	9.9	26	0.82	4.3	15	30	-	2.5	1.8	2.0	2.6
EPG_110	2157	1659	37	8.2	26	847	9.1	18	0.87	4.3	15	30	-	2.8	1.8	2.0	2.0
EPG_110	2216	1690	38	8.1	26	851	12	21	0.83	4.1	15	30	0.03	2.6	1.9	2.0	1.8
EPG_110	2276	1720	39	8.0	28	857	9.2	23	0.75	4.5	14	31	0.10	2.6	1.8	2.0	2.5
EPG_110	2335	1673	39	7.5	27	849	9.4	25	0.75	4.0	15	30	0.03	2.8	1.9	2.0	2.6
EPG_110	2394	1688	38	7.9	27	850	9.5	29	0.84	4.1	15	35	-	2.8	2.0	2.0	3.1
EPG_184	2926	2246	37	5.8	28	594	9	15	0.88	4.4	16	33	-	3.3	1.0	3.8	1.8
EPG_184	2985	2209	37	6.3	28	594	8	15	0.92	4.2	16	33	0.00	3.3	1.0	3.7	1.8
EPG_184	3044	2233	37	5.7	27	588	9	16	0.74	4.2	16	32	-	3.3	1.0	3.8	1.7
EPG_184	3103	2198	36	5.4	27	590	8	15	0.81	4.1	16	33	0.01	3.4	1.0	3.7	1.8
EPG_184	3162	2254	37	5.2	27	588	8	16	0.79	4.4	16	32	-	3.3	1.0	3.8	1.9
EPG_184	3222	2225	37	5.9	27	583	8	16	0.77	4.1	16	32	-	3.4	0.9	3.8	1.9
EPG_184	3281	2261	37	5.5	28	593	9	17	0.82	4.2	16	32	0.01	3.2	1.1	3.8	1.9
EPG_184	3340	2247	37	5.6	27	597	8	17	0.87	4.1	16	33	0.02	3.3	0.9	3.8	2.0
EPG_184	3399	2221	37	5.7	27	593	8	16	0.81	4.2	16	33	0.01	3.2	1.0	3.7	1.9
EPG_184	3458	2239	37	6.2	27	592	8	17	0.77	4.0	16	32	0.10	3.1	1.0	3.8	2.0
EPG_184	3517	2190	36	5.3	27	581	8	16	0.74	4.1	16	32	0.02	3.5	1.0	3.8	1.9
EPG_184	3576	2179	39	5.5	27	591	8	16	0.78	4.1	16	32	0.04	3.2	0.9	3.7	1.9

Table A3.10 continued

	Time sec	Ti ppt	V ppt	As ppt	Rb ppt	Sr ppt	Y ppt	Zr ppt	Cs ppt	Ba ppt	La ppt	Ce ppt	Bi ppt	Th ppt	U ppt	Ti/Sr	Zr/Y
EPG_344	4109	3769	73	6.7	63	548	28	37	3.5	11	44	84	0.07	12	13	6.9	1.3
EPG_344	4168	3690	67	7.1	59	558	29	43	3.8	12	45	82	0.15	13	13	6.6	1.5
EPG_344	4227	5856	69	6.9	66	549	28	38	3.3	11	44	85	0.07	12	13	10.7	1.3
EPG_344	4286	3550	67	6.6	60	547	29	51	3.3	12	44	84	0.15	12	13	6.5	1.8
EPG_344	4345	4122	67	7.1	57	549	29	41	3.3	12	46	86	0.18	12	13	7.5	1.4
EPG_344	4404	3712	68	7.4	60	551	29	46	3.4	11	46	87	0.13	12	13	6.7	1.6
EPG_344	4463	3684	69	7.2	61	557	29	39	4.1	11	46	88	0.20	12	15	6.6	1.3
EPG_344	4522	3625	68	7.2	56	548	29	43	3.2	13	46	84	0.13	12	13	6.6	1.5
EPG_344	4582	3664	71	7.3	66	557	29	46	3.6	10	46	88	0.12	13	13	6.6	1.6
EPG_344	4641	3677	62	6.8	56	557	30	44	3.1	12	46	85	0.13	13	13	6.6	1.5
EPG_344	4700	3579	67	7.0	59	560	29	42	3.3	11	46	85	0.17	13	13	6.4	1.4
EPG_344	4759	3701	66	8.8	59	554	29	41	3.5	11	47	87	0.09	13	13	6.7	1.4
EPG_344	4818	3633	67	6.7	67	556	30	39	3.4	11	46	85	0.11	13	14	6.5	1.3
EPG_344	4877	3778	66	7.2	62	570	29	40	3.3	13	46	89	0.13	12	14	6.6	1.4
EPG_290	5232	3066	48	8.6	49	496	39	23	2.8	11	40	86	0.18	9.0	6.8	6.2	0.6
EPG_290	5291	3044	46	8.7	43	488	38	23	2.7	11	41	87	0.20	9.1	6.6	6.2	0.6
EPG_290	5350	3060	49	8.4	44	485	39	28	2.6	12	40	86	0.21	9.5	6.8	6.3	0.7
EPG_290	5409	3036	48	8.3	43	488	40	23	2.6	12	40	86	0.17	9.7	6.3	6.2	0.6
EPG_290	5469	3031	46	7.7	43	478	43	25	2.6	12	40	87	0.12	9.2	6.6	6.3	0.6
EPG_290	5528	3007	46	8.9	43	479	38	22	3.2	11	40	88	0.14	9.4	6.6	6.3	0.6
EPG_290	5587	2956	49	8.5	41	486	39	24	2.8	11	41	88	0.26	9.9	6.5	6.1	0.6
EPG_290	5646	3062	47	8.6	44	485	38	23	2.7	11	41	87	0.14	10	6.7	6.3	0.6
EPG_290	5705	3012	47	8.9	42	498	38	24	2.7	12	41	87	0.19	10	6.6	6.1	0.6
EPG_290	5764	3006	47	8.5	42	486	40	24	2.7	11	41	88	0.22	9.8	6.6	6.2	0.6
EPG_290	5823	2928	45	8.5	47	484	39	294	2.6	11	41	87	0.17	9.7	6.8	6.0	7.6
EPG_290	5882	3030	47	8.8	43	476	38	375	2.8	12	41	88	0.16	9.5	6.5	6.4	9.9
EPG_290	5942	2867	47	8.4	43	467	37	24	2.7	11	39	84	0.18	9.5	6.2	6.1	0.6
EPG_072	6237	9581	144	28	96	1776	49	86	4.9	27	95	196	0.40	19	6.3	5.4	1.8
EPG_072	6296	9398	143	28	97	1768	48	111	4.7	26	95	193	0.41	19	6.3	5.3	2.3
EPG_072	6355	9136	138	28	94	1772	48	95	4.6	26	94	196	0.43	19	6.1	5.2	2.0
EPG_072	6415	8890	135	27	92	1751	47	97	4.8	26	94	195	0.46	19	6.0	5.1	2.0
EPG_072	6474	8969	139	28	97	1747	48	95	4.6	26	94	192	0.38	19	6.1	5.1	2.0
EPG_072	6533	9050	136	27	96	1714	48	95	4.8	26	93	192	0.43	19	6.3	5.3	2.0
EPG_072	6592	8984	135	28	94	1736	47	97	4.5	26	93	191	0.38	19	5.9	5.2	2.0
EPG_072	6651	8830	135	28	92	1728	47	95	4.8	26	93	190	0.46	19	6.0	5.1	2.0
EPG_072	6710	8801	136	27	93	1722	47	107	4.5	26	94	191	0.44	19	5.9	5.1	2.3
EPG_072	6769	8632	132	27	91	1697	46	94	4.7	26	92	191	0.43	19	5.8	5.1	2.0
EPG_072	6829	8697	131	27	94	1709	47	103	4.7	26	93	191	0.38	19	5.8	5.1	2.2
EPG_072	6888	8752	131	26	96	1734	46	95	4.7	26	92	191	0.43	19	6.1	5.0	2.0
EPG_072	6947	8671	134	26	91	1696	46	94	4.4	25	91	187	0.39	18	5.7	5.1	2.0
EPG_072	7006	8469	130	26	89	1692	45	96	4.7	25	90	187	0.41	18	5.7	5.0	2.1
EPG_072	7065	8634	133	27	91	1701	46	93	4.6	25	91	188	0.43	19	5.8	5.1	2.0
EPG_072	7124	8714	131	24	89	1568	43	96	4.5	25	87	180	0.47	18	5.6	5.6	2.2

	Time sec	Ti ppt	V ppt	As ppt	Rb ppt	Sr ppt	Y ppt	Zr ppt	Cs ppt	Ba ppt	La ppt	Ce ppt	Bi ppt	Th ppt	U ppt	Ti/Sr	Zr/Y
SLRS-4	7538	86	30	67	141	2570	12	10.7	0.6	79	25	34	0.15	2.0	4.6	0.033	0.9
SLRS-4	7597	92	30	69	144	2563	13	9.7	0.6	80	26	34	0.15	2.1	4.5	0.036	0.8
SLRS-4	7656	96	30	69	142	2616	12	9.2	0.6	79	26	34	0.13	1.9	4.6	0.037	0.7
SLRS-4	7715	92	30	68	142	2628	13	8.9	0.5	82	26	34	0.20	2.1	4.6	0.035	0.7
SLRS-4	7775	90	30	68	143	2633	13	8.7	0.5	81	26	34	0.15	2.1	4.5	0.034	0.7
SLRS-4	7834	90	29	68	143	2573	12	8.5	0.5	80	25	34	0.13	2.0	4.5	0.035	0.7
SLRS-4	7893	90	29	69	142	2610	12	8.3	0.6	81	26	34	0.17	2.1	4.6	0.035	0.7
SLRS-4	7952	96	29	69	142	2584	12	8.3	0.6	81	26	34	0.15	2.0	4.7	0.037	0.7
SLRS-4	8011	93	29	67	140	2519	12	8.1	0.5	80	26	34	0.19	2.1	4.5	0.037	0.7
SLRS-4	8070	91	30	68	141	2507	12	8.1	0.5	81	26	34	0.13	2.0	4.6	0.036	0.7
SLRS-4	8129	90	29	69	140	2540	12	8.3	0.5	79	25	33	0.19	2.1	4.6	0.035	0.7
SLRS-4	8189	90	29	68	140	2542	12	8.1	0.6	79	25	33	0.13	2.0	4.5	0.035	0.7
SLRS-4	8248	90	29	67	140	2505	12	8.5	0.6	80	25	34	0.14	2.1	4.6	0.036	0.7
10 ppb Mg_std	8839	871	89	195	195	989	9.6	91	9.9	63	10.0	10.1	10.0	9.7	10.4	0.88	9.4
10 ppb Mg_std	8898	943	97	202	206	1011	10.4	95	10.5	66	10.5	10.5	10.6	10.7	10.7	0.93	9.2
10 ppb Mg_std	8957	941	97	201	204	1009	10.1	95	10.2	65	10.4	10.3	10.4	10.8	10.8	0.93	9.5
Averages																	
10 ppb Mg_std		1285	124	220	220	1069	10.8	91	10.2	62	10.0	9.8	9.32	10.0	9.6	1.2	8.4
EPG_240		276	7.6	3.6	6.7	73	2.7	3.8	0.3	1.2	3.6	7.3	0.05	0.9	0.7	3.8	1.3
EPG_110		1698	39	7.7	27	848	10.0	22	0.8	4.2	15	30	0.04	2.8	1.9	2.0	2.2
EPG_184		2225	37	5.7	27	590	8.5	16	0.8	4.2	16	32	0.03	3.3	1.0	3.8	1.9
EPG_344		3860	67	7.2	61	554	29	42	3.4	12	46	85	0.13	12.4	13	7.0	1.5
EPG_290		3008	47	8.5	44	484	39	72	2.7	11.3	41	87	0.18	9.6	6.6	6.2	1.9
EPG_072		8888	135	27	93	1719	47	97	4.7	26	92	191	0.42	18.8	6.0	5.2	2.1
SLRS-4		91	29	68	141	2568	12	8.7	0.6	80	26	34	0.15	2.0	4.6	0.0	0.7
10 ppb Mg_std		918	94	199	202	1003	10.0	94	10.2	64	10.3	10.3	10.4	10.4	10.7	0.9	9.4
2σ																	
10 ppb Mg_std		22	0.5	6.9	2.8	19	0.2	2.0	0.2	1.2	0.3	0.2	0.38	0.2	0.2	0.0	0.4
EPG_240		32	1.1	0.6	0.5	2	1.4	10.2	0.1	0.2	0.2	0.3	0.03	0.1	0.1	0.4	2.9
EPG_110		48	1.4	0.7	0.8	12	2.1	6.7	0.1	0.3	0.3	3.4	0.07	0.6	0.1	0.1	0.9
EPG_184		53	1.5	0.7	1.0	9	0.6	1.0	0.1	0.2	0.3	0.7	0.06	0.2	0.1	0.1	0.2
EPG_344		1181	5.1	1.1	7.2	13	1.0	7.7	0.5	1.4	1.8	3.7	0.08	0.6	1.3	2.2	0.3
EPG_290		117	2.4	0.6	4.1	16	2.8	236	0.3	0.6	1.0	2.3	0.07	0.7	0.4	0.2	6.2
EPG_072		587	8.0	2.3	5.5	98	2.6	11.6	0.3	0.9	4.0	7.8	0.06	0.7	0.4	0.3	0.3
SLRS-4		5.7	0.8	1.7	2.8	89	0.3	1.5	0.1	2.0	0.6	0.7	0.05	0.1	0.2	0.0	0.1
10 ppb Mg_std		82	8.9	8.0	11.8	24	0.7	5.6	0.6	3.5	0.5	0.4	0.63	1.2	0.4	0.1	0.3
2 rsd (%)																	
10 ppb Mg_std		2	0	3	1	2	2	2	2	2	3	2	4	2	2	0	4
EPG_240		12	14	17	7	3	52	266	18	17	4	4	61	14	10	11	224
EPG_110		3	4	9	3	1	21	30	11	8	2	11	184	21	8	3	39
EPG_184		2	4	12	4	2	7	6	14	6	2	2	235	6	12	2	8
EPG_344		31	8	15	12	2	3	18	14	12	4	4	59	5	9	31	19
EPG_290		4	5	7	9	3	7	329	12	5	3	3	40	8	5	4	331
EPG_072		7	6	8	6	6	12	6	12	6	4	4	14	4	8	6	13
SLRS-4		6	3	2	2	3	2	17	12	2	2	2	32	7	4	6	16
10 ppb Mg_std		9	9	4	6	2	7	6	6	5	5	4	6	12	4	6	3

Table A3.11 Trace element chemistry of EPG snow samples measured by non-collision cell ICP-MS. Values below the detection limit are shown in grey.

Sample	Depth cm	Ti	V	Cr	Ni	Cu	Zn	As	Rb	Sr	Y	Zr	Sb	Cs	Ba	La	Ce	Pb	Bi	Th	U	Ti/Sr	Zr/Y
Average		11840	205	190	103	162	268	22	164	2467	51	336	3.0	8.7	431	105	208	32	0.39	36	8.9	4.9	6.6
2σ		42553	676	568	352	495	836	60	536	8927	170	1189	19	28	1516	355	712	82	1.01	232	26	5.7	5.1
2 rsd (%)		359	330	299	343	306	312	272	327	362	332	354	626	322	352	339	343	257	260	637	292	115	77.5
Min		44	3.1	1.1	1.4	0.67	2.7	0.31	3.0	32.2	1.00	3.0	0.03	0.08	4.8	1.00	1.70	1.32	0.009	0.04	0.170	0.08	0.22
Max		151058	2227	1735	1246	1636	3012	199	1731	31450	709	5630	121	95	5841	1362	2665	324	4.3	1339	94	16	17
Detection limit		22	1.8	27	2.8	17	48	6.7	0.86	0.62	0.21	1.0	1.2	0.28	1.3	0.16	0.22	2.9	0.41	0.29	0.30		
SLRS-4 2 rsd (%)		10	7	30	13	18	30	6	5	5	6	15	5	13	5	5	6	9	26	10	9	7	11
EPG_379	1	134355	1958	702	1140	1599	2841	106	1429	11665	585	3655	3.4	93	5056	1199	2391	324	3.0	236	89	12	6.2
EPG_377	3	29003	436	203	245	228	238	28	407	3104	147	1012	1.2	26	1059	313	644	88	0.70	145	23	9.3	6.9
EPG_375	5	757	16	14	3.3	16	52	1.2	15	200	3.0	34	0.39	0.90	37	7.3	14	4.1	0.011	1.7	1.2	3.8	11
EPG_373	7	656	15	14	4.5	63	9.3	0.6	11	187	4.1	21	0.16	0.51	25	6.7	19	2.5	0.023	3.5	1.1	3.5	5.2
EPG_371	9	829	16	21	5.4	12	27	1.3	16	188	3.0	22	0.03	1.0	34	6.5	13	4.6	0.037	2.1	1.3	4.4	7.5
EPG_369	11	777	17	23	5.0	17	38	2.9	13	190	2.9	28	0.38	0.89	37	6.7	13	5.1	0.051	1.6	1.1	4.1	9.5
EPG_367	13	748	17	26	6.0	13	26	1.8	13	189	4.7	21	0.43	0.68	63	6.7	15	3.0	0.035	2.7	1.4	4.0	4.6
EPG_365	15	550	15	30	4.3	9.4	8.4	2.4	10	195	2.7	18	0.22	0.48	26	6.2	12	2.4	0.056	1.2	0.9	2.8	6.6
EPG_363	17	28393	425	286	226	274	533	37	334	4440	93	743	1.4	16	979	215	427	51	0.77	46	13	6.4	8.0
EPG_361	19	18984	298	247	129	119	129	29	249	3659	83	586	1.4	12	655	164	319	32	0.65	32	11	5.2	7.0
EPG_359	21	8137	132	108	62	94	151	13	99	1398	31	229	0.75	5.0	308	66	135	17	0.26	13	4.2	5.8	7.3
EPG_357	23	8117	118	95	62	97	190	10	88	1177	22	189	1.1	4.3	379	52	103	19	0.32	10	3.5	6.9	8.7
EPG_355	25	9267	144	85	71	141	309	12	168	1241	45	249	1.4	9.9	364	78	151	39	0.34	20	13	7.5	5.6
EPG_353	27	5544	105	62	62	225	433	9.5	101	848	39	183	0.87	7.2	299	77	144	49	0.36	29	20	6.5	4.7
EPG_351	29	3182	73	49	52	144	178	7.7	75	534	20	113	0.72	5.1	170	40	74	26	0.19	13	15	6.0	5.6
EPG_349	31	4602	90	45	52	174	178	7.5	109	640	31	159	1.2	7.1	232	60	112	33	0.27	21	15	7.2	5.2
EPG_347	33	4405	92	50	56	181	220	8.9	106	735	41	158	1.5	7.4	229	66	126	33	0.26	20	21	6.0	3.9
EPG_345	35	3428	71	43	40	118	172	6.3	71	526	24	116	1.0	5.1	170	54	103	24	0.22	22	15	6.5	4.7
EPG_343	37	3117	70	42	40	148	173	7.4	76	624	29	116	0.97	5.2	168	120	229	25	0.30	18	15	5.0	4.1
EPG_341	39	3438	82	42	48	196	561	7.2	84	676	33	156	0.66	5.9	199	53	105	32	0.24	18	16	5.1	4.8
EPG_339	41	3561	77	41	48	141	160	7.1	77	560	24	136	0.74	5.5	177	51	106	22	0.22		9.0	6.4	5.7
EPG_337	43	1069	19	20	9.7	46	159	2.9	28	208	5.8	42	1.4	1.8	61	12	27	9.8	0.048	3.1	2.7	5.1	7.3
EPG_335	45	1479	30	19	17	51	147	3.8	26	235	10	62	3.4	1.7	59	20	36	13	0.33	4.7	2.7	6.3	6.1
EPG_333	47	1133	20	14	11	34	87	3.3	22	185	7.1	61	1.1	1.3	58	15	24	11	0.083	3.1	2.2	6.1	8.6
EPG_331	49	879	17	8.0	11	33	63	2.4	18	172	5.6	43	0.79	1.1	44	11	21	8.0	0.066	2.7	1.9	5.1	7.7
EPG_329	51	1070	17	6.3	7.9	21	62	2.8	18	177	6.8	53	0.95	0.92	60	11	22	10	0.042	3.1	1.5	6.0	7.8
EPG_327	53	1007	20	25	11	23	-	2.5	21	204	5.5	40	0.89	1.1	50	11	23	7.2	0.070	2.5	1.4	4.9	7.3
EPG_325	55	360	8.2	22	3.7	8.2	-	2.2	8.1	113	2.2	22	1.0	0.42	15	3.9	7.8	3.5	0.077	0.80	0.34	3.2	10
EPG_323	57	292	6.3	18	4.4	5.0	-	1.9	6.8	123	1.6	17	1.8	0.26	11	2.8	5.5	2.9	0.042	0.57	0.38	2.4	11
EPG_321	59	175	4.2	5.2	1.6	0.7	-	0.6	4.7	76	1.3	12	1.2	0.15	6.7	2.4	4.6	1.5	0.045	0.44	0.20	2.3	9.5
EPG_319	61	204	3.1	5.8	8.1	23	-	1.3	3.0	54	1.1	11	1.8	0.08	16	1.8	3.4	15	0.095	0.30	0.17	3.8	9.9
EPG_317	63	7061	114	45	62	88	-	6.9	101	768	29	247	1.5	5.6	268	56	106	21	0.26	15	5.3	9.2	8.6
EPG_315	65	2920	79	81	45	43	406	12	44	613	14	115	2.3	2.3	110	27	52	15	0.25	4.8	2.6	4.8	8.5
EPG_313	67	297	11	32	5.9	2.1	537	4.8	5.3	49	1.6	14	1.7	0.30	11	3.3	6.6	3.0	0.14	0.59	0.22	6.1	8.7
EPG_311	69	6347	102	94	68	79	184	9.6	86	877	28	253	2.8	4.9	210	53	103	12	0.22	12	5.2	7.2	9.2

Table A3.11 continued.

Sample	Depth cm	Ti ppt	V ppt	Cr ppt	Ni ppt	Cu ppt	Zn ppt	As ppt	Rb ppt	Sr ppt	Y ppt	Zr ppt	Sb ppt	Cs ppt	Ba ppt	La ppt	Ce ppt	Pb ppt	Bi ppt	Th ppt	U ppt	Ti/Sr	Zr/Y
EPG_309	71	29272	499	525	291	436	-	41	409	6207	132	1017	3.7	22	1134	269	546	95	0.85	55	24	4.7	7.7
EPG_307	73	71532	1178	888	609	889	1771	115	928	14596	296	2093	6.9	51	2464	748	1400	151	2.0	174	44	4.9	7.1
EPG_305	75	151058	2227	1206	1246	1636	3012	170	1731	21467	709	5630	12	95	5841	1362	2665	303	4.3	313	94	7.0	7.9
EPG_302	78	15735	247	110	151	232	453	21	228	1688	75	499	7.1	15	663	178	336	88	0.82	55	23	9.3	6.6
EPG_301	79	18103	275	141	157	254	-	18	278	1742	89	592	10.0	18	736	183	369	89	0.97	60	24	10	6.6
EPG_299	81	16312	249	118	131	235	414	14	279	1569	77	420	18	18	614	147	283	71	0.56	56	25	10	5.4
EPG_297	83	18430	293	189	155	319	543	21	294	2680	111	527	18	18	897	210	405	89	0.66	59	34	6.9	4.8
EPG_295	85	15336	232	130	124	236	512	14	271	1840	66	462	28	15	553	139	283	64	0.53	39	20	8.3	7.0
EPG_293	87	5837	95	54	59	114	198	6.1	82	216	121	146	0.90	4.0	215	54	107	20	0.19	12	4.6	6.9	7.8
EPG_291	89	4250	58	39	44	53	128	5.6	63	430	18	146	0.90	3.8	152	37	77	22	0.20	14	4.6	9.9	8.2
EPG_289	91	3409	57	39	27	67	139	7.0	61	406	15	91	1.7	3.4	139	36	85	24	0.28	6.6	3.6	8.4	6.1
EPG_287	93	1055	23	32	11	27	46	4.0	18	381	5.1	44	1.0	0.65	44	11	21	6.5	0.050	1.6	0.95	2.8	8.5
EPG_285	95	907	13	5.5	8.9	29	68	1.7	11	94	2.7	33	0.45	3.2	33	5.9	12	7.4	0.073	1.2	0.39	9.7	12
EPG_283	97	208	4.4	9.5	4.6	9.4	99	1.2	3.3	32	1.1	11	0.99	0.15	9.0	1.9	3.8	7.0	0.074	0.33	0.18	6.4	10
EPG_281	99	33942	481	240	321	310	773	32	432	4258	135	1645	2.3	23	1233	299	585	71	0.90	73	16	8.0	12
EPG_279	101	39860	508	232	349	365	972	34	458	4449	129	1312	2.0	25	1156	279	557	88	0.96	69	19	9.0	10
EPG_277	103	12435	197	84	143	170	487	16	183	1391	45	437	0.75	11	437	90	180	40	0.30	22	8.3	8.9	9.6
EPG_275	105	1630	26	22	12	21	138	4.0	21	211	6.3	64	0.50	0.98	60	19	39	6.7	0.11	2.6	2.2	7.7	10
EPG_273	107	1217	29	31	15	26	77	4.9	23	333	7.6	53	0.68	1.1	65	15	32	8.5	0.13	2.0	2.0	3.7	7.0
EPG_271	109	4838	82	67	42	76	245	13	80	817	20	154	1.3	4.2	171	40	80	37	0.44	8.5	3.3	5.9	7.6
EPG_269	111	6014	88	53	41	48	85	5.9	78	655	25	79	0.86	4.0	264	54	102	14	0.20	12	3.2	9.2	3.1
EPG_267	113	6762	114	79	64	75	128	6.7	104	801	25	152	0.75	5.9	289	59	113	21	0.28	16	4.0	8.4	6.0
EPG_265	115	17246	269	133	147	173	453	15	269	1839	51	540	1.1	16	570	115	231	43	0.92	29	8.0	9.4	11
EPG_263	117	18645	294	158	175	165	446	17	271	2167	52	582	2.4	16	600	114	225	36	0.72	26	8.5	8.6	11
EPG_261	119	20452	303	140	174	188	395	16	265	1724	76	629	1.1	15	798	170	336	46	0.80	40	8.7	12	8.3
EPG_259	121	9940	159	96	109	103	232	16	153	1133	51	485	1.8	7.9	334	113	222	33	0.56	23	5.0	8.8	9.4
EPG_257	123	15592	236	126	139	181	365	16	251	2094	75	354	0.81	14	606	172	327	45	0.40	52	11	7.4	4.7
EPG_255	125	3952	63	40	30	50	26	5.4	43	387	22	110	1.8	2.4	125	35	67	9.3	0.12	6.6	3.9	10	5.0
EPG_253	127	1764	33	33	19	86	197	5.9	28	371	14	53	1.2	1.8	63	28	51	21	0.16	4.0	2.7	4.7	3.9
EPG_251	129	15085	201	95	89	124	348	14	167	1302	51	345	1.2	8.8	537	109	223	43	0.41	32	8.6	12	6.8
EPG_249	131	3979	55	28	28	47	146	13	62	253	17	106	1.4	3.1	146	34	65	45	0.48	11	2.9	16	6.1
EPG_247	133	596	14	10	10	22	123	8.1	13	78	3.0	15	1.2	0.80	25	6.3	12	24	0.26	1.7	0.90	7.6	5.0
EPG_245	135	544	13	9.1	9.3	23	412	5.9	14	88	3.8	14	0.62	0.92	30	6.4	12	18	0.24	2.0	1.1	6.2	3.8
EPG_244	136	273	7.6	-	6.1	10	23	4.0	7.5	70	2.3	4.4	0.85	0.42	22	4.2	7.7	8.4	0.065	1.2	0.94	3.9	1.9
EPG_243	137	482	12	9.7	8.9	21	42	3.2	10	88	3.2	13	1.8	0.68	26	5.5	10	11	0.12	1.5	1.2	5.5	4.0
EPG_241	139	376	9.6	7.1	6.1	14	23	2.6	9.2	68	2.5	11	1.0	0.61	21	4.1	7.8	8.4	0.079	1.2	0.75	5.5	4.2
EPG_239	141	696	14	6.3	8.7	20	57	6.6	13	113	3.4	18	0.84	0.80	30	6.7	12	19	0.20	1.5	1.0	6.1	5.4
EPG_237	143	779	14	11	11	11	57	12	14	137	3.4	24	1.0	0.76	31	7.0	14	35	0.36	1.4	0.75	5.7	7.0
EPG_235	145	380	7.5	1.1	3.7	7.4	21	8.9	8.2	77	1.6	9.5	2.6	0.40	17	3.6	6.8	19	0.17	0.36	0.40	5.0	5.8
EPG_233	147	780	14	19	8.3	53	95	12	14	142	3.1	25	1.9	0.80	31	6.2	8.1	33	0.31	1.0	0.68	5.5	8.1
EPG_227	153	3589	64	61	29	50	144	7.0	43	685	12	129	0.56	1.9	109	23	46	12	0.16	4.4	1.5	5.2	10
EPG_225	155	11491	184	142	86	117	183	14	127	2028	36	374	1.8	6.0	374	80	163	21	0.34	16	5.8	5.7	10
EPG_223	157	12867	198	187	94	141	300	20	150	2332	42	460	1.6	6.7	431	94	184	27	0.31	19	6.5	5.5	11

Table A3.11 continued.

Sample	Depth cm	Ti ppt	V ppt	Cr ppt	Ni ppt	Cu ppt	Zn ppt	As ppt	Rb ppt	Sr ppt	Y ppt	Zr ppt	Sb ppt	Cs ppt	Ba ppt	La ppt	Ce ppt	Pb ppt	Bi ppt	Th ppt	U ppt	Ti/Sr	Zr/Y
EPG_221	159	15967	242	186	110	157	345	18	155	2284	48	483	1.1	7.8	523	106	207	27	0.41	21	6.4	7.0	10
EPG_219	161	13465	209	154	146	153	365	18	148	2002	50	389	3.2	7.7	437	111	246	38	0.43	20	8.3	6.7	7.8
EPG_217	163	28438	417	186	192	500	886	23	373	2501	139	568	2.0	25	1026	546	996	107	0.74	369	30	11	4.1
EPG_215	165	17196	263	168	149	355	535	16	222	2240	80	462	1.1	13	639	181	334	61	0.48	74	21	7.7	5.8
EPG_213	167	18966	327	216	190	439	758	21	280	2684	150	511	1.0	18	916	202	387	85	0.66	52	25	7.1	3.4
EPG_211	169	16302	271	226	159	366	533	19	208	2110	80	429	1.2	14	630	175	451	66	0.58	56	23	7.7	5.4
EPG_209	171	22883	330	225	176	420	635	24	269	2710	118	538	1.4	17	893	298	702	73	0.56	179	20	8.4	4.6
EPG_207	173	9434	157	129	74	190	255	13	150	1374	110	251	0.95	9.0	365	96	201	28	0.32	20	11	6.9	2.3
EPG_205	175	18608	284	201	174	316	454	20	251	2201	75	487	1.0	16	791	174	329	80	0.58	46	15	8.5	6.2
EPG_203	177	17820	283	219	172	346	470	23	250	2148	83	460	0.80	16	712	165	313	63	0.62	40	17	8.3	5.5
EPG_201	179	38567	468	298	289	304	331	29	458	2876	113	798	1.9	29	1429	285	560	80	0.83	68	21	13	7.1
EPG_199	181	38124	593	596	285	403	366	51	479	6133	147	922	1.2	29	1428	399	602	70	1.0	85	23	6.2	6.3
EPG_197	183	14449	343	543	115	250	205	39	324	5109	76	317	1.4	16	671	130	234	58	0.38	27	17	2.8	4.2
EPG_195	185	16183	284	325	104	170	162	24	281	3078	64	259	1.6	16	519	161	239	58	1.2	94	13	5.3	4.0
EPG_193	187	7878	103	129	35	71	148	12	156	1366	24	56	1.0	4.9	711	37	67	14	0.099	4.2	2.8	5.8	2.3
EPG_191	189	1021	24	27	10	15	22	1.8	22	196	4.0	40	0.31	0.60	37	8.6	17	3.4	0.009	2.8	0.72	5.2	10
EPG_190	190	562	18	50	7.0	25	43	8.3	16	460	4.4	10	0.95	0.76	35	7.3	13	7.6	0.22	1.5	1.8	1.2	2.3
EPG_188	192	1389	34	79	13	23	47	8.7	23	632	13	33	1.4	0.78	55	13	28	5.5	0.063	2.0	0.90	2.2	2.4
EPG_187	193	5712	117	210	37	61	83	16	71	1957	22	185	0.69	2.7	191	61	341	11	0.15	61	4.2	2.9	8.5
EPG_185	195	26807	423	467	181	212	184	41	356	5464	87	693	2.0	19	720	262	515	35	0.66	61	11	4.9	7.9
EPG_183	197	3567	187	538	44	96	38	38	80	3391	12	114	1.0	2.2	124	25	45	11	0.070	4.9	2.9	1.1	9.1
EPG_181	199	42947	716	652	369	655	808	74	536	12002	115	1033	2.4	26	1252	264	519	71	1.0	58	18	3.6	9.0
EPG_179	201	1659	141	447	23	79	49	31	57	2701	15	59	0.85	1.5	68	27	49	10	0.14	4.3	2.4	0.6	3.9
EPG_178	202	2277	119	438	19	76	52	27	58	2292	8.2	79	0.99	1.6	84	20	38	13	0.12	4.5	2.0	1.0	9.7
EPG_176	204	20549	456	520	257	456	430	34	312	2906	136	599	1.1	22	821	256	487	84	0.86	101	20	7.1	4.4
EPG_175	205	65448	1132	880	577	972	2093	93	837	14398	237	1376	6.0	45	2639	484	923	132	1.7	100	51	4.5	5.8
EPG_174	206	49803	924	1360	272	420	441	81	549	11843	217	399	2.8	22	2020	439	850	97	1.0	72	27	4.2	1.8
EPG_173	207	81301	1342	1016	608	983	1503	115	1092	16004	243	1639	2.4	53	2963	561	1091	123	1.6	125	36	5.1	6.7
EPG_171	209	82814	1224	1107	582	545	491	86	892	10912	271	1819	2.2	48	2347	570	1093	104	1.4	1339	37	7.6	6.7
EPG_169	211	9254	192	264	69	120	110	26	139	2732	37	266	2.7	6.3	363	183	321	24	0.21	25	7.0	3.4	7.1
EPG_167	213	3488	65	58	40	57	198	26	65	728	16	140	6.0	3.9	181	31	59	34	0.40	6.2	3.5	4.8	8.6
EPG_165	215	1654	38	50	27	49	116	23	28	253	7.4	52	5.8	2.4	72	14	33	22	0.34	5.2	2.4	6.5	7.1
EPG_163	217	1155	33	51	24	57	83	24	24	290	7.0	44	5.6	2.0	46	12	23	10	0.30	2.7	3.3	4.0	6.3
EPG_161	219	5370	93	64	46	53	126	27	81	965	36	229	5.6	4.7	211	56	110	30	0.46	14	6.0	5.6	6.4
EPG_159	221	7234	125	74	63	82	121	31	111	1777	38	331	5.5	7.9	320	85	162	27	0.59	17	6.6	4.1	8.6
EPG_157	223	8579	200	145	78	149	161	42	123	2877	33	322	6.1	7.0	265	68	132	21	0.42	13	5.0	9.7	7.1
EPG_155	225	12939	263	172	106	162	211	47	158	4633	48	481	6.1	6.9	381	97	190	31	0.49	16	6.4	2.8	10
EPG_153	227	4170	103	97	47	71	124	31	79	1124	17	129	5.9	3.1	132	35	65	16	0.31	6.0	3.1	3.7	7.7
EPG_151	229	5084	138	115	56	86	271	35	109	1846	23	161	5.8	5.5	193	67	126	24	0.35	13	5.3	2.8	6.9
EPG_149	231	8864	243	610	101	137	153	34	141	4251	34	233	1.6	6.0	268	63	124	18	0.32	17	4.5	2.1	6.9
EPG_148	232	15006	307	651	84	179	167	37	165	6005	57	153	0.76	6.0	1023	120	224	26	0.28	21	10	2.5	2.7
EPG_147	233	36774	496	203	217	291	501	56	354	5991	117	814	6.6	17	1092	226	453	64	0.71	37	13	6.1	7.0
EPG_145	235	31532	411	158	188	181	382	46	305	4383	95	716	3.3	15	855	180	359	50	0.67	37	12	7.2	7.6

Table A3.11 continued.

Sample	Depth cm	Ti ppt	V ppt	Cr ppt	Ni ppt	Cu ppt	Zn ppt	As ppt	Rb ppt	140	138	12	31	Zr ppt	Sb ppt	Cs ppt	Ba ppt	La ppt	Ce ppt	Pb ppt	Bi ppt	Th ppt	U ppt	Ti/Sr	Zr/Y
										140 ppt	138 ppt	12 ppt	31 ppt												
EPG_144	236	5420	89	55	35	39	46	4.9	63	175	1.2	3.1	191	47	89	8.6	0.15	9.2	5.2	7.2	7.9	7.9			
EPG_142	238	449	8.6	10	3.4	-	5.4	1.5	7.5	31	-	0.44	20	6.2	9.8	-	0.015	1.1	0.82	2.8	6.2	6.2			
EPG_138	242	1272	21	25	6.0	8.5	17	4.8	22	31	0.94	1.3	61	17	34	3.0	0.058	2.9	2.0	3.9	2.7	2.7			
EPG_136	244	825	18	29	4.9	9.0	13	5.1	19	124	0.57	1.1	33	10	20	4.2	0.056	2.6	1.1	2.4	1.7	1.7			
EPG_134	246	781	18	34	5.9	6.1	7.5	4.9	15	41	8.3	0.69	35	8.1	15	1.8	0.035	2.0	1.1	2.2	4.9	4.9			
EPG_132	248	1673	29	33	13	44	68	7.6	25	67	0.44	1.4	72	20	40	15	0.19	4.7	4.1	4.8	4.9	4.9			
EPG_130	250	10999	196	185	69	104	60	29	129	161	0.58	6.8	451	146	264	25	0.42	30	11	4.4	2.1	2.1			
EPG_128	252	25743	519	488	227	307	231	57	401	896	1.9	24	907	247	472	55	0.91	64	24	4.7	7.6	7.6			
EPG_127	253	340	75	150	51	151	194	28	82	6.5	0.44	1.2	39	43	75	6.1	0.049	1.2	11	0.1	0.22	0.22			
EPG_126	254	18113	395	358	205	267	144	36	285	560	9.6	19	659	227	424	44	0.81	41	16	4.7	5.9	5.9			
EPG_124	256	4542	118	152	64	73	35	15	98	119	0.70	5.8	186	53	95	11	0.15	10	6.0	2.4	3.9	3.9			
EPG_121	259	44	6.0	18	5.9	0.7	9.7	8.6	4.8	3.3	2.2	0.49	5.3	1.1	1.9	1.6	0.022	0.13	0.34	0.4	3.3	3.3			
EPG_119	261	295	9.4	68	6.3	20	83	7.0	7.9	5.0	5.0	0.61	15	4.4	8.5	3.6	0.045	0.34	0.35	3.2	2.6	2.6			
EPG_117	263	256	10	71	5.7	19	29	7.1	8.0	338	7.1	0.50	15	7.2	15	4.9	0.021	0.90	0.92	2.0	2.2	2.2			
EPG_115	265	571	14	74	7.0	17	44	7.7	10	353	8.3	0.64	19	5.3	9.5	6.1	0.038	1.0	0.61	4.1	4.5	4.5			
EPG_113	267	317	15	81	7.2	16	58	8.4	11	347	14	0.72	16	4.5	8.5	7.1	0.048	0.71	0.37	1.6	5.6	5.6			
EPG_111	269	2140	52	170	25	54	62	11	34	2477	76	0.32	19	72	32	6.7	0.059	3.0	1.8	2.4	6.4	6.4			
EPG_108	272	730	23	43	9.0	17	29	6.0	16	5536	11	0.62	42	7.4	14	5.3	0.062	0.90	0.92	1.6	3.4	3.4			
EPG_106	274	100	3.6	9.3	1.4	4.5	75	2.6	3.3	30	0.92	0.18	4.8	1.0	1.7	3.3	0.048	0.10	0.17	1.3	2.5	2.5			
EPG_104	276	114	9.8	28	3.7	12	13	4.9	5.0	3834	95	0.40	6.2	1.9	3.2	3.1	0.036	0.04	0.33	0.7	0.90	0.90			
EPG_102	278	363	12	23	8.8	13	34	8.5	9.1	1903	30	0.34	21	3.7	7.5	14	0.17	0.66	0.26	1.4	9.0	9.0			
EPG_100	280	135	6.8	16	1.7	5.1	28	8.0	4.7	106	1.0	0.13	5.9	1.2	2.3	13	0.11	0.17	0.17	1.1	4.0	4.0			
EPG_096	284	5447	223	465	87	156	108	36	127	31	2.8	0.89	4.8	4.3	81	13	0.15	8.8	3.3	1.5	7.4	7.4			
EPG_094	286	10096	274	360	139	281	430	32	207	127	2.6	1.1	8.6	63	122	23	0.26	13	5.5	2.2	5.4	5.4			
EPG_092	288	19292	471	653	235	538	505	73	372	139	4.7	1.3	15	158	311	39	0.52	36	14	1.5	5.3	5.3			
EPG_090	290	4151	128	261	38	98	94	20	82	202	2.3	1.1	5.0	2.6	52	9.6	0.15	4.9	2.4	1.9	7.6	7.6			
EPG_088	292	3089	98	219	28	75	61	17	56	399	9.3	0.42	1.8	103	23	46	0.11	4.3	1.7	2.4	6.8	6.8			
EPG_086	294	45464	924	731	462	658	878	80	593	469	5.6	1.8	26	1314	1570	69	1.3	681	44	3.5	5.2	5.2			
EPG_084	296	91032	1653	1726	709	1181	1379	199	1381	75	1.2	3.0	51	552	1097	126	1.7	148	44	2.9	6.2	6.2			
EPG_082	298	96174	1708	1735	904	1132	1423	197	1480	161	4.2	4.6	50	2968	591	115	1.7	107	39	3.1	5.0	5.0			
EPG_079	301	50221	1029	1110	490	678	1156	113	1012	360	3.5	2.6	59	1810	349	668	1.4	89	24	2.9	9.3	9.3			
EPG_077	303	13827	259	361	135	192	378	30	198	561	2.9	7.4	473	130	256	26	0.39	36	8.3	3.3	9.8	9.8			
EPG_075	305	3833	75	89	39	67	140	13	61	127	2.1	2.8	136	33	59	14	0.14	6.1	5.0	4.4	8.4	8.4			
EPG_073	307	682	20	26	9.9	17	84	6.8	16	4610	25	0.64	34	10	21	14	0.087	1.5	0.77	2.1	6.4	6.4			
EPG_071	309	7923	133	104	80	82	307	23	101	408	0.99	4.9	253	59	116	21	0.64	12	4.7	6.9	13	13			
EPG_069	311	2273	49	61	27	19	45	14	39	117	1.1	1.8	72	22	42	12	0.14	3.3	1.7	3.7	9.6	9.6			
EPG_067	313	2628	58	89	26	40	119	13	50	106	2.0	2.5	96	28	54	12	0.14	4.6	3.0	2.8	6.8	6.8			
EPG_065	315	3304	72	91	37	70	113	10	68	119	1.5	3.6	127	40	76	18	0.20	10	5.7	3.5	6.6	6.6			
EPG_063	317	1487	42	73	19	51	97	10	36	64	1.5	1.9	84	57	68	10	0.15	9.4	3.8	2.1	4.4	4.4			
EPG_061	319	3318	86	102	36	99	97	14	36	112	0.74	3.6	155	43	80	14	0.60	9.0	4.8	3.0	4.4	4.4			
EPG_059	321	3511	67	133	33	52	152	12	46	95	5.0	2.4	153	27	50	12	0.26	4.7	2.4	3.8	7.5	7.5			
EPG_057	323	274	11	26	4.4	12	34	4.9	8.1	59	0.34	0.26	35	3.0	5.8	4.6	0.076	0.37	0.37	1.1	8.8	8.8			
EPG_055	325	2248	48	74	39	37	51	9.1	31	135	1.1	1.4	87	18	36	6.3	0.11	3.0	1.3	3.0	8.1	8.1			

Table A3.11 continued.

Sample	Depth cm	Ti ppt	V ppt	Cr ppt	Ni ppt	Cu ppt	Zn ppt	As ppt	Rb ppt	Sr ppt	Y ppt	Zr ppt	Sb ppt	Cs ppt	Ba ppt	La ppt	Ce ppt	Pb ppt	Bi ppt	Th ppt	U ppt	Ti/Sr	Zr/Y
EPG_053	327	22156	318	319	71	155	165	30	229	4055	69	853	1.1	11	523	136	267	26	0.40	25	7.6	5.5	12
EPG_051	329	9756	166	165	71	103	102	30	126	2204	37	280	1.4	6.1	326	73	139	20	0.30	18	7.1	4.4	7.1
EPG_049	331	3334	72	83	33	93	88	16	58	892	21	104	1.3	3.2	130	41	84	19	0.18	14	6.1	3.7	4.9
EPG_047	333	1203	30	43	22	39	48	10	30	356	18	65	1.3	1.8	58	19	41	14	0.16	4.6	4.9	3.4	3.6
EPG_045	335	4518	143	241	44	144	109	25	93	2583	22	109	0.81	4.4	194	43	74	17	0.18	8.9	6.7	1.7	4.9
EPG_043	337	3989	129	242	31	103	56	23	66	2531	14	117	0.87	2.1	121	27	54	7.1	0.11	4.3	2.1	1.6	8.3
EPG_041	339	565	26	69	7.7	52	149	7.0	19	655	27	222	0.82	0.36	19	4.7	8.8	6.8	0.039	0.72	0.52	0.9	8.2
EPG_039	341	152	21	62	4.0	34	75	6.6	13	606	1.8	5.3	1.5	0.21	8.2	2.3	4.2	2.3	0.060	0.26	0.42	0.2	3.0
EPG_037	343	147	19	58	4.3	17	11	5.7	11	579	1.5	3.2	1.7	0.21	7.5	2.1	3.7	1.3	0.027	0.16	0.47	0.3	2.2
EPG_035	345	240	27	80	5.9	35	26	11	17	864	3.3	17	0.36	0.31	13	3.5	6.5	2.5	0.042	0.41	0.71	0.3	5.2
EPG_033	347	202	37	138	5.3	39	26	11	20	1065	9.0	60	0.87	0.36	11	3.0	5.5	3.2	0.049	0.53	0.70	0.2	6.6
EPG_031	349	168	41	133	3.8	26	2.7	11	20	1198	7.7	30	0.72	0.26	8.7	3.0	4.9	1.8	0.062	0.27	0.81	0.1	3.8
EPG_030	350	206	50	185	5.7	50	54	14	22	1443	3.6	16	0.74	0.44	11	3.0	5.6	3.6	0.070	0.39	1.1	0.1	4.4
EPG_028	352	2596	52	57	31	54	67	9.3	47	810	21	70	1.2	2.8	111	37	72	14	0.18	5.7	3.4	3.2	3.4
EPG_026	354	3390	66	44	30	52	82	9.5	46	605	36	109	2.4	2.7	140	79	158	14	0.20	5.7	3.5	5.6	3.1
EPG_024	356	1366	28	29	15	11	29	4.6	20	254	6.5	46	0.32	1.1	52	11	22	7.0	0.072	1.7	0.85	5.4	7.0
EPG_023	357	3112	52	40	35	75	116	7.3	40	504	17	122	0.52	2.0	133	27	50	17	0.24	5.2	2.1	6.2	7.3
EPG_020	360	1797	35	34	22	26	122	5.8	27	480	15	132	1.5	1.6	72	16	31	11	0.15	2.9	1.4	3.7	8.9
EPG_017	363	3606	67	72	30	53	101	11	48	626	18	143	0.90	2.9	120	28	56	19	0.19	5.1	1.9	5.8	8.0
EPG_016	364	2175	40	38	21	25	94	7.5	28	463	34	294	0.85	1.4	81	17	35	10	0.19	3.5	1.2	4.7	8.6
EPG_014	366	1281	27	34	13	24	100	5.7	22	477	42	343	3.7	1.1	50	12	23	10	0.12	2.0	0.95	2.7	8.2
EPG_013	367	3577	55	42	29	48	113	9.1	34	428	26	170	1.8	1.7	118	30	62	12	0.18	6.9	1.5	8.4	6.6
EPG_012	368	930	47	51	48	94	99	40	49	490	9.8	97	10	10	100	10	10	51	-	20	10	1.9	9.9
EPG_010	370	1111	28	51	16	31	95	6.7	21	500	40	290	0.72	0.97	45	19	36	7.5	0.070	7.3	0.97	2.2	7.2
EPG_008	372	3396	80	114	37	76	81	15	63	1204	24	135	1.1	3.3	127	35	73	16	0.18	8.4	3.6	2.8	5.6
EPG_006	374	5234	124	168	53	123	116	21	83	2232	29	184	1.6	3.9	223	57	109	19	0.22	11	4.9	2.3	6.3
EPG_005	375	9065	185	224	86	102	82	27	126	2919	49	369	1.6	5.9	347	89	174	22	0.31	23	7.3	3.1	7.5
EPG_003	377	14632	252	259	118	134	112	27	172	3608	83	563	2.1	9.4	433	123	221	32	0.36	54	8.5	4.1	6.8
EPG_002	378	6855	137	162	75	149	271	19	110	2524	84	437	1.5	5.6	268	68	127	49	0.25	13	6.0	2.7	5.2
EPG_001	379	15727	276	334	144	237	267	27	171	4176	98	591	1.2	9.3	480	141	268	48	0.39	29	9.3	3.8	6.0

Table A3.12 Correlation coefficients of EPG major and trace element chemistry measured by ICP-MS

r^2	Na	Mg	Al	Ca	Mn	Fe	Ba	Ti	V	Cr	Ni	Cu	Zn	As	Rb	Sr	Y	Zr	Cd	Sb	Cs	Ba	La	Ce	Pb	Bi	Th	U
Na	1.00																											
Mg	0.94	1.00																										
Al	0.28	0.37	1.00																									
Ca	0.76	0.81	0.73	1.00																								
Mn	0.29	0.38	0.97	0.75	1.00																							
Fe	0.27	0.36	0.99	0.71	0.96	1.00																						
Ba	0.29	0.38	0.90	0.74	0.97	0.89	1.00																					
Ti	0.54	0.53	0.53	0.76	0.56	0.51	0.59	1.00																				
V	0.66	0.65	0.52	0.82	0.54	0.49	0.56	0.98	1.00																			
Cr	0.82	0.79	0.25	0.68	0.27	0.24	0.29	0.68	0.79	1.00																		
Ni	0.57	0.57	0.57	0.80	0.59	0.54	0.61	0.98	0.98	0.70	1.00																	
Cu	0.59	0.58	0.52	0.78	0.53	0.48	0.57	0.92	0.94	0.70	0.95	1.00																
Zn	0.41	0.43	0.58	0.69	0.61	0.55	0.65	0.84	0.83	0.49	0.87	0.90	1.00															
As	0.82	0.81	0.34	0.76	0.37	0.32	0.39	0.79	0.87	0.90	0.81	0.80	0.62	1.00														
Rb	0.65	0.67	0.52	0.82	0.54	0.50	0.57	0.96	0.98	0.79	0.97	0.93	0.81	0.87	1.00													
Sr	0.85	0.85	0.30	0.74	0.31	0.28	0.33	0.74	0.84	0.93	0.76	0.77	0.58	0.96	0.85	1.00												
Y	0.44	0.44	0.59	0.73	0.62	0.55	0.66	0.95	0.91	0.56	0.94	0.90	0.86	0.68	0.89	0.62	1.00											
Zr	0.38	0.40	0.64	0.69	0.69	0.61	0.73	0.90	0.85	0.50	0.90	0.81	0.81	0.63	0.83	0.56	0.94	1.00										
Cd	0.06	0.07	0.08	0.10	0.09	0.07	0.10	0.14	0.13	0.05	0.13	0.11	0.12	0.20	0.12	0.09	0.13	0.16	1.00									
Sb	0.00	0.00	0.00	0.00	0.01	0.00	0.01	0.01	0.01	0.00	0.01	0.01	0.01	0.00	0.01	0.00	0.01	0.17	0.01	1.00								
Cs	0.49	0.52	0.64	0.78	0.65	0.61	0.67	0.95	0.94	0.63	0.95	0.92	0.85	0.73	0.95	0.67	0.93	0.89	0.13	0.01	1.00							
Ba	0.48	0.48	0.57	0.74	0.60	0.54	0.63	0.98	0.95	0.62	0.97	0.93	0.88	0.73	0.94	0.67	0.96	0.92	0.14	0.01	0.96	1.00						
La	0.43	0.43	0.59	0.72	0.63	0.56	0.67	0.94	0.90	0.54	0.93	0.90	0.85	0.66	0.88	0.59	0.96	0.91	0.12	0.01	0.93	0.95	1.00					
Ce	0.43	0.43	0.56	0.71	0.60	0.53	0.63	0.91	0.88	0.53	0.91	0.88	0.83	0.64	0.85	0.59	0.93	0.87	0.12	0.01	0.90	0.92	0.98	1.00				
Pb	0.31	0.32	0.60	0.64	0.62	0.57	0.65	0.86	0.80	0.42	0.85	0.85	0.86	0.55	0.80	0.47	0.91	0.85	0.14	0.01	0.90	0.90	0.91	0.88	1.00			
Bi	0.42	0.44	0.56	0.69	0.61	0.54	0.66	0.91	0.88	0.54	0.90	0.86	0.85	0.69	0.87	0.60	0.92	0.91	0.20	0.01	0.91	0.92	0.91	0.89	0.89	1.00		
Th	0.14	0.10	0.08	0.17	0.09	0.07	0.09	0.32	0.30	0.24	0.28	0.23	0.15	0.20	0.27	0.18	0.28	0.24	0.00	0.00	0.28	0.26	0.33	0.37	0.22	0.25	1.00	
U	0.36	0.36	0.53	0.65	0.55	0.49	0.59	0.85	0.82	0.47	0.86	0.89	0.84	0.59	0.81	0.54	0.90	0.80	0.10	0.01	0.88	0.88	0.91	0.90	0.92	0.86	0.29	1.00

Table A3.13 Density and temperature measurements of the EPG snow pit profile.

Depth (cm)	Density (kg m ⁻³)	Water equivalent depth (cm)	Snow temperature (°C)
0	0.27	0.0	-7.9
5	0.37	1.9	-7.9
10	0.45	2.2	-8.1
15	0.37	1.9	-8.9
20	0.37	1.9	-9.9
25	0.41	2.1	-10.5
30	0.43	2.2	-11.5
35	0.49	2.5	-11.3
40	0.51	2.6	-12.5
45	0.45	2.3	-12.7
50	0.45	2.3	-13.6
55	0.37	1.9	-13.6
60	0.33	1.7	-15.0
65	0.31	1.6	-14.7
70	0.41	2.1	-15.4
75	0.41	2.1	-14.5
80	0.57	2.9	-15.5
85	0.37	1.9	-16.1
90	0.31	1.6	-16.9
95	0.33	1.7	-16.3
100	0.35	1.8	-18.0
105	0.35	1.8	-17.4
110	0.31	1.6	-18.7
115	0.43	2.2	-17.9
120	0.41	2.1	-18.8
125	0.41	2.1	-18.6
130	0.35	1.8	-19.5
135	0.41	2.1	-19.5
140	0.44	2.2	-19.4
145	0.39	2.0	-18.4
150	0.37	1.9	-18.6
155	0.45	2.3	-19.5
160	0.49	2.5	-20.9
165	0.43	2.2	-20.9
170	0.45	2.3	-21.1
175	0.49	2.5	-22.7
180	0.39	2.0	-22.0
185	0.37	1.9	-22.5
190	0.43	2.2	-23.0
195	0.49	2.5	-21.8
200	0.47	2.4	-23.0
205	0.41	2.1	-22.7
210	0.32	1.6	-24.1
215	0.40	2.0	-22.3
220	0.43	2.2	-22.5
225	0.41	2.1	-21.3
230	0.46	2.3	-23.2
235	0.48	2.4	-21.6
240	0.49	2.5	-22.7
245	0.41	2.1	-21.8
250	0.47	2.4	-24.1
255	0.38	1.9	-23.9
260	0.46	2.3	-25.3
265	0.45	2.3	-24.6
270	0.51	2.6	-25.8
275	0.53	2.7	-24.8
280	0.50	2.5	-26.5
285	0.37	1.9	-26
290	0.51	2.6	-26.9
295	0.53	2.6	-25.5
300	0.41	2.1	-27.4

Table A3.13 continued.

Depth (cm)	Density (kg m ⁻³)	Water equivalent depth (cm)	Snow temperature (°C)
305	0.43	2.2	-25.8
310	0.53	2.7	-27.6
315	0.53	2.7	-26.7
320	0.51	2.5	-27.4
325	0.49	2.5	-26.7
330	0.49	2.5	-29.9
335	0.51	2.5	-26.7
340	0.51	2.6	-28.1
345	0.55	2.8	-26.9
350	0.50	2.5	-28.1
355	0.49	2.5	-27.2
360	0.55	2.8	-28.3
365	0.54	2.7	-27.6
370	0.39	2.0	-28.6
375	0.41	2.1	-28.6

**Appendix Four: Stable isotope, major and trace element chemistry
(ICP-OES and IC analysis), and density measurements of WHG
snow profiles**

Table A4.1 Oxygen ($\delta^{18}\text{O}$) and hydrogen (δD) isotopic ratios of WHG_1 snow samples. The second order parameter deuterium excess (d) is calculated as $d = \delta\text{D} - 8 \cdot \delta^{18}\text{O}$. Analytical precision is typically $< 0.1 \text{ ‰}$ for $\delta^{18}\text{O}$, $< 1.0 \text{ ‰}$ δD , and $< 1.0 \text{ ‰}$ d excess. Dating is based on comparison of $\delta^{18}\text{O}$ with Cape Hallett temperature changes. δD values in light grey are not considered reliable. Fresh surface samples of snow (WHG_FS) have also been measured.

Sample	Depth (cm)	Date (yr)	$\delta^{18}\text{O}$ (‰)	δD (‰)	2σ (‰)	d excess (‰)
WHG 2006/07 (FS) 001			-22.9	-176	0.6	7
WHG 2006/07 (FS) 002			-21.4	-171	0.5	0
WHG 2006/07 (FS) 003			-22.1	-174	0.4	3
WHG 2006/07 (1) 214	9	2006.69	-35.0	-275	0.2	5
WHG 2006/07 (1) 213	10	2006.68	-35.8	-280	0.2	7
WHG 2006/07 (1) 212	11	2006.68	-35.9	-282	0.1	5
WHG 2006/07 (1) 211	12	2006.67	-35.9	-281	0.1	6
WHG 2006/07 (1) 210	13	2006.67	-35.3	-274	0.0	9
WHG 2006/07 (1) 209	14	2006.66	-33.9	-262	0.1	9
WHG 2006/07 (1) 208	15	2006.66	-31.6	-243	0.1	9
WHG 2006/07 (1) 207	16	2006.65	-30.4	-233	0.1	10
WHG 2006/07 (1) 206	17	2006.65	-29.7	-228	0.0	10
WHG 2006/07 (1) 205	18	2006.64	-29.0	-221	0.0	11
WHG 2006/07 (1) 204	19	2006.64	-28.8	-220	0.0	10
WHG 2006/07 (1) 203	20	2006.63	-28.6	-218	0.1	10
WHG 2006/07 (1) 202	21	2006.63	-28.5	-218	0.1	10
WHG 2006/07 (1) 201	22	2006.62	-28.5	-218	0.4	10
WHG 2006/07 (1) 200	23	2006.61	-28.5	-218	0.2	10
WHG 2006/07 (1) 199	24	2006.61	-28.5	-218	0.1	10
WHG 2006/07 (1) 198	25	2006.60	-28.4	-218	0.0	9
WHG 2006/07 (1) 197	26	2006.60	-28.4	-217	0.0	10
WHG 2006/07 (1) 196	27	2006.59	-28.3	-217	0.0	10
WHG 2006/07 (1) 195	28	2006.58	-28.3	-216	0.1	10
WHG 2006/07 (1) 194	29	2006.58	-28.2	-215	0.1	11
WHG 2006/07 (1) 193	30	2006.58	-28.3	-215	0.2	11
WHG 2006/07 (1) 192	31	2006.58	-28.9	-220	0.1	12
WHG 2006/07 (1) 191	32	2006.58	-29.2	-222	0.4	12
WHG 2006/07 (1) 190	33	2006.58	-32.4	-249	0.0	10
WHG 2006/07 (1) 189	34	2006.58	-35.3	-272	0.1	10
WHG 2006/07 (1) 188	35	2006.57	-38.4	-302	0.1	5
WHG 2006/07 (1) 187	36	2006.57	-41.0	-323	0.1	5
WHG 2006/07 (1) 186	37	2006.57	-41.7	-329	0.1	5
WHG 2006/07 (1) 185	38	2006.56	-42.1	-331	0.1	6
WHG 2006/07 (1) 184	39	2006.56	-42.2	-331	0.1	6
WHG 2006/07 (1) 183	40	2006.55	-42.2	-332	0.0	6
WHG 2006/07 (1) 182	41	2006.55	-42.2	-332	0.0	6
WHG 2006/07 (1) 181	42	2006.54	-42.1	-330	0.1	7
WHG 2006/07 (1) 180	43	2006.54	-42.2	-331	0.1	7
WHG 2006/07 (1) 179	44	2006.53	-42.3	-336	0.1	2
WHG 2006/07 (1) 178	45	2006.53	-41.9	-329	0.2	6
WHG 2006/07 (1) 177	46	2006.52	-39.1	-307	0.0	6
WHG 2006/07 (1) 176	47	2006.52	-36.5	-287	0.2	5
WHG 2006/07 (1) 175	48	2006.52	-35.0	-274	0.2	6
WHG 2006/07 (1) 174	49	2006.47	-34.1	-266	0.3	7
WHG 2006/07 (1) 173	50	2006.46	-34.0	-266	0.2	6
WHG 2006/07 (1) 172	51	2006.46	-34.0	-267	0.3	5
WHG 2006/07 (1) 171	52	2006.46	-34.0	-268	0.0	4
WHG 2006/07 (1) 170	53	2006.46	-34.0	-269	0.0	4
WHG 2006/07 (1) 169	54	2006.46	-33.9	-264	0.2	7
WHG 2006/07 (1) 168	55	2006.46	-33.4	-260	0.1	7
WHG 2006/07 (1) 167	56	2006.46	-32.5	-249	0.1	11
WHG 2006/07 (1) 166	57	2006.46	-32.0	-244	0.1	12
WHG 2006/07 (1) 165	58	2006.46	-31.7	-244	0.5	10
WHG 2006/07 (1) 164	59	2006.46	-31.6	-242	0.0	11
WHG 2006/07 (1) 163	60	2006.45	-31.5	-243	0.3	9
WHG 2006/07 (1) 162	61	2006.45	-31.4	-243	0.2	9
WHG 2006/07 (1) 161	62	2006.45	-31.5	-240	0.0	12
WHG 2006/07 (1) 160	63	2006.44	-31.5	-243	0.0	9

Table A4.1 continued.

Sample	Depth (cm)	Date (yr)	$\delta^{18}\text{O}$ (‰)	δD (‰)	2σ (‰)	d excess (‰)
WHG 2006/07 (1) 159	64	2006.44	-31.5	-243	0.0	10
WHG 2006/07 (1) 158	65	2006.44	-31.6	-242	0.4	11
WHG 2006/07 (1) 157	66	2006.44	-31.6	-241	0.4	12
WHG 2006/07 (1) 156	67	2006.43	-31.6	-240	0.4	12
WHG 2006/07 (1) 155	68	2006.43	-31.7	-243	0.1	10
WHG 2006/07 (1) 154	69	2006.43	-31.7	-241	0.2	13
WHG 2006/07 (1) 153	70	2006.42	-31.8	-243	0.5	11
WHG 2006/07 (1) 152	71	2006.42	-31.7	-244	0.3	10
WHG 2006/07 (1) 151	72	2006.42	-31.9	-245	0.0	10
WHG 2006/07 (1) 150	73	2006.41	-32.2	-247	0.2	11
WHG 2006/07 (1) 149	74	2006.41	-32.5	-249	0.1	11
WHG 2006/07 (1) 148	75	2006.41	-32.8	-253	0.1	9
WHG 2006/07 (1) 147	76	2006.41	-33.6	-260	0.7	9
WHG 2006/07 (1) 146	77	2006.35	-34.1	-265	0.6	8
WHG 2006/07 (1) 145	78	2006.34	-34.2	-266	0.2	8
WHG 2006/07 (1) 144	79	2006.33	-33.3	-258	0.4	9
WHG 2006/07 (1) 143	80	2006.31	-32.9	-253	0.2	9
WHG 2006/07 (1) 142	81	2006.30	-32.5	-251	0.2	9
WHG 2006/07 (1) 141	82	2006.29	-32.3	-248	0.8	11
WHG 2006/07 (1) 140	83	2006.28	-31.6	-247	0.1	6
WHG 2006/07 (1) 139	84	2006.26	-31.1	-243	0.3	5
WHG 2006/07 (1) 138	85	2006.25	-30.1	-236	0.2	5
WHG 2006/07 (1) 137	86	2006.23	-29.1	-228	0.2	5
WHG 2006/07 (1) 136	87	2006.21	-27.5	-213	0.2	7
WHG 2006/07 (1) 135	88	2006.18	-26.1	-200	0.2	9
WHG 2006/07 (1) 134	89	2006.14	-23.5	-177	0.0	11
WHG 2006/07 (1) 133	90	2006.11	-21.8	-163	0.0	11
WHG 2006/07 (1) 132	91	2006.07	-20.7	-155	0.3	11
WHG 2006/07 (1) 131	92	2006.03	-20.2	-151	0.1	11
WHG 2006/07 (1) 130	93	2006.02	-20.0	-148	0.1	12
WHG 2006/07 (1) 129	94	2006.02	-18.9	-135	0.3	16
WHG 2006/07 (1) 128	95	2006.01	-18.2	-129	0.6	17
WHG 2006/07 (1) 127	96	2006.01	-17.8	-123	0.3	20
WHG 2006/07 (1) 126	97	2006.00	-17.7	-123	0.7	19
WHG 2006/07 (1) 125	98	2005.99	-17.8	-123	0.7	19
WHG 2006/07 (1) 124	99	2005.98	-18.0	-126	0.1	18
WHG 2006/07 (1) 123	100	2005.96	-18.4	-130	0.2	17
WHG 2006/07 (1) 122	101	2005.96	-19.1	-139	1.2	14
WHG 2006/07 (1) 121	102	2005.96	-19.5	-143	0.2	13
WHG 2006/07 (1) 120	103	2005.96	-19.8	-147	0.3	12
WHG 2006/07 (1) 119	104	2005.96	-20.1	-150	0.6	10
WHG 2006/07 (1) 118	105	2005.95	-20.0	-150	0.7	10
WHG 2006/07 (1) 117	106	2005.95	-20.1	-152	0.9	9
WHG 2006/07 (1) 116	107	2005.95	-20.0	-150	0.1	10
WHG 2006/07 (1) 115	108	2005.95	-19.9	-149	0.3	10
WHG 2006/07 (1) 114	109	2005.94	-19.8	-148	0.5	11
WHG 2006/07 (1) 113	110	2005.94	-19.8	-147	1.0	11
WHG 2006/07 (1) 112	111	2005.94	-19.8	-149	0.0	10
WHG 2006/07 (1) 111	112	2005.94	-19.9	-149	0.2	10
WHG 2006/07 (1) 110	113	2005.93	-20.1	-150	0.6	11
WHG 2006/07 (1) 109	114	2005.92	-20.1	-151	0.2	10
WHG 2006/07 (1) 108	115	2005.91	-20.5	-157	0.0	7
WHG 2006/07 (1) 107	116	2005.90	-21.1	-162	0.2	7
WHG 2006/07 (1) 106	117	2005.89	-21.7	-167	0.2	6
WHG 2006/07 (1) 105	118	2005.88	-22.1	-170	0.1	7
WHG 2006/07 (1) 104	119	2005.88	-22.4	-172	0.1	7
WHG 2006/07 (1) 103	120	2005.88	-22.5	-173	0.4	7
WHG 2006/07 (1) 102	121	2005.87	-22.6	-173	0.1	8
WHG 2006/07 (1) 101	122	2005.87	-22.7	-174	0.2	8
WHG 2006/07 (1) 100	123	2005.86	-22.8	-178	0.9	4
WHG 2006/07 (1) 099	124	2005.86	-22.9	-177	0.6	6
WHG 2006/07 (1) 098	125	2005.85	-22.9	-178	1.4	6

Table A4.1 continued.

Sample	Depth (cm)	Date (yr)	$\delta^{18}\text{O}$ (‰)	δD (‰)	2σ (‰)	d excess (‰)
WHG 2006/07 (1) 097	126	2005.85	-23.1	-177	0.4	7
WHG 2006/07 (1) 096	127	2005.85	-23.0	-177	0.5	6
WHG 2006/07 (1) 095	128	2005.85	-22.9	-177	1.1	6
WHG 2006/07 (1) 094	129	2005.85	-22.6	-176	0.4	5
WHG 2006/07 (1) 093	130	2005.85	-22.3	-173	0.3	5
WHG 2006/07 (1) 092	131	2005.84	-22.2	-174	0.9	4
WHG 2006/07 (1) 091	132	2005.84	-22.0	-173	0.4	3
WHG 2006/07 (1) 090	133	2005.84	-21.7	-172	0.9	2
WHG 2006/07 (1) 089	134	2005.84	-21.5	-167	0.7	5
WHG 2006/07 (1) 088	135	2005.83	-21.2	-166	1.0	4
WHG 2006/07 (1) 087	136	2005.83	-21.1	-164	0.8	5
WHG 2006/07 (1) 086	137	2005.83	-21.7	-163	0.4	11
WHG 2006/07 (1) 085	138	2005.82	-21.2	-163	1.1	6
WHG 2006/07 (1) 084	139	2005.82	-21.5	-167	0.4	5
WHG 2006/07 (1) 083	140	2005.82	-22.1	-173	0.8	3
WHG 2006/07 (1) 082	141	2005.82	-22.6	-177	0.7	4
WHG 2006/07 (1) 081	142	2005.81	-23.5	-184	0.9	3
WHG 2006/07 (1) 080	143	2005.81	-23.8	-188	0.2	3
WHG 2006/07 (1) 079	144	2005.81	-24.1	-189	0.3	4
WHG 2006/07 (1) 078	145	2005.81	-24.4	-190	1.1	6
WHG 2006/07 (1) 077	146	2005.80	-24.4	-190	0.1	6
WHG 2006/07 (1) 076	147	2005.80	-24.6	-191	0.6	5
WHG 2006/07 (1) 075	148	2005.79	-24.7	-193	0.7	4
WHG 2006/07 (1) 074	149	2005.78	-24.6	-191	0.2	6
WHG 2006/07 (1) 073	150	2005.77	-24.6	-191	0.7	6
WHG 2006/07 (1) 072	151	2005.77	-24.7	-193	0.9	5
WHG 2006/07 (1) 071	152	2005.77	-24.8	-193	0.5	5
WHG 2006/07 (1) 070	153	2005.76	-24.9	-196	0.4	3
WHG 2006/07 (1) 069	154	2005.76	-25.3	-199	0.9	4
WHG 2006/07 (1) 068	155	2005.76	-25.6	-202	0.7	3
WHG 2006/07 (1) 067	156	2005.76	-25.9	-206	1.2	2
WHG 2006/07 (1) 066	157	2005.76	-26.7	-214	0.1	0
WHG 2006/07 (1) 065	158	2005.76	-27.0	-216	0.1	-1
WHG 2006/07 (1) 064	159	2005.76	-27.5	-222	1.0	-2
WHG 2006/07 (1) 063	160	2005.76	-28.4	-229	0.3	-2
WHG 2006/07 (1) 062	161	2005.76	-28.9	-233	1.2	-2
WHG 2006/07 (1) 061	162	2005.76	-29.3	-233	0.5	2
WHG 2006/07 (1) 060	163	2005.75	-29.8	-239	0.2	-1
WHG 2006/07 (1) 059	164	2005.75	-30.3	-244	0.3	-2
WHG 2006/07 (1) 058	165	2005.75	-30.7	-245	0.7	0
WHG 2006/07 (1) 057	166	2005.75	-31.5	-252	0.4	0
WHG 2006/07 (1) 056	167	2005.75	-32.4	-258	0.5	1
WHG 2006/07 (1) 055	168	2005.75	-33.2	-263	1.7	2
WHG 2006/07 (1) 054	169	2005.75	-34.6	-278	0.4	-2
WHG 2006/07 (1) 053	170	2005.75	-36.0	-291	0.4	-2
WHG 2006/07 (1) 052	171	2005.75	-37.6	-303	2.1	-2
WHG 2006/07 (1) 051	172	2005.75	-38.4	-309	0.2	-2
WHG 2006/07 (1) 050	173	2005.75	-39.1	-315	1.9	-3
WHG 2006/07 (1) 049	174	2005.74	-39.4	-317	0.5	-2
WHG 2006/07 (1) 048	175	2005.74	-39.5	-317	1.0	-1
WHG 2006/07 (1) 047	176	2005.73	-39.7	-316	0.7	1
WHG 2006/07 (1) 046	177	2005.72	-39.7	-319	1.0	-2
WHG 2006/07 (1) 045	178	2005.71	-39.7	-319	0.6	-1
WHG 2006/07 (1) 044	179	2005.70	-39.6	-316	1.1	1
WHG 2006/07 (1) 043	180	2005.70	-39.8	-318	0.2	1
WHG 2006/07 (1) 042	181	2005.69	-39.5	-316	0.2	0
WHG 2006/07 (1) 041	182	2005.68	-39.3	-316	0.2	-1
EPG-2006/07_039	183	2005.67	-28.5	-11	0.7	217
EPG-2006/07_038	184	2005.66	-28.0	-21	0.3	203
EPG-2006/07_037	185	2005.65	-27.5	-14	0.9	206
EPG-2006/07_036	186	2005.65	-26.9	-21	0.8	194
EPG-2006/07_035	187	2005.64	-26.2	-21	1.6	189

Table A4.1 continued.

Sample	Depth (cm)	Date (yr)	$\delta^{18}\text{O}$ (‰)	δD (‰)	2σ (‰)	d excess (‰)
EPG-2006/07_034	188	2005.63	-25.4	-6	0.1	197
EPG-2006/07_033	189	2005.62	-25.1	-20	0.4	181
EPG-2006/07_032	190	2005.61	-24.3	-32	1.1	163
EPG-2006/07_031	191	2005.60	-23.7	-32	0.8	158
EPG-2006/07_030	192	2005.60	-22.9	-31	0.8	152
EPG-2006/07_029	193	2005.59	-22.2	-32	1.2	146
EPG-2006/07_028	194	2005.58	-21.7	-33	0.3	140
EPG-2006/07_027	195	2005.57	-21.1	-33	0.5	136
EPG-2006/07_026	196	2005.56	-20.8	-33	0.8	133
EPG-2006/07_025	197	2005.56	-20.3	-32	0.0	131
EPG-2006/07_024	198	2005.55	-20.3	-33	0.2	130
EPG-2006/07_023	199	2005.54	-20.4	-33	0.8	131
EPG-2006/07_022	200	2005.53	-20.6	-38	0.9	127
EPG-2006/07_021	201	2005.52	-20.8	-39	1.2	128
EPG-2006/07_020	202	2005.51	-21.2	-2	0.5	168
EPG-2006/07_019	203	2005.51	-21.3	4	0.3	175
EPG-2006/07_018	204	2005.50	-21.8	-5	0.0	170
EPG-2006/07_017	205	2005.49	-22.4	0	0.3	179
EPG-2006/07_016	206	2005.48	-23.0	-11	0.5	173
EPG-2006/07_015	207	2005.47	-23.6	-11	0.1	178
EPG-2006/07_014	208	2005.46	-24.1	-12	0.6	181
EPG-2006/07_013	209	2005.46	-24.6	-12	0.1	185
EPG-2006/07_012	210	2005.45	-25.4	-12	0.4	191
EPG-2006/07_011	211	2005.44	-25.9	-12	0.1	196
EPG-2006/07_010	212	2005.43	-26.4	-1	1.2	210
EPG-2006/07_009	213	2005.42	-26.7	9	0.3	223
EPG-2006/07_008	214	2005.41	-26.9	-47	0.2	168
EPG-2006/07_007	215	2005.41	-27.0	-48	0.4	168
EPG-2006/07_006	216	2005.40	-26.9	-37	0.3	178
EPG-2006/07_005	217	2005.39	-26.6	-26	0.8	187
EPG-2006/07_004	218	2005.38	-26.6	-62	0.4	151
EPG-2006/07_003	219	2005.37	-26.2	-60	0.4	150
EPG-2006/07_002	220	2005.36	-26.0	-59	0.9	149
EPG-2006/07_001	221	2005.36	-26.0	-63	1.3	146

Table A4.2 Oxygen ($\delta^{18}\text{O}$) and hydrogen (δD) isotopic ratios of WHG_1b snow samples. The second order parameter deuterium excess (d) is calculated as $d = \delta\text{D} - 8 \cdot \delta^{18}\text{O}$. Analytical precision is typically < 0.1 ‰ for $\delta^{18}\text{O}$, < 1.0 ‰ δD , and < 1.0 ‰ d excess. Dating is based on comparison of $\delta^{18}\text{O}$ with Cape Hallett temperature changes.

Sample	Depth (cm)	WHG_1 equiv. depth (cm)	Date (yr)	$\delta^{18}\text{O}$ (‰)	δD (‰)	2σ (‰)	d excess (‰)
WHG 2006/07 (1b) 090	190	199	2005.71	-34.5	-270	0.7	6
WHG 2006/07 (1b) 089	191	200	2005.69	-34.8	-272	0.4	6
WHG 2006/07 (1b) 088	192	201	2005.67	-34.9	-274	0.5	5
WHG 2006/07 (1b) 087	193	202	2005.65	-34.9	-274	0.2	5
WHG 2006/07 (1b) 086	194	203	2005.63	-35.1	-277	0.5	3
WHG 2006/07 (1b) 085	195	204	2005.60	-35.0	-277	0.7	3
WHG 2006/07 (1b) 084	196	205	2005.58	-34.9	-276	0.1	3
WHG 2006/07 (1b) 083	197	206	2005.56	-34.0	-269	0.3	4
WHG 2006/07 (1b) 082	198	207	2005.54	-33.8	-265	0.7	6
WHG 2006/07 (1b) 081	199	208	2005.52	-33.4	-260	0.2	7
WHG 2006/07 (1b) 080	200	209	2005.50	-33.1	-257	0.0	8
WHG 2006/07 (1b) 079	201	210	2005.48	-32.8	-252	0.1	10
WHG 2006/07 (1b) 078	202	211	2005.46	-32.8	-253	0.0	9
WHG 2006/07 (1b) 077	203	212	2005.44	-32.9	-255	0.4	9
WHG 2006/07 (1b) 076	204	213	2005.42	-33.5	-259	0.7	9
WHG 2006/07 (1b) 075	205	214	2005.39	-34.3	-264	0.6	10
WHG 2006/07 (1b) 074	206	215	2005.39	-34.4	-265	0.1	10
WHG 2006/07 (1b) 073	207	216	2005.38	-34.6	-266	0.3	11
WHG 2006/07 (1b) 072	208	217	2005.38	-34.9	-268	0.8	11
WHG 2006/07 (1b) 071	209	218	2005.37	-35.1	-269	0.1	12
WHG 2006/07 (1b) 070	210	219	2005.37	-35.3	-271	0.1	11
WHG 2006/07 (1b) 069	211	220	2005.36	-35.4	-272	0.4	12
WHG 2006/07 (1b) 068	212	221	2005.36	-35.4	-273	0.6	11
WHG 2006/07 (1b) 067	213	222	2005.35	-35.2	-272	0.5	10
WHG 2006/07 (1b) 066	214	223	2005.35	-35.2	-273	0.4	8
WHG 2006/07 (1b) 065	215	224	2005.34	-34.8	-269	0.3	9
WHG 2006/07 (1b) 064	216	225	2005.33	-34.6	-269	0.4	8
WHG 2006/07 (1b) 063	217	226	2005.32	-34.1	-263	0.9	9
WHG 2006/07 (1b) 062	218	227	2005.31	-33.5	-259	0.8	9
WHG 2006/07 (1b) 061	219	228	2005.30	-32.5	-250	0.7	10
WHG 2006/07 (1b) 060	220	229	2005.29	-31.8	-244	0.3	11
WHG 2006/07 (1b) 059	221	230	2005.28	-31.1	-238	0.3	11
WHG 2006/07 (1b) 058	222	231	2005.27	-30.1	-230	0.7	11
WHG 2006/07 (1b) 057	223	232	2005.26	-29.3	-223	0.3	11
WHG 2006/07 (1b) 056	224	233	2005.25	-27.9	-212	0.8	11
WHG 2006/07 (1b) 055	225	234	2005.24	-26.1	-195	0.6	14
WHG 2006/07 (1b) 054	226	235	2005.23	-24.3	-180	0.3	15
WHG 2006/07 (1b) 053	227	236	2005.22	-22.5	-163	0.4	17
WHG 2006/07 (1b) 052	228	237	2005.21	-21.0	-151	0.2	18
WHG 2006/07 (1b) 051	229	238	2005.19	-19.4	-138	0.2	17
WHG 2006/07 (1b) 050	230	239	2005.17	-18.5	-133	0.0	16
WHG 2006/07 (1b) 049	231	240	2005.15	-18.1	-133	0.7	13
WHG 2006/07 (1b) 048	232	241	2005.13	-18.0	-129	0.4	15
WHG 2006/07 (1b) 047	233	242	2005.13	-18.2	-132	0.3	14
WHG 2006/07 (1b) 046	234	243	2005.13	-18.5	-135	0.3	12
WHG 2006/07 (1b) 045	235	244	2005.12	-18.7	-138	0.1	12
WHG 2006/07 (1b) 044	236	245	2005.12	-19.2	-143	0.2	11
WHG 2006/07 (1b) 043	237	246	2005.12	-19.7	-147	0.2	11
WHG 2006/07 (1b) 042	238	247	2005.12	-19.9	-149	0.7	10
WHG 2006/07 (1b) 041	239	248	2005.12	-20.1	-150	0.2	11
WHG 2006/07 (1b) 040	240	249	2005.12	-20.3	-153	0.2	10
WHG 2006/07 (1b) 039	241	250	2005.12	-20.2	-152	0.1	10
WHG 2006/07 (1b) 038	242	251	2005.11	-20.0	-150	0.3	10
WHG 2006/07 (1b) 037	243	252	2005.11	-19.7	-147	0.5	11
WHG 2006/07 (1b) 036	244	253	2005.11	-19.5	-144	0.1	12

Table A4.2 continued.

Sample	Depth (cm)	WHG_1 equiv. depth (cm)	Date (yr)	$\delta^{18}\text{O}$ (‰)	δD (‰)	2σ (‰)	d excess (‰)
WHG 2006/07 (1b) 035	245	254	2005.11	-19.3	-144	0.5	10
WHG 2006/07 (1b) 034	246	255	2005.10	-19.1	-142	0.1	11
WHG 2006/07 (1b) 033	247	256	2005.10	-19.1	-144	0.1	9
WHG 2006/07 (1b) 032	248	257	2005.09	-19.0	-144	0.3	8
WHG 2006/07 (1b) 031	249	258	2005.09	-18.8	-144	0.0	7
WHG 2006/07 (1b) 030	250	259	2005.08	-18.7	-144	0.1	6
WHG 2006/07 (1b) 029	251	260	2005.08	-18.6	-143	0.1	5
WHG 2006/07 (1b) 028	252	261	2005.07	-18.2	-142	0.1	4
WHG 2006/07 (1b) 027	253	262	2005.07	-17.9	-138	0.9	5
WHG 2006/07 (1b) 026	254	263	2005.06	-17.6	-137	0.2	4
WHG 2006/07 (1b) 025	255	264	2005.06	-17.2	-133	0.1	5
WHG 2006/07 (1b) 024	256	265	2005.05	-16.7	-129	0.2	4
WHG 2006/07 (1b) 023	257	266	2005.05	-16.3	-126	0.1	4
WHG 2006/07 (1b) 022	258	267	2005.04	-15.9	-122	0.5	5
WHG 2006/07 (1b) 021	259	268	2005.04	-15.4	-119	0.1	5
WHG 2006/07 (1b) 020	260	269	2005.03	-14.9	-115	0.2	5
WHG 2006/07 (1b) 019	261	270	2005.03	-14.7	-113	0.6	5
WHG 2006/07 (1b) 018	262	271	2005.02	-14.7	-112	0.2	5
WHG 2006/07 (1b) 017	263	272	2005.02	-14.5	-111	0.0	5
WHG 2006/07 (1b) 016	264	273	2005.01	-14.4	-111	0.1	4
WHG 2006/07 (1b) 015	265	274	2005.01	-14.4	-112	0.3	4
WHG 2006/07 (1b) 014	266	275	2005.01	-14.7	-114	0.4	4
WHG 2006/07 (1b) 013	267	276	2005.01	-14.8	-114	0.5	4
WHG 2006/07 (1b) 012	268	277	2005.01	-15.7	-122	0.3	3
WHG 2006/07 (1b) 011	269	278	2005.01	-15.6	-121	0.2	3
WHG 2006/07 (1b) 010	270	279	2004.93	-16.5	-128	0.4	3
WHG 2006/07 (1b) 009	271	280	2004.92	-17.5	-137	0.1	3
WHG 2006/07 (1b) 008	272	281	2004.90	-17.5	-138	0.3	2
WHG 2006/07 (1b) 007	273	282	2004.89	-19.0	-150	0.6	2
WHG 2006/07 (1b) 006	274	283	2004.87	-20.9	-166	0.3	1
WHG 2006/07 (1b) 005	275	284	2004.87	-21.6	-171	0.3	2
WHG 2006/07 (1b) 004	276	285	2004.86	-22.3	-178	0.3	1
WHG 2006/07 (1b) 003	277	286	2004.86	-23.2	-184	0.7	2
WHG 2006/07 (1b) 002	278	287	2004.86	-23.8	-189	0.1	2
WHG 2006/07 (1b) 001	279	288	2004.85	-24.0	-190	0.6	3

Table A4.3 Oxygen ($\delta^{18}\text{O}$) and hydrogen (δD) isotopic ratios of WHG_2 snow samples. The second order parameter deuterium excess (d) is calculated as $d = \delta\text{D} - 8 \cdot \delta^{18}\text{O}$. Analytical precision is typically $< 0.1 \text{ ‰}$ for $\delta^{18}\text{O}$, $< 1.0 \text{ ‰}$ δD , and $< 1.0 \text{ ‰}$ d excess. Dating is based on comparison of $\delta^{18}\text{O}$ with Cape Hallett temperature changes.

Sample	Depth (cm)	Date (yr)	$\delta^{18}\text{O}$ (‰)	δD (‰)	2σ (‰)	d excess (‰)
WHG 2006/07 (2) 170	1	2006.84	-25.3	-199.1	0.0	3.2
WHG 2006/07 (2) 168	2	2006.84	-26.2	-206.2	0.3	3.3
WHG 2006/07 (2) 169	3	2006.84	-25.3	-198.0	0.3	4.6
WHG 2006/07 (2) 165	4	2006.81	-26.6	-208.1	0.3	5.0
WHG 2006/07 (2) 167	5	2006.82	-26.2	-206.1	0.6	3.3
WHG 2006/07 (2) 166	6	2006.81	-26.3	-206.9	0.6	3.7
WHG 2006/07 (2) 164	7	2006.81	-27.3	-214.6	0.1	3.9
WHG 2006/07 (2) 163	8	2006.80	-28.3	-221.6	0.3	4.7
WHG 2006/07 (2) 158	9	2006.78	-29.2	-227.6	0.2	5.8
WHG 2006/07 (2) 162	10	2006.80	-28.9	-225.8	0.5	5.6
WHG 2006/07 (2) 161	11	2006.79	-29.1	-227.2	0.5	5.5
WHG 2006/07 (2) 160	12	2006.79	-29.2	-226.8	0.1	6.7
WHG 2006/07 (2) 159	13	2006.79	-29.2	-227.5	0.0	6.2
WHG 2006/07 (2) 157	14	2006.78	-29.2	-225.9	1.1	7.5
WHG 2006/07 (2) 156	15	2006.78	-29.2	-226.2	0.2	7.2
WHG 2006/07 (2) 155	16	2006.78	-29.2	-227.9	0.0	5.5
WHG 2006/07 (2) 154	17	2006.77	-29.2	-227.6	0.3	5.9
WHG 2006/07 (2) 153	18	2006.77	-29.2	-227.4	0.6	6.2
WHG 2006/07 (2) 152	19	2006.76	-29.2	-228.6	0.1	5.1
WHG 2006/07 (2) 151	20	2006.76	-29.1	-227.8	0.1	5.3
WHG 2006/07 (2) 150	21	2006.76	-29.2	-227.8	0.5	5.5
WHG 2006/07 (2) 149	22	2006.75	-29.4	-228.0	0.2	7.3
WHG 2006/07 (2) 148	23	2006.75	-28.8	-224.9	0.5	5.7
WHG 2006/07 (2) 147	24	2006.74	-27.8	-214.8	0.7	7.6
WHG 2006/07 (2) 146	25	2006.73	-27.6	-211.5	0.0	9.2
WHG 2006/07 (2) 145	26	2006.72	-27.5	-211.4	0.1	8.5
WHG 2006/07 (2) 144	27	2006.72	-27.5	-210.7	0.6	8.9
WHG 2006/07 (2) 142	28	2006.71	-27.9	-214.7	0.4	8.3
WHG 2006/07 (2) 143	29	2006.72	-27.5	-211.2	0.3	8.8
WHG 2006/07 (2) 141	30	2006.71	-29.1	-227.0	0.1	5.5
WHG 2006/07 (2) 140	31	2006.69	-30.5	-238.8	0.2	4.9
WHG 2006/07 (2) 139	32	2006.68	-30.9	-241.6	0.2	5.7
WHG 2006/07 (2) 138	33	2006.68	-31.2	-241.4	0.4	7.8
WHG 2006/07 (2) 137	34	2006.67	-31.1	-239.1	0.5	9.5
WHG 2006/07 (2) 136	35	2006.67	-30.5	-234.4	0.1	9.4
WHG 2006/07 (2) 135	36	2006.66	-29.8	-227.3	0.1	10.8
WHG 2006/07 (2) 134	37	2006.66	-29.4	-224.6	0.1	10.2
WHG 2006/07 (2) 133	38	2006.65	-29.2	-224.4	0.0	9.1
WHG 2006/07 (2) 132	39	2006.65	-29.1	-224.9	0.3	8.1
WHG 2006/07 (2) 131	40	2006.64	-29.2	-225.9	0.0	7.5
WHG 2006/07 (2) 130	41	2006.64	-29.3	-226.7	0.0	7.3
WHG 2006/07 (2) 129	42	2006.64	-29.4	-228.3	0.2	6.7
WHG 2006/07 (2) 128	43	2006.63	-29.5	-229.5	0.3	6.2
WHG 2006/07 (2) 127	44	2006.63	-29.6	-231.6	0.3	5.2
WHG 2006/07 (2) 126	45	2006.62	-29.7	-232.0	0.5	5.3
WHG 2006/07 (2) 125	46	2006.62	-29.7	-233.0	0.5	4.4
WHG 2006/07 (2) 124	47	2006.61	-29.6	-231.6	0.6	5.1
WHG 2006/07 (2) 123	48	2006.61	-29.7	-232.4	0.4	5.4
WHG 2006/07 (2) 122	49	2006.60	-29.8	-229.7	0.0	8.3
WHG 2006/07 (2) 121	50	2006.60	-29.7	-231.1	0.1	6.8
WHG 2006/07 (2) 120	51	2006.59	-29.6	-228.2	0.2	8.8
WHG 2006/07 (2) 119	52	2006.58	-29.4	-225.3	0.2	10.2
WHG 2006/07 (2) 118	53	2006.58	-29.6	-225.7	0.3	11.3
WHG 2006/07 (2) 117	54	2006.58	-29.7	-227.8	0.3	10.1
WHG 2006/07 (2) 116	55	2006.58	-30.1	-231.0	0.1	9.4
WHG 2006/07 (2) 115	56	2006.58	-30.5	-235.8	0.0	8.5
WHG 2006/07 (2) 114	57	2006.58	-31.2	-241.0	0.2	8.2
WHG 2006/07 (2) 113	58	2006.58	-31.4	-243.4	0.1	8.1
WHG 2006/07 (2) 112	59	2006.58	-31.7	-244.7	0.1	8.7
WHG 2006/07 (2) 111	60	2006.57	-32.2	-248.2	0.0	9.6
WHG 2006/07 (2) 110	61	2006.57	-33.0	-254.1	0.2	9.7
WHG 2006/07 (2) 109	62	2006.57	-34.2	-265.5	0.2	8.2

Table A4.3 continued.

Sample	Depth (cm)	Date (yr)	$\delta^{18}\text{O}$ (‰)	δD (‰)	2σ (‰)	d excess (‰)
WHG 2006/07 (2) 108	63	2006.57	-37.1	-289.6	0.3	7.1
WHG 2006/07 (2) 107	64	2006.57	-40.6	-319.1	0.1	5.8
WHG 2006/07 (2) 106	65	2006.57	-41.2	-324.0	0.5	5.7
WHG 2006/07 (2) 105	66	2006.57	-41.8	-327.9	0.2	6.1
WHG 2006/07 (2) 104	67	2006.57	-42.6	-333.4	0.5	7.1
WHG 2006/07 (2) 103	68	2006.56	-42.6	-333.1	0.1	7.9
WHG 2006/07 (2) 102	69	2006.55	-42.6	-330.7	0.1	9.9
WHG 2006/07 (2) 101	70	2006.55	-42.1	-329.9	0.1	6.7
WHG 2006/07 (2) 100	71	2006.54	-38.6	-302.4	0.2	6.7
WHG 2006/07 (2) 099	72	2006.54	-38.2	-298.6	0.3	6.9
WHG 2006/07 (2) 098	73	2006.54	-35.6	-277.7	0.1	6.8
WHG 2006/07 (2) 097	74	2006.53	-34.9	-272.6	0.2	6.9
WHG 2006/07 (2) 096	75	2006.53	-34.2	-267.0	0.2	6.2
WHG 2006/07 (2) 095	76	2006.52	-34.1	-266.9	0.3	6.2
WHG 2006/07 (2) 094	77	2006.51	-34.2	-267.0	0.6	6.4
WHG 2006/07 (2) 093	78	2006.50	-34.4	-270.2	0.1	4.7
WHG 2006/07 (2) 092	79	2006.49	-34.7	-271.4	0.2	5.8
WHG 2006/07 (2) 091	80	2006.49	-34.9	-273.1	0.7	6.1
WHG 2006/07 (2) 090	81	2006.48	-35.0	-276.4	0.6	3.9
WHG 2006/07 (2) 089	82	2006.47	-35.2	-278.3	0.0	3.2
WHG 2006/07 (2) 088	83	2006.47	-34.8	-275.6	0.1	3.1
WHG 2006/07 (2) 087	84	2006.47	-33.6	-263.0	0.1	5.6
WHG 2006/07 (2) 086	85	2006.46	-32.9	-254.4	0.2	9.0
WHG 2006/07 (2) 085	86	2006.46	-32.4	-249.0	0.5	10.1
WHG 2006/07 (2) 084	87	2006.46	-32.2	-246.6	0.1	11.1
WHG 2006/07 (2) 083	88	2006.42	-32.3	-246.6	0.1	11.8
WHG 2006/07 (2) 082	89	2006.42	-32.3	-248.2	0.0	10.5
WHG 2006/07 (2) 081	90	2006.42	-32.4	-247.9	0.3	11.4
WHG 2006/07 (2) 080	91	2006.42	-32.7	-250.8	0.1	10.4
WHG 2006/07 (2) 079	92	2006.41	-32.8	-250.5	0.0	11.7
WHG 2006/07 (2) 078	93	2006.41	-32.8	-251.1	0.0	11.1
WHG 2006/07 (2) 077	94	2006.41	-32.9	-253.3	0.1	10.2
WHG 2006/07 (2) 076	95	2006.41	-33.0	-254.0	0.1	9.7
WHG 2006/07 (2) 075	96	2006.41	-33.1	-255.3	0.6	9.6
WHG 2006/07 (2) 074	97	2006.41	-33.5	-257.3	0.4	10.5
WHG 2006/07 (2) 073	98	2006.40	-33.5	-259.8	0.3	8.0
WHG 2006/07 (2) 072	99	2006.40	-34.4	-268.6	0.4	6.8
WHG 2006/07 (2) 071	100	2006.40	-34.9	-273.2	0.1	6.3
WHG 2006/07 (2) 070	101	2006.40	-35.6	-278.3	0.4	6.6
WHG 2006/07 (2) 069	102	2006.36	-35.6	-279.3	0.6	5.5
WHG 2006/07 (2) 068	103	2006.33	-35.7	-277.5	0.3	8.1
WHG 2006/07 (2) 067	104	2006.31	-35.4	-275.5	0.4	8.0
WHG 2006/07 (2) 066	105	2006.29	-35.0	-272.6	0.1	7.7
WHG 2006/07 (2) 065	106	2006.27	-33.5	-260.4	0.1	7.5
WHG 2006/07 (2) 064	107	2006.25	-31.9	-245.6	0.3	9.4
WHG 2006/07 (2) 063	108	2006.22	-28.2	-213.7	0.1	11.7
WHG 2006/07 (2) 062	109	2006.19	-24.2	-179.2	0.4	14.1
WHG 2006/07 (2) 061	110	2006.18	-23.1	-170.3	0.3	14.2
WHG 2006/07 (2) 060	111	2006.16	-22.2	-162.8	0.4	14.7
WHG 2006/07 (2) 059	112	2006.16	-22.0	-161.5	0.3	14.7
WHG 2006/07 (2) 058	113	2006.15	-22.1	-161.8	0.1	14.8
WHG 2006/07 (2) 057	114	2006.14	-22.0	-161.3	0.0	14.9
WHG 2006/07 (2) 056	115	2006.14	-21.9	-159.5	0.1	15.5
WHG 2006/07 (2) 055	116	2006.13	-21.7	-158.5	0.1	14.9
WHG 2006/07 (2) 054	117	2006.12	-21.7	-157.2	0.3	16.2
WHG 2006/07 (2) 053	118	2006.12	-21.5	-157.1	0.1	15.2
WHG 2006/07 (2) 052	119	2006.11	-21.5	-157.5	0.1	14.1
WHG 2006/07 (2) 051	120	2006.10	-21.4	-158.7	0.3	12.2
WHG 2006/07 (2) 050	121	2006.10	-21.4	-158.4	0.1	12.4
WHG 2006/07 (2) 049	122	2006.09	-21.4	-161.8	0.2	9.7
WHG 2006/07 (2) 048	123	2006.08	-21.4	-162.0	0.1	8.9
WHG 2006/07 (2) 047	124	2006.08	-21.2	-160.2	0.1	9.4

Table A4.3 continued.

Sample	Depth (cm)	Date (yr)	$\delta^{18}\text{O}$ (‰)	δD (‰)	2σ (‰)	d excess (‰)
WHG 2006/07 (2) 046	125	2006.07	-20.8	-156.3	0.0	9.9
WHG 2006/07 (2) 045	126	2006.06	-20.9	-156.2	0.1	11.1
WHG 2006/07 (2) 044	127	2006.05	-20.2	-151.3	0.4	9.9
WHG 2006/07 (2) 043	128	2006.05	-20.2	-150.1	0.0	11.1
WHG 2006/07 (2) 042	129	2006.04	-19.6	-145.1	0.1	11.7
WHG 2006/07 (2) 041	130	2006.03	-19.7	-145.2	0.0	12.2
WHG 2006/07 (2) 040	131	2006.03	-19.6	-145.7	0.0	10.9
WHG 2006/07 (2) 039	132	2006.02	-18.8	-138.9	0.2	11.7
WHG 2006/07 (2) 038	133	2006.01	-18.4	-136.0	0.2	10.9
WHG 2006/07 (2) 037	134	2006.01	-17.8	-130.1	0.3	12.2
WHG 2006/07 (2) 036	135	2006.00	-17.6	-129.4	0.1	11.6
WHG 2006/07 (2) 035	136	2005.99	-17.8	-131.1	0.2	11.3
WHG 2006/07 (2) 034	137	2005.98	-18.2	-135.0	0.0	10.3
WHG 2006/07 (2) 033	138	2005.96	-18.6	-139.1	0.1	9.3
WHG 2006/07 (2) 031	140	2005.94	-19.9	-152.3	0.6	7.1
WHG 2006/07 (2) 030	141	2005.91	-21.3	-163.7	0.1	6.9
WHG 2006/07 (2) 029	142	2005.90	-21.9	-168.4	0.2	6.9
WHG 2006/07 (2) 028	143	2005.89	-22.3	-171.6	0.0	7.0
WHG 2006/07 (2) 027	144	2005.89	-22.6	-172.4	0.1	8.2
WHG 2006/07 (2) 026	145	2005.89	-22.6	-172.3	0.1	8.7
WHG 2006/07 (2) 025	146	2005.89	-22.6	-172.8	0.1	8.2
WHG 2006/07 (2) 024	147	2005.88	-22.6	-171.8	0.1	8.8
WHG 2006/07 (2) 023	148	2005.88	-22.5	-171.4	0.0	8.9
WHG 2006/07 (2) 022	149	2005.88	-22.4	-169.2	0.2	9.9
WHG 2006/07 (2) 021	150	2005.87	-22.4	-171.4	0.1	7.8
WHG 2006/07 (2) 020	151	2005.87	-22.5	-173.6	0.1	6.2
WHG 2006/07 (2) 019	152	2005.87	-22.7	-176.0	0.2	5.4
WHG 2006/07 (2) 018	153	2005.86	-22.6	-177.9	0.2	3.1
WHG 2006/07 (2) 017	154	2005.86	-22.8	-178.2	0.1	4.1
WHG 2006/07 (2) 016	155	2005.85	-22.8	-179.1	0.1	3.5
WHG 2006/07 (2) 015	156	2005.85	-22.7	-178.2	0.5	3.6
WHG 2006/07 (2) 014	157	2005.85	-22.5	-177.5	0.2	2.7
WHG 2006/07 (2) 013	158	2005.85	-22.1	-172.9	0.1	4.1
WHG 2006/07 (2) 012	159	2005.85	-21.5	-168.1	0.2	4.0
WHG 2006/07 (2) 011	160	2005.84	-20.5	-158.8	0.2	4.9
WHG 2006/07 (2) 010	161	2005.84	-19.6	-149.8	0.1	6.8
WHG 2006/07 (2) 008	163	2005.84	-18.8	-146.3	0.0	4.1
WHG 2006/07 (2) 007	164	2005.83	-18.5	-140.9	0.1	7.1
WHG 2006/07 (2) 006	165	2005.83	-18.1	-140.0	0.2	5.0
WHG 2006/07 (2) 005	166	2005.83	-17.6	-134.1	0.0	6.8
WHG 2006/07 (2) 004	167	2005.83	-17.5	-131.6	0.4	8.7
WHG 2006/07 (2) 003	168	2005.83	-17.7	-133.3	0.2	8.5
WHG 2006/07 (2) 002	169	2005.82	-18.3	-137.8	0.2	8.2
WHG 2006/07 (2) 001	170	2005.82	-18.4	-139.4	0.3	7.5

Table A4.4 Oxygen ($\delta^{18}\text{O}$) and hydrogen (δD) isotopic ratios of WHG_3 snow samples. The second order parameter deuterium excess (d) is calculated as $d = \delta\text{D} - 8 \cdot \delta^{18}\text{O}$. Analytical precision is typically $< 0.1 \text{ ‰}$ for $\delta^{18}\text{O}$, $< 1.0 \text{ ‰}$ δD , and $< 1.0 \text{ ‰}$ d excess. Dating is based on comparison of $\delta^{18}\text{O}$ with Cape Hallett temperature changes.

Sample	Depth (cm)	Date (yr)	$\delta^{18}\text{O}$ (‰)	δD (‰)	2σ (‰)	d excess (‰)
WHG 2006/07 (3) 112	1	2006.86	-24.5	-195	0.1	1
WHG 2006/07 (3) 111	2	2006.86	-25.0	-196	1.1	4
WHG 2006/07 (3) 110	3	2006.85	-25.3	-203	0.3	-1
WHG 2006/07 (3) 109	4	2006.84	-26.0	-204	0.4	4
WHG 2006/07 (3) 108	5	2006.84	-25.8	-205	0.3	1
WHG 2006/07 (3) 107	6	2006.83	-25.8	-206	0.1	1
WHG 2006/07 (3) 106	7	2006.82	-26.2	-206	0.5	4
WHG 2006/07 (3) 105	8	2006.82	-25.5	-203	0.2	1
WHG 2006/07 (3) 104	9	2006.81	-25.5	-202	0.2	2
WHG 2006/07 (3) 103	10	2006.80	-25.8	-202	0.0	4
WHG 2006/07 (3) 102	11	2006.80	-26.3	-207	0.1	4
WHG 2006/07 (3) 101	12	2006.79	-27.0	-212	0.4	3
WHG 2006/07 (3) 100	13	2006.78	-27.7	-218	0.4	4
WHG 2006/07 (3) 099	14	2006.78	-28.0	-221	0.5	4
WHG 2006/07 (3) 098	15	2006.77	-28.2	-221	0.2	5
WHG 2006/07 (3) 097	16	2006.77	-28.7	-221	0.8	8
WHG 2006/07 (3) 096	17	2006.76	-28.2	-221	0.3	5
WHG 2006/07 (3) 095	18	2006.76	-28.4	-222	0.5	6
WHG 2006/07 (3) 094	19	2006.76	-28.5	-225	0.1	3
WHG 2006/07 (3) 093	20	2006.76	-29.0	-227	0.6	5
WHG 2006/07 (3) 092	21	2006.76	-29.2	-228	0.5	5
WHG 2006/07 (3) 091	22	2006.76	-29.3	-228	0.1	6
WHG 2006/07 (3) 090	23	2006.76	-29.3	-228	0.7	7
WHG 2006/07 (3) 089	24	2006.76	-29.3	-229	1.0	6
WHG 2006/07 (3) 088	25	2006.76	-29.4	-229	0.1	5
WHG 2006/07 (3) 087	26	2006.75	-29.5	-230	0.1	6
WHG 2006/07 (3) 086	27	2006.75	-29.4	-230	0.1	5
WHG 2006/07 (3) 085	28	2006.75	-29.6	-231	0.0	6
WHG 2006/07 (3) 084	29	2006.75	-29.6	-232	0.3	5
WHG 2006/07 (3) 083	30	2006.75	-29.4	-231	1.0	5
WHG 2006/07 (3) 082	31	2006.75	-29.4	-229	0.1	6
WHG 2006/07 (3) 081	32	2006.75	-29.2	-229	0.4	5
WHG 2006/07 (3) 080	33	2006.74	-29.2	-228	0.0	6
WHG 2006/07 (3) 079	34	2006.74	-29.2	-226	0.3	7
WHG 2006/07 (3) 078	35	2006.74	-29.1	-228	0.7	5
WHG 2006/07 (3) 077	36	2006.73	-29.1	-228	0.1	5
WHG 2006/07 (3) 076	37	2006.73	-29.1	-228	0.8	4
WHG 2006/07 (3) 075	38	2006.73	-29.0	-227	0.4	5
WHG 2006/07 (3) 074	39	2006.73	-28.7	-225	0.1	5
WHG 2006/07 (3) 073	40	2006.72	-28.0	-221	1.0	3
WHG 2006/07 (3) 072	41	2006.72	-27.9	-218	0.3	5
WHG 2006/07 (3) 071	42	2006.72	-28.3	-217	0.0	9
WHG 2006/07 (3) 070	43	2006.72	-28.3	-220	0.0	6
WHG 2006/07 (3) 069	44	2006.71	-28.9	-221	0.1	10
WHG 2006/07 (3) 068	45	2006.71	-29.1	-227	0.2	6
WHG 2006/07 (3) 067	46	2006.71	-31.0	-244	0.4	4
WHG 2006/07 (3) 066	47	2006.70	-34.6	-270	0.8	7
WHG 2006/07 (3) 065	48	2006.68	-36.3	-286	0.1	4
WHG 2006/07 (3) 064	49	2006.67	-36.5	-288	0.4	4
WHG 2006/07 (3) 063	50	2006.66	-36.5	-286	0.1	6
WHG 2006/07 (3) 062	51	2006.66	-35.6	-282	0.1	2
WHG 2006/07 (3) 061	52	2006.66	-33.4	-265	0.6	2
WHG 2006/07 (3) 060	53	2006.66	-31.3	-248	0.5	2
WHG 2006/07 (3) 059	54	2006.65	-30.7	-241	0.4	4
WHG 2006/07 (3) 058	55	2006.65	-30.3	-237	0.1	6
WHG 2006/07 (3) 057	56	2006.64	-30.6	-237	0.2	8
WHG 2006/07 (3) 056	57	2006.64	-29.9	-235	0.1	4
WHG 2006/07 (3) 055	58	2006.63	-29.8	-235	0.2	4

Table A4.4 continued.

Sample	Depth (cm)	Date (yr)	$\delta^{18}\text{O}$ (‰)	δD (‰)	2σ (‰)	d excess (‰)
WHG 2006/07 (3) 054	59	2006.63	-30.2	-237.7	0.2	4
WHG 2006/07 (3) 053	60	2006.62	-30.4	-238.8	0.2	5
WHG 2006/07 (3) 052	61	2006.62	-30.9	-243.2	0.2	4
WHG 2006/07 (3) 051	62	2006.61	-31.6	-247.3	0.2	5
WHG 2006/07 (3) 050	63	2006.61	-31.7	-249.0	0.0	4
WHG 2006/07 (3) 049	64	2006.61	-32.0	-251.4	0.8	4
WHG 2006/07 (3) 048	65	2006.60	-31.0	-244.5	0.3	4
WHG 2006/07 (3) 047	66	2006.60	-30.4	-235.6	0.3	8
WHG 2006/07 (3) 046	67	2006.59	-29.4	-230.7	0.4	5
WHG 2006/07 (3) 045	68	2006.59	-28.3	-218.5	0.2	8
WHG 2006/07 (3) 044	69	2006.59	-27.8	-213.9	0.1	9
WHG 2006/07 (3) 043	70	2006.58	-27.3	-213.2	0.9	5
WHG 2006/07 (3) 042	71	2006.58	-27.7	-211.2	0.1	10
WHG 2006/07 (3) 041	72	2006.58	-27.7	-213.8	0.4	8
WHG 2006/07 (3) 040	73	2006.58	-28.2	-217.3	0.6	8
WHG 2006/07 (3) 039	74	2006.57	-29.9	-231.8	0.5	7
WHG 2006/07 (3) 038	75	2006.57	-33.7	-264.5	0.2	5
WHG 2006/07 (3) 037	76	2006.57	-37.2	-298.0	0.1	0
WHG 2006/07 (3) 036	77	2006.56	-40.9	-324.1	0.0	3
WHG 2006/07 (3) 035	78	2006.56	-41.3	-328.9	0.5	1
WHG 2006/07 (3) 034	79	2006.55	-41.1	-326.3	0.0	3
WHG 2006/07 (3) 033	80	2006.55	-39.3	-313.9	0.2	0
WHG 2006/07 (3) 032	81	2006.54	-37.6	-295.6	0.4	5
WHG 2006/07 (3) 031	82	2006.54	-36.0	-282.1	0.4	6
WHG 2006/07 (3) 030	83	2006.53	-34.8	-274.9	0.6	3
WHG 2006/07 (3) 029	84	2006.53	-33.3	-265.6	0.2	1
WHG 2006/07 (3) 028	85	2006.52	-33.0	-263.6	0.0	0
WHG 2006/07 (3) 027	86	2006.51	-33.3	-264.7	0.5	2
WHG 2006/07 (3) 026	87	2006.50	-33.5	-267.3	0.2	0
WHG 2006/07 (3) 025	88	2006.48	-33.6	-269.8	0.4	-1
WHG 2006/07 (3) 024	89	2006.47	-33.7	-266.8	0.4	3
WHG 2006/07 (3) 023	90	2006.47	-33.2	-257.6	0.8	8
WHG 2006/07 (3) 022	91	2006.46	-32.5	-251.6	0.3	9
WHG 2006/07 (3) 021	92	2006.46	-31.4	-239.6	0.3	12
WHG 2006/07 (3) 020	93	2006.46	-31.4	-239.1	0.3	12
WHG 2006/07 (3) 019	94	2006.46	-31.1	-238.1	0.1	11
WHG 2006/07 (3) 018	95	2006.45	-31.0	-238.0	0.1	10
WHG 2006/07 (3) 017	96	2006.45	-31.1	-239.1	0.1	10
WHG 2006/07 (3) 016	97	2006.45	-31.3	-240.5	0.7	10
WHG 2006/07 (3) 015	98	2006.44	-31.3	-239.6	1.1	11
WHG 2006/07 (3) 014	99	2006.44	-32.0	-242.2	0.3	13
WHG 2006/07 (3) 013	100	2006.42	-31.6	-242.7	0.2	10
WHG 2006/07 (3) 012	101	2006.42	-31.6	-242.6	0.4	10
WHG 2006/07 (3) 011	102	2006.42	-31.8	-243.8	0.5	10
WHG 2006/07 (3) 010	103	2006.42	-31.7	-243.3	0.7	10
WHG 2006/07 (3) 009	104	2006.42	-32.9	-249.7	0.2	13
WHG 2006/07 (3) 008	105	2006.41	-33.5	-258.4	0.5	10
WHG 2006/07 (3) 007	106	2006.40	-29.3	-228.7	0.1	5
WHG 2006/07 (3) 006	107	2006.36	-35.5	-278.3	0.1	6
WHG 2006/07 (3) 005	108	2006.29	-35.2	-274.5	0.0	7
WHG 2006/07 (3) 004	109	2006.27	-34.1	-263.5	0.3	9
WHG 2006/07 (3) 003	110	2006.25	-32.5	-249.1	0.1	11
WHG 2006/07 (3) 002	111	2006.24	-28.4	-214.8	0.4	12
WHG 2006/07 (3) 001	112	2006.18	-23.6	-177.9	0.3	11

Table A4.5 Oxygen ($\delta^{18}\text{O}$) and hydrogen (δD) isotopic ratios of WHG_4 snow samples. The second order parameter deuterium excess (d) is calculated as $d = \delta\text{D} - 8 \cdot \delta^{18}\text{O}$. Analytical precision is typically $< 0.1 \text{ ‰}$ for $\delta^{18}\text{O}$, $< 1.0 \text{ ‰}$ δD , and $< 1.0 \text{ ‰}$ d excess. Dating is based on comparison of $\delta^{18}\text{O}$ with Cape Hallett temperature changes.

Sample	Depth (cm)	Date (yr)	$\delta^{18}\text{O}$ (‰)	δD (‰)	d excess (‰)
2006/06 (4)_102	1	2006.86	-25.5	-203	1
2006/06 (4)_101	2	2006.85	-27.2	-210	8
2006/06 (4)_100	3	2006.85	-27.7	-213	9
2006/06 (4)_099	4	2006.84	-27.5	-212	7
2006/06 (4)_098	5	2006.83	-27.5	-212	7
2006/06 (4)_097	6	2006.82	-27.5	-213	7
2006/06 (4)_096	7	2006.81	-27.5	-213	7
2006/06 (4)_095	8	2006.81	-28.2	-216	10
2006/06 (4)_094	9	2006.81	-28.3	-221	6
2006/06 (4)_093	10	2006.80	-29.0	-227	6
2006/06 (4)_092	11	2006.80	-29.4	-229	6
2006/06 (4)_091	12	2006.80	-29.7	-231	7
2006/06 (4)_090	13	2006.80	-29.7	-231	7
2006/06 (4)_089	14	2006.80	-30.1	-230	10
2006/06 (4)_088	15	2006.79	-30.1	-230	11
2006/06 (4)_087	16	2006.79	-29.8	-231	8
2006/06 (4)_086	17	2006.79	-29.8	-230	8
2006/06 (4)_085	18	2006.79	-29.7	-229	9
2006/06 (4)_084	19	2006.79	-29.7	-230	8
2006/06 (4)_083	20	2006.78	-30.0	-231	10
2006/06 (4)_082	21	2006.78	-29.6	-230	6
2006/06 (4)_081	22	2006.78	-29.5	-230	6
2006/06 (4)_080	23	2006.78	-29.5	-229	7
2006/06 (4)_079	24	2006.78	-29.9	-230	9
2006/06 (4)_078	25	2006.78	-29.8	-230	9
2006/06 (4)_077	26	2006.77	-29.4	-229	6
2006/06 (4)_076	27	2006.77	-29.4	-229	6
2006/06 (4)_075	28	2006.77	-29.3	-229	5
2006/06 (4)_074	29	2006.76	-29.3	-228	6
2006/06 (4)_073	30	2006.76	-29.3	-228	6
2006/06 (4)_072	31	2006.75	-29.4	-228	8
2006/06 (4)_071	32	2006.75	-29.3	-228	6
2006/06 (4)_070	33	2006.74	-29.4	-227	9
2006/06 (4)_069	34	2006.74	-29.3	-225	10
2006/06 (4)_068	35	2006.73	-29.2	-226	7
2006/06 (4)_067	36	2006.73	-29.1	-225	8
2006/06 (4)_066	37	2006.72	-29.1	-225	8
2006/06 (4)_065	38	2006.72	-29.1	-226	7
2006/06 (4)_064	39	2006.70	-29.1	-226	7
2006/06 (4)_063	40	2006.68	-29.5	-226	10
2006/06 (4)_062	41	2006.67	-29.1	-226	6
2006/06 (4)_061	42	2006.67	-29.1	-226	7
2006/06 (4)_060	43	2006.67	-29.2	-226	7
2006/06 (4)_059	44	2006.66	-29.2	-228	6
2006/06 (4)_058	45	2006.66	-29.2	-226	7
2006/06 (4)_057	46	2006.66	-29.2	-227	6
2006/06 (4)_056	47	2006.65	-29.1	-227	6
2006/06 (4)_055	48	2006.65	-29.2	-227	7
2006/06 (4)_054	49	2006.65	-29.1	-226	7
2006/06 (4)_053	50	2006.64	-29.0	-224	8
2006/06 (4)_052	51	2006.64	-28.7	-224	6
2006/06 (4)_051	52	2006.64	-28.6	-223	6
2006/06 (4)_050	53	2006.63	-28.4	-221	6
2006/06 (4)_049	54	2006.62	-28.4	-221	7
2006/06 (4)_048	55	2006.62	-28.5	-222	6
2006/06 (4)_047	56	2006.61	-28.6	-222	6
2006/06 (4)_046	57	2006.60	-28.5	-222	6
2006/06 (4)_045	58	2006.59	-28.4	-221	7
2006/06 (4)_044	59	2006.58	-28.3	-220	6
2006/06 (4)_043	60	2006.58	-28.4	-221	6
2006/06 (4)_042	61	2006.58	-28.7	-224	6
2006/06 (4)_041	62	2006.58	-28.8	-224	6

Table A4.5 continued.

Sample	Depth (cm)	Date (yr)	$\delta^{18}\text{O}$ (‰)	δD (‰)	d excess (‰)
2006/06 (4)_040	63	2006.58	-29.0	-227	6
2006/06 (4)_039	64	2006.57	-29.2	-227	6
2006/06 (4)_038	65	2006.57	-29.9	-233	6
2006/06 (4)_037	66	2006.57	-30.7	-238	8
2006/06 (4)_036	67	2006.57	-32.0	-251	5
2006/06 (4)_035	68	2006.57	-34.2	-270	4
2006/06 (4)_034	69	2006.57	-34.9	-275	4
2006/06 (4)_033	70	2006.56	-35.1	-276	5
2006/06 (4)_032	71	2006.51	-35.2	-276	5
2006/06 (4)_031	72	2006.50	-35.2	-277	5
2006/06 (4)_030	73	2006.49	-35.3	-278	5
2006/06 (4)_029	74	2006.49	-35.5	-279	4
2006/06 (4)_028	75	2006.48	-35.6	-281	4
2006/06 (4)_027	76	2006.47	-35.1	-275	5
2006/06 (4)_026	77	2006.47	-33.7	-262	7
2006/06 (4)_025	78	2006.47	-32.7	-252	10
2006/06 (4)_024	79	2006.46	-32.3	-247	12
2006/06 (4)_023	80	2006.45	-32.3	-247	12
2006/06 (4)_022	81	2006.44	-32.4	-247	12
2006/06 (4)_021	82	2006.42	-32.4	-247	13
2006/06 (4)_020	83	2006.41	-32.6	-250	10
2006/06 (4)_019	84	2006.41	-33.0	-253	11
2006/06 (4)_018	85	2006.41	-33.4	-258	10
2006/06 (4)_017	86	2006.40	-34.3	-267	7
2006/06 (4)_016	87	2006.40	-35.1	-273	8
2006/06 (4)_015	88	2006.40	-35.6	-279	7
2006/06 (4)_014	89	2006.39	-36.2	-280	9
2006/06 (4)_013	90	2006.39	-36.5	-284	9
2006/06 (4)_012	91	2006.39	-36.0	-282	6
2006/06 (4)_011	92	2006.39	-36.2	-282	8
2006/06 (4)_010	93	2006.39	-35.5	-276	8
2006/06 (4)_009	94	2006.38	-35.4	-275	8
2006/06 (4)_008	95	2006.38	-35.5	-276	8
2006/06 (4)_007	96	2006.37	-35.1	-275	6
2006/06 (4)_006	97	2006.37	-34.5	-270	6
2006/06 (4)_005	98	2006.36	-34.0	-263	9
2006/06 (4)_004	99	2006.33	-30.9	-237	11
2006/06 (4)_003	100	2006.29	-30.4	-232	10
2006/06 (4)_002	101	2006.25	-28.7	-218	12
2006/06 (4)_001	102	2006.21	-26.4	-198	13

Table A4.6 Repeated measurement of the quality control standard QC_2 by ICP-OES to determine analytical precision.

Standard	Al ppb	Ca ppb	K ppb	Mg ppb	Na ppb	S ppb	Si ppb	Sr ppb
Spectrum	396.2	396.8	766.5	285.2	330.2	180.7	251.6	421.6
Average	3	22	25	22	115	24	2	0.22
2 σ	0.5	2	1	2	36	2	1	0.03
2 rsd	19	9	5	11	32	8	35	12
QC_2 1	2.4	23	25	22	130	24	2.2	0.21
QC_2 2	2.5	23	24	22	112	24	1.6	0.21
QC_2 3	2.5	22	25	23	124	24	1.9	0.21
QC_2 4	2.5	22	25	22	108	24	2.2	0.20
QC_2 5	2.8	22	25	22	122	25	1.9	0.20
QC_2 6	2.6	21	25	22	94	24	2.8	0.20
QC_2 7	2.7	21	25	22	97	24	1.9	0.20
QC_2 8	2.5	23	25	22	95	24	2.4	0.21
QC_2 9	2.6	22	25	22	110	25	2.5	0.21
QC_2 10	2.7	21	24	21	97	24	2.4	0.20
QC_2 11	2.7	21	25	21	106	25	2.3	0.20
QC_2 12	2.4	21	25	21	91	23	1.9	0.21
QC_2 13	2.8	20	25	21	112	24	1.8	0.21
QC_2 14	2.8	21	25	21	125	25	2.3	0.22
QC_2 15	2.8	21	24	21	114	23	1.6	0.24
QC_2 16	3.2	22	26	21	150	25	2.0	0.25
QC_2 17	2.9	21	25	20	114	24	1.5	0.24
QC_2 18	2.7	21	25	20	135	23	1.8	0.23
QC_2 19	2.7	21	25	21	125	23	2.0	0.24
QC_2 20	2.6	24	26	25	128	25	3.0	0.24
QC_2 21	2.7	23	25	22	117	25	1.5	0.21
QC_2 22	2.7	23	25	23	133	25	2.0	0.22
QC_2 23	2.6	23	25	24	135	25	2.6	0.22
QC_2 24	2.8	24	26	24	150	25	2.5	0.23
QC_2 25	2.7	24	25	24	117	25	2.4	0.23
QC_2 26	2.8	23	25	23	126	24	2.0	0.22
QC_2 27	2.7	23	25	24	137	25	2.5	0.22
QC_2 28	2.5	23	25	23	136	25	1.7	0.21
QC_2 29	2.6	23	25	23	151	25	2.4	0.21
QC_2 30	2.7	23	25	23	140	25	2.0	0.22
QC_2 31	2.0	22	27	24	104	23	1.4	0.22
QC_2 32	2.4	22	25	23	89	23	2.0	0.22
QC_2 33	2.2	21	26	22	115	23	2.1	0.21
QC_2 34	2.5	22	26	22	135	22	2.0	0.22
QC_2 35	2.3	21	26	22	118	22	2.3	0.21
QC_2 36	2.2	22	26	22	142	23	2.2	0.21
QC_2 37	2.4	22	26	22	127	23	2.1	0.22
QC_2 38	2.5	22	26	22	114	23	1.6	0.22
QC_2 39	2.2	21	25	22	106	23	2.4	0.21
QC_2 40	2.5	22	25	21	105	23	2.1	0.21
QC_2 41	2.1	22	26	21	98	24	2.7	0.21
QC_2 42	2.4	21	26	21	117	23	1.8	0.21
QC_2 43	2.3	22	25	22	130	24	2.4	0.22
QC_2 44	2.4	21	26	22	86	23	2.5	0.22
QC_2 45	2.3	21	26	21	116	24	3.0	0.21
QC_2 46	2.1	22	25	22	90	24	2.3	0.22
QC_2 47	2.5	21	26	21	94	25	2.0	0.22
QC_2 48	2.2	21	25	21	92	26	2.0	0.22
QC_2 49	2.3	20	26	20	102	24	1.5	0.22
QC_2 50	2.3	21	26	20	81	24	2.2	0.24
QC_2 51	2.3	20	26	19	86	24	1.9	0.24
QC_2 52	2.4	20	26	19	105	24	1.7	0.24
QC_2 53	2.7	21	26	20	110	24	2.0	0.26

Table A4.7 Measured concentrations of blanks used to determine the detection limits of elements measured by ICP-OES analysis.

Blanks	Al ppb	Ca ppb	K ppb	Mg ppb	Na ppb	S ppb	Si ppb	Sr ppb
3 σ	0.40	4.61	0.35	0.29	39.56	0.59	0.79	0.0043
Blank_01	0.48	5.55	4.91	-1.25	-34.9	-2.63	-0.15	-0.007
Blank_02	0.49	3.83	5.12	-1.32	-26.2	-2.82	0.11	-0.010
Blank_03	0.65	3.86	4.88	-1.32	-41.9	-2.98	0.42	-0.011
Blank_04	0.63	2.53	5.02	-1.50	-34.0	-2.94	0.36	-0.012
Blank_05	0.55	2.42	4.90	-1.44	-44.9	-2.86	0.40	-0.010
Blank_06	0.55	1.61	4.91	-1.46	-38.6	-2.70	0.67	-0.010
Blank_07	0.62	1.04	5.16	-1.49	-43.8	-2.58	0.05	-0.009
Blank_08	0.22	0.72	5.16	-1.53	-14.5	-3.09	-0.09	-0.008
Blank_09	0.66	1.02	4.87	-1.45	-32.1	-2.45	0.45	-0.009
Blank_10	0.63	2.38	4.95	-1.32	-64.8	-2.81	0.23	-0.010

Table A4.8 Major and trace element chemistry of WHG_1 snow samples measured by ICP-OES. Analytical precision is determined by repeated measurement of quality control standard (QC_2). Values shown in grey are below the detection limit.

Sample	Depth cm	Al ppb	Ca ppb	K ppb	Mg ppb	Na ppb	S ppb	Si ppb	Sr ppb
Spectrum measured		396.2	396.8	766.5	285.2	330.2	180.7	251.6	421.6
Detection limit (3 σ blanks)		0.40	4.6	0.35	0.29	40	0.59	0.79	0.004
Sample average		1.9	49	50	136	1178	102	1.9	0.70
Sample 2 rsd (%)		111	254	265	285	313	260	156	279
Sample max		6	433	487	1390	13800	896	9	7
Sample min		BDL	BDL	BDL	BDL	BDL	BDL	BDL	BDL
WHG_2006/07 (1)_214	9	4.6	8	14	15	133	31	1	0.08
WHG_2006/07 (1)_213	10	0.8	7	10	8	66	21	1.6	0.05
WHG_2006/07 (1)_212	11	1.4	7	11	14	114	22	1.0	0.08
WHG_2006/07 (1)_211	12	1.3	8	12	17	130	21	1.2	0.10
WHG_2006/07 (1)_210	13	1.1	7	10	12	107	18	0.4	0.07
WHG_2006/07 (1)_209	14	1.2	16	13	20	223	19	0.9	0.12
WHG_2006/07 (1)_208	15	1.0	24	27	53	593	37	1.7	0.32
WHG_2006/07 (1)_207	16	1.3	29	38	74	850	44	0.7	0.44
WHG_2006/07 (1)_206	17	1.1	34	38	89	891	47	0.6	0.51
WHG_2006/07 (1)_205	18	1.7	41	42	104	986	52	1.0	0.58
WHG_2006/07 (1)_204	19	1.1	40	48	124	1120	60	0.6	0.66
WHG_2006/07 (1)_203	20	1.2	40	47	121	1100	60	0.5	0.65
WHG_2006/07 (1)_202	21	1.4	43	50	130	1200	63	0.7	0.70
WHG_2006/07 (1)_201	22	1.6	48	50	125	1150	63	1.0	0.67
WHG_2006/07 (1)_200	23	1.4	45	50	129	1160	63	1.3	0.70
WHG_2006/07 (1)_199	24	1.0	40	50	126	1220	62	0.7	0.70
WHG_2006/07 (1)_198	25	1.5	49	52	134	1210	63	1.3	0.71
WHG_2006/07 (1)_197	26	1.6	44	49	132	1180	63	1.2	0.69
WHG_2006/07 (1)_195	27	1.3	28	25	64	620	33	0.8	0.31
WHG_2006/07 (1)_194	28	1.3	0	6	1	32	-1	-2.5	0.00
WHG_2006/07 (1)_193	29	1.5	39	47	127	1100	58	0.9	0.61
WHG_2006/07 (1)_192	30	1.7	39	47	131	1090	58	1.6	0.62
WHG_2006/07 (1)_191	31	1.4	50	48	139	1150	62	1.3	0.66
WHG_2006/07 (1)_190	32	1.4	69	77	133	1990	87	3.8	1.04
WHG_2006/07 (1)_189	33	1.3	17	21	48	435	31	1.7	0.24
WHG_2006/07 (1)_188	34	1.0	22	13	22	200	19	1.8	0.12
WHG_2006/07 (1)_187	35	1.2	4	8	8	50	8	1.7	0.05
WHG_2006/07 (1)_186	36	1.2	8	8	8	45	8	1.9	0.04
WHG_2006/07 (1)_185	37	1.4	7	8	8	42	8	1.9	0.04
WHG_2006/07 (1)_184	38	1.3	14	8	8	78	8	2.3	0.05
WHG_2006/07 (1)_183	39	1.3	0	6	1	40	-1	-2.2	0.00
WHG_2006/07 (1)_182	40	1.6	6	8	8	50	8	2.0	0.04
WHG_2006/07 (1)_181	41	2.0	7	9	8	76	8	2.1	0.04
WHG_2006/07 (1)_180	42	1.5	9	8	9	35	8	1.7	0.05
WHG_2006/07 (1)_179	43	1.3	6	8	9	52	9	1.4	0.05
WHG_2006/07 (1)_178	44	1.4	5	9	13	76	14	1.1	0.06
WHG_2006/07 (1)_177	45	1.3	31	30	70	746	58	1.8	0.39
WHG_2006/07 (1)_176	46	1.8	43	47	118	1050	69	3.2	0.61
WHG_2006/07 (1)_175	47	1.4	40	45	118	1020	64	1.4	0.58
WHG_2006/07 (1)_174	48	1.3	41	46	122	1040	67	1.9	0.59
WHG_2006/07 (1)_173	49	1.8	51	46	122	1050	66	1.6	0.61
WHG_2006/07 (1)_172	50	1.6	41	46	125	1030	67	2.3	0.61
WHG_2006/07 (1)_171	51	1.5	42	45	124	1040	66	1.5	0.62
WHG_2006/07 (1)_170	52	1.8	40	43	119	1000	61	2.3	0.59
WHG_2006/07 (1)_169	53	1.4	36	41	106	949	56	1.7	0.53
WHG_2006/07 (1)_168b	54	1.5	41	40	99	871	54	2.0	0.55
WHG_2006/07 (1)_168	55	1.5	47	42	106	988	67	0.9	0.61
WHG_2006/07 (1)_167	56	1.5	37	34	78	835	60	1.8	0.49
WHG_2006/07 (1)_166	57	1.3	23	23	54	507	35	1.6	0.26
WHG_2006/07 (1)_165	58	1.5	22	23	53	493	34	1.4	0.26
WHG_2006/07 (1)_164	59	1.3	17	23	52	498	34	1.5	0.25
WHG_2006/07 (1)_163	60	1.1	19	22	54	488	33	1.6	0.26
WHG_2006/07 (1)_162	61	1.6	19	24	54	475	35	1.3	0.26
WHG_2006/07 (1)_161	62	1.3	32	21	54	434	34	2.3	0.25
WHG_2006/07 (1)_160	63	1.3	24	21	55	435	34	2.2	0.25
WHG_2006/07 (1)_159	64	1.1	75	22	61	457	36	1.6	0.29
WHG_2006/07 (1)_158	65	0.9	7	10	16	125	9	0.7	0.07

Table A4.8 continued.

Sample	Depth cm	Al ppb	Ca ppb	K ppb	Mg ppb	Na ppb	S ppb	Si ppb	Sr ppb
WHG_2006/07 (1)_157	66	1.3	23	22	63	469	32	1.4	0.28
WHG_2006/07 (1)_156	67	1.3	21	27	65	454	33	1.2	0.26
WHG_2006/07 (1)_155	68	1.2	19	24	67	471	33	1.0	0.27
WHG_2006/07 (1)_154	69	1.2	22	24	69	488	32	1.0	0.28
WHG_2006/07 (1)_153	70	1.2	23	24	68	511	32	1.5	0.28
WHG_2006/07 (1)_152	71	1.3	24	23	69	462	32	0.8	0.28
WHG_2006/07 (1)_151	72	1.2	27	28	71	524	33	0.8	0.31
WHG_2006/07 (1)_150	73	1.0	32	27	75	592	34	1.7	0.32
WHG_2006/07 (1)_149	74	1.3	34	37	104	850	45	1.3	0.47
WHG_2006/07 (1)_148	75	1.5	38	39	118	858	49	1.3	0.53
WHG_2006/07 (1)_147	76	1.3	47	44	122	969	54	2.1	0.55
WHG_2006/07 (1)_146	77	1.3	43	51	148	1150	62	1.6	0.67
WHG_2006/07 (1)_145	78	1.7	111	125	342	3000	201	2.5	1.70
WHG_2006/07 (1)_144	79	3.4	433	487	1390	13800	896	8.3	6.89
WHG_2006/07 (1)_143	80	2.8	416	454	1290	12800	835	7.6	6.42
WHG_2006/07 (1)_142	81	2.4	391	440	1240	12300	811	7.0	6.11
WHG_2006/07 (1)_141	82	2.8	398	443	1250	12200	810	8.8	6.18
WHG_2006/07 (1)_140	83	1.9	101	104	270	2520	194	3.1	1.48
WHG_2006/07 (1)_139	84	1.3	26	28	68	641	53	2.1	0.33
WHG_2006/07 (1)_138	85	1.2	10	12	20	204	17	0.9	0.10
WHG_2006/07 (1)_137	86	1.3	12	13	22	223	20	1.9	0.11
WHG_2006/07 (1)_136	87	1.5	12	15	28	314	31	2.0	0.15
WHG_2006/07 (1)_135	88	1.6	23	21	45	511	64	2.4	0.26
WHG_2006/07 (1)_134	89	1.7	15	19	42	381	78	2.4	0.18
WHG_2006/07 (1)_133	90	1.5	33	33	85	850	104	1.7	0.42
WHG_2006/07 (1)_132	91	1.8	19	21	49	479	79	1.4	0.24
WHG_2006/07 (1)_131	92	1.8	22	25	59	557	91	1.6	0.29
WHG_2006/07 (1)_130	93	1.7	23	25	55	530	82	2.0	0.26
WHG_2006/07 (1)_129	94	1.6	87	81	215	2120	267	2.1	1.13
WHG_2006/07 (1)_128	95	2.7	80	87	231	2210	282	1.9	1.21
WHG_2006/07 (1)_127	96	2.2	93	86	238	2300	295	1.6	1.24
WHG_2006/07 (1)_126	97	2.2	80	85	237	2220	294	1.1	1.22
WHG_2006/07 (1)_125	98	2.0	76	84	233	2240	290	1.1	1.17
WHG_2006/07 (1)_124	99	2.3	83	85	246	2270	311	1.2	1.24
WHG_2006/07 (1)_123	100	2.0	82	81	244	2210	310	1.5	1.25
WHG_2006/07 (1)_122	101	2.2	54	50	140	1350	193	1.1	0.73
WHG_2006/07 (1)_121	102	2.1	12	18	33	289	68	1.2	0.15
WHG_2006/07 (1)_120	103	1.8	6	10	16	152	89	1.0	0.07
WHG_2006/07 (1)_119	104	1.8	19	13	25	223	150	2.1	0.12
WHG_2006/07 (1)_118	105	1.6	14	16	34	342	165	0.9	0.17
WHG_2006/07 (1)_117	106	1.6	10	14	29	288	202	1.5	0.14
WHG_2006/07 (1)_116	107	1.3	7	11	18	179	100	1.2	0.09
WHG_2006/07 (1)_115	108	1.7	9	12	21	212	109	1.4	0.11
WHG_2006/07 (1)_114	109	1.6	12	17	36	362	135	1.2	0.17
WHG_2006/07 (1)_113	110	1.8	21	21	49	488	155	1.3	0.24
WHG_2006/07 (1)_112	111	1.6	18	19	40	396	143	0.7	0.19
WHG_2006/07 (1)_111	112	1.5	11	13	25	240	113	0.9	0.12
WHG_2006/07 (1)_110	113	2.2	15	18	36	395	152	1.7	0.17
WHG_2006/07 (1)_109	114	1.9	34	22	46	492	172	1.2	0.25
WHG_2006/07 (1)_108	115	1.9	14	14	30	251	87	0.7	0.16
WHG_2006/07 (1)_107	116	1.2	9	10	15	141	48	0.6	0.08
WHG_2006/07 (1)_106	117	1.3	6	9	13	115	40	1.0	0.07
WHG_2006/07 (1)_105	118	1.6	5	8	9	63	44	1.0	0.05
WHG_2006/07 (1)_104	119	2.0	7	7	8	74	45	1.1	0.05
WHG_2006/07 (1)_103	120	1.6	14	7	9	64	46	1.1	0.05
WHG_2006/07 (1)_102	121	1.3	3	7	7	65	45	0.6	0.03
WHG_2006/07 (1)_101	122	1.2	5	7	7	72	44	1.2	0.04
WHG_2006/07 (1)_100	123	1.5	4	7	5	35	40	1.3	0.03
WHG_2006/07 (1)_099	124	1.6	5	7	6	37	42	1.5	0.03
WHG_2006/07 (1)_098	125	1.6	6	7	5	18	37	2.1	0.03
WHG_2006/07 (1)_094	126	1.8	2	6	3	15	52	0.7	0.02
WHG_2006/07 (1)_097	127	1.3	4	6	4	9	36	1.0	0.02
WHG_2006/07 (1)_096	128	1.5	12	6	4	25	34	1.0	0.02
WHG_2006/07 (1)_095	129	1.1	3	6	3	28	43	0.5	0.02
WHG_2006/07 (1)_094	130	1.3	0	6	1	62	-1	-2.4	0.00
WHG_2006/07 (1)_092	131	1.8	4	7	5	-3	67	1.1	0.03
WHG_2006/07 (1)_091	132	4.0	3	6	4	9	69	1.7	0.03
WHG_2006/07 (1)_090	133	1.4	4	7	5	31	66	0.2	0.03

Table A4.8 continued.

Sample	Depth cm	Al ppb	Ca ppb	K ppb	Mg ppb	Na ppb	S ppb	Si ppb	Sr ppb
WHG_2006/07 (1)_089	134	1.4	25	11	21	200	126	0.9	0.11
WHG_2006/07 (1)_088	135	1.5	8	11	20	201	130	0.7	0.09
WHG_2006/07 (1)_087	136	1.7	13	11	23	193	134	1.1	0.12
WHG_2006/07 (1)_086	137	1.4	6	10	14	127	127	0.4	0.07
WHG_2006/07 (1)_085	138	1.9	9	11	17	163	124	1.0	0.09
WHG_2006/07 (1)_084	139	2.1	10	14	26	212	63	0.4	0.12
WHG_2006/07 (1)_083	140	3.4	61	58	159	1430	195	2.1	0.94
WHG_2006/07 (1)_082	141	3.9	88	88	257	2140	246	2.9	1.35
WHG_2006/07 (1)_081	142	4.9	120	111	333	2810	282	3.4	1.73
WHG_2006/07 (1)_080	143	2.7	113	118	332	2790	278	2.4	1.70
WHG_2006/07 (1)_079	144	4.5	123	112	334	2670	280	3.2	1.76
WHG_2006/07 (1)_078	145	4.6	111	112	318	2670	268	3.6	1.66
WHG_2006/07 (1)_077	146	1.3	104	114	295	2670	282	3.7	1.46
WHG_2006/07 (1)_076	147	4.7	125	112	332	2710	274	2.7	1.77
WHG_2006/07 (1)_075	148	4.8	120	121	350	2920	281	2.6	1.85
WHG_2006/07 (1)_074	149	5.9	136	136	404	3220	315	3.4	2.09
WHG_2006/07 (1)_073	150	5.6	149	137	411	3310	327	2.8	2.17
WHG_2006/07 (1)_072	151	4.6	148	137	400	3320	318	3.4	2.10
WHG_2006/07 (1)_071	152	5.3	142	138	409	3370	326	3.2	2.16
WHG_2006/07 (1)_070	153	4.7	156	149	440	3700	350	4.2	2.29
WHG_2006/07 (1)_069	154	4.5	163	160	478	3990	371	3.0	2.47
WHG_2006/07 (1)_068	155	5.3	192	180	581	4760	439	4.5	2.93
WHG_2006/07 (1)_067	156	5.4	141	126	383	3160	303	4.6	2.04
WHG_2006/07 (1)_066	157	4.4	52	44	100	845	96	2.9	0.62
WHG_2006/07 (1)_065	158	4.5	54	35	87	710	86	6.1	0.58
WHG_2006/07 (1)_064	159	3.2	41	35	83	704	87	3.4	0.51
WHG_2006/07 (1)_063	160	2.7	43	35	89	734	87	3.8	0.53
WHG_2006/07 (1)_062	161	1.3	0	6	1	40	-1	-2.3	0.00
WHG_2006/07 (1)_061	162	2.3	40	31	78	635	83	4.0	0.47
WHG_2006/07 (1)_060	163	3.6	41	28	68	523	73	5.2	0.44
WHG_2006/07 (1)_059	164	3.7	52	50	121	889	84	3.7	0.69
WHG_2006/07 (1)_058	165	4.4	122	115	298	2310	140	7.5	1.70
WHG_2006/07 (1)_057	166	4.8	188	167	535	4060	187	5.8	2.76
WHG_2006/07 (1)_056	167	4.6	146	139	406	3070	159	7.3	2.19
WHG_2006/07 (1)_055	168	2.7	98	108	259	2060	131	2.7	1.52
WHG_2006/07 (1)_054	169	1.6	82	80	211	1760	92	1.8	1.15
WHG_2006/07 (1)_053	170	1.0	70	77	217	1530	51	1.8	1.07
WHG_2006/07 (1)_052	171	1.5	69	78	233	1560	51	2.2	1.14
WHG_2006/07 (1)_051	172	1.7	73	79	239	1580	53	2.2	1.16
WHG_2006/07 (1)_050	173	1.3	74	80	247	1600	54	1.8	1.21
WHG_2006/07 (1)_049	174	1.8	70	78	237	1540	53	1.8	1.14
WHG_2006/07 (1)_048	175	1.5	67	72	226	1480	54	1.5	1.08
WHG_2006/07 (1)_047	176	1.7	67	72	221	1420	54	1.9	1.06
WHG_2006/07 (1)_046	177	1.8	63	69	200	1310	54	2.0	0.98
WHG_2006/07 (1)_045	178	1.4	56	63	186	1250	55	1.6	0.94
WHG_2006/07 (1)_044	179	1.5	51	57	164	1160	54	2.2	0.83
WHG_2006/07 (1)_043	180	1.3	49	52	151	1100	50	1.3	0.77
WHG_2006/07 (1)_042	181	1.3	47	50	141	1090	49	1.3	0.75
WHG_2006/07 (1)_041	182	1.2	43	48	134	1040	48	1.5	0.68
WHG_2006/07 (1)_040	183	1.1	42	47	133	1020	48	1.6	0.67
WHG_2006/07 (1)_039	184	1.3	43	48	133	1030	47	1.4	0.68
WHG_2006/07 (1)_038	185	1.1	43	47	132	1030	47	1.4	0.67
WHG_2006/07 (1)_037	186	1.4	40	48	132	1040	47	1.5	0.65
WHG_2006/07 (1)_036	187	1.5	47	53	150	1160	51	1.5	0.76
WHG_2006/07 (1)_035	188	1.3	43	47	141	1040	47	1.5	0.72
WHG_2006/07 (1)_034	189	1.5	41	45	130	998	43	1.5	0.65
WHG_2006/07 (1)_033	190	1.2	40	45	123	973	39	1.2	0.62
WHG_2006/07 (1)_032	191	1.5	38	42	117	931	36	1.1	0.60
WHG_2006/07 (1)_031	192	1.3	38	40	114	863	33	1.2	0.58
WHG_2006/07 (1)_030	193	1.3	35	39	110	837	31	1.8	0.54
WHG_2006/07 (1)_029	194	1.6	37	40	110	829	30	1.3	0.55
WHG_2006/07 (1)_028	195	1.7	34	38	98	790	34	1.5	0.50
WHG_2006/07 (1)_027	196	1.3	35	35	94	777	45	2.2	0.50
WHG_2006/07 (1)_026	197	1.4	39	37	105	882	52	2.3	0.57
WHG_2006/07 (1)_025	198	1.7	46	36	103	912	61	2.7	0.58
WHG_2006/07 (1)_024	199	1.7	41	38	108	941	67	1.9	0.60
WHG_2006/07 (1)_023	200	1.3	56	47	134	1170	77	2.7	0.72

Table A4.8 continued.

Sample	Depth cm	Al ppb	Ca ppb	K ppb	Mg ppb	Na ppb	S ppb	Si ppb	Sr ppb
WHG_2006/07 (1)_022	201	1.6	49	46	138	1120	70	2.8	0.70
WHG_2006/07 (1)_021	202	1.5	44	46	139	1140	70	2.4	0.70
WHG_2006/07 (1)_020	203	1.8	44	45	133	1120	68	1.9	0.66
WHG_2006/07 (1)_019	204	1.5	45	46	133	1120	67	1.8	0.67
WHG_2006/07 (1)_018	205	1.9	44	46	129	1070	67	2.0	0.65
WHG_2006/07 (1)_017	206	1.7	42	45	130	1090	67	1.8	0.62
WHG_2006/07 (1)_016	207	1.3	49	47	139	1160	71	2.3	0.69
WHG_2006/07 (1)_015	208	1.5	45	47	141	1190	71	1.8	0.71
WHG_2006/07 (1)_014	209	1.8	47	47	143	1110	72	1.9	0.73
WHG_2006/07 (1)_013	210	2.0	44	43	130	1060	64	2.4	0.68
WHG_2006/07 (1)_012	211	1.4	34	37	104	886	52	2.2	0.50
WHG_2006/07 (1)_011	212	2.0	30	34	90	763	45	2.5	0.43
WHG_2006/07 (1)_010	213	1.2	30	31	87	771	52	2.4	0.43
WHG_2006/07 (1)_009	214	1.5	43	35	96	932	75	1.4	0.58
WHG_2006/07 (1)_008	215	1.8	50	35	90	927	83	2.1	0.57
WHG_2006/07 (1)_007	216	1.7	34	27	70	771	67	2.3	0.46
WHG_2006/07 (1)_006	217	1.7	24	22	53	458	32	2.3	0.28
WHG_2006/07 (1)_005	218	1.5	22	22	51	447	32	2.5	0.27
WHG_2006/07 (1)_004	219	2.1	28	23	53	452	32	2.4	0.30
WHG_2006/07 (1)_003	220	1.6	24	22	49	436	34	1.6	0.28
WHG_2006/07 (1)_002	221	1.4	23	19	47	382	42	2.2	0.26
WHG_2006/07 (1)_001	222	1.3	31	19	43	354	48	2.6	0.22

Table A4.9 Major and trace element chemistry of WHG_1b snow samples measured by ICP-OES. Analytical precision is determined by repeated measurement of quality control standard (QC_2). Values shown in grey are below the detection limit.

Sample	Depth cm	WHG_1 equiv. depth (cm)	Al ppb	Ca ppb	K ppb	Mg ppb	Na ppb	S ppb	Si ppb	Sr ppb
Spectrum measured			396.2	396.8	766.5	285.2	330.2	180.7	251.6	421.6
Detection limit (3 σ blanks)			0.40	4.6	0.35	0.29	40	0.59	0.79	0.00
Sample average			0.64	15	28	52	495	145	-5	0.26
Sample 2 std (%)			146	258	114	201	170	202	-53	256
Sample max			2.5	101	103	318	2490	501	BDL	1.88
Sample min			BDL	BDL	11	4	BDL	BDL	BDL	BDL
<hr/>										
WHG_2006/07 (1b)_090	190	199	0.31	17	35	59	632	40	-4.66	0.29
WHG_2006/07 (1b)_089	191	200	0.61	17	32	66	629	40	-4.75	0.32
WHG_2006/07 (1b)_088	192	201	0.75	21	35	70	656	46	-3.99	0.36
WHG_2006/07 (1b)_087	193	202	0.65	-7	11	4	128	-4	-8.38	-0.04
WHG_2006/07 (1b)_086	194	203	0.94	37	38	73	886	76	-4.94	0.55
WHG_2006/07 (1b)_085	195	204	0.94	3	21	33	291	10	-3.91	0.04
WHG_2006/07 (1b)_084	196	205	0.45	11	20	41	310	16	-4.16	0.15
WHG_2006/07 (1b)_083	197	206	0.93	34	47	111	960	60	-4.21	0.58
WHG_2006/07 (1b)_082	198	207	1.04	39	52	130	1120	69	-3.22	0.71
WHG_2006/07 (1b)_081	199	208	0.79	55	64	166	1320	86	-4.28	0.93
WHG_2006/07 (1b)_080	200	209	1.02	53	65	164	1320	87	-4.01	0.91
WHG_2006/07 (1b)_079	201	210	0.89	49	62	166	1360	87	-3.53	0.89
WHG_2006/07 (1b)_078	202	211	0.35	49	60	158	1210	81	-4.55	0.84
WHG_2006/07 (1b)_077	203	212	0.63	65	57	146	1120	75	-5.23	0.81
WHG_2006/07 (1b)_076	204	213	0.64	58	55	129	1460	149	-4.56	0.94
WHG_2006/07 (1b)_075	205	214	0.61	18	34	63	607	29	-4.64	0.32
WHG_2006/07 (1b)_074	206	215	0.55	25	34	57	577	24	-4.27	0.28
WHG_2006/07 (1b)_073	207	216	0.61	16	32	51	525	22	-4.76	0.26
WHG_2006/07 (1b)_072	208	217	0.47	14	33	50	508	22	-4.34	0.26
WHG_2006/07 (1b)_071	209	218	0.41	14	31	52	527	22	-4.53	0.27
WHG_2006/07 (1b)_070	210	219	0.30	15	30	51	527	22	-4.46	0.26
WHG_2006/07 (1b)_069	211	220	0.57	14	29	54	534	23	-4.05	0.27
WHG_2006/07 (1b)_068	212	221	0.48	14	29	53	523	22	-3.88	0.26
WHG_2006/07 (1b)_067	213	222	0.52	14	29	52	535	24	-3.88	0.29
WHG_2006/07 (1b)_066	214	223	0.70	22	30	49	580	37	-3.73	0.36
WHG_2006/07 (1b)_065	215	224	0.52	9	22	36	343	18	-4.42	0.14
WHG_2006/07 (1b)_064	216	225	0.76	15	27	50	499	33	-4.56	0.24
WHG_2006/07 (1b)_063	217	226	0.39	19	27	51	572	45	-4.53	0.31
WHG_2006/07 (1b)_062	218	227	0.73	9	26	33	337	24	-4.02	0.12
WHG_2006/07 (1b)_061	219	228	0.53	7	19	27	292	31	-3.69	0.11
WHG_2006/07 (1b)_060	220	229	0.87	32	23	31	300	41	-3.83	0.14
WHG_2006/07 (1b)_059	221	230	0.99	7	19	31	260	43	-2.52	0.11
WHG_2006/07 (1b)_058	222	231	1.73	16	26	45	425	58	-2.46	0.24
WHG_2006/07 (1b)_057	223	232	2.13	23	28	55	511	65	-1.19	0.32
WHG_2006/07 (1b)_056	224	233	2.04	26	29	59	577	68	-1.62	0.35
WHG_2006/07 (1b)_055	225	234	2.07	22	31	61	583	74	-0.878	0.37
WHG_2006/07 (1b)_054	226	235	1.74	22	31	62	608	79	-2.77	0.37
WHG_2006/07 (1b)_053	227	236	0.79	13	30	56	524	77	-4.87	0.25
WHG_2006/07 (1b)_052	228	237	0.39	17	28	56	562	84	-5.4	0.26
WHG_2006/07 (1b)_051	229	238	0.57	14	28	59	574	93	-5.34	0.29
WHG_2006/07 (1b)_050	230	239	0.23	14	27	54	515	91	-5.5	0.26
WHG_2006/07 (1b)_049	231	240	0.38	14	27	51	525	91	-5.74	0.25
WHG_2006/07 (1b)_048	232	241	0.49	6	23	31	330	58	-5.64	0.11
WHG_2006/07 (1b)_047	233	242	0.21	4	21	27	304	51	-5.31	0.10
WHG_2006/07 (1b)_046	234	243	0.12	5	21	28	295	52	-5.65	0.11
WHG_2006/07 (1b)_045	235	244	0.19	4	22	23	263	47	-5.4	0.08
WHG_2006/07 (1b)_044	236	245	0.33	5	16	17	206	36	-4.87	0.04
WHG_2006/07 (1b)_043	237	246	0.40	2	14	15	173	29	-5.22	0.03
WHG_2006/07 (1b)_042	238	247	0.51	1	22	14	178	31	-5.07	0.02
WHG_2006/07 (1b)_041	239	248	0.21	1	15	13	147	26	-5.02	0.01
WHG_2006/07 (1b)_040	240	249	0.23	8	15	14	176	28	-4.33	0.02
WHG_2006/07 (1b)_039	241	250	0.29	6	17	24	246	38	-4.58	0.07
WHG_2006/07 (1b)_038	242	251	0.23	11	27	44	358	51	-4.61	0.16
WHG_2006/07 (1b)_037	243	252	0.96	96	92	266	2300	327	-5.71	1.80
WHG_2006/07 (1b)_036	244	253	1.27	101	103	318	2490	354	-5	1.88

Table A4.9 continued.

Sample	Depth cm	WHG_1 equiv. depth (cm)	Al ppb	Ca ppb	K ppb	Mg ppb	Na ppb	S ppb	Si ppb	Sr ppb
WHG_2006/07 (1b)_035	245	254	0.70	19	44	95	673	146	-5.54	0.35
WHG_2006/07 (1b)_034	246	255	1.38	44	39	97	909	257	-6.15	0.61
WHG_2006/07 (1b)_033	247	256	0.52	6	25	46	391	214	-6.37	0.14
WHG_2006/07 (1b)_032	248	257	0.29	0	16	17	193	192	-6.49	0.04
WHG_2006/07 (1b)_031	249	258	2.53	1	16	15	190	195	-5.86	0.03
WHG_2006/07 (1b)_030	250	259	0.40	1	15	14	168	211	-6.53	0.03
WHG_2006/07 (1b)_029	251	260	0.17	-2	13	9	144	213	-6.52	-0.01
WHG_2006/07 (1b)_028	252	261	0.14	-3	12	6	104	220	-6.38	-0.03
WHG_2006/07 (1b)_027	253	262	0.15	-3	12	6	119	253	-6.08	-0.02
WHG_2006/07 (1b)_026	254	263	0.42	-3	12	7	97.8	263	-5.78	-0.02
WHG_2006/07 (1b)_025	255	264	0.26	0	13	9	120	302	-6.55	-0.01
WHG_2006/07 (1b)_024	256	265	0.61	0	20	14	173	419	-6.81	0.02
WHG_2006/07 (1b)_023	257	266	0.46	5	19	21	232	488	-6.25	0.07
WHG_2006/07 (1b)_022	258	267	0.50	4	19	25	277	501	-6.33	0.10
WHG_2006/07 (1b)_021	259	268	0.67	5	21	32	328	492	-6.72	0.13
WHG_2006/07 (1b)_020	260	269	0.64	7	23	37	368	484	-6.8	0.16
WHG_2006/07 (1b)_019	261	270	0.52	9	30	39	390	485	-6.86	0.17
WHG_2006/07 (1b)_018	262	271	0.83	12	31	43	414	479	-6.86	0.20
WHG_2006/07 (1b)_017	263	272	0.66	12	33	45	446	478	-6.19	0.21
WHG_2006/07 (1b)_016	264	273	0.34	14	31	53	509	468	-6.82	0.26
WHG_2006/07 (1b)_015	265	274	0.26	13	30	51	488	412	-6.43	0.25
WHG_2006/07 (1b)_014	266	275	0.46	11	30	46	447	364	-5.96	0.22
WHG_2006/07 (1b)_013	267	276	0.45	10	30	42	414	322	-7.19	0.18
WHG_2006/07 (1b)_012	268	277	0.24	6	22	32	341	248	-6.6	0.13
WHG_2006/07 (1b)_011	269	278	0.37	8	22	39	392	271	-6.79	0.17
WHG_2006/07 (1b)_010	270	279	0.26	4	20	31	307	223	-6.31	0.11
WHG_2006/07 (1b)_009	271	280	0.00	2	18	24	256	192	-6.21	0.10
WHG_2006/07 (1b)_008	272	281	0.56	1	17	20	244	177	-5.27	0.06
WHG_2006/07 (1b)_007	273	282	0.24	0	15	16	188	142	-5.75	0.03
WHG_2006/07 (1b)_006	274	283	0.46	-2	14	12	149	119	-5.44	0.01
WHG_2006/07 (1b)_005	275	284	0.46	-2	14	11	154	112	-5.64	0.01
WHG_2006/07 (1b)_004	276	285	0.60	0	14	11	158	103	-5.76	0.01
WHG_2006/07 (1b)_003	277	286	0.47	-2	14	12	172	105	-5.32	0.01
WHG_2006/07 (1b)_002	278	287	0.75	-2	14	11	149	86	-4.95	0.01
WHG_2006/07 (1b)_001	279	288	1.05	-1	15	12	169	66	-4.37	0.02

Table A4.10 Major and trace element chemistry of WHG_2 snow samples measured by ICP-OES. Analytical precision is determined by repeated measurement of quality control standard (QC_2). Values shown in grey are below the detection limit.

Sample	Depth cm	Al ppb	Ca ppb	K ppb	Mg ppb	Na ppb	S ppb	Si ppb	Sr ppb
Spectrum		396.2	396.8	766.5	285.2	330.2	180.7	251.6	421.6
Detection limit (3 σ blanks)		0.40	4.6	0.35	0.29	40	0.59	0.79	0.004
Sample average		1	26	30	73	613	88	1	0
Sample 2 rsd (%)		221	165	139	165	161	159	144	166
Sample max		11	156	136	435	3560	296	3.1	2.4
Sample min		BDL	BDL	6	BDL	BDL	BDL	BDL	BDL
WHG_2006/07 (2)_170	1	3.2	74	90	181	1520	236	1.5	1.02
WHG_2006/07 (2)_169	2	5.4	51	95	135	1270	169	1.7	0.70
WHG_2006/07 (2)_168	3	2.8	78	95	185	1630	240	1.3	1.02
WHG_2006/07 (2)_167	4	2.2	72	92	188	1720	244	2.0	1.01
WHG_2006/07 (2)_166	5	2.4	78	103	186	1660	288	1.0	1.06
WHG_2006/07 (2)_165	6	2.3	64	75	150	1310	225	1.8	0.85
WHG_2006/07 (2)_164	7	2.2	41	46	108	920	145	1.7	0.58
WHG_2006/07 (2)_163	8	3.0	27	30	74	662	96	2.1	0.38
WHG_2006/07 (2)_162	9	2.2	59	55	129	1100	222	1.5	0.77
WHG_2006/07 (2)_161	10	3.3	16	22	45	473	73	1.5	0.29
WHG_2006/07 (2)_160	11	0.7	17	19	37	403	67	0.4	0.24
WHG_2006/07 (2)_159	12	3.8	14	19	39	392	67	1.2	0.26
WHG_2006/07 (2)_158	13	5.7	15	20	42	381	67	1.1	0.27
WHG_2006/07 (2)_157	14	11.2	15	20	41	376	69	1.6	0.27
WHG_2006/07 (2)_156	15	10.8	16	19	40	408	67	1.5	0.26
WHG_2006/07 (2)_155	16	0.9	-3	6	-2	-88	-4	-2.7	-0.01
WHG_2006/07 (2)_154	17	1.5	15	19	42	376	69	1.2	0.27
WHG_2006/07 (2)_153	18	1.9	15	20	42	402	68	0.0	0.27
WHG_2006/07 (2)_152	19	1.1	17	19	43	411	69	1.0	0.29
WHG_2006/07 (2)_151	20	1.7	14	20	42	399	70	1.2	0.27
WHG_2006/07 (2)_150	21	1.5	14	20	41	404	69	1.1	0.26
WHG_2006/07 (2)_149	22	1.5	16	20	38	392	68	0.9	0.25
WHG_2006/07 (2)_148	23	1.5	13	18	34	360	61	0.3	0.22
WHG_2006/07 (2)_147	24	1.2	5	11	15	145	23	0.3	0.09
WHG_2006/07 (2)_146	25	0.9	5	11	12	114	18	0.3	0.07
WHG_2006/07 (2)_145	26	0.8	5	11	12	132	16	0.7	0.08
WHG_2006/07 (2)_144	27	0.8	3	11	12	129	18	0.3	0.08
WHG_2006/07 (2)_143	28	1.1	3	11	11	120	17	0.8	0.07
WHG_2006/07 (2)_142	29	0.8	5	13	15	158	23	0.4	0.10
WHG_2006/07 (2)_141	30	0.8	10	17	30	260	34	0.7	0.18
WHG_2006/07 (2)_140	31	0.6	10	18	36	327	35	0.5	0.21
WHG_2006/07 (2)_139	32	0.3	11	18	35	309	33	0.2	0.20
WHG_2006/07 (2)_138	33	0.5	11	17	34	288	32	0.9	0.19
WHG_2006/07 (2)_137	34	0.5	16	23	51	494	35	0.6	0.31
WHG_2006/07 (2)_136	35	0.8	27	35	80	742	42	0.6	0.48
WHG_2006/07 (2)_135	36	0.7	32	42	103	998	55	0.3	0.62
WHG_2006/07 (2)_134	37	0.7	45	53	143	1280	75	0.7	0.86
WHG_2006/07 (2)_133	38	0.6	50	55	155	1340	81	1.1	0.95
WHG_2006/07 (2)_132	39	0.8	48	52	143	1230	84	1.0	0.86
WHG_2006/07 (2)_131	40	0.8	42	50	132	1200	82	1.4	0.78
WHG_2006/07 (2)_130	41	0.9	39	48	126	1180	82	0.8	0.76
WHG_2006/07 (2)_129	42	0.9	38	47	121	1140	79	1.0	0.71
WHG_2006/07 (2)_128	43	0.8	36	44	112	1090	74	1.1	0.66
WHG_2006/07 (2)_127	44	0.8	37	41	108	994	71	1.6	0.66
WHG_2006/07 (2)_126	45	0.8	34	37	94	874	66	0.5	0.54
WHG_2006/07 (2)_125	46	1.1	29	35	86	808	62	1.5	0.51
WHG_2006/07 (2)_124	47	0.6	28	36	89	846	64	0.5	0.52
WHG_2006/07 (2)_123	48	0.7	25	35	84	797	64	1.5	0.47
WHG_2006/07 (2)_122	49	1.1	26	31	76	669	54	1.9	0.42
WHG_2006/07 (2)_121	50	0.3	33	28	62	605	52	1.3	0.34
WHG_2006/07 (2)_120	51	0.7	23	29	74	663	54	1.2	0.41
WHG_2006/07 (2)_119	52	0.5	25	30	76	677	55	1.1	0.40
WHG_2006/07 (2)_118	53	0.8	26	32	83	726	56	1.1	0.45
WHG_2006/07 (2)_117	54	0.7	26	32	80	721	55	1.1	0.44

Table A4.10 continued.

Sample	Depth cm	Al ppb	Ca ppb	K ppb	Mg ppb	Na ppb	S ppb	Si ppb	Sr ppb
WHG_2006/07 (2)_116	55	0.8	25	33	80	722	55	0.7	0.44
WHG_2006/07 (2)_115	56	0.4	26	33	82	770	56	1.0	0.46
WHG_2006/07 (2)_114	57	0.6	29	35	85	779	55	0.5	0.50
WHG_2006/07 (2)_113	58	0.7	27	35	87	783	56	1.1	0.49
WHG_2006/07 (2)_112	59	0.8	27	35	85	791	55	0.6	0.46
WHG_2006/07 (2)_111	60	0.5	28	37	91	862	57	1.3	0.50
WHG_2006/07 (2)_110	61	0.9	28	36	83	794	54	1.1	0.46
WHG_2006/07 (2)_109	62	1.0	29	33	84	766	54	1.4	0.49
WHG_2006/07 (2)_108	63	0.7	29	23	52	466	38	0.9	0.33
WHG_2006/07 (2)_107	64	0.7	4	10	12	83	9	1.2	0.07
WHG_2006/07 (2)_106	65	0.5	5	9	8	42	6	1.6	0.05
WHG_2006/07 (2)_105	66	0.5	8	9	5	49	5	0.9	0.03
WHG_2006/07 (2)_104	67	0.6	1	11	6	6	6	0.6	0.03
WHG_2006/07 (2)_103	68	0.7	4	8	6	38	5	0.6	0.03
WHG_2006/07 (2)_102	69	0.6	1	8	6	16	5	0.4	0.03
WHG_2006/07 (2)_101	70	0.7	2	9	6	2	5	0.9	0.04
WHG_2006/07 (2)_100	71	0.7	31	30	73	734	60	0.6	0.49
WHG_2006/07 (2)_099	72	1.3	34	34	85	702	49	0.9	0.51
WHG_2006/07 (2)_098	73	0.9	47	48	129	1130	77	1.4	0.75
WHG_2006/07 (2)_097	74	1.0	48	50	134	1100	74	1.3	0.76
WHG_2006/07 (2)_096	75	1.1	45	50	138	1130	73	1.7	0.76
WHG_2006/07 (2)_095	76	1.3	54	52	147	1160	80	1.1	0.82
WHG_2006/07 (2)_094	77	1.5	54	55	154	1250	86	1.1	0.87
WHG_2006/07 (2)_093	78	1.0	43	46	124	1040	68	1.0	0.66
WHG_2006/07 (2)_092	79	0.8	41	43	123	974	61	1.3	0.65
WHG_2006/07 (2)_091	80	1.3	39	44	117	938	61	1.5	0.70
WHG_2006/07 (2)_090	81	0.9	32	36	99	761	47	1.1	0.53
WHG_2006/07 (2)_089	82	0.7	26	26	66	492	33	1.1	0.33
WHG_2006/07 (2)_088	83	0.8	31	36	89	726	47	1.4	0.48
WHG_2006/07 (2)_087	84	0.8	60	60	166	1390	94	0.9	0.98
WHG_2006/07 (2)_086	85	1.2	69	66	176	1450	106	0.9	1.06
WHG_2006/07 (2)_085	86	0.6	36	41	117	887	55	1.0	0.57
WHG_2006/07 (2)_084	87	0.5	33	36	112	777	45	0.7	0.54
WHG_2006/07 (2)_083	88	0.6	41	38	124	804	47	0.8	0.62
WHG_2006/07 (2)_082	89	0.5	33	39	125	843	50	1.7	0.55
WHG_2006/07 (2)_081	90	0.6	39	40	119	867	50	1.2	0.52
WHG_2006/07 (2)_080	91	0.9	38	49	138	1040	52	1.0	0.64
WHG_2006/07 (2)_079	92	0.8	46	50	151	1100	57	1.3	0.75
WHG_2006/07 (2)_078	93	0.9	45	50	149	1060	53	1.2	0.69
WHG_2006/07 (2)_077	94	0.5	47	52	158	1160	56	0.9	0.79
WHG_2006/07 (2)_076	95	0.7	48	55	160	1210	59	1.2	0.77
WHG_2006/07 (2)_075	96	0.9	47	53	163	1180	57	1.4	0.78
WHG_2006/07 (2)_074	97	1.2	104	94	294	2350	164	2.5	1.61
WHG_2006/07 (2)_073	98	1.9	156	136	435	3560	283	3.1	2.38
WHG_2006/07 (2)_072	99	1.3	56	55	168	1290	97	2.1	0.89
WHG_2006/07 (2)_071	100	2.0	46	45	127	990	71	2.4	0.67
WHG_2006/07 (2)_070	101	0.4	30	28	83	518	27	1.2	0.45
WHG_2006/07 (2)_069	102	0.5	33	36	110	399	24	0.4	0.54
WHG_2006/07 (2)_068	103	0.8	44	39	132	383	22	0.5	0.74
WHG_2006/07 (2)_067	104	0.6	33	38	114	376	22	0.4	0.55
WHG_2006/07 (2)_066	105	0.5	23	26	75	261	20	0.2	0.38
WHG_2006/07 (2)_065	106	0.7	14	22	50	243	19	0.6	0.23
WHG_2006/07 (2)_064	107	1.0	17	27	52	329	31	0.1	0.27
WHG_2006/07 (2)_063	108	0.8	30	31	78	713	89	0.9	0.43
WHG_2006/07 (2)_062	109	0.8	39	34	98	846	127	1.0	0.56
WHG_2006/07 (2)_061	110	1.1	44	42	118	1100	166	1.1	0.60
WHG_2006/07 (2)_060	111	0.8	34	30	81	752	127	0.5	0.43
WHG_2006/07 (2)_059	112	0.9	42	33	98	893	142	0.7	0.53
WHG_2006/07 (2)_058	113	0.7	20	26	66	642	116	0.4	0.32
WHG_2006/07 (2)_057	114	0.6	24	25	64	616	114	0.0	0.32
WHG_2006/07 (2)_056	115	0.8	22	25	63	630	119	0.8	0.30
WHG_2006/07 (2)_055	116	1.1	22	26	62	611	119	1.0	0.30
WHG_2006/07 (2)_054	117	0.7	22	26	66	631	121	0.7	0.32
WHG_2006/07 (2)_053	118	1.2	23	27	66	643	124	0.2	0.34
WHG_2006/07 (2)_052	119	0.8	20	25	62	606	123	0.8	0.29
WHG_2006/07 (2)_051	120	0.7	10	17	28	288	96	0.1	0.13

Table A4.10 continued.

Sample	Depth cm	Al ppb	Ca ppb	K ppb	Mg ppb	Na ppb	S ppb	Si ppb	Sr ppb
WHG_2006/07 (2)_050	121	0.5	10	16	31	303	99	0.7	0.15
WHG_2006/07 (2)_049	122	0.7	7	12	18	192	110	0.4	0.09
WHG_2006/07 (2)_048	123	0.9	9	15	30	284	153	0.4	0.15
WHG_2006/07 (2)_047	124	0.7	12	15	29	293	178	-0.3	0.14
WHG_2006/07 (2)_046	125	1.1	21	23	44	413	232	0.0	0.22
WHG_2006/07 (2)_045	126	1.0	16	21	48	463	246	0.1	0.23
WHG_2006/07 (2)_044	127	1.2	24	23	63	547	262	0.5	0.35
WHG_2006/07 (2)_043	128	1.2	21	23	52	519	247	0.0	0.26
WHG_2006/07 (2)_042	129	1.6	19	22	50	497	200	1.2	0.25
WHG_2006/07 (2)_041	130	1.2	32	24	59	557	229	-0.2	0.31
WHG_2006/07 (2)_040	131	0.9	27	26	66	613	255	0.1	0.32
WHG_2006/07 (2)_039	132	0.8	28	26	74	637	200	0.2	0.40
WHG_2006/07 (2)_038	133	1.4	23	28	66	649	196	0.2	0.32
WHG_2006/07 (2)_037	134	1.0	21	27	65	644	251	0.3	0.31
WHG_2006/07 (2)_036	135	1.4	23	25	60	590	264	0.3	0.30
WHG_2006/07 (2)_035	136	0.9	26	23	60	575	288	0.3	0.30
WHG_2006/07 (2)_034	137	1.4	23	26	61	555	296	0.3	0.30
WHG_2006/07 (2)_033	138	1.9	30	29	73	696	288	0.9	0.41
WHG_2006/07 (2)_031	140	1.1	8	14	21	212	76	0.6	0.10
WHG_2006/07 (2)_030	141	1.0	4	11	15	150	47	1.0	0.07
WHG_2006/07 (2)_029	142	0.7	3	10	12	134	44	0.8	0.06
WHG_2006/07 (2)_028	143	0.7	4	8	5	43	42	0.9	0.02
WHG_2006/07 (2)_027	144	0.9	6	8	4	32	27	1.1	0.02
WHG_2006/07 (2)_026	145	0.8	4	12	4	31	41	0.9	0.03
WHG_2006/07 (2)_025	146	0.8	1	7	3	46	38	0.3	0.01
WHG_2006/07 (2)_024	147	0.6	1	7	3	19	39	1.2	0.01
WHG_2006/07 (2)_023	148	0.9	2	8	4	17	42	0.4	0.02
WHG_2006/07 (2)_022	149	0.6	4	7	6	29	47	0.1	0.03
WHG_2006/07 (2)_021	150	0.6	3	7	6	53	64	0.7	0.03
WHG_2006/07 (2)_020	151	0.8	1	7	1	-11	62	0.9	0.00
WHG_2006/07 (2)_019	152	0.9	1	7	1	9	57	0.2	0.01
WHG_2006/07 (2)_018	153	0.7	0	6	1	-8	54	-0.4	0.00
WHG_2006/07 (2)_017	154	1.0	5	8	2	21	65	0.9	0.01
WHG_2006/07 (2)_016	155	0.6	0	6	0	-29	61	0.5	0.00
WHG_2006/07 (2)_015	156	0.4	0	6	-1	-31	46	0.5	0.00
WHG_2006/07 (2)_014	157	1.0	0	7	0	-21	45	0.7	0.00
WHG_2006/07 (2)_013	158	0.7	0	7	2	11	54	0.5	0.01
WHG_2006/07 (2)_012	159	0.9	7	11	16	136	101	0.5	0.08
WHG_2006/07 (2)_011	160	0.7	5	12	20	194	131	0.4	0.09
WHG_2006/07 (2)_010	161	2.2	18	16	34	323	143	1.8	0.22
WHG_2006/07 (2)_008	163	2.5	20	18	35	319	144	2.1	0.21
WHG_2006/07 (2)_007	164	1.7	16	15	31	248	106	1.2	0.20
WHG_2006/07 (2)_006	165	1.5	12	15	27	210	78	1.3	0.16
WHG_2006/07 (2)_005	166	1.1	10	15	30	290	65	0.7	0.14
WHG_2006/07 (2)_004	167	1.2	11	16	35	329	69	0.6	0.17
WHG_2006/07 (2)_003	168	0.8	11	15	34	269	67	0.3	0.16
WHG_2006/07 (2)_002	169	1.1	10	15	32	224	62	0.7	0.14
WHG_2006/07 (2)_001	170	1.4	20	17	34	243	65	1.7	0.16

Table A4.11 Major and trace element chemistry of WHG_3 snow samples measured by ICP-OES. Analytical precision is determined by repeated measurement of quality control standard (QC_2). Values shown in grey are below the detection limit.

Sample	Depth	Al ppb	Ca ppb	K ppb	Mg ppb	Na ppb	S ppb	Si ppb	Sr ppb
Spectrum		396.2	396.8	766.5	285.2	330.2	180.7	251.6	421.6
Detection limit (3 σ blanks)		0.40	4.6	0.35	0.29	40	0.59	0.79	0.004
Sample average	1	33	37	86	743	68	2	0	
Sample 2 rsd (%)	68	144	132	169	159	159	176	169	
Sample max	3	123	116	356	2930	286	5	2	
Sample min	1	BDL	6	1	BDL	BDL	BDL	BDL	
WHG_2006/07 (3)_112	1	2.6	74	83	210	1820	210	4.5	1.10
WHG_2006/07 (3)_111	2	2.5	76	79	206	1700	198	4.1	1.10
WHG_2006/07 (3)_110	3	2.4	69	70	205	1730	194	5.0	1.07
WHG_2006/07 (3)_109	4	2.1	75	68	197	1680	188	4.1	1.03
WHG_2006/07 (3)_108	5	2.3	74	69	209	1790	193	4.4	1.10
WHG_2006/07 (3)_107	6	2.3	75	71	216	1750	191	3.7	1.19
WHG_2006/07 (3)_106	7	1.9	69	71	209	1830	192	4.3	1.09
WHG_2006/07 (3)_105	8	3.2	123	116	356	2930	286	4.5	1.94
WHG_2006/07 (3)_104	9	2.6	84	86	256	2110	221	3.9	1.33
WHG_2006/07 (3)_103	10	2.3	85	82	247	1980	203	2.7	1.34
WHG_2006/07 (3)_102	11	1.8	56	55	165	1400	152	2.3	0.86
WHG_2006/07 (3)_101	12	1.1	36	33	89	754	96	1.7	0.47
WHG_2006/07 (3)_100	13	1.3	20	25	55	453	75	1.4	0.28
WHG_2006/07 (3)_099	14	1.1	18	20	43	377	65	2.6	0.22
WHG_2006/07 (3)_098	15	1.1	13	20	40	346	60	1.9	0.20
WHG_2006/07 (3)_097	16	0.8	13	19	38	325	56	2.1	0.19
WHG_2006/07 (3)_096	17	0.7	19	19	41	326	59	1.6	0.20
WHG_2006/07 (3)_095	18	1.1	18	23	56	456	75	2.8	0.28
WHG_2006/07 (3)_094	19	1.4	21	27	63	508	83	2.4	0.30
WHG_2006/07 (3)_093	20	1.4	24	30	73	591	82	3.7	0.38
WHG_2006/07 (3)_092	21	1.6	25	29	66	573	78	3.8	0.34
WHG_2006/07 (3)_091	22	1.9	22	29	62	532	74	3.9	0.32
WHG_2006/07 (3)_090	23	1.5	22	29	63	572	74	3.5	0.32
WHG_2006/07 (3)_089	24	1.7	25	25	65	548	76	3.3	0.33
WHG_2006/07 (3)_088	25	1.7	20	31	59	504	73	3.8	0.30
WHG_2006/07 (3)_087	26	1.6	21	27	55	465	67	3.6	0.28
WHG_2006/07 (3)_086	27	1.7	25	24	62	483	67	3.1	0.35
WHG_2006/07 (3)_085	28	1.4	17	26	52	464	66	3.5	0.27
WHG_2006/07 (3)_084	29	1.4	17	23	53	448	65	3.4	0.27
WHG_2006/07 (3)_083	30	1.5	21	27	62	531	73	4.0	0.32
WHG_2006/07 (3)_082	31	1.7	27	24	63	484	73	3.9	0.33
WHG_2006/07 (3)_081	32	1.6	29	23	61	493	73	3.6	0.32
WHG_2006/07 (3)_080	33	1.6	30	24	61	452	72	3.0	0.32
WHG_2006/07 (3)_079	34	1.3	33	23	58	478	70	2.8	0.31
WHG_2006/07 (3)_078	35	1.9	21	24	44	440	66	2.5	0.27
WHG_2006/07 (3)_077	36	1.6	15	16	23	233	38	1.9	0.14
WHG_2006/07 (3)_076	37	2.1	22	23	46	477	68	3.2	0.29
WHG_2006/07 (3)_075	38	1.8	23	25	43	433	67	3.0	0.27
WHG_2006/07 (3)_074	39	2.0	18	21	40	424	63	4.1	0.25
WHG_2006/07 (3)_073	40	1.3	0	6	1	69	-1	-2.6	0.00
WHG_2006/07 (3)_072	41	1.2	9	10	7	46	16	1.3	0.05
WHG_2006/07 (3)_071	42	1.3	8	13	5	39	13	0.3	0.03
WHG_2006/07 (3)_070	43	1.0	8	10	4	45	11	-0.1	0.03
WHG_2006/07 (3)_069	44	1.3	0	6	1	58	-1	-2.6	0.00
WHG_2006/07 (3)_068	45	1.0	6	8	5	27	12	0.2	0.03
WHG_2006/07 (3)_067	46	1.2	10	15	9	65	18	0.5	0.06
WHG_2006/07 (3)_066	47	1.1	6	15	9	64	21	0.5	0.06
WHG_2006/07 (3)_065	48	1.0	7	10	10	114	21	0.7	0.06
WHG_2006/07 (3)_064	49	1.3	6	14	10	104	21	0.1	0.06
WHG_2006/07 (3)_063	50	0.9	6	12	10	83	20	0.4	0.06
WHG_2006/07 (3)_062	51	1.0	10	12	10	98	20	0.6	0.06
WHG_2006/07 (3)_061	52	1.1	12	14	21	219	30	0.9	0.12
WHG_2006/07 (3)_060	53	1.2	18	21	36	343	41	0.7	0.22
WHG_2006/07 (3)_059	54	1.0	16	21	34	344	41	0.4	0.21
WHG_2006/07 (3)_058	55	1.1	15	21	35	341	42	0.8	0.21

Table A4.11 continued.

Sample	Depth	Al ppb	Ca ppb	K ppb	Mg ppb	Na ppb	S ppb	Si ppb	Sr ppb
WHG_2006/07 (3)_057	56	1.1	16	19	30	303	38	0.5	0.18
WHG_2006/07 (3)_056	57	1.2	17	18	30	286	39	0.8	0.19
WHG_2006/07 (3)_055	58	1.0	16	21	29	301	37	1.2	0.18
WHG_2006/07 (3)_054	59	1.1	13	18	28	279	37	0.7	0.17
WHG_2006/07 (3)_053	60	1.1	15	19	31	279	38	1.0	0.18
WHG_2006/07 (3)_052	61	1.1	21	21	38	349	34	0.5	0.22
WHG_2006/07 (3)_051	62	0.9	23	25	52	496	33	0.7	0.30
WHG_2006/07 (3)_050	63	1.2	31	37	74	693	38	1.4	0.45
WHG_2006/07 (3)_049	64	1.3	34	37	84	753	38	1.2	0.51
WHG_2006/07 (3)_048	65	1.0	21	29	54	562	33	0.4	0.33
WHG_2006/07 (3)_047	66	1.0	24	31	48	500	31	1.1	0.30
WHG_2006/07 (3)_046	67	1.1	18	24	46	507	30	1.1	0.28
WHG_2006/07 (3)_045	68	1.1	33	34	73	785	44	1.2	0.46
WHG_2006/07 (3)_044	69	1.3	32	41	95	928	54	0.9	0.56
WHG_2006/07 (3)_043	70	0.9	42	43	103	1000	57	0.6	0.60
WHG_2006/07 (3)_042	71	1.2	39	45	111	1060	61	1.3	0.65
WHG_2006/07 (3)_041	72	1.0	41	49	119	1100	62	1.4	0.70
WHG_2006/07 (3)_040	73	0.9	41	45	109	1040	58	0.6	0.65
WHG_2006/07 (3)_039	74	0.9	41	48	117	1120	64	1.0	0.69
WHG_2006/07 (3)_038	75	1.3	31	36	78	787	49	1.2	0.50
WHG_2006/07 (3)_037	76	1.0	15	19	24	248	19	0.6	0.16
WHG_2006/07 (3)_036	77	0.8	8	11	8	63	8	0.6	0.05
WHG_2006/07 (3)_035	78	0.9	10	12	8	56	8	1.1	0.05
WHG_2006/07 (3)_034	79	1.1	12	13	8	46	8	1.2	0.06
WHG_2006/07 (3)_033	80	1.1	15	15	14	167	16	0.8	0.10
WHG_2006/07 (3)_032	81	1.1	20	26	42	457	34	0.8	0.27
WHG_2006/07 (3)_031	82	1.2	33	33	67	701	48	1.7	0.43
WHG_2006/07 (3)_030	83	1.6	42	49	104	1100	69	1.3	0.66
WHG_2006/07 (3)_029	84	1.6	61	72	174	1640	97	1.3	1.07
WHG_2006/07 (3)_028	85	1.2	74	74	177	1670	99	1.4	1.05
WHG_2006/07 (3)_027	86	0.9	52	55	131	1180	66	0.4	0.78
WHG_2006/07 (3)_026	87	1.4	35	36	85	666	27	0.5	0.50
WHG_2006/07 (3)_025	88	1.1	34	42	94	668	25	0.3	0.53
WHG_2006/07 (3)_024	89	0.8	49	61	145	1100	36	0.3	0.84
WHG_2006/07 (3)_023	90	1.2	86	99	264	1880	108	0.4	1.57
WHG_2006/07 (3)_022	91	1.1	94	109	293	2170	140	0.7	1.74
WHG_2006/07 (3)_021	92	1.3	89	104	277	2090	148	0.9	1.64
WHG_2006/07 (3)_020	93	1.2	59	67	169	1310	91	0.7	0.98
WHG_2006/07 (3)_019	94	1.1	39	39	86	735	49	0.7	0.49
WHG_2006/07 (3)_018	95	1.1	24	27	64	559	37	0.3	0.35
WHG_2006/07 (3)_017	96	0.9	26	27	59	515	35	0.5	0.33
WHG_2006/07 (3)_016	97	1.0	26	29	75	574	37	1.0	0.39
WHG_2006/07 (3)_015	98	1.1	29	33	78	674	39	0.4	0.42
WHG_2006/07 (3)_014	99	1.0	38	34	92	705	39	0.5	0.53
WHG_2006/07 (3)_013	100	1.0	35	34	86	745	43	0.4	0.46
WHG_2006/07 (3)_012	101	0.9	30	33	86	705	41	0.9	0.45
WHG_2006/07 (3)_011	102	0.9	31	38	93	750	43	0.7	0.49
WHG_2006/07 (3)_010	103	1.0	36	37	91	709	43	1.2	0.46
WHG_2006/07 (3)_009	104	1.2	33	43	99	773	46	0.6	0.50
WHG_2006/07 (3)_008	105	1.1	39	47	112	1000	53	1.4	0.60
WHG_2006/07 (3)_006	107	1.5	59	83	159	1350	71	1.4	0.87
WHG_2006/07 (3)_005	108	1.5	53	63	165	1380	74	2.0	0.90
WHG_2006/07 (3)_004	109	1.5	54	70	161	1450	87	1.9	0.93
WHG_2006/07 (3)_003	110	1.6	66	66	158	1500	103	1.7	0.99
WHG_2006/07 (3)_002	111	1.9	63	66	125	1280	130	1.8	0.90
WHG_2006/07 (3)_001	112	2.3	46	82	78	799	107	0.9	0.52

Table A4.12 Major and trace element chemistry of WHG_4 snow samples measured by ICP-OES. Analytical precision is determined by repeated measurement of quality control standard (QC_2). Values shown in grey are below the detection limit.

Sample	Depth cm	Al ppb	Ca ppb	K ppb	Mg ppb	Na ppb	S ppb	Si ppb	Sr ppb
Spectrum		396.2	396.8	766.5	285.2	330.2	180.7	251.6	421.6
Detection limit (3 σ blanks)		0.40	4.6	0.35	0.29	40	0.59	0.79	0.004
Sample average		1	42	53	145	1086	74	BDL	1
Sample 2 rsd (%)		154	261	194	229	224	272	BDL	245
Sample max		3	357	349	1090	8160	654	6	5
Sample min		BDL	BDL	11	4	61	BDL	BDL	BDL
WHG_2006/07 (4)_102	1	0.88	9	23	30	337	31	-4	0.13
WHG_2006/07 (4)_101	2	0.40	5	18	25	292	19	-4	0.09
WHG_2006/07 (4)_100	3	0.39	4	18	25	261	18	-4	0.09
WHG_2006/07 (4)_099	4	0.57	4	19	25	265	19	-5	0.09
WHG_2006/07 (4)_098	5	0.82	2	17	24	253	19	-4	0.08
WHG_2006/07 (4)_097	6	0.37	2	18	25	269	18	-4	0.09
WHG_2006/07 (4)_096	7	0.52	2	18	25	250	18	-5	0.08
WHG_2006/07 (4)_095	8	0.48	7	22	33	358	24	-4	0.15
WHG_2006/07 (4)_094	9	0.43	26	41	76	821	45	-4	0.47
WHG_2006/07 (4)_093	10	0.53	27	43	94	866	42	-5	0.51
WHG_2006/07 (4)_092	11	0.81	40	45	104	852	46	-4	0.61
WHG_2006/07 (4)_091	12	0.39	29	43	95	871	44	-4	0.52
WHG_2006/07 (4)_090	13	0.43	28	43	99	847	43	-4	0.53
WHG_2006/07 (4)_089	14	0.41	28	43	99	852	43	-4	0.54
WHG_2006/07 (4)_088	15	0.41	38	42	102	845	45	-4	0.53
WHG_2006/07 (4)_087	16	0.62	30	42	102	862	45	-4	0.53
WHG_2006/07 (4)_086	17	0.56	28	43	102	890	44	-5	0.52
WHG_2006/07 (4)_085	18	0.29	28	43	100	882	44	-4	0.52
WHG_2006/07 (4)_084	19	0.39	28	42	103	865	45	-4	0.54
WHG_2006/07 (4)_083	20	0.67	-7	11	4	61	-4	-9	-0.04
WHG_2006/07 (4)_082	21	0.49	30	47	113	946	51	-4	0.55
WHG_2006/07 (4)_081	22	0.65	37	52	133	1040	62	-4	0.64
WHG_2006/07 (4)_080	23	0.64	38	52	135	1020	60	-4	0.65
WHG_2006/07 (4)_079	24	0.31	36	51	133	1010	60	-3	0.63
WHG_2006/07 (4)_078	25	0.55	36	51	134	1030	61	-4	0.64
WHG_2006/07 (4)_077	26	0.47	43	53	145	1060	64	-4	0.70
WHG_2006/07 (4)_076	27	0.61	38	53	140	1070	65	-4	0.66
WHG_2006/07 (4)_075	28	0.66	40	53	143	1050	64	-4	0.68
WHG_2006/07 (4)_074	29	0.49	38	51	137	1030	61	-4	0.67
WHG_2006/07 (4)_073	30	0.41	39	52	141	1050	64	-4	0.69
WHG_2006/07 (4)_072	31	0.50	41	51	137	1030	65	-4	0.66
WHG_2006/07 (4)_071	32	0.52	40	50	133	1030	65	-4	0.64
WHG_2006/07 (4)_070	33	0.41	40	51	134	1010	63	-4	0.63
WHG_2006/07 (4)_069	34	0.68	39	52	144	1060	67	-3	0.69
WHG_2006/07 (4)_068	35	0.62	38	53	137	1030	66	-4	0.64
WHG_2006/07 (4)_067	36	0.67	47	53	144	1060	68	-4	0.67
WHG_2006/07 (4)_066	37	0.74	39	52	146	1070	69	-3	0.68
WHG_2006/07 (4)_065	38	0.48	40	51	139	1030	70	-4	0.64
WHG_2006/07 (4)_064	39	0.88	39	51	139	1030	70	-3	0.64
WHG_2006/07 (4)_063	40	0.91	39	51	139	1040	70	-3	0.63
WHG_2006/07 (4)_062	41	0.34	40	51	142	1130	72	-3	0.67
WHG_2006/07 (4)_061	42	0.55	39	50	137	1060	69	-3	0.61
WHG_2006/07 (4)_060	43	0.56	36	51	131	1030	67	-3	0.59
WHG_2006/07 (4)_059	44	0.36	37	51	135	1060	71	-3	0.62
WHG_2006/07 (4)_058	45	0.94	40	51	139	1080	70	-3	0.64
WHG_2006/07 (4)_057	46	0.71	41	50	140	1060	72	-3	0.63
WHG_2006/07 (4)_056	47	0.52	36	49	128	1010	66	-3	0.56
WHG_2006/07 (4)_055	48	0.64	34	45	118	938	60	-3	0.52
WHG_2006/07 (4)_054	49	0.70	34	46	121	950	63	-3	0.54
WHG_2006/07 (4)_053	50	0.39	34	46	122	869	63	-4	0.52
WHG_2006/07 (4)_052	51	0.58	29	43	110	818	57	-4	0.45
WHG_2006/07 (4)_051	52	0.65	29	37	99	710	54	-3	0.40
WHG_2006/07 (4)_050	53	0.41	29	41	118	843	61	-3	0.49
WHG_2006/07 (4)_049	54	0.76	38	47	135	909	70	-2	0.56

Table A4.12 continued.

Sample	Depth cm	Al ppb	Ca ppb	K ppb	Mg ppb	Na ppb	S ppb	Si ppb	Sr ppb
WHG_2006/07 (4)_048	55	0.40	42	47	144	1020	74	-3	0.63
WHG_2006/07 (4)_047	56	0.78	36	46	130	888	67	-4	0.53
WHG_2006/07 (4)_046	57	0.71	32	40	115	880	64	-3	0.49
WHG_2006/07 (4)_045	58	0.74	32	44	113	816	58	-4	0.48
WHG_2006/07 (4)_044	59	0.75	27	38	106	764	58	-4	0.43
WHG_2006/07 (4)_043	60	0.59	27	38	107	760	57	-4	0.42
WHG_2006/07 (4)_042	61	0.67	30	42	116	831	63	-4	0.46
WHG_2006/07 (4)_041	62	0.75	32	43	120	894	65	-3	0.49
WHG_2006/07 (4)_040	63	0.50	32	45	119	903	66	-4	0.49
WHG_2006/07 (4)_039	64	0.45	33	46	128	944	67	-4	0.53
WHG_2006/07 (4)_038	65	0.69	63	46	128	929	67	-4	0.57
WHG_2006/07 (4)_037	66	0.51	35	44	124	934	66	-4	0.54
WHG_2006/07 (4)_036	67	0.80	35	43	113	903	62	-4	0.53
WHG_2006/07 (4)_035	68	0.50	43	41	104	856	67	-4	0.56
WHG_2006/07 (4)_034	69	0.48	40	44	122	897	60	-5	0.58
WHG_2006/07 (4)_033	70	0.66	32	42	120	821	45	-4	0.51
WHG_2006/07 (4)_032	71	0.68	36	45	127	876	49	-3	0.55
WHG_2006/07 (4)_031	72	0.79	36	43	124	855	47	-4	0.54
WHG_2006/07 (4)_030	73	0.77	29	41	112	764	45	-4	0.45
WHG_2006/07 (4)_029	74	0.78	25	38	101	724	43	-3	0.40
WHG_2006/07 (4)_028	75	0.59	20	31	79	597	36	-4	0.32
WHG_2006/07 (4)_027	76	0.49	20	30	72	584	39	-4	0.33
WHG_2006/07 (4)_026	77	0.30	31	36	92	757	51	-5	0.46
WHG_2006/07 (4)_025	78	0.23	22	33	89	629	38	-5	0.35
WHG_2006/07 (4)_024	79	0.34	19	33	89	622	35	-5	0.33
WHG_2006/07 (4)_023	80	0.15	28	39	111	748	40	-5	0.44
WHG_2006/07 (4)_022	81	0.24	31	43	123	802	44	-5	0.48
WHG_2006/07 (4)_021	82	0.39	28	42	126	827	44	-4	0.48
WHG_2006/07 (4)_020	83	0.43	31	42	128	831	45	-4	0.50
WHG_2006/07 (4)_019	84	0.37	33	44	130	837	46	-4	0.53
WHG_2006/07 (4)_018	85	0.45	36	47	140	913	48	-4	0.56
WHG_2006/07 (4)_017	86	0.78	40	53	155	1040	57	-4	0.66
WHG_2006/07 (4)_016	87	0.64	48	58	163	1080	59	-3	0.73
WHG_2006/07 (4)_015	88	0.73	48	60	170	1140	62	-3	0.76
WHG_2006/07 (4)_014	89	0.61	45	61	170	1120	63	-3	0.74
WHG_2006/07 (4)_013	90	0.45	50	62	175	1160	66	-3	0.77
WHG_2006/07 (4)_012	91	0.88	72	85	250	1630	106	-3	1.13
WHG_2006/07 (4)_011	92	1.08	86	95	285	1900	139	-2	1.34
WHG_2006/07 (4)_010	93	2.85	265	261	822	5770	472	5	3.98
WHG_2006/07 (4)_009	94	3.17	357	347	1090	8160	650	5	5.35
WHG_2006/07 (4)_008	95	3.36	356	349	1080	8160	654	6	5.19
WHG_2006/07 (4)_007	96	2.22	218	215	652	4870	407	2	3.21
WHG_2006/07 (4)_006	97	0.83	67	71	202	1570	127	-3	0.99
WHG_2006/07 (4)_005	98	0.35	18	29	65	553	38	-4	0.26
WHG_2006/07 (4)_004	99	0.32	2	16	23	230	14	-5	0.06
WHG_2006/07 (4)_003	100	0.09	4	18	25	258	17	-5	0.07
WHG_2006/07 (4)_002	101	0.46	9	22	31	322	29	-4	0.12
WHG_2006/07 (4)_001	102	0.36	15	28	45	481	50	-5	0.20

Table A4.13 Major ionic chemistry of WHG_1 snow samples measured by IC.

Sample	Depth (cm)	Na (ppb)	K (ppb)	Mg (ppb)	Ca (ppb)	MS (ppb)	Cl (ppb)	NO ₃ (ppb)	SO ₄ (ppb)
Sample average		1193	51	173	57	28	2530	65	322
Sample 2 rsd (%)		276	253	255	258	290	273	149	287
Sample max		11948	454	1565	518	209	25581	246	3312
Sample min		26	6	4	2	0	50	20	32
<hr/>									
WHG_2006/07 (1)_214	9	145	15	21	8	3	324	42	100
WHG_2006/07 (1)_213	10	100	10	16	7	3	250	42	83
WHG_2006/07 (1)_212	11	140	13	22	9	3	325	46	77
WHG_2006/07 (1)_211	12	168	13	26	10	3	423	59	80
WHG_2006/07 (1)_210	13	131	12	23	9	3	338	63	71
WHG_2006/07 (1)_209	14	222	14	33	13	3	516	58	75
WHG_2006/07 (1)_208	15	643	27	81	31	2	1454	54	130
WHG_2006/07 (1)_207	16	900	39	113	39	0	2023	51	161
WHG_2006/07 (1)_206	17	979	40	129	42	0	2177	41	165
WHG_2006/07 (1)_205	18	1086	43	150	46	0	2423	40	186
WHG_2006/07 (1)_204	19	1229	49	176	52	0	2867	40	220
WHG_2006/07 (1)_203	20	1256	50	181	53	0	3065	41	233
WHG_2006/07 (1)_202	21	1279	51	183	55	0	3005	41	228
WHG_2006/07 (1)_201	22	1287	52	184	54	0	3138	43	238
WHG_2006/07 (1)_200	23	1251	51	178	54	2	2989	42	228
WHG_2006/07 (1)_199	24	1223	50	173	52	0	2872	40	216
WHG_2006/07 (1)_198	25	1248	51	176	53	0	2850	41	215
WHG_2006/07 (1)_197	26	1250	50	182	52	0	2809	42	209
WHG_2006/07 (1)_195	27	1465	56	219	64	0	3296	51	250
WHG_2006/07 (1)_194	28	1271	56	183	52	0	2878	44	214
WHG_2006/07 (1)_193	29	653	29	93	25	0	1481	21	112
WHG_2006/07 (1)_192	30	1075	43	145	41	0	2424	37	165
WHG_2006/07 (1)_191	31	1216	46	182	52	2	2885	50	216
WHG_2006/07 (1)_190	32	935	34	131	50	2	2154	50	182
WHG_2006/07 (1)_189	33	495	20	70	21	2	1151	53	114
WHG_2006/07 (1)_188	34	242	11	33	10	3	557	52	69
WHG_2006/07 (1)_187	35	82	7	12	4	3	199	52	38
WHG_2006/07 (1)_186	36	79	7	12	4	4	193	52	37
WHG_2006/07 (1)_185	37	81	7	13	5	4	199	51	38
WHG_2006/07 (1)_184	38	79	7	12	4	3	194	52	37
WHG_2006/07 (1)_183	39	78	6	13	4	4	185	49	37
WHG_2006/07 (1)_182	40	80	7	13	5	3	191	51	38
WHG_2006/07 (1)_181	41	83	8	14	6	1	179	50	37
WHG_2006/07 (1)_180	42	80	8	15	5	3	164	44	36
WHG_2006/07 (1)_179	43	88	11	15	5	0	209	49	41
WHG_2006/07 (1)_178	44	113	9	20	8	2	271	27	49
WHG_2006/07 (1)_177	45	780	29	99	39	2	1696	40	195
WHG_2006/07 (1)_176	46	1129	44	146	65	0	2518	46	233
WHG_2006/07 (1)_175	47	1063	42	163	53	0	2202	38	198
WHG_2006/07 (1)_174	48	1069	42	163	53	0	2497	43	219
WHG_2006/07 (1)_173	49	1104	45	164	52	1	2388	41	209
WHG_2006/07 (1)_172	50	1082	43	166	53	2	2457	42	215
WHG_2006/07 (1)_171	51	1109	46	164	52	2	2388	41	208
WHG_2006/07 (1)_170	52	1065	41	158	50	2	2356	43	199
WHG_2006/07 (1)_169	53	985	40	144	46	1	1859	36	154
WHG_2006/07 (1)_168b	54	955	41	142	47	0	2255	45	187
WHG_2006/07 (1)_168	55	1053	41	141	53	2	2369	44	224
WHG_2006/07 (1)_167	56	870	31	107	43	3	1887	39	196
WHG_2006/07 (1)_166	57	538	21	78	24	3	1237	36	118
WHG_2006/07 (1)_165	58	523	22	75	22	3	1235	40	120
WHG_2006/07 (1)_164	59	516	22	75	22	4	1168	38	114
WHG_2006/07 (1)_163	60	503	19	76	23	3	1156	37	113
WHG_2006/07 (1)_162	61	512	22	75	21	3	976	32	97
WHG_2006/07 (1)_161	62	477	18	75	21	4	1148	40	117
WHG_2006/07 (1)_160	63	473	19	78	22	3	1100	38	114

Table A4.13 continued.

Sample	Depth (cm)	Na (ppb)	K (ppb)	Mg (ppb)	Ca (ppb)	MS (ppb)	Cl (ppb)	NO ₃ (ppb)	SO ₄ (ppb)
WHG_2006/07 (1)_159	64	499	21	82	22	3	1153	36	112
WHG_2006/07 (1)_158	65	502	22	86	24	0	1170	38	111
WHG_2006/07 (1)_157	66	500	21	86	23	2	1168	33	110
WHG_2006/07 (1)_156	67	503	27	90	25	2	1188	33	114
WHG_2006/07 (1)_155	68	504	20	94	24	2	1212	33	115
WHG_2006/07 (1)_154	69	544	22	96	25	2	1265	33	113
WHG_2006/07 (1)_153	70	525	21	93	25	2	1221	32	109
WHG_2006/07 (1)_152	71	486	21	92	25	2	1128	32	103
WHG_2006/07 (1)_151	72	546	24	98	26	2	1288	33	112
WHG_2006/07 (1)_150	73	601	24	109	28	2	1404	32	117
WHG_2006/07 (1)_149	74	831	36	141	39	2	1941	34	149
WHG_2006/07 (1)_148	75	920	37	158	46	0	2034	33	156
WHG_2006/07 (1)_147	76	1012	42	167	48	0	2268	31	173
WHG_2006/07 (1)_146	77	1154	49	190	56	0	2472	28	189
WHG_2006/07 (1)_145	78	2706	120	388	125	0	5906	42	627
WHG_2006/07 (1)_144	79	11948	454	1565	518	0	25581	165	3312
WHG_2006/07 (1)_143	80	11071	427	1444	480	0	23819	145	3065
WHG_2006/07 (1)_142	81	10732	416	1399	464	0	22822	139	2923
WHG_2006/07 (1)_141	82	10845	435	1390	471	0	22891	138	2919
WHG_2006/07 (1)_140	83	2735	111	359	124	5	5536	75	661
WHG_2006/07 (1)_139	84	713	31	100	29	4	1446	54	161
WHG_2006/07 (1)_138	85					10	273	31	32
WHG_2006/07 (1)_137	86	243	21	33	12	20	515	57	58
WHG_2006/07 (1)_136	87	337	17	44	17	13	679	59	88
WHG_2006/07 (1)_135	88	556	22	65	27	20	1081	58	184
WHG_2006/07 (1)_134	89	431	21	65	18	24	894	46	224
WHG_2006/07 (1)_133	90	913	37	121	36	46	1844	85	298
WHG_2006/07 (1)_132	91	534	24	74	21	49	1111	56	206
WHG_2006/07 (1)_131	92	621	27	85	25	58	1327	58	236
WHG_2006/07 (1)_130	93	534	27	80	24	55	1222	53	202
WHG_2006/07 (1)_129	94	2178	86	277	94	75	4342	91	817
WHG_2006/07 (1)_128	95	2449	95	310	104	111	4758	87	905
WHG_2006/07 (1)_127	96	2359	98	306	101	113	4705	94	902
WHG_2006/07 (1)_126	97	2557	100	332	107	66	5136	108	1005
WHG_2006/07 (1)_125	98	2333	89	306	97	114	4610	92	904
WHG_2006/07 (1)_124	99	2390	90	322	103	121	4672	91	961
WHG_2006/07 (1)_123	100	2330	86	315	99	126	4544	97	938
WHG_2006/07 (1)_122	101	1423	53	185	58	106	2828	82	560
WHG_2006/07 (1)_121	102	336	20	43	13	71	837	57	151
WHG_2006/07 (1)_120	103	163	12	23	7	104	371	50	201
WHG_2006/07 (1)_119	104	256	13	34	10	159	484	38	368
WHG_2006/07 (1)_118	105	297	15	37	11	136	620	26	302
WHG_2006/07 (1)_117	106	321	14	42	14	209	583	25	501
WHG_2006/07 (1)_116	107	199	11	24	14	143	379	21	203
WHG_2006/07 (1)_115	108	230	13	31	10	132	443	21	237
WHG_2006/07 (1)_114	109	392	17	52	16	135	758	24	321
WHG_2006/07 (1)_113	110	539	22	69	21	142	1008	29	393
WHG_2006/07 (1)_112	111	328	18	29	8	67	723	35	167
WHG_2006/07 (1)_111	112	270	15	36	12	130	585	75	259
WHG_2006/07 (1)_110	113	405	20	51	17	103	760	102	401
WHG_2006/07 (1)_109	114	533	25	63	22	100	926	120	493
WHG_2006/07 (1)_108	115	302	18	39	13	56	592	178	234
WHG_2006/07 (1)_107	116	192	14	24	8	27	407	220	134
WHG_2006/07 (1)_106	117	137	9	17	7	27	294	176	101
WHG_2006/07 (1)_105	118	91	9	12	5	26	198	161	111
WHG_2006/07 (1)_104	119	82	9	11	5	27	171	149	117
WHG_2006/07 (1)_103	120	78	9	11	4	27	162	145	116
WHG_2006/07 (1)_102	121	76	7	10	3	28	156	139	116
WHG_2006/07 (1)_101	122	70	8	9	3	28	147	143	114
WHG_2006/07 (1)_100	123	53	10	6	3	19	126	147	94
WHG_2006/07 (1)_099	124	56	8	7	4	25	115	123	106

Table A4.13 continued.

Sample	Depth (cm)	Na (ppb)	K (ppb)	Mg (ppb)	Ca (ppb)	MS (ppb)	Cl (ppb)	NO ₃ (ppb)	SO ₄ (ppb)
WHG_2006/07 (1)_098	125	43	8	6	4	24	88	102	95
WHG_2006/07 (1)_097	127	28	7	4	2	36	54	64	76
WHG_2006/07 (1)_096	128	26	8	4	3	53	50	58	84
WHG_2006/07 (1)_095	129	26	7	4	3	72	53	59	102
WHG_2006/07 (1)_094	130	31	7	5	3	80	65	69	123
WHG_2006/07 (1)_094	126	40	7	6	3	25	84	95	91
WHG_2006/07 (1)_092	131	39	9	6	3	84	79	61	135
WHG_2006/07 (1)_091	132	34	8	5	3	85	69	60	142
WHG_2006/07 (1)_090	133	49	8	8	5	104	100	71	122
WHG_2006/07 (1)_089	134	203	12	28	18	111	355	61	312
WHG_2006/07 (1)_088	135	210	13	29	8	120	375	63	323
WHG_2006/07 (1)_087	136	198	13	26	8	129	344	58	311
WHG_2006/07 (1)_086	137	148	12	21	7	119	258	64	303
WHG_2006/07 (1)_085	138	153	12	25	10	101	297	84	313
WHG_2006/07 (1)_084	139	444	22	80	25	74	1000	63	360
WHG_2006/07 (1)_083	140	1527	62	219	74	103	3078	102	566
WHG_2006/07 (1)_082	141	2205	90	325	106	90	4443	131	727
WHG_2006/07 (1)_081	142	2823	115	417	135	62	5712	167	892
WHG_2006/07 (1)_080	143	2771	118	407	132	56	5639	162	875
WHG_2006/07 (1)_079	144	2791	115	413	137	54	5662	161	882
WHG_2006/07 (1)_078	145	2694	112	394	128	51	5463	160	834
WHG_2006/07 (1)_077	146	2655	114	385	126	49	5453	164	812
WHG_2006/07 (1)_076	147	2715	114	405	134	51	5545	169	846
WHG_2006/07 (1)_075	148	2987	125	443	145	51	6066	188	923
WHG_2006/07 (1)_074	149	3243	136	490	161	55	6653	220	1007
WHG_2006/07 (1)_073	150	3302	138	499	166	54	6699	224	1033
WHG_2006/07 (1)_072	151	3297	138	488	162	54	6642	204	1029
WHG_2006/07 (1)_071	152	3340	139	485	171	53	6697	202	1023
WHG_2006/07 (1)_070	153	3732	152	533	173	45	7592	195	1171
WHG_2006/07 (1)_069	154	3477	141	468	159	40	6857	165	1295
WHG_2006/07 (1)_068	155	4756	189	691	221	51	8549	246	1306
WHG_2006/07 (1)_067	156	3219	129	460	159	42	6059	161	892
WHG_2006/07 (1)_066	157	878	47	129	58	36	2309	74	352
WHG_2006/07 (1)_065	158	746	37	113	55	33	1843	73	278
WHG_2006/07 (1)_064	159	721	36	112	52	39	1705	83	270
WHG_2006/07 (1)_063	160	755	38	118	53	44	1722	86	268
WHG_2006/07 (1)_062	161	710	35	110	50	40	1583	79	259
WHG_2006/07 (1)_061	162	679	34	106	49	37	1457	74	248
WHG_2006/07 (1)_060	163	548	32	93	44	23	1339	63	256
WHG_2006/07 (1)_059	164	955	51	165	66	12	2230	55	270
WHG_2006/07 (1)_058	165	2373	117	364	137	13	5307	95	443
WHG_2006/07 (1)_057	166	3923	162	611	205	18	8679	152	582
WHG_2006/07 (1)_056	167	3185	143	487	166	13	6952	106	499
WHG_2006/07 (1)_055	168	2177	113	325	118	7	4951	58	452
WHG_2006/07 (1)_054	169	1900	85	271	93	5	3625	34	257
WHG_2006/07 (1)_053	170	1603	79	274	80	7	3837	38	164
WHG_2006/07 (1)_052	171	1620	80	292	82	6	3337	32	142
WHG_2006/07 (1)_051	172	1661	81	300	84	8	4034	37	169
WHG_2006/07 (1)_050	173	1641	79	307	86	8	4137	37	171
WHG_2006/07 (1)_049	174	1614	83	298	83	9	3814	35	166
WHG_2006/07 (1)_048	175	1517	75	290	82	10	3533	33	159
WHG_2006/07 (1)_047	176	1456	75	271	79	8	2885	27	138
WHG_2006/07 (1)_046	177	1559	85	281	82	7	3101	31	157
WHG_2006/07 (1)_045	178	1306	65	239	69	11	2981	30	165
WHG_2006/07 (1)_044	179	1228	58	210	61	11	2749	30	155
WHG_2006/07 (1)_043	180	1147	55	188	55	11	2656	29	156
WHG_2006/07 (1)_042	181	1004	51	133	39	7	2081	20	111
WHG_2006/07 (1)_041	182	1096	50	174	52	11	2524	29	156
WHG_2006/07 (1)_040	183	1042	46	170	50	11	2433	30	152
WHG_2006/07 (1)_039	184	1058	48	169	51	11	2424	31	150
WHG_2006/07 (1)_038	185	1046	48	167	51	11	2396	31	146

Table A4.13 continued.

Sample	Depth (cm)	Na (ppb)	K (ppb)	Mg (ppb)	Ca (ppb)	MS (ppb)	Cl (ppb)	NO ₃ (ppb)	SO ₄ (ppb)
WHG_2006/07 (1)_037	186	984	45	135	44	7	2152	25	119
WHG_2006/07 (1)_036	187	1037	44	160	63	9	2191	31	134
WHG_2006/07 (1)_035	188	1032	45	174	50	9	2344	34	141
WHG_2006/07 (1)_034	189	1018	43	165	48	9	2291	36	131
WHG_2006/07 (1)_033	190	974	43	159	48	7	2244	37	124
WHG_2006/07 (1)_032	191	916	42	153	47	6	1918	34	111
WHG_2006/07 (1)_031	192	878	39	150	46	6	2041	39	105
WHG_2006/07 (1)_030	193	858	49	139	40	30	1989	42	99
WHG_2006/07 (1)_029	194	851	40	138	40	5	1941	47	99
WHG_2006/07 (1)_028	195	1031	51	162	51	0	2340	77	137
WHG_2006/07 (1)_027	196	799	32	124	43	3	1803	44	140
WHG_2006/07 (1)_026	197	885	35	131	45	2	1634	37	133
WHG_2006/07 (1)_025	198	909	36	131	47	0	1836	41	181
WHG_2006/07 (1)_024	199	995	37	139	51	2	2026	43	218
WHG_2006/07 (1)_023	200	1246	45	166	55	0	2570	52	242
WHG_2006/07 (1)_022	201	1200	45	169	52	0	2464	41	219
WHG_2006/07 (1)_021	202	1169	44	169	51	2	2458	36	219
WHG_2006/07 (1)_020	203	1108	41	164	49	0	2397	31	214
WHG_2006/07 (1)_019	204	1140	42	163	49	0	2357	27	212
WHG_2006/07 (1)_018	205	1133	43	160	50	0	2369	28	214
WHG_2006/07 (1)_017	206	1131	42	164	50	1	2384	32	216
WHG_2006/07 (1)_016	207	1195	44	174	53	1	2492	27	229
WHG_2006/07 (1)_015	208	1194	44	173	52	1	2489	27	228
WHG_2006/07 (1)_014	209	1186	44	171	52	0	2487	33	228
WHG_2006/07 (1)_013	210	1086	39	155	47	2	2250	26	203
WHG_2006/07 (1)_012	211	894	32	130	39	0	1792	21	158
WHG_2006/07 (1)_011	212	752	28	113	34	0	1559	21	136
WHG_2006/07 (1)_010	213	789	27	109	35	0	1607	21	161
WHG_2006/07 (1)_009	214	956	31	114	47	2	1865	24	233
WHG_2006/07 (1)_008	215	938	30	107	54	3	1798	26	250
WHG_2006/07 (1)_007	216	752	23	84	37	5	1420	26	194
WHG_2006/07 (1)_006	217	482	17	66	26	9	1003	26	98
WHG_2006/07 (1)_005	218	463	17	65	28	12	957	28	92
WHG_2006/07 (1)_004	219	468	18	66	31	12	976	29	94
WHG_2006/07 (1)_003	220	488	17	61	32	19	972	30	94
WHG_2006/07 (1)_002	221	397	13	54	29	18	788	26	114
WHG_2006/07 (1)_001	222	340	14	44	46	17	680	26	132

Table A4.14 Major ionic chemistry of WHG_1b snow samples measured by IC.

Sample	Depth (cm)	WHG_1 equiv. depth (cm)	Na (ppb)	K (ppb)	Mg (ppb)	Ca (ppb)	MS (ppb)	Cl (ppb)	NO ₃ (ppb)	SO ₄ (ppb)
Sample average			510	21	67	23	222	1023	30	343
Sample 2 std (%)			205	156	199	189	232	202	103	181
Sample max			2929	97	387	118	773	5643	101	1155
Sample min			23	5	4	2	4	41	10	46
WHG_2006/07 (1b)_090	190	199	89	8	11	11	59	160	32	158
WHG_2006/07 (1b)_089	191	200	81	7	11	8	74	146	30	208
WHG_2006/07 (1b)_088	192	201	87	8	12	6	99	161	29	255
WHG_2006/07 (1b)_087	193	202	71	7	10	5	121	127	26	226
WHG_2006/07 (1b)_086	194	203	84	10	11	5	161	149	24	256
WHG_2006/07 (1b)_085	195	204	85	6	11	5	170	151	18	238
WHG_2006/07 (1b)_084	196	205	123	6	16	5	236	219	13	258
WHG_2006/07 (1b)_083	197	206	181	9	24	7	292	325	12	327
WHG_2006/07 (1b)_082	198	207	204	9	27	9	308	366	12	357
WHG_2006/07 (1b)_081	199	208	276	11	37	11	368	503	13	436
WHG_2006/07 (1b)_080	200	209	355	12	46	13	452	650	13	494
WHG_2006/07 (1b)_079	201	210	288	12	38	10	448	528	14	440
WHG_2006/07 (1b)_078	202	211	384	23	51	15	559	724	16	615
WHG_2006/07 (1b)_077	203	212	410	23	55	16	581	752	17	729
WHG_2006/07 (1b)_076	204	213	473	23	63	19	661	873	17	846
WHG_2006/07 (1b)_075	205	214	480	24	63	19	729	882	20	958
WHG_2006/07 (1b)_074	206	215	409	26	54	17	732	767	22	1014
WHG_2006/07 (1b)_073	207	216	387	24	50	17	746	729	23	1009
WHG_2006/07 (1b)_072	208	217	355	23	46	14	756	669	24	1026
WHG_2006/07 (1b)_071	209	218	332	15	43	12	773	628	26	1004
WHG_2006/07 (1b)_070	210	219	282	13	36	11	766	516	25	1082
WHG_2006/07 (1b)_069	211	220	215	11	28	8	743	388	22	1155
WHG_2006/07 (1b)_068	212	221	172	11	22	8	716	295	21	1155
WHG_2006/07 (1b)_067	213	222	111	12	14	6	678	189	19	905
WHG_2006/07 (1b)_066	214	223	50	6	7	5	601	88	14	568
WHG_2006/07 (1b)_065	215	224	34	5	5	3	500	54	11	491
WHG_2006/07 (1b)_064	216	225	26	5	4	2	435	42	10	478
WHG_2006/07 (1b)_063	217	226	23	5	4	2	373	41	14	445
WHG_2006/07 (1b)_062	218	227	57	7	7	3	302	106	27	458
WHG_2006/07 (1b)_061	219	228	106	8	13	4	273	200	37	485
WHG_2006/07 (1b)_060	220	229	123	9	16	7	243	243	47	460
WHG_2006/07 (1b)_059	221	230	142	9	18	7	186	303	57	472
WHG_2006/07 (1b)_058	222	231	343	18	56	11	121	755	40	598
WHG_2006/07 (1b)_057	223	232	1008	32	120	47	121	1798	40	786
WHG_2006/07 (1b)_056	224	233	708	37	122	28	106	1585	33	390
WHG_2006/07 (1b)_055	225	234	2929	97	387	118	217	5643	101	1014
WHG_2006/07 (1b)_054	226	235	2764	86	329	116	223	5272	98	937
WHG_2006/07 (1b)_053	227	236	336	18	62	16	59	828	35	113
WHG_2006/07 (1b)_052	228	237	208	9	33	9	40	461	28	98
WHG_2006/07 (1b)_051	229	238	99	7	15	6	26	195	14	67
WHG_2006/07 (1b)_050	230	239	99	7	14	7	26	194	13	68
WHG_2006/07 (1b)_049	231	240	115	14	16	10	28	220	13	77
WHG_2006/07 (1b)_048	232	241	117	6	17	6	29	223	12	78
WHG_2006/07 (1b)_047	233	242	144	8	20	8	32	277	11	89
WHG_2006/07 (1b)_046	234	243	230	13	30	11	40	442	12	120
WHG_2006/07 (1b)_045	235	244	261	13	32	15	44	502	10	132
WHG_2006/07 (1b)_044	236	245	253	12	34	12	43	494	14	130
WHG_2006/07 (1b)_043	237	246	291	15	41	13	42	596	21	154
WHG_2006/07 (1b)_042	238	247	532	19	68	21	52	1032	27	250
WHG_2006/07 (1b)_041	239	248	529	20	71	23	51	1038	30	249
WHG_2006/07 (1b)_040	240	249	586	21	78	23	48	1152	37	263
WHG_2006/07 (1b)_039	241	250	543	20	74	21	41	1074	35	236
WHG_2006/07 (1b)_038	242	251	525	22	74	22	42	1063	37	218
WHG_2006/07 (1b)_037	243	252	609	22	80	32	51	1223	44	215
WHG_2006/07 (1b)_036	244	253	578	22	79	33	56	1193	44	185

Table A4.14 continued.

Sample	Depth (cm)	WHG_1 equiv. depth (cm)	Na (ppb)	K (ppb)	Mg (ppb)	Ca (ppb)	MS (ppb)	Cl (ppb)	NO ₃ (ppb)	SO ₄ (ppb)
WHG_2006/07 (1b)_035	245	254	555	21	78	32	54	1142	35	172
WHG_2006/07 (1b)_034	246	255	506	19	70	29	46	1040	32	165
WHG_2006/07 (1b)_033	247	256	416	17	59	26	38	861	28	153
WHG_2006/07 (1b)_032	248	257	231	11	38	13	22	489	28	117
WHG_2006/07 (1b)_031	249	258	260	14	38	38	22	507	26	114
WHG_2006/07 (1b)_030	250	259	267	10	34	16	19	528	25	89
WHG_2006/07 (1b)_029	251	260	309	18	42	14	15	647	30	75
WHG_2006/07 (1b)_028	252	261	615	19	67	32	12	1205	37	141
WHG_2006/07 (1b)_027	253	262	498	19	66	22	10	1045	32	106
WHG_2006/07 (1b)_026	254	263	329	13	47	15	6	736	30	64
WHG_2006/07 (1b)_025	255	264	614	21	61	27		1217	33	119
WHG_2006/07 (1b)_024	256	265	539	23	65	23		1138	34	80
WHG_2006/07 (1b)_023	257	266	534	21	69	23		1145	34	76
WHG_2006/07 (1b)_022	258	267	534	22	69	22	5	1145	32	75
WHG_2006/07 (1b)_021	259	268	533	23	69	24		1151	34	76
WHG_2006/07 (1b)_020	260	269	530	24	67	22		1143	33	76
WHG_2006/07 (1b)_019	261	270	535	27	68	24		1155	32	77
WHG_2006/07 (1b)_018	262	271	538	25	69	24	4	1154	27	76
WHG_2006/07 (1b)_017	263	272	567	27	73	24		1215	26	77
WHG_2006/07 (1b)_016	264	273	653	27	83	29		1391	28	102
WHG_2006/07 (1b)_015	265	274	1703	47	170	73		3151	38	523
WHG_2006/07 (1b)_014	266	275	1336	51	186	58		2804	39	248
WHG_2006/07 (1b)_013	267	276	1459	54	209	60		3071	40	276
WHG_2006/07 (1b)_012	268	277	1559	56	217	64	4	3223	43	290
WHG_2006/07 (1b)_011	269	278	1578	59	212	62		3230	44	289
WHG_2006/07 (1b)_010	270	279	1620	59	208	68		3345	49	300
WHG_2006/07 (1b)_009	271	280	1275	46	169	50	4	2665	44	236
WHG_2006/07 (1b)_008	272	281	1086	41	144	43		2266	44	199
WHG_2006/07 (1b)_007	273	282	293	12	51	13		679	32	62
WHG_2006/07 (1b)_006	274	283	239	13	44	9		587	34	46
WHG_2006/07 (1b)_005	275	284	990	31	95	47	4	1897	50	255
WHG_2006/07 (1b)_004	276	285	726	27	88	31	5	1447	41	153
WHG_2006/07 (1b)_003	277	286	732	29	90	32		1477	42	157
WHG_2006/07 (1b)_002	278	287	660	25	85	29	4	1351	35	135
WHG_2006/07 (1b)_001	279	288	769	34	97	33		1581	40	160

Table A4.15 Density measurements of the four WHG snow profiles.

WHG_1		WHG_1b		WHG_2		WHG_3		WHG_4	
Depth (cm)	Density (kg m ⁻³)	Depth (cm)	Density (kg m ⁻³)	Depth (cm)	Density (kg m ⁻³)	Depth (cm)	Density (kg m ⁻³)	Depth (cm)	Density (kg m ⁻³)
9	361	193	497	0	409	0	290	1	370
12	391	196	482	3	389	4	290	4	397
15	410	198	482	5	419	7	295	6	384
17	401	200	489	8	384	8	285	8	370
20	364	202	486	10	389	12	300	11	366
23	373	206	494	15	365	14	265	13	364
26	383	208	486	17	396	16	350	14	364
29	380	213	485	21	327	18	373	18	363
32	384	215	482	24	375	21	375	20	369
34	403	220	478	27	364	23	374	23	376
35	408	221	477	29	360	27	374	25	384
39	421	224	474	32	356	29	385	27	386
43	421	228	456	33	348	31	386	30	392
45	408	233	461	37	358	34	383	33	398
47	425	235	459	39	365	39	346	36	402
50	428	239	456	42	362	41	348	38	400
52	428	241	426	44	356	44	384	41	408
56	415	245	430	47	377	49	374	43	406
59	416	248	419	49	380	50	378	46	411
60	422	252	432	51	375	53	371	48	410
63	421	253	431	54	393	57	371	51	418
65	423	256	451	57	386	58	365	54	405
69	422	258	461	59	399	62	382	56	412
72	440	261	471	61	399	64	394	58	418
75	448	265	492	64	402	67	397	61	412
77	440	267	454	66	417	69	387	64	418
80	426	269	460	69	413	73	396	66	426
84	424	272	459	71	417	76	401	69	419
86	400	275	465	74	422	77	404	71	414
90	378	277	467	76	424	80	401	74	426
92	388	285	470	79	418	82	405	76	427
95	402	289	461	82	413	84	394	79	425
98	446			84	420	86	400	81	426
101	374			86	418	90	402	84	442
103	364			89	423	93	397	88	435
105	383			92	434	96	409	89	418
106	386			93	434	97	414	93	423
110	390			97	412	101	417	96	424
113	361			99	432	103	417	98	401
115	381			103	424	105	414	100	349
117	378			106	410	108	334	103	390
121	380			109	380	109	338	106	388
124	378			112	377	111	340	108	346
126	376			116	403	114	409	111	376
127	380			119	404	118	413	114	376
130	388			123	362	120	378	117	8368
132	383			124	346	123	407	121	378
134	393			128	374	125	339	124	399
137	431			133	367	127	334	129	374
141	420			135	388	130	358	133	410
141	428			138	391	135	362	136	408
145	492			142	376	138	376	140	369
148	436			144	386	140	380	143	391
150	446			147	378			148	388
154	389			150	374				
157	393			152	376				
159	390			156	379				
162	424			155	371				
165	420			159	364				
168	428			163	378				
172	448			166	381				
174	463			169	448				
178	477								
180	465								
183	471								
185	468								
187	480								
191	495								
195	482								
198	482								
201	455								
205	460								
207	478								
208	473								

